

# Handover in Digital Cellular Mobile Communication Systems

Mahmood Mohseni Zonoozi

B.Sc. (Eng) (Hon), M. E. E.

*A thesis submitted in fulfilment of the requirements for the degree of  
Doctor of Philosophy*



Department of Electrical and Electronic Engineering  
Faculty of Engineering  
Victoria University of Technology,  
Melbourne, Australia

March 1997

FTS THESIS  
621.38456 ZON  
30001005085313  
Zonoozi, Mahmood Mohseni  
Handover in digital cellular  
mobile communication systems



## ***Abstract***

A mathematical formulation is developed for systematic tracking of the random movement of a mobile station in a cellular environment. It incorporates mobility parameters under generalized conditions, so that the model could be tailored to be applicable in most cellular environments. This model is then used to characterize different mobility-related traffic parameters in a cellular system. These include the cell residence time of both new and handover calls, channel holding time and the average number of handovers per call. It is shown that the cell residence time can be described by the *generalized gamma distribution*, while the channel holding time can be best approximated by the negative exponential distribution. Based on these findings a teletraffic model that takes the user mobility into account is presented and is substantiated using a computer simulation. Further, the influence of cell size on new and handover call blocking probabilities is examined. The effect of the handover channel reservation on call dropout probability is also examined to determine the optimum number of reserved channels required for handover. Improvement to handover performance is investigated in terms of reduction in the number of unnecessary handovers as well as reduction in handover delay time. For this purpose an analytical method is developed which determines the optimum hysteresis level and the signal averaging time under shadow fading. The results are applicable in both micro- and macro-cellular systems.

## *Declaration*

I declare that, to the best of my knowledge, the research described herein is the result of my own work, except where otherwise stated in the text. It is submitted in fulfilment of the candidature for the degree of Doctor of Philosophy of Victoria University of Technology, Australia. No part of it has already been submitted for any degree nor is being submitted concurrently for any other degree.

Mahmood Mohseni Zonoozi

March 1997.

## ***Acknowledgment***

I am most grateful to my supervisor, **Dr. Prem Dassanayake** who has guided me through this work. I am indebted to him for his unceasing encouragement, support and advice. I wish to thank my co-supervisor **Assoc. Prof. Mike Faulkner**, the ex-Head of Department **Assoc. Prof. Wally Evans**, the Deputy Dean of Faculty **Assoc. Prof. Patrick Leung**, and the Head of Department **Prof. Akhtar Kalam**.

Many thanks should also go to my fellow research students in the department of Electrical and Electronic Engineering with whom I had many helpful discussions throughout the last four years. The memories I shared with **Reza, Nasser, Mehrdad, Omar, Iqbal, Osama, Adrian, Mahabir, Rushan, Zahidul, Vallipuram, Ranjan, Olivia, Tuan** and **Mark** will always be in my mind. A special note of appreciation is extended to the **people of Iran** who have financed my education for nearly 24 years. Their sacrifice cannot be paid, I will honour it.

Words cannot express my deepest gratitude and appreciation to my wife, **Mahin** for her patience throughout the period of this work when I had to spend all day at my work. She never ran out of encouragement during the most difficult and vulnerable parts of my stay in Melbourne. Her emotional support and motivation helped the speedy completion of this thesis without which this work may not have materialised. I would also like to acknowledge my son **Farhad** who throughout many late nights stayed with me at the university putting independent efforts in learning so many details about computing and computer technology that projected his ability and tenacity with a mature image and won him the admiration of many staff and students in the department. My acknowledgement extends to my little beautiful daughter **Shahrzad** for assuring me with her pleasant smile and sweet warmth while she was around whenever work turned tense. Last but by no means least, my **mother, mother-in-law, father and father-in-law** should be recognized for their everlasting encouragement and support.

*With love to my wife  
Mahin*

# *Table of Contents*

<b>Abstract</b> .....	<b>i</b>
<b>Declaration</b> .....	<b>ii</b>
<b>Acknowledgment</b> .....	<b>iii</b>
<b>Table of Contents</b> .....	<b>v</b>
<b>List of Figures</b> .....	<b>viii</b>
<b>List of Tables</b> .....	<b>x</b>
<b>Acronyms</b> .....	<b>xi</b>
<b>Notations</b> .....	<b>xiii</b>
<b>Chapter 1. Introduction</b> .....	<b>1</b>
1.1. Historical Overview .....	2
1.2. Ongoing Work and the Future.....	6
1.3. Scope of Thesis .....	11
1.3.1. Effect of mobility on handover.....	11
1.3.2. Effect of handover on teletraffic performance criteria .....	11
1.3.3. Effect of propagation environment on handover decision making.....	12
<b>Chapter 2. Trends in Handover Processes</b> .....	<b>13</b>
2.1. Cell Structures .....	15
2.2. Handover Performance Measures .....	17
2.2.1. Performance evaluation by means of traffic analysis .....	18
2.2.2. Performance evaluation by means of handover administration.....	18
2.3. Handover Algorithms .....	19
2.3.1. Signal strength based handover algorithm .....	20
2.3.2. Co-channel interference based handover algorithm .....	21
2.3.3. BER and pseudo BER based handover algorithm.....	21
2.3.4. Distance based handover algorithm .....	23
2.3.5. Velocity adaptive handover algorithm.....	23
2.3.6. Direction biased handover algorithm .....	25
2.3.7. Multi-criteria based handover algorithm.....	26
2.4. Handover Strategies .....	27
2.4.1. Network Controlled Handover (NCHO) .....	27
2.4.2. Mobile Assisted Handover (MAHO) .....	29
2.4.3. Mobile Controlled Handover (MCHO).....	30
2.5. Soft handover .....	31
2.6. Conclusions and Summary .....	35



<b>Chapter 3. Stochastic Mobility Modelling.....</b>	<b>36</b>
3.1. Tracing of a mobile inside the cell .....	38
3.2. Tracing of mobile outside the cell.....	48
3.3. Conclusions .....	52
<b>Chapter 4. Cell Residence Time and Channel Holding Time Distributions</b>	<b>53</b>
4.1. Cell Residence Time Distribution .....	57
4.1.1. Simplified Case .....	58
4.1.2. Generalized Case.....	62
4.2. Mean Cell Residence Time .....	76
4.3. Effect of Change in Direction and Speed.....	78
4.4. Average Number of Handovers.....	85
4.4.1. Method I.....	86
4.4.2. Method II.....	88
4.5. Channel Holding Time Distribution.....	91
4.6. Conclusions .....	97
<b>Chapter 5. Effect of Handover on the Teletraffic Performance Criteria....</b>	<b>98</b>
5.1. Radio Resource Allocation.....	99
5.1.1. Fixed Channel Assignment (FCA).....	100
5.1.2. Dynamic Channel Assignment (DCA).....	100
5.1.3. Flexible Channel Assignment .....	102
5.2. Teletraffic Performance Parameters.....	104
5.2.1. Setup channel blocking probability.....	104
5.2.2. New call blocking probability .....	105
5.2.3. Fixed network blocking probability .....	105
5.2.4. Handover attempt failure probability .....	106
5.2.5. Dropout probability .....	106
5.2.6. Unsuccessful call probability .....	108
5.3. Teletraffic Analysis .....	108
5.4. Handover Prioritization Schemes.....	113
5.4.1. Reserved channel scheme.....	114
5.4.2. Queueing prioritization schemes.....	118
5.5. Simulation model .....	121
5.5.1. Cellular Mobile Coverage Area .....	122
5.5.2. Analysis of computer simulation results .....	123
5.6. Conclusions .....	132
<b>Chapter 6. Mobile Radio Channel Modelling for Handover Analysis .....</b>	<b>134</b>

6.1. Radio Signal Components .....	135
6.1.1. Multipath fading component .....	136
6.1.2. Shadow fading component .....	138
6.1.3. Path loss component .....	139
6.2. Mobile Radio Channel Characterization for Handover Analysis.....	143
6.3. Conclusions .....	148
<b>Chapter 7. Optimum Hysteresis Level, Signal Averaging Time and Handover Delay .....</b>	<b>149</b>
7.1. Handover Initiation Parameters.....	152
7.2. Received Signal Statistics .....	155
7.2.1. Mean of the received signal level .....	156
7.2.2. Variance of the received signal level .....	156
7.3. Handover Algorithm with Hysteresis.....	159
7.4. Unnecessary Handovers .....	162
7.5. Handover Delay.....	170
7.5.1. Handover delay in macrocells .....	171
7.5.2. Handover delay in microcells.....	176
7.6. Conclusions .....	178
<b>Chapter 8. Conclusions .....</b>	<b>180</b>
8.1. Effect of mobility on handover .....	181
8.2. Effect of handover on teletraffic performance criteria.....	182
8.3. Effect of propagation environment on handover decision making .....	183
<b>References.....</b>	<b>185</b>
<b>Appendix A User Distribution.....</b>	<b>203</b>
<b>Appendix B User's Speed Distribution.....</b>	<b>206</b>
<b>Appendix C Minimum Value of Two Random Variables.....</b>	<b>208</b>
<b>Appendix D Expected Value of a Distribution.....</b>	<b>210</b>
<b>Appendix E Source Codes.....</b>	<b>212</b>

## *List of Figures*

Fig.1.1	Network development and integration. ....	10
Fig.2.1	A typical components of a cellular system. ....	14
Fig.3.1	Trajectory of a randomly moving mobile in the cellular environment. ....	38
Fig.3.2	Four different cases for a mobile path. ....	39
Fig.3.3	An example for movement of a mobile from location A to E passing through the regions of 1 (ABC), 2 (CD), & 4 (DE). ....	42
Fig.3.4	Illustration of different regions. ....	42
Fig.3.5	Movement of mobiles between different regions. ....	44
Fig.3.6	Permissible state diagram for mobile movement. ....	46
Fig.3.7	Relations to trace a mobile between different regions. ....	47
Fig.3.8	Coordinates of a mobile position at point A with respect to two different coordinates systems. ....	49
Fig.3.9	Neighbour cells numbering. ....	49
Fig.3.10	Geometric relations between real location of a mobile A, and its image A' in the substitute cell. ....	51
Fig.4.1	Representation of cell residence time in time and space domains for a mobile moving across cells. ....	57
Fig.4.2	Cell residence time illustration for two different cases. ....	60
Fig.4.3	Simplified flow diagram for analysing boundary crossing. ....	64
Fig.4.4	Mobile movement in permissible directions. ....	67
Fig.4.5	New and handover calls' cell residence time distributions obtained analytically (Eqs. (4.6) and (4.9)) and by simulation with the same assumptions. ....	70
Fig.4.6	Paths of five sample mobile users. ....	71
Fig.4.7	Examples of generalized gamma density functions. ....	73
Fig.4.8	New call cell residence time pdf. ....	76
Fig.4.9	New and handover call cell residence time cdf obtained by the simulation and by the assumption of the equivalent generalized gamma distributions. ....	77
Fig.4.10	Effect of change in mobile direction on the boundary crossing probability. ....	80
Fig.4.11	Excess cell radius for different values of drift limits (in degrees). ....	83
Fig.4.12	Excess cell radius for different values of mean initial speed. ....	84
Fig.4.13	Cell residence times for a mobile travelling across cells. ....	89
Fig.4.14	Average number of handovers experienced by a call for different probabilities of handover failures. ....	91
Fig.4.15	Illustration of handover within various call duration. ....	92
Fig.4.16	Illustration of the new and handover call cell residence time. ....	93
Fig.4.17	Cdf of different random variables for a cell size of 3 Km. ....	95
Fig.4.18	Variation of the average channel holding time with cell size in the reference cell. ....	96
Fig.5.1	Markov chain representation of two cells with n channels. ....	109

Fig.5.2	Blocking probabilities for the networks with reserved channel scheme ....	116
Fig.5.3	Efficiency of the reserved channel scheme. ....	117
Fig.5.4	Layout for a toroidal 49-cell system (reuse cluster for the cell number 33 highlighted).....	123
Fig.5.5	New and handover call blocking probabilities for different cell sizes. ....	124
Fig.5.6	Comparison of offered traffic for different cell sizes. ....	125
Fig.5.7	Dropout probability versus handover call blocking probability. (No channel reservation). ....	126
Fig.5.8	Dropout probability versus new call attempt rate. (No channel reservation) ...	127
Fig.5.9	New and handover call blocking probabilities with reserved channels for handover calls. ....	128
Fig.5.10	Dropout probability variation with the number of reserved channels for handover. ....	130
Fig.5.11	Optimum number of reserved channels for different dropout levels.....	131
Fig.6.1	Illustration of the parameters for determination of the LOS and NLOS path losses.....	143
Fig.6.2	Digital filter for producing slow fading signal component. ....	146
Fig.6.3	Received signal level along a LOS and a NLOS streets in a microcell with superimposed correlated shadow fading.....	147
Fig.6.4	Received signal level along a path in a macrocell with superimposed correlated shadow fading.....	147
Fig.7.1	Control channel measuring sequence. Cell number 0 stands for the current cell and other cell numbers stand for the neighbour cells [61]. ....	155
Fig.7.2	Standard deviation as a function of averaging period. ....	160
Fig.7.3	Received signal level from two base stations without shadow fading. ....	161
Fig.7.4	Conversion of the normal distributions to the equivalent standardized normal distributions. ....	164
Fig.7.5	Unnecessary handover probability versus path loss difference normalised to hysteresis level.....	166
Fig.7.6	Effect of shadow fading variance and hysteresis level on unnecessary handover probability.....	167
Fig.7.8	Relation between three parameters of h, T, Pu.....	168
Fig.7.7	Unnecessary handover probability versus hysteresis level for different signal averaging time. ....	169
Fig.7.9	Definition of parameters for delay calculation. ....	171
Fig.7.10	Handover delay versus hysteresis levels for different signal averaging periods and cell sizes.....	174
Fig.7.11	Handover delay versus signal averaging period and hysteresis level as a function of unnecessary handovers for different cell sizes.....	175
Fig.7.12	Illustration of handover delay parameters in a micro-cell (figure (b) shows a zoomed region of figure (a) around the optimal point). ....	177
Fig.A.1	User distribution in a strip. ....	204
Fig.C.1	Region for a random variable Z which is the minimum of the two other random variables.....	210

## *List of Tables*

Table 3.1	Equations for calculation of mobile new location. ....	46
Table 4.1	Different distributions derived from generalized gamma distribution. ....	73
Table 4.2	Best fitted gamma distribution parameters value for the new and handover call residence time. ....	74
Table 4.3	Comparison of results obtained from (4.25)-(4.26) with (4.23)-(4.24). ....	79

# *Acronyms*

ADC	American Digital Cellular
ALT	Automatic Link Transfer
AMPS	Advanced Mobile Phone Service
AR-1	Auto-Regressive of the first order
BCC	Blocked-Calls-Cleared
BER	Bit Error Rate
B-ISDN	Broad-band Integrated Services Digital Network
CBD	Central business district
Cdf	Cumulative distribution function
CDMA	Code Division Multiple Access
CDPC	Cellular Digital Packet data
CEC	Commission of the European Community
CEPT	Conférence Européenne des postes et Télécommunications
CT	Cordless Telephone
DCA	Dynamic Channel Assignment
DECT	Digital European Cordless Telecommunications
EIA	Electronic Industries Association (US)
ETSI	European Telecommunications Standards Institute
FIFO	First-In-First-Out
FCA	Fixed Channel Assignment
FDMA	Frequency Division Multiple Access
FPLMTS	Future Public Land Mobile Telecommunication Systems
GoS	Grade-of-Service
GSM	Global System for Mobile communications <sup>1</sup>
IID	Independent and Identically Distributed
IN	Intelligent Networks
INMARSAT	International Maritime Satellite Organization
IP	Internet Protocol
IS	Interim Standard (TIA/EIA cellular network signalling standard, US)
ISDN	Integrated Services Digital Network
ITU	International Telecommunication Union
IVHS	Intelligent Vehicle Highway Systems
JDC	Japanese Digital Cellular
JMPS	Japanese Mobile Phone System
LCR	level crossing rates
LEO	Low Earth Orbit
MAHO	Mobile Assisted Handover

---

1. This abbreviation earlier stood for Groupé Spéciale Mobile

---

MBPS	Measurement-Based Priority Scheme
MCHO	Mobile Controlled Handover
MSS	Mobile Satellite Systems
MSC	Mobile Switching Centre
NCHO	Network Controlled Handover
NMT	Nordic Mobile Telephone
PACS	Personal Access Communications Services
PCS	Personal Communication System
Pdf	Probability density function
PHS	Personal Handyphone System
PIN	Personal Identification Number
PMR	Private Mobile Radio
PN	Pseudo random Noise
PSTN	Public Switched Telephone Network
QoS	Quality-of-Service
QPSK	Quadrature Phase Shift Keyed
RACE	Research on Advanced Communications for Europe
RSS	Received Signal Strength
RV	Random variable
SAT	Supervisory Audio Tone
SER	Symbol Error Rate
SIR	Signal to Interference Ratio
SRS	Sub-Rating Scheme
TACS	Total Access Communications System
TDMA	Time Division Multiple Access
TIA	Telecommunications Industry Association
UDPC	Universal Digital Portable Communications
UMTS	Universal Mobile Telecommunication System
UPT	Universal Personal Telecommunication
WACS	Wireless Access Communications Systems
ZCR	Zero Crossing Rates

# *Notations*

## *Generic notations and operators*

$Cov(\tau)$	Auto-covariance function
$E[ \ ]$	Expectation operator
$F_X(x)$	Cdf of the random variable $x$ .
$I_0( \ )$	Modified Bessel function of the first kind zero order.
$Prob\{ \ }$	Probability operator
$R_x(\tau)$	Auto-correlation function of random variable $x$
$U( \ )$	Unit step function
$Var\{X\}$	Variance of the random variable $x$
$(X, Y), (X', Y')$	Coordinate systems with the origin locating at the base station site
$X Y$	Random variable $x$ given random variable $y$
$\bar{x}$	Mean of random variable $x$ .
$f_X(x), f(x)$	Pdf of the random variable $x$
$\Gamma(a)$	Gamma function
$^\circ$	Degrees
$\mathcal{S}^{-1}[ \ ]$	Inverse Fourier transform

## *Variables*

$A_{cell}$	Cell area
$BC_{nk}$	Status of $k^{\text{th}}$ mobile in a cell with the of radius $nR$
$C$	Number of channels allocated to a cell
$C_h$	Number of reserved channels
$Cor(\Delta d)$	Spatial correlation between two signal samples separated by a distance $\Delta d$
$D$	Distance between two Base stations
$D_R$	Minimum distance to prevent co-channel interference
$H$	Number of handovers per call
$K$	Normalization constant
$K_{Rv}$	Normalized cell size with respect to the speed
$K_\alpha, K_v$	Proportionality factor
$L$	Drop in signal level at the street corner in $dB$ .
$L_p$	Median path loss in decibels
$L(x)$	Path loss for LOS
$L(y)$	Path loss for NLOS
$M$	Mobile population in a cell



$N$	Number of cells
$P_B$	Overall blocking probability per cell
$P_{Bl}$	Fixed network blocking probability
$P_{Bn}$	New call blocking probability
$P_{Bs}$	Setup channel blocking probability
$P_D$	Dropout probability
$P_{Fh}$	Handover attempt failure probability
$P_{Hd}$	Probability of a handover call being delayed
$P_U$	Unnecessary handover probability
$P_u$	Unsuccessful call probability
$P(B \alpha=0)$	Boundary crossing probability in the reference cell
$P(B \alpha=\varphi)$	Boundary crossing probability in a cell with a drift in the range $(-\varphi, +\varphi)$
$P(0)$	Normalizing factor
$P(i)$	Probability of being in state $i$
$P_h$	Probability that a non-failed handover call requires another handover
$P_n$	Probability that a non-blocked new call requires at least one handover
$P_{Tx}$	Transmitter signal power in $dB$
$P_{rx}$	Received signal power in $dB$
$R$	Radius of the equivalent circle for a hexagonal cell
$R\#n$	Region No. $n$
$R_{hex}$	Cell radius for a hexagonal cell shape
$R_v$	Radius of a cell in which mobiles move with zero drift (similar to the reference cell) and a truncated Gaussian speed pdf with an average value of $v \neq \mu_v$ and standard deviation of $\sigma_v = (v-5)/3 [Km/h]$
$R_\alpha$	Radius of a cell in which mobiles move with a drift pdf in the range $(-\varphi^\circ, +\varphi^\circ)$ and speed pdf similar to that of the reference cell.
$S$	Normal variable denoting local mean signal level in $dB$ .
$S_s(f)$	Power spectrum of the shadow fading
$S(n)$	$n^{\text{th}}$ sample of the slow fading signal level
$SEER_i$	Symbol error rate for the base station $i$
$T$	Received signal averaging time
$T_H$	Channel holding time of the handover call.
$T_N$	Channel holding time of the new call
$T_c$	Call holding time
$T_{ch}$	Channel holding time in a cell
$T_h$	Handover call cell residence time
$T_n$	New call cell residence time
$V_0, v_0$	Mobile initial speed
$V, V_c, v_c, v$	Mobile current speed
$V_p, v_p$	Mobile previous speed
$V_m$	Maximum mobile speed $Km/h$
$V_{max}$	Maximum mobile initial speed $Km/h$
$V_{min}$	Minimum mobile initial speed $Km/h$
$a, b, c$	Location, scale and shape parameters of the generalized gamma

	distribution
$d$	Distance traversed by the mobile
$f_m$	Maximum shadow fading rate
$f_T(t; a, b, c)$	Generalized gamma pdf
$f_h^*(\mu_c)$	Laplace transform of the handover call cell residence time
$f_n^*(\mu_c)$	Laplace transform of the new call cell residence time
$h$	Hysteresis level
$h_b$	Base station effective antenna height
$n$	Maximum number of calls in a cell
$n_1$	Number of calls in cell 1
$n_2$	Number of calls in cell 2
$p(n_1, n_2)$	Steady state probability of having $n_1$ calls in cell 1 and $n_2$ calls in cell 2
$p_0$	Normalization constant
$p_{rx}$	Received signal strength power at a distance of $x$
$p_t$	Transmitter output power
$q$	Form factor
$r$	Random received signal level
$\hat{r}$	Sample mean of the received signal level
$\hat{r}_{\#0}$	Estimated received signal level from the communicating base station, $BS_0$
$\hat{r}_{\#1}$	Estimated received signal level from the neighbouring base station $BS_1$
$r(t)$	Received signal level in time domain
$r(x)$	Received signal level in the space domain
$r_o(t)$	Multipath fading component
$r_o(x)$	Multipath fading component in the space domain
$r_o$	Random multipath fading component
$r_i$	Sampled signal level at time $i\Delta T$
$s_o(t)$	Local mean signal level (shadow fading component)
$s_o(x)$	Local mean signal level (shadow fading component) in the space domain
$s_o$	Random shadow fading component
$s$	Normal variable denoting local mean signal level in $db$
$t_0$	Maximum channel holding time
$(x, y)$	Location of a mobile in a cell with respect to its own coordinate system
$(x', y')$	Corresponding location of a mobile in the replaced cell coordinate system
$(x'_1, y'_1)$	Location of a mobile in a cell with respect to the neighbour cell coordinate system
$x_a$	Fictitious transmitter point from the base station
$x_L$	Breakpoint distance
$\Delta L$	Difference between the two received signal levels
$\Delta R_\alpha$	Excess cell radius for a cell with the radius of $R_\alpha$
$\Delta R_v$	Excess cell radius for a cell with the radius of $R_v$
$\Delta d$	Distance between two signal samples
$\Delta T$	Period between sampling times
$\Delta \tau$	Time interval between two successive locations of a mobile
$(P_\tau, \Theta_\tau)$	Location of a collection of mobiles in different cells in polar coordinates

	at instant of $\tau$ .
$\alpha$	Magnitude of the change in direction of the mobile with respect to the current direction in the range $(-\varphi^\circ, +\varphi^\circ)$
$\alpha_0$	Initial direction angle of the mobile, also the start angle of the mobile's new direction in the substitute cell.
$\alpha_\tau$	Amount of change in direction at instant of $\tau$ with respect to the previous direction.
$\beta_\tau$	Magnitude of the angle between line joining the mobile's current position to the reference point (base station), and its previous direction at the instant of $\tau$ .
$\gamma$	Propagation slope factor
$\gamma_\tau$	Supplementary angle between the mobile's current direction and the line connecting the mobile's previous position to the base station.
$\delta$	Maximum divergence between two observed and hypothesized distributions.
$\delta_H$	Hysteresis delay in macrocells
$\delta_{HM}$	Handover delay in macrocells
$\delta_h$	Hysteresis delay in microcell
$\delta_{h\mu}$	Handover delay in microcells
$\delta P_{\alpha(B)}$	Relative boundary crossing probability between drift of $0^\circ$ and drift in the range $(-\varphi^\circ, +\varphi^\circ)$
$\varepsilon_k$	Reserved channel efficiency
$\zeta$	Fraction of the average non-blocked new calls out of average total number of calls in a cell
$\eta_\tau$	Angle between two successive locations of a mobile
$\theta_1$	Location angle of the mobile with respect to the original cell
$\theta_2$	Location angle of the mobile with respect to the substitute cell
$\theta_\tau$	Location of the mobile at time $\tau$ in polar coordinates (angle)
$\lambda$	Wavelength
$\lambda_h$	Handover call arrival rate per cell
$\lambda_n$	New call arrival rate per cell
$\lambda_t$	Total call arrival rate per cell
$\mu$	Logarithmic average of the received signal local mean power [dBm].
$\mu_0, \mu_1$	Average received signal levels from the communicating and the neighbouring base stations
$\mu_0(d), \mu_0'(d)$	Average received signal levels from the communicating and the neighbouring base stations at a point $d$ from $BS0$
$\mu_c$	Call completion rate.
$\mu_{ch}$	Total channel service rate
$\mu_e$	Effective call completion rate
$\mu_h$	Handover rate
$\mu_v$	Average initial speed of mobile [Km/h] in reference cell
$\mu'_v$	Average initial speed of mobile [Km/h]
$\xi$	Offset value from the Rayleigh distribution (amplitude of direct wave)

---

$\pi$	Number 3.14
$\rho$	Autocorrelation factor
$\rho_{d_0}$	Spatial correlation factor at a distance $d_0$
$\rho_c$	Total effective traffic intensity per cell
$\rho_h$	Offered traffic per cell by handover calls
$\rho_o$	Offered traffic intensity
$\rho_\tau$	Location of the mobile at time $\tau$ in polar coordinates (magnitude)
$\rho_0, \theta_0$	Initial location of a mobile in polar coordinates
$(\rho_{nk}, \theta_{nk})$	Location of $k^{\text{th}}$ mobile in a cell of radius $nR$ at time $\tau$ in polar coordinates
$(\rho_\tau, \theta_\tau)$	Location of a mobile at time $\tau$ in polar coordinates
$\sigma$	Standard deviation of the received signal in $dB$
$\sigma_s$	Standard deviation of the shadow fading in $dB$
$\sigma_v$	Standard deviation of the initial speed of mobile [ $Km/h$ ]
$\tau$	Time after initiation of a call
$\varphi$	Range of change in direction of mobile.
$\varphi(t)$	Phase angle of the received signal
$\mathcal{N}(0, 1)$	Normal variable with mean of 0 and standard deviation of 1
$\mathfrak{R}_\alpha$	Equivalent reference cell radius for a cell supporting freedom on mobile's drift with a uniform pdf in the range $(-\varphi^\circ, +\varphi^\circ)$ and speed pdf similar to that of the reference cell.
$\mathfrak{R}_{\alpha v}$	Equivalent reference cell radius for a cell supporting freedom on mobile's drift with a uniform pdf in the range $(-\varphi^\circ, +\varphi^\circ)$ and speed with a truncated Gaussian speed pdf having an average and standard deviation different from reference cell.
$\mathfrak{R}_v$	Equivalent reference cell radius for a cell supporting freedom on mobile's speed with a truncated Gaussian pdf having an average and standard deviation different from reference cell. Mobiles are allowed only to move on straight path without any drift.

# *Chapter 1*

## *Introduction*

The worldwide communication network is probably the greatest achievement of the mankind. Many aspects of our lives today are dependent on this network so that even a modest failure of it would impact on our lives by way of a major disruption of our day to day activity in this modern society. The conventional telephone network, better known as the Public Switched Telephone Network (PSTN), that provides national and international coverage through its fixed structure has been in existence for a considerable time. However, the emerging trends indicate that the evolution of communication from place based system to a person based system has already begun and its universal spread is imminent. Having access to information and being able to communicate easily and securely, in any medium or a combination of media (voice, data, image, video, or multimedia) in a cost effective manner is something that has taken for granted by the modern society. Further, the importance of such systems is

highlighted by the fact that the mobile communication facility advocates the notion that communication should be possible at any time from any where to any one. It is believed that in next decade the portable phone will replace the 'telephone in the house' of today. The cellular mobile radio systems have been recognised as the most promising stepping stone to this future goal. It is anticipated that the expansion of cellular communication networks will be a major activity throughout the world in this decade.

## 1.1 Historical Overview

In the early mobile systems a user was free to move only within the coverage area of a single base station. In these systems, known as Private Mobile Radio (PMR), each user was allocated a particular frequency band (channel). However, to really allow the users to be mobile, the service area has to cover a wide region. This would involve a large number of users and the required number of channels could not be found within the available spectrum. Therefore, the *cellular* concept of using the same frequency at different places was introduced by MacDonald [1] in 1979. The cellular concept allows an infinitely large area to be served by a limited frequency band. In a cellular system the entire area in which the network operates is divided into cells, and the available spectrum is shared among a cluster of cells. The clusters are repeated to cover the entire area. Associated with each cell is a base station which handles all the calls made by the mobiles in the cell area using a set of channels assigned to the cell.

The first cellular system, AMPS [2, 3], was developed during the 1970s by Bell

Laboratories. This first generation analog cellular system has been available since 1983. It used FDMA technology to achieve radio communications. With FDMA, voice channels are carried by different radio frequencies. A total of 50 MHz in the band 824-849 MHz and 869-894 MHz is allocated for AMPS. This spectrum is divided into 832 frequency channels or 416 downlinks and 416 uplinks. TACS, NMT and JMPS are among other first generation cellular system. Although cell division techniques are frequently employed by the first generation, reduction of cell sizes to below a few hundred meters would eventually render cell division no longer feasible. Moreover, analog modulation is sensitive to interference from other users in the system, and the voice quality is quite vulnerable to various kinds of noise. As a consequence of these, other means of capacity improvement such as efficient modulation schemes were sought for the second generation.

In the second generation cellular systems, digital technology enables the use of signal processing techniques to increase the robustness against interference. It also reduces the spectral bandwidth required for each user and hence provides higher capacity. The second generation provides about 3 to 4 times the capacity of the first generation without adding new base stations. Since digital systems are more immune to noise, a SIR ratio of 7 dB could be tolerated for a digital system whereas 15 dB is required for the analog systems under same circumstances [4]. This allows for smaller reuse clusters, thereby increasing the capacity of the system. The control signalling in the second generation cellular system can easily be hidden from the users, whereas in the first generation it appears as annoying noise bursts to the users. Unlike the first generation where handover decisions are completely managed by the network and terminals are passive in the handover process, in the second generation the terminals

are active in the handover process by supplying measurement values to the network. In the second generation, three major cellular systems (namely GSM [5], ADC [6], JDC [7]) have been launched that employ a circuit switching hybrid FDMA/TDMA scheme on the radio channel, and there is another standard under evaluation that uses CDMA technology [8, 9, 10].

GSM is widely used in Europe, Australia and Asia. In GSM every frequency carrier is divided into fixed time slots that supports up to eight voice channels. The speech coding rate is 13 Kb/s in GSM. With TDMA, the radio hardware in the base station can be shared among multiple users. In North America, however, the main design objective has been to make a smooth transition from the low capacity analog systems to high capacity digital systems. This is possible since digital technology enables allocation of three TDMA channels on the same radio frequency as one FDMA channel in the AMPS system. Such a mixed system, known as ADC (DAMPS or IS-54 standard) enhances the capacity of the system three times just by exchanging the analog FDMA transceivers to digital TDMA transceivers. The speech coding rate is 7.95 kb/s in ADC. The Japanese have designed a digital system, known as JDC where the transmission part resembles the American IS-54 standard and the protocols for communication resembles the GSM standard. JDC and ADC systems have high modulation efficiency due to the use of QPSK modulation and low bit rate codecs. Therefore both systems have more system capacity than GSM.

Recently a new standard employing CDMA technology, IS-95, has been developed in North America which claims to have many advantages over TDMA technology, including improvement to capacity up to 10 to 12 times over the analog systems.



However, these claims have not yet been fully accepted by the advocates of TDMA and the issue is still of considerable controversy. At the moment the CDMA standard is undergoing field tests.

Another system, similar to the cellular system, which has the same basic purpose of providing its users access to the PSTN without any constraint of a wire connection, is the cordless telephone system. In a cordless telephone system each user has his/her own base station attached to his/her subscriber line. In general, the digital cordless systems are optimized for low-complexity equipment and high-quality speech in a quasi-static environment (with respect to user mobility). Conversely, the digital cellular air interfaces are geared toward maximizing bandwidth efficiency and frequency reuse. This is achieved at the price of increased complexity in the terminal and base station. While a cordless phone and its base station comprise an autonomous communication system, cellular phones rely on complicated coordination under the control of a central processor. In a similar manner to the cellular systems, the cordless telephone system has undergone a change from an analog stage (first generation) to a digital revolutionary phase (second generation). The third generation mobile systems will be an integrated service facility which will combine the cellular and cordless services.

The most serious drawback of the first generation cordless telephone is the operating range which is limited to tens of meters from a single base station. Another big problem is the vulnerability to interference from other cordless telephones. Most of the first generation cordless telephones have access to only one channel and the user can do nothing to avoid interference from someone nearby using the same channel.

Of the cordless phones that have access to several channels, almost all rely on manual channel selection to avoid interference. The second generation cordless phone is able to communicate with many base stations and it automatically selects the best available radio channel. Examples of this system are CT2 [11], DECT [12], PHS [13, 14], WACS [15, 16] and PACS [17].

## **1.2 Ongoing Work and the Future**

The current demand for mobile communication facilities and the dramatic increase in its growth rate reveal that even the second generation systems cannot be expected to fulfil all demands. Moreover, with emerging multimedia applications it is believed that an entirely new generation cellular system is required to handle the new applications. Continuous improvements in microelectronic technology and radio link techniques coupled with advances in network signalling and control capabilities will support increasingly sophisticated features and services. Part of the challenge in planning future wireless systems is to determine the services that they would be required to support. It is not unrealistic to envision in very near future subscribers with small pocket-size flip-top terminals with keyboard and display being capable of originating or receiving calls of voice, video and data including fax and electronic mail. The ability to integrate these services and convert between media will give the subscriber not only the ability to select the most convenient terminal, but also the most convenient medium.

During the development phase of the GSM system another research initiative was launched by the European Community to develop an advanced communication

network for Europe which is intended to incorporate the same service on fixed as well as on mobile radio networks. The idea is to establish a Personal Communication System [18, 19] (PCS<sup>1</sup>) that allows mobility of both users and services. The main feature of PCS is the concept of personal mobility. Whether a subscriber is in the house, in the car or in the office, they should be able to use the same terminal, at any time with any of the allowed access methods using their personal identification number. In addition, the advanced service features and variety of data transmission types will have to be supported by such systems. It is anticipated that PCS will need an enormous capacity, which must be met with new technology. The mixture of applications implies that new access methods must be negotiated in order to host different data types, such as speech and video. Also the cell sizes have to become smaller to allow higher capacity in city environments. Since the users of cellular phones are getting used to pocket sized telephones, one cannot expect that the phones of PCS to be any larger. Therefore, the batteries have to be efficient enough to allow the use of high power transmissions in rural areas.

There are some situations in which providing radio coverage with terrestrial based cellular networks is either not economically viable (such as remote, sparsely-populated areas), or physically impractical (such as over large bodies of water). In these cases, satellite based cellular systems can be the best solution [20]. By the use of many LEO satellites a complete coverage of the world is possible with low power telephones. Motorola's Iridium project [21] is an example of such a system. It seems that PCS will consist of a mixture of technologies, and the mobile

---

1. PCS is termed by International Telecommunication Union (ITU) as Universal Personal Telecommunication (UPT).

terminal must be able to switch between systems so that a system that fits the user's occasion best is used. In this case, another kind of handover, to be referred as *intersystem handover*, will be essential.

It is conceivable that the current pan European digital mobile telephone network will not satisfy the telecommunication needs of a future society in terms of user capacity and service provisions. To satisfy the needs of future customers of mobile telecommunication services the Commission of the European Community (CEC) has launched an ambitious research initiative under the Research on Advanced Communications for Europe (RACE) program. The program's purpose is to study and develop the enabling techniques for creating a third generation mobile communication system by the turn of the century and to integrate similar services as provided in fixed networks such as ISDN and B-ISDN. Therefore, it is necessary to study the technological aspects of mobile telecommunications to see how they can influence its user capacity and services.

It is anticipated that the third generation wireless systems (e.g. FPLMTS, UMTS [22, 23]) will be operational by the year 2000. These would aim to consolidate on the developments and services (voice, video, data, etc.) offered by fixed (PSTN, ISDN), cordless, paging and cellular mobile (terrestrial and satellite) networks, to form a common integrated network. The transmission plan for this new global system needs to be flexible enough to support both personal and terminal<sup>1</sup> mobilities. The emergence of the third generation wireless system is set to make a lasting impact on

---

1. Terminal mobility is accommodated using a portable terminal through a wireless access to a fixed base station. Personal mobility can be accommodated either through a wired access or through wireless access using a portable identity card [24].

the telecommunication field. However achieving its goals will be a long-drawn-out task with many stumbling blocks to overcome. The most important issue here is related to the large amount of signalling information which the network has to handle in paging, channel assignment, handover, user location updating, registration, security clearance, and the like. Fig. 1.1 illustrates some perspectives of this network development and its integration trend.

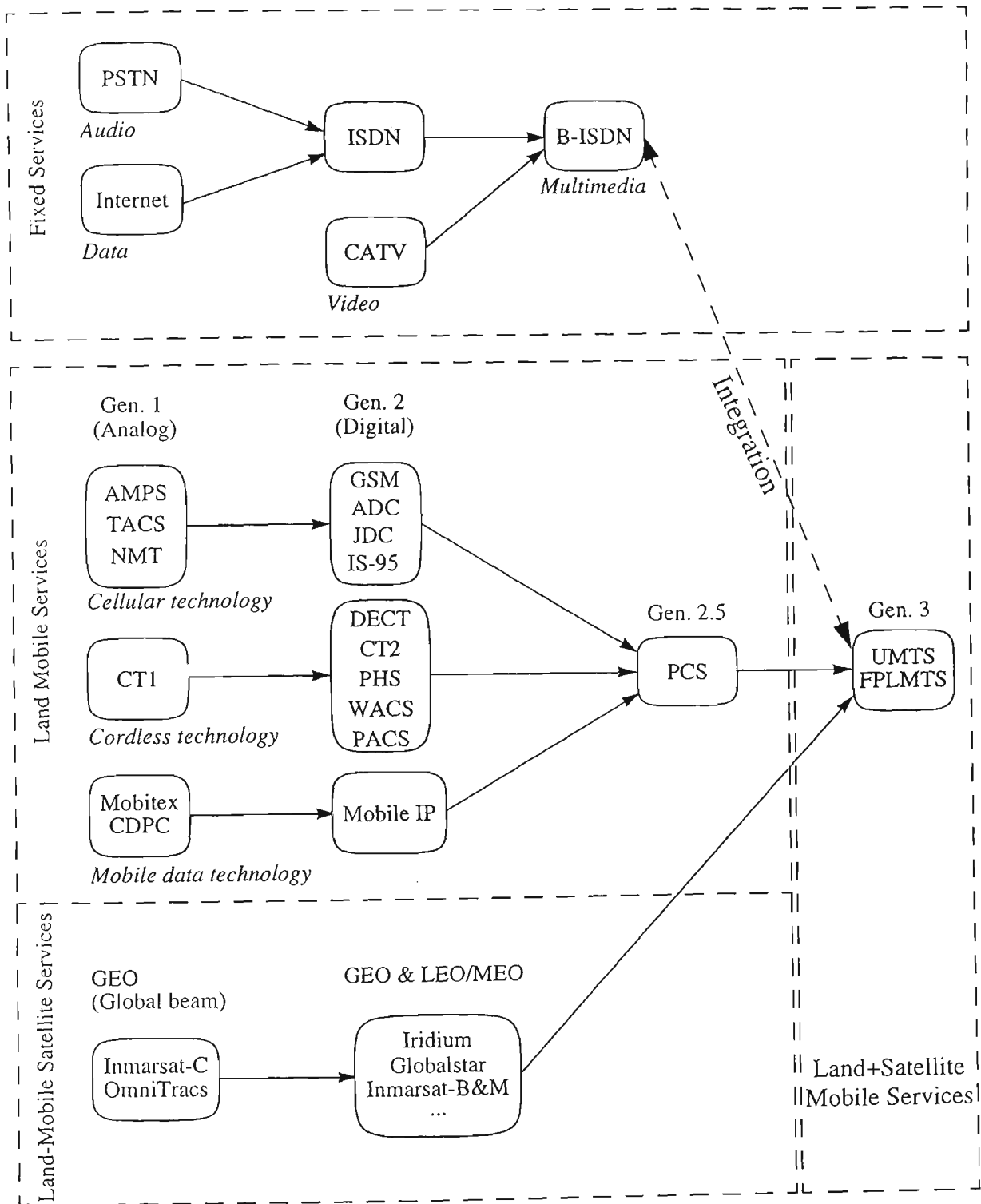


Fig. 1.1. Network development and integration.

## **1.3 Scope of Thesis**

This thesis is focused mainly on three important issues concerning the handover process in cellular mobile systems. These include the following:

- Effect of mobility on handover,
- Effect of handover on teletraffic performance criteria,
- Effect of propagation environment on handover decision making.

### **1.3.1 Effect of mobility on handover**

In Chapter 3 a mathematical formulation is developed for systematic tracking of the random movement of a mobile station in a cellular environment. It incorporates mobility parameters under most generalized conditions, so that the model could be tailored to be applicable in most cellular environments. Using the developed mobility model, the characterisation of different mobility-related parameters in cellular systems is studied in Chapter 4. These include the distribution of the cell residence time of both new and handover calls, channel holding time and the average number of handovers per call. It is shown that the cell residence time can be described by the generalized gamma distribution while the channel holding time can be best approximated by negative exponential distribution [25- 36].

### **1.3.2 Effect of handover on teletraffic performance criteria**

Based on the results obtained for cell residence time distribution, a teletraffic model that takes user mobility into account is formulated in Chapter 5. This is supported by a computer simulation using the next-event time-advance approach also described in Chapter 5. Furthermore, the influence of cell size on new and handover call blocking probabilities is examined. The effect of the handover channel reservation on call dropout probability is investigated to determine the optimum number of reserved channels required for handover [37- 39].

### **1.3.3 Effect of propagation environment on handover decision making**

A mobile radio channel is usually characterized by superposition of three independent components which reflect small-, medium-, and large-scale propagation effects. In Chapter 6, contributions of each of these components are considered. Emphasis is made on the effect of shadow fading (the medium-scale propagation component), which is important in handover decision making in cellular networks.

In Chapter 7, improvement to handover performance is investigated in terms of reductions in unnecessary handovers and handover delay time. An analytical method is described to determine the optimum hysteresis level and signal averaging time for both micro- and macro-cells. Results demonstrate the possible compromise between handover parameters, i.e. signal averaging time and hysteresis level, under the influence of shadow fading. These results could be used in setting the parameters of the handover algorithm to minimise delay in handover decision making while minimising unnecessary handovers [40- 46].



# *Chapter 2*

## *Trends in Handover Processes*

A cellular network can be viewed as an interface between mobile units and a telecommunication infrastructure (e.g., PSTN). A mobile station (MS) is a low-power communication device that has a limited radio coverage area with radius ranging from a few kilometres (macrocells) to several hundreds of meters (microcells). In a cellular environment, a large geographical area is divided into small areas each covered by a cell-site or base station (BS). When an MS places a call, a dedicated circuit has to be established between the MS and the called party. The first link of the circuit is a wireless link between the MS and the closest BS. The second link is established between the BS and mobile switching centre (MSC), which can be through a wireless or a wired media. A typical cellular system is illustrated in Fig. 2.1 [47].

An important feature of the cellular mobile communication systems is the initiation and maintenance of a reliable and good quality radio link to support a voice or data transaction, despite the movement or physical positioning of the subscriber. Therefore, the network should be equipped to recognize any cell boundary crossings and to hand the mobile unit from its original base station to the most appropriate neighbour. This function called *handover*, or handoff<sup>1</sup> as is used in some literature interchangeably, automatically connects the mobile to the base station that provides the best signal quality. The handover can be considered as an adaptive method for keeping cell areas as compact as possible and consequently leading to a decrease of cell-to-cell interference. The concept of handover constitutes one of the most complex functions within a cellular radio system. It ensures continuity of calls while the users are on the move and cross the boundaries of areas covered by different base stations. When the signal quality drops at the mobile station, two different types of

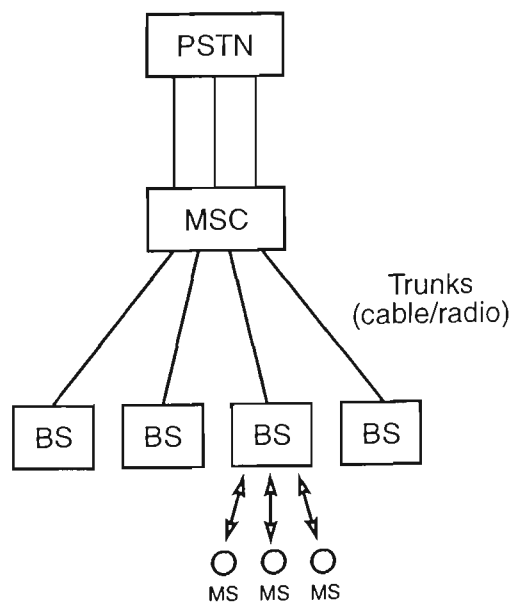


**Fig. 2.1.** A typical components of a cellular system.

1. Handover is called ALT (Automatic Link Transfer) in Personal Communication Systems (PCS)

handover, namely inter-cell or intra-cell, could take place. In cases when there is a strong interferer on a channel, it may be sufficient to switch to another channel, but remain connected to the same base station. This type of handover is called an intra-cell handover. The primary purpose of an inter-cell handover is to switch a call in progress from the serving base station to a neighbouring base station whenever the existing radio link suffers from degradation.

This Chapter explains briefly issues affecting the handover process, or being effected by the handover process, explicitly or implicitly. The aim is not to describe each phenomenon in detail but to present the issues so that the flavour of current trends could be observed.

## 2.1 Cell Structures

The dramatic increase in demand for mobile communication systems has motivated many researchers to place a greater emphasis on maximising the system capacity. Conventionally the capacity of a network could be enhanced by deployment of different methods such as efficient modulation schemes, improved speech coding techniques, appropriate channel coding, frequency spectrum allocation. Nevertheless, there is an exclusive elaborate approach for increasing capacity in the Cellular mobile communications systems, and that is by reducing the cell size. Theoretically, a reduction of cell radius by  $n$  times could enhance mobile system capacity by  $n^2$  times. Application of different cell sizes such as: picocells, microcells, macrocells, mixed cells, overlapped cells, highway microcells appears to be suitable solution to the complicated problem of different traffic demands in various areas.

Implementation of cells of smaller size is seen as the obvious way to increase system capacity which would effectively cater for higher demands. Smaller cells, however, come with their own drawbacks in cellular system design. Apart from the network complexity, the main difficulty is the increased proportion of handovers that occurs during one particular call.

Labeledz [48] has shown that the number of cell boundary crossings per call is inversely proportional to the cell radius. In addition, Nanda [49] has found that while the handover rate only increases with the square root of call density in macrocells, it increases linearly with the call density in microcells. Since the mobile has a certain probability of encountering a dropped call at every boundary crossing, handover algorithms must become more robust as the cell size decreases.

Due to the small cell dimensions in microcellular systems, a rapidly moving mobile will cause a high work load for the handover management system since the mobile will cross cell borders at a high rate. The rapidly changing signal quality, and frequent requirement for handovers during a call, leads to the risk of a dropped call in fast mobiles. It has therefore been suggested that some channels are assigned to base stations with antennas placed high above the ground level and relatively free from obstructions. Thus, the coverage areas of these overlaid cells will be large and therefore the handover rate will be much lower than for microcells, and the call reliability will improve. For this scheme to be useful, the system must provide some means to measure the mobile's velocity so that the fast mobiles could be assigned to umbrella cells. One raw method could be to monitor the frequency of handovers, and if the terminal has made a large number of handovers within a short period of time, it

is probably moving fast and should be connected to an umbrella cell. A moving terminal also generates a Doppler spread [4] of the received signal, and a large Doppler spread indicates that the terminal should be handed over from the microcellular system. The deployment of a multi-tier system with macrocells overlaying microcells offers system providers new opportunities. Clever use of the two tiers can lead to increased end-user performance and system capacity. For example, stationary users can be assigned to microcells so that they operate at reduced power and cause significantly less interference; when the microcellular capacity is exhausted, the overflow traffic can be assigned to the macrocells. As another example, a business area with building and parking facilities may employ microcell base stations to cover the outdoor areas together with picocells to provide radio coverage to indoor areas and offices. Behaviour of the handover in all these circumstances raises issues that need to be discussed.

## 2.2 Handover Performance Measures

Many criteria for determining the efficiency of a handover algorithm are discussed in the literature [50, 51, 52, 53] and may be used in optimal design. To completely evaluate the performance of a handover scheme one should build a full system and collect data for evaluation. This, of course, is not practicable. The second best method would be to build a complete simulation model of the system and emulate the actions of users and handover algorithms. This would lead to extremely complex simulation models which again would not be practicable. Simpler scenarios must therefore be used focusing attention on particular problems. Solving these individual problems, one could obtain information necessary to assess the system performance

for handover schemes. In this section, different aspects of handover performance evaluation will be described.

### **2.2.1 Performance evaluation by means of traffic analysis**

To evaluate the effect of handover on the capacity of a cellular system, it is possible to use traffic performance evaluations. By assuming that originating calls and handovers to a cell can be modelled as Markovian “birth-death” processes, and that the unencumbered call duration and channel holding time can be modelled as negative exponentially distributed random variables, it is possible to obtain analytical results for a number of performance measures. The unencumbered call duration and channel holding time are the time for an uninterrupted call to be completed, and the time a user is active on a channel in a cell before the channel is released (by call completion or handover), respectively. In Chapter 5, different teletraffic performance parameters are defined. These parameters can be obtained for a number of resource assignment schemes and platform types.

### **2.2.2 Performance evaluation by means of handover administration**

The methods treated by traffic performance ignores the dynamic performance. Hence, other methods are needed to evaluate the administration load imposed by the resource allocation schemes. It is therefore common to identify some scenario that provides desired information. To establish the trade-off between the signal quality and the handover management load a commonly used method is to let a terminal move between two base stations while the signal quality and the handover activity is

monitored. This method has been used for simulations in [54, 55, 56] and for analytic evaluations in [57]. Among the quantities that are monitored during one trip are: the mean number of handovers, probability of unnecessary handovers, duration of interruption, number of unnecessary handovers, delay in making a handover and the distance at which handover occurs.

### 2.3 Handover Algorithms

Handover algorithms are decision systems in which decisions are triggered by channel degradation or network criteria. Channel degradation criterion can be realized by different measurements such as the received signal strength [54, 58, 59, 60, 61, 62], received signal to interference ratio (SIR) [63], bit error rate (BER) [64, 65], and estimated distance from base stations [60, 66]. In the network criterion, the handover decisions are made by reasons other than degradation of the current channel such as teletraffic load and the decisions are taken by the network management centre of the cellular system. In [67], the handover problem in a stochastic control frame is introduced and a Markov decision process formulation is used to derive optimal handover.

Handover algorithms should be robust to variations in propagation, mobile station velocity, and co-channel interference. Ideally they should perform only one handover per cell boundary crossing, and this handover should occur quickly and as close to the boundary as possible. A literature review of the existing and proposed algorithms is summarized in the following sub-section.

### 2.3.1 Signal strength based handover algorithm

The signal strength based handover algorithm compares signal strength averages measured over a time interval, and executes a handover if the average signal strength of an alternative base station is larger than that of the serving base station. This method is shown to stimulate too many unnecessary handovers when the current base station signal is still adequate [57, 59, 61, 62]. This problem can be alleviated by introducing a hysteresis margin. This allows a user to hand over only if the new base station is sufficiently stronger (by a hysteresis margin) than the current one. This technique prevents the so-called *ping-pong* effect. The ping-pong effect is the repeated handovers between two base stations caused by rapid fluctuations in the received signal strengths from both base stations. This matter is addressed in Chapter 7.

Loew [68] describes a relative signal strength based handover algorithm which uses the signal strength difference coupled with an absolute level requirement. In this manner, the signal strength difference is only compared if the average signal strength is below an absolute threshold level. Zhang et al. [69] provide an analytical method to evaluate the performance of this algorithm. Muñoz-Rodríguez et al. [70] provide a neural circuit to perform this algorithm.

In general, the handover initiation criteria analysed in the literature are based on essentially four variables: the length and shape of the averaging window, the threshold level, and the hysteresis margin.



Prediction techniques base the handover decision on the expected future value of the received signal strength. A technique based on this has been proposed and shown (through simulation) to be better, in terms of reduction in the number of unnecessary handovers, than both the relative signal strength and relative signal strength with hysteresis and threshold methods [71].

### **2.3.2 Co-channel interference based handover algorithm**

Although signal strength based algorithms are useful, they do not take into account of the co-channel interference. In [63] a handover algorithm is developed under the assumption that the mobile station or the base station has access to real time SIR measurements. Nevertheless, obtaining these measurements is difficult in practice [72, 73], and only few papers [73, 74, 75] have investigated methods to actually monitor the co-channel interference. Kozono [74] suggests a method for measuring co-channel interference in the first generation cellular systems, AMPS, by separating two terms at different frequencies which are both known functions of the signal and interference. An interference measurement circuit is used to perform this separation and estimate the co-channel interference. Yoshida [73] suggests a method for in-service monitoring of multipath delay spread and co-channel interference for a QPSK signal. He reports that the co-channel interference can be monitored for multipath fading channels provided the delay spread is negligible.

### **2.3.3 BER and pseudo BER based handover algorithm**

Bit error rate based methods are desirable since they give a good indicator of speech

quality. Steele [65] investigated estimating the BER by counting the number of errors from the error locator polynomial assuming Reed Solomon encoding. Using the derived symbol error rate  $SER_i$  for the base station  $i$ , the suggested handover algorithm computes whether  $SER_0/SER_i$  is less than some threshold. A variable  $P_j$  is assigned a one if it was true and a zero if it was false, where  $j$  denotes the current decision point. Afterwards, a weighted sum of the  $P_j$ 's is formed and compared to a new threshold. A handover is activated if the weighted average is greater than the threshold, and  $SER_0$  is greater than an unacceptable symbol error threshold. Steele used this algorithm in a two cell cluster, and found a slight delay in handover in the presence of co-channel interferers. Cornett et al. [64] have showed two methods to estimate the BER in a Rayleigh fading channel. The first derives the BER from an autocorrelation parameter in the receiver, given that a pseudo random noise sequence is interleaved in the data. The second shows if symbol interleaving is used in a Reed-Solomon-based system, then side information from a bounded distance decoder can be used for a raw channel BER.

Pseudo error rate methods have also been studied in [76, 77]. Kostic et al. [76] have derived a pseudo error rate method for PSK modulation. Nagura et al. [77] have investigated the use of the eye-opening as a measure of the signal quality. Here, a pseudo error is said to occur when the eye-opening height falls below a certain threshold. The channel is assumed acceptable until the pseudo error rate is above the threshold and its slope is positive.

### 2.3.4 Distance based handover algorithm

Knowing the distance between mobile station and base station, it is possible to control the movement of the mobile in the cell structure. This avoids using a channel outside the planned cell area. A variety of methods have been published that determine the mobile's position in macrocells such as angle of arrival techniques from multibeam antennas [78] and antenna arrays [79], time-of-arrival methods [80, 81], and crude signal strength methods [82]. With the current interest in intelligent vehicle highway systems (IVHS), a substantial amount of research is aimed at investigating these and other methods for vehicle location and tracking in microcells. Currently known methods are not accurate enough to base handover on position information alone [83].

### 2.3.5 Velocity adaptive handover algorithm

If handover requests from rapidly moving mobile stations are not processed quickly, excessive dropped calls may occur. Fast temporal based handover algorithms have been shown to be able to partially solve this problem [61] by using short temporal averaging windows to detect large, sudden, drops in signal strength. However, the shortness of a temporal window is a relative quantity to the mobile station velocity and, furthermore, a fixed time averaging interval makes the handover performance sensitive to velocity, with best performance being achieved only at a particular velocity. To overcome this problem, velocity adaptive handover algorithms have been proposed to provide good and consistent handover performance for mobile stations having different velocities. Different velocity estimators have been

investigated which were based on following techniques:

- *Level Crossing Rates (LCR)* with respect to the signal envelope;
- *Zero Crossing Rates (ZCR)* of the in-phase and quadrature components of the signal envelope;
- Covariance approximation method;
- Eigen-based Doppler estimation for differentially coherent CPM.

LCR is defined as the average number of times the signal envelope crosses a specified level in the positive direction. Likewise, ZCR is defined as the average number of zero crossings a signal makes per second. It is well known that the LCR or ZCR are functions of the mobile velocity [4, 84] and can be used for velocity prediction. Austin et al. [85] has derived a velocity estimator based on the LCRs of the received signal which is robust to the Rice factor.

Covariance approximation is a velocity estimator method that relies on an estimate of the autocovariance between faded samples of the signal. This method is based on estimating the maximum Doppler frequency as a means to obtain mobile velocity. The procedure which estimates the Doppler frequency from the squared deviations of the signal envelope originally is put forth by Holtzman and Sampath [86]. This model is later shown robust to Rice factors and white Gaussian noise [87].

For some modulation schemes, it may also be possible to measure the velocity from the Doppler shift in the signal. Common methods for Doppler estimation such as automatic frequency control loops are often inappropriate due to burst intervals where the acquisition time consumes a large portion of the data interval. Open loop

Doppler estimation has been considered [88] for PSK signals and extended to differentially coherent CPM by Biglieri [89]. Austin [90] considers a generalization of Biglieri's method whereby the Doppler is estimated by using a set of averages each obtained from a separate differential detection of a CPM waveform. The averages are shown to have the same form as the autocorrelations of a complex exponential at a known multiple of the Doppler frequency in noise, and therefore, eigen-based line spectral estimation methods can be used to estimate the Doppler frequency.

### 2.3.6 Direction biased handover algorithm

The majority of previous handover algorithm studies [54, 56, 57, 59, 61, 62, 70, 91, 92] have concentrated on handover decisions between two base stations only. Mende [60] simulated the case of multiple base stations, but no conclusions were made. In urban microcells, the mobile is likely to have multiple base stations that are handover candidates at any instant. For example, consider a Manhattan type street layout consisting of streets on a rectangular grid. One proposed method to cover such an area is to place base stations at every other intersection. Thus, as soon as a mobile moves into an intersection without a base station, four base stations become candidates for handovers. One method to accomplish a proper handover is encouraging handovers to base stations that the mobile is moving towards and discouraging handovers to base stations that the mobile is moving away from. Three basic approaches to accomplish the direction biasing are proposed. The first two approaches use direction adjusted hysteresis levels, while the third approach uses a fuzzy handover algorithm in which the membership functions will be direction biased.

The direction biased handover algorithms presented only need the subscribers' moving direction; precise position is not necessary. Thus, simpler estimation techniques can be used; such as monitoring the direction of the Doppler shift (positive or negative) [89, 90], monitoring the time variation of the signal strength, or even determining the direction from the location of past handovers. Unfortunately, Doppler (velocity) estimation techniques which derive estimates from the covariance or level crossing rates [85, 86, 87] are not useful because these techniques only yield the magnitude of the Doppler. A simple direction estimator is based on monitoring the time variation of the signal strength. Austin [93] has investigated multi-cell handover characteristics of classical handover algorithms by using a Manhattan microcell environment with base stations located at every other intersection.

### **2.3.7 Multi-criteria based handover algorithm**

Conceivably, a handover should be made on a variety of statistics that are related to the capacity of the system. Current systems such as GSM [66] now trigger a handover if any individual handover statistic suggests the need for a handover. New research is just beginning on how to incorporate multiple criteria such as distance, BER, co-channel interference, signal strength, and so on all into a single handover algorithm. Muñoz-Rodríguez et al. [94, 95] have suggested various fuzzy set combinations and neural network methods [70] by which various criteria can be combined into a handover algorithm. Nevertheless, no insight has been given on how to optimize or choose the various parameters for multiple criteria handover algorithms. However, a combined BER and signal strength algorithm is developed by Kumar et al. [96].

## 2.4 Handover Strategies

The mobile unit and the base station are connected via radio links which carry data as well as signalling information. In case a signal deterioration occurs, three different handover strategies have been proposed for transferring the connection to a new base station [54]. Depending on the handover decision process being applied as a centralized, half centralized or decentralized phenomena, three different types of handover strategies can be defined respectively as:

- Network Controlled Handover (NCHO)
- Mobile Assisted Handover (MAHO)
- Mobile Controlled Handover (MCHO)

Since the number of handovers increases with decreasing cell size, it will be an almost impossible task to make a handover decision for every mobile by one central switch (centralized). Moreover, in microcells the connection between MS and BS can deteriorate very quickly. A typical situation is when the mobile turns round a street corner (street corner effect). Fast handover decisions required in such situations can be achieved more readily by decentralizing the handover decision process.

### 2.4.1 Network Controlled Handover (NCHO)

This method is widely used in first generation cellular systems, where the MSC is solely in charge of the handover process and the mobile stations are completely passive. The base stations monitor the quality of the current connection by measuring

the received signal strength (RSS) of connected stations. Also the signal to interference ratio (SIR) is measured by means of a supervisory audio tone (SAT). This is accomplished by the base station transmitting a tone with a frequency outside the audio range. This tone is echoed by the terminal, and from the received signal the base station can estimate the degree of interference by evaluating the quality of the received SAT. If the received signal deteriorates below some threshold, and/or the quality of the SAT is degrading, the base station sends a request for handover to the mobile switching centre (MSC). Meanwhile, the MSC orders all the surrounding base stations to tune into the channel used by the terminal to measure the received signal strength from the mobile and to respond with the result. The MSC then decides to which base station the mobile should be handed over, and assigns a new channel frequency. The new channel is instructed as to both the mobile (through the old base station) and the new base station.

Once the target base station and the mobile station are synchronized the handover is completed. After that the old channel, and the link between the MSC and the old base station are released. The signalling involved here leads to a long reaction time in handover. Further, there is always the possibility of interpreting data as signals in error leading to failed handovers. The typical handover time, i.e. the time between detection of a necessary handover and the completion of the handover, has been found to be of the order of 5-10 seconds. Therefore, this type of network controlled handovers (NCHO) is not suitable in rapidly changing radio environments. In addition, NCHO can not be used in systems with a high concentration of users, since the MSC may be overloaded with processing of handovers. One advantage with centralized handover, however, is that the information about the signal quality of all



users is located at a single point. This can be utilized for resource allocation purposes which require centralized knowledge about the system.

### 2.4.2 Mobile Assisted Handover (MAHO)

To improve on handover reaction time, and reduce handover administration load of the MSC, the handover decisions should be distributed towards the mobile stations. One way to achieve this could be to let the mobile stations make the measurements and the MSC make the decisions, as is done in the second generation cellular systems (e.g., GSM [5]). For example, the mobile station can monitor the quality of the current link and measure the signal strengths of the surrounding base stations. The measurements are forwarded to the current base station twice a second. The base station is also responsible for supervising the received signal strength (RSS) and the channel quality (BER) in the uplink. If the signal quality is degrading, or a new base station becomes much stronger, the serving base station sends a request to the MSC for a handover to the strongest base station. If channels are available at that base station, links are set up between the MSC and the target base station, and the terminal is instructed to tune in to the new channel. Hence, much of the delay due to the measurement requests between MSC and other base stations will be eliminated. In this scheme the mobile terminal assists the MSC in the handover process by supplying measurements and therefore this scheme is often called mobile assisted handover, (MAHO). The time between detection of a handover requirement until its execution is typically of the order of 1 second. This may still be too long to avoid dropping a call due to street corner effect.

### 2.4.3 Mobile Controlled Handover (MCHO)

It is also possible to go one step further and let the mobile station perform both the measurements and the handover decisions. In this method, the mobile continuously monitors the signal strength and quality from the accessed BS and several handover candidate BSs. When some handover criteria is met, the MS checks the best candidate BS for an available traffic channel and launches a handover request. This handover strategy supports both inter- and intra-cell handovers. If it is discovered after a handover that the interference in the uplink is too high, or it becomes poor during conversation, an intracell handover to a better channel can be performed.

Such a scheme has a very short handover reaction time and could be useful in microcellular systems where there is a high concentration of users and the radio environment changes rapidly. Once a handover has been decided, a request is sent from the mobile station to the target base station for a particular channel, or for any channel if no channel allocation is incorporated in the handover algorithm. If there is a channel available at the target base station, a link between the MSC and the target base station is established and the terminal and the target base station tune in to the new channel. This arrangement can improve reliability in rapidly changing environments since handovers can then be executed fast (reaction time of the order of 0.1 second). One disadvantage of MCHO is that the mobile does not have information about the signal quality of other users and the handover algorithm must be designed according to some statistical rule so that other users are not harmed by interference from this user. MCHO method is employed by both DECT and WACS air interface protocols.

In the MCHO scheme the handover request must somehow be transferred to the target base station. There are two ways how this could be done: (i) the request could be sent to the current base station and then to the target base station via the MSC, or (ii) directly from the terminal to the target base station. The first method is referred to as backward handover and the main advantage in this method is that the request is transmitted on an existing radio channel. This scheme is suitable in environments where the channel quality is likely to remain satisfactory until the handover is completed. However, if the signal quality of the existing link suddenly drops before a new link is established, there is a risk that the call may be dropped. In the other method, i.e. forward handover, the mobile terminal must first accomplish synchronization on a multi access channel with the target base station before a handover request can be transmitted. Unless the synchronization process is slow, this scheme could be useful in rapidly changing radio environments since the mobile will have contact with the target base station even if the old link deteriorates.

It should be noted that if all signalling on the air interface were error free, there would not be a major difference in performance between MAHO and MCHO. The critical difference is that in MAHO a handover request is transmitted from the base station to the mobile station. If that message is not received correctly the call may be dropped. Also if new base stations are not identified or recent measurement reports are missing, the handover request might be delayed causing a call dropout.

## 2.5 Soft handover

In conventional handover algorithms, the radio link from the old serving base station

is dropped as soon as a handover is made to the new base station. This method has difficulties in situations such as the street corner effect. To increase handover reliability it is possible to let a mobile, which is located in the transition region between cells, simultaneously be connected to two or more base stations until the mobile is safely inside the target cell. Then the connections to all base stations except the target base station are released. By doing this, the signal strength from one base station may be allowed to suddenly drop out because of fading while the path to the other base station may still be good. This make-before-break method is known as soft handover. Soft handover provides macroscopic diversity and improves handover success probability. Not only does this greatly minimize the probability of a dropped call, but it also makes the handover virtually undetectable by the user.

CDMA is particularly suited for soft handovers since multiple radio links can be obtained by simply de-spreading the pseudo random noise (PN) sequences associated with each base station. The analog system (and the digital TDMA-based system) provides a break-before-make switching function whereas the CDMA-based soft handover system provides a make-before-break switching function. The soft handover scheme changes the distribution of SIR, since mobiles which are further away from base stations can receive more signal energy. Thus, a soft handover scheme may reduce outage probability. In addition, since the mobile is connected to all neighbouring base stations while it is located in the border region between cells, the fluctuations in signal quality will not lead to flip-flopping of a call since the mobile is continuously connected to all base stations. Hence, soft handover can provide diversity against rapidly changing signal quality without a high handover management load to the system. One drawback is that a user in soft handover will

occupy links between several base stations and the mobile switching centre.

In a series of articles Bernhardt [97, 98] investigated soft handover as a means to provide macroscopic diversity in a Universal Digital Portable Communication (UDPC) system. In [99] the impact of macroscopic diversity on received signal strength was investigated for different base station configurations in an environment with lognormal fading. A diversity gain of 13 dB was experienced for a four base station configuration compared to a system with a single base station. This improvement could be used to reduce the base station density thereby to cut the cost of the system. This cost issue was elaborated in [97]. In [98], Bernhardt expanded his studies to incorporate a cellular system where each group of base stations was reused across the service area. Hence the influence of channel reuse on capacity was addressed. The results showed that when using macroscopic diversity the improved signal quality could allow the use of a shorter reuse distance which increases the capacity.

An important issue is that when soft handover is used, more transmitters will be active in the downlink, thus causing more interference. During soft handover there is no increase of interference in the uplink; diversity is obtained since several ports are used to decode the signal. The base stations receive different copies of the same transmitted signal. In the downlink the same signal is transmitted by several base stations. Therefore the interference level will increase in the downlink and the question is whether the macroscopic diversity can be used to counteract the effects of increased downlink interference level.

In the downlink the base stations can use orthogonal, or the same carrier channel when simulcasting the signal to the mobile. When the same carrier channels are used by the simulcasting base stations the terminal perceives this as multipath propagation of the signal from a single transmitter. In any case, using soft handover in the downlink requires a receiver at the terminal that is able to decode the delayed copies of the same transmitted signal.

Another aspect, that does not influence the signal quality but is essential for the willingness of the operator to implement soft handover, is the network overhead that arises from soft handover. In conventional handover schemes there is only one link between the MSC and a base station per user; with soft handover one link is needed per base station which increases the required capacity of traffic in the fixed network. It is not only the radio channels that are scarce resources, but also the wired channels in cellular systems. If soft handover is implemented in the system the number of wired channels may also have to be increased. The more base stations that are allowed to be involved in soft handover the greater the traffic will be in the fixed network. It is therefore interesting to measure the effects of increased traffic in installing a soft handover.

In [100] the tradeoff between the improved signal quality and the network overhead was addressed when soft handover was used in a cellular CDMA system. It was concluded that for an acceptable tradeoff the system could allow for three participating base stations in soft handover and the difference in received signal power of these base stations should not exceed 5 dB.

In Qualcomm's CDMA proposal [10] the users transmit wideband signals on the same carrier frequency. The users/base stations are distinguished by means of pseudo random signature sequences. In this wideband system a RAKE receiver can be utilized to measure the received power from surrounding base stations, by assigning one finger of the RAKE receiver to scan the codes of the base stations (which actually are time shifted versions of the same code). These codes are transmitted on pilot signals that use the same transmitter power. The performance of the traffic channel is strongly dependent on efficient power control. If the terminal notices that another base station becomes stronger, it will send a request to the MSC to set up a link between the MSC and that base station. Thereafter the terminal uses one finger for the signal from each base station. In the uplink the base stations forward the received signals to the MSC for diversity decoding. When one base station becomes much weaker than the other the connection to this base station is released (the finger used for this base station can then be used to handle multipath propagation).

## **2.6 Conclusions and Summary**

A background of issues on traditional topics in handover research has been presented. These included an overview of cell structures, common handover performance criteria, handover algorithms, handover strategies and soft handover.

# *Chapter 3*

## *Stochastic Mobility Modelling*

Mobility of users is a major difference between fixed and mobile telephony. It is one of the key concerns in the design and performance analysis of cellular mobile networks. The mobility model plays an important role in examining different issues involved in a cellular system such as handover, offered traffic, dimensioning of signalling network, user location updating, registration, paging, multilayer network management and the like. In the general case, the mobility modelling should include changes in both direction and speed of the mobile. Since the moving direction and the speed of a mobile are both non-deterministic variables, the path of a mobile will be a random trajectory. In order to trace this trajectory, it requires a systematic formulation of the geometrical relations governing the complex problem of random movement.



Mobility models developed in the literature [101, 102] assume constant speeds drawn from a given probability distributions. Guérin [103] has developed a mobility model where the direction of a mobile is allowed to change at certain points in time. Tekinay [104] has proposed an approach based on the two dimensional random walk where the users are uniformly distributed in the area. This characterizes the mobile movement as a modified Brownian motion. Kim et. al [105] have used random walk mobility model to study different mobile registration schemes. In [106], a mobility pattern is proposed in which movement of the mobile stations consist of moving and stopping time intervals consistent with traffic in a city centre. Thomas et. al [107] have analysed the mobility by using a fluid flow model under the assumption that users are moving randomly. Moreover, some of the works consider mobility models for specific application purposes, such as grid patterns for two dimensional space [108, 109] and highway patterns for one dimensional space [110, 111]. In [108] a mobility model in three dimensional space has been proposed. The main weakness of this model, i.e. in up-down (vertical) motions, has been addressed later [112] by applying some boundary conditions on each floor and vertical motions in staircase regions.

While all the above-mentioned literature have modelled mobility in various methods, none of those have proposed any straight forward procedure for tracing a mobile station in order to obtain different mobility-related parameters. This Chapter presents a mathematical formulation for systematic tracking of the random movement of a mobile station in a cellular environment. The proposed mobility model takes into consideration all the possible mobility related parameters including: mobile origin attributes (initial position, direction and speed), ongoing attributes (changes in



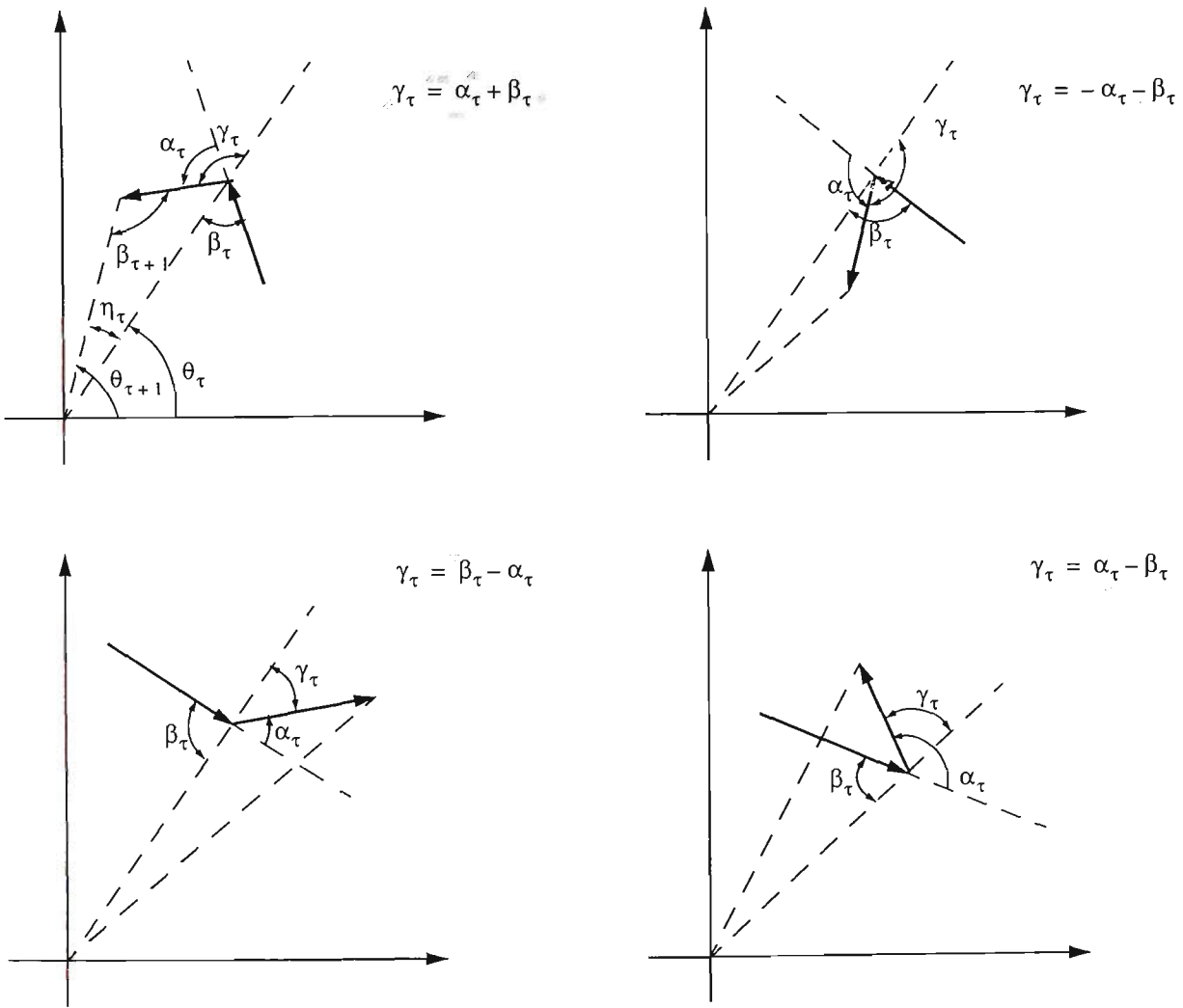


Fig. 3.2. Four different cases for a mobile path.

$$\theta_{\tau+1} = \theta_{\tau} \pm \eta_{\tau} \quad (3.2)$$

where  $\gamma_{\tau}$  is the supplementary angle between the of the mobile's current direction and the line connecting the mobile's previous position to the base station,  $\eta_{\tau}$  is the difference between angles location's of two successive locations of a mobile, and  $d$  is the distance traversed during the time interval  $\Delta\tau$  between  $\tau$  and  $\tau+1$ . If the mobile speed during  $\Delta\tau$  is assumed to be  $v$ , then,

$$d = v \cdot \Delta\tau \quad (3.3)$$

As it is shown in Fig. 3.2, depending on the direction and position of the mobile  $\gamma_{\tau}$  and  $\eta_{\tau}$  will be,

$$\begin{aligned} \gamma_{\tau} &= \pm\alpha_{\tau} \pm \beta_{\tau} \\ \eta_{\tau} &= \gamma_{\tau} - \beta_{\tau+1} \end{aligned} \quad (3.4)$$

Therefore, successive locations of the mobile can be traced by the following regressive relations,

$$\theta_{\tau+1} = \theta_{\tau} \pm \alpha_{\tau} \pm \beta_{\tau} \pm \beta_{\tau+1} \quad (3.5)$$

In the above relations,  $\alpha_{\tau}$  is the amount of change in direction at time  $\tau$  with respect to the previous direction and  $\beta_{\tau}$  is the magnitude of the angle between mobiles's previous direction and the line joining the mobile's current position to the reference point (base station). Signs + or - depend on the successive positioning of the mobile

and have to be ascertained as shown later. In order to simplify the formulation, a coordinate system is defined with its origin at the current location of the mobile. In this coordinate system, the positive  $x$ -axis coincides with the mobile's previous moving direction and the  $y$ -axis coincides with the line joining the current mobile location to the base station. The positive direction of  $y$ -axis is obtained by turning counter clockwise from the  $x$ -axis until the  $y$ -axis is met. The angle between the two axes can be any value between  $0$  and  $\pi$ , depending on the previous direction of the mobile (Fig. 3.3). Such a coordinate system is dynamic in the sense that its origin and axes orientation change according to the successive locations and directions of the mobile. Further, it can be seen that the positive  $y$ -axis can be either towards or outwards from the base station depending on the mobile movement direction.

Consider a mobile located at point  $A$  at time  $\tau$ . If the mobile approaches the point  $A$  as shown in Fig. 3.4a, then the positive  $y$ -axis is towards the base station. However, if the mobile approaches the point  $A$  as shown in Fig. 3.4b, then the positive  $y$ -axis is outwards from the base station. Notice that the line joining the mobile to the base station  $AO$  divides the cell space into two regions. If the positive  $y$ -axis at point  $A$  is towards the base station, then  $\alpha_\tau$  will relate to  $\beta_\tau$  such that the two regions can be identified as:

$$\begin{aligned} \text{Region No. 1 (R\#1)} & \quad -\beta_\tau \leq \alpha_\tau \leq \pi - \beta_\tau \\ \text{Region No. 2 (R\#2)} & \quad \alpha_\tau < -\beta_\tau \text{ or } \alpha_\tau > \pi - \beta_\tau \end{aligned} \tag{3.6}$$

Similarly, If the positive  $y$ -axis at point  $A$  is outwards from the base station, then the two regions can be identified as:

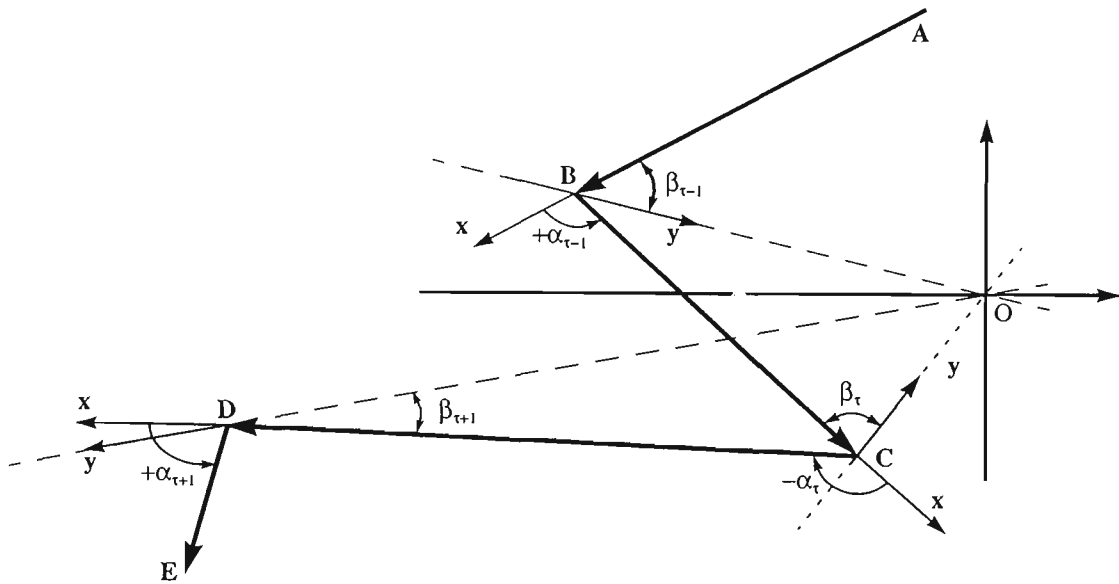


**Fig. 3.3.** An example for movement of a mobile from location A to E passing through the regions of 1 (ABC), 2 (CD), & 4 (DE).

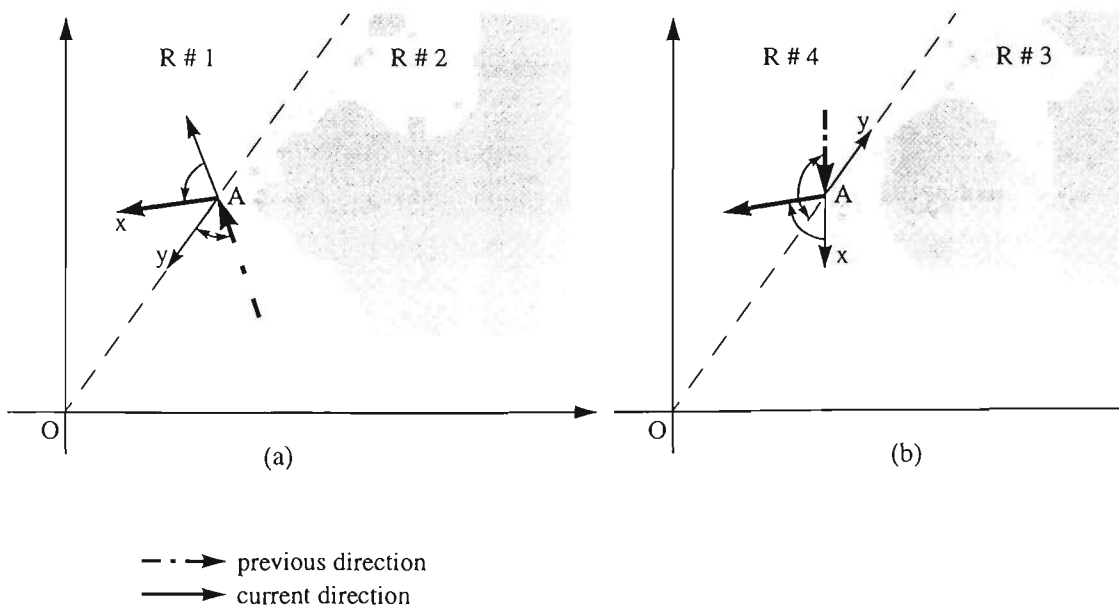


**Fig. 3.4.** Illustration of different regions.

$$\begin{array}{ll}
\text{Region No. 3 (R\#3)} & \beta_\tau \geq \alpha_\tau \geq \beta_\tau - \pi \\
\text{Region No. 4 (R\#4)} & \alpha_\tau > \beta_\tau \text{ or } \alpha_\tau < \beta_\tau - \pi
\end{array} \tag{3.7}$$

Since any value of  $\alpha_\tau$  may satisfy one of (3.6) and one of (3.7), to determine  $\alpha_\tau$  unequivocally, we proceed as follows:

Consider two successive points  $E$  and  $F$  in the mobile path (Fig. 3.5). Let  $OE$  and  $OF$  be the lines joining the base station to the points  $E$  and  $F$ . Depending on the directions of the mobile at time  $\tau$  and  $\tau - 1$ , one of the following cases can occur:

$$\begin{array}{l}
\text{case I} \left\{ \begin{array}{l} \text{direction} \Rightarrow \text{from } E \text{ to } F \\ \text{last location} \Rightarrow \text{lower side of the line } OE \end{array} \right. \\
\text{case II} \left\{ \begin{array}{l} \text{direction} \Rightarrow \text{from } F \text{ to } E \\ \text{last location} \Rightarrow \text{lower side of the line } OF \end{array} \right. \\
\text{case III} \left\{ \begin{array}{l} \text{direction} \Rightarrow \text{from } F \text{ to } E \\ \text{last location} \Rightarrow \text{upper side of the line } OF \end{array} \right. \\
\text{case IV} \left\{ \begin{array}{l} \text{direction} \Rightarrow \text{from } E \text{ to } F \\ \text{last location} \Rightarrow \text{upper side of the line } OE \end{array} \right.
\end{array} \tag{3.8}$$

Inspection of any of these cases would reveal that the mobile movement is related to the regional transitions. That is, in *case I*, the mobile movement is such that it enters the region  $R\#1$  at point  $E$ . This mobile has the option of moving either to  $R\#1$  or to  $R\#2$  in continuing its movement at point  $F$ . As another example, consider *case II*. At point  $E$ , the mobile enters the region  $R\#2$ . At point  $F$  it has the option of moving either to  $R\#3$  or to  $R\#4$ . The same argument could be put in *case III*

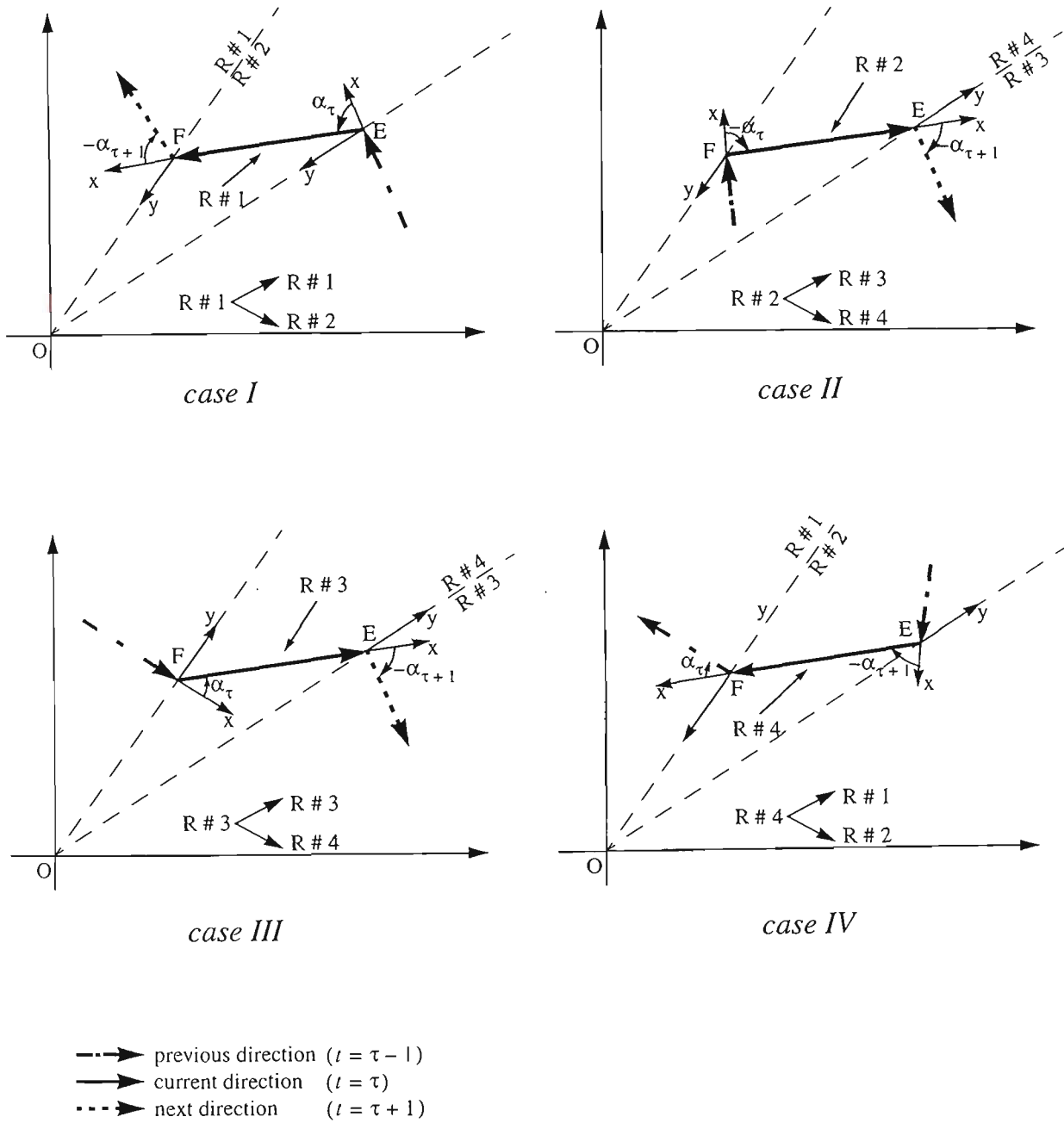


Fig. 3.5. Movement of mobiles between different regions.



and *case IV*. These can be summarised as follows:

$$\begin{aligned}
 \text{case I} &\Rightarrow \text{a mobile moving in } R\#1 \text{ continues either in } R\#1 \text{ or } R\#2 \\
 \text{case II} &\Rightarrow \text{a mobile moving in } R\#2 \text{ continues either in } R\#3 \text{ or } R\#4 \\
 \text{case III} &\Rightarrow \text{a mobile moving in } R\#3 \text{ continues either in } R\#3 \text{ or } R\#4 \\
 \text{case IV} &\Rightarrow \text{a mobile moving in } R\#4 \text{ continues either in } R\#1 \text{ or } R\#2
 \end{aligned} \tag{3.9}$$

Examination of the successive positions of the mobile reveals that the mobile movement could be tagged to the regional transitions as shown in the state diagram of Fig. 3.6. This diagram shows permissible movement from one region to another. For instance a mobile in region  $R\#1$  at time  $\tau$  can remain in region  $R\#1$  or move to region  $R\#2$  at time  $\tau + 1$ . A mobile in region  $R\#2$  at time  $\tau$  can move to either region  $R\#3$  or region  $R\#4$  at time  $\tau + 1$ , and so on.

The value of  $\theta_\tau$  depends on the current and the previous state of the mobile. For instance, if the mobile arrives at time  $\tau$  to region  $R\#1$  (either from region  $R\#1$  or region  $R\#4$ ),  $\theta_\tau$  is given by  $\theta_\tau = \theta_{\tau-1} + \gamma_{\tau-1} - \beta_\tau$ , where  $\gamma_{\tau-1} = \alpha_{\tau-1} + \beta_{\tau-1}$  (Fig. 3.7). Further, the condition for arrival at region  $R\#1$  is given by  $\gamma_{\tau-1} > 0$ . Similarly the condition for arrival at other states and the corresponding expressions for  $\theta_\tau$  can be found accordingly. The equations for calculation of mobile new location are tabulated in Table 3.1.

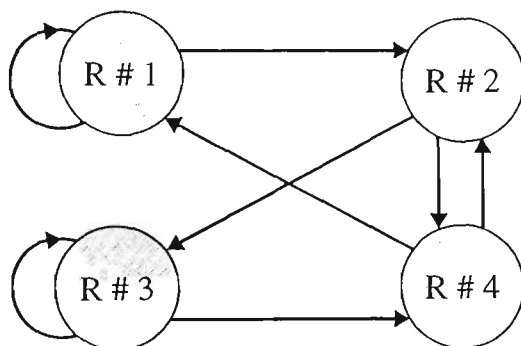


Fig. 3.6. Permissible state diagram for mobile movement.

Table 3.1 Equations for calculation of mobile new location.

State Changes	Equations
1 ⇒ 1 or 4 ⇒ 1	$\gamma_{\tau-1} = \alpha_{\tau-1} + \beta_{\tau-1} > 0$ $\theta_{\tau} = \theta_{\tau-1} + \gamma_{\tau-1} - \beta_{\tau}$
1 ⇒ 2 or 4 ⇒ 2	$\gamma_{\tau-1} = \alpha_{\tau-1} + \beta_{\tau-1} < 0$ $\theta_{\tau} = \theta_{\tau-1} + \gamma_{\tau-1} + \beta_{\tau}$
2 ⇒ 3 or 3 ⇒ 3	$\gamma_{\tau-1} = \alpha_{\tau-1} - \beta_{\tau-1} < 0$ $\theta_{\tau} = \theta_{\tau-1} + \gamma_{\tau-1} + \beta_{\tau}$
2 ⇒ 4 or 3 ⇒ 4	$\gamma_{\tau-1} = \alpha_{\tau-1} - \beta_{\tau-1} > 0$ $\theta_{\tau} = \theta_{\tau-1} + \gamma_{\tau-1} - \beta_{\tau}$

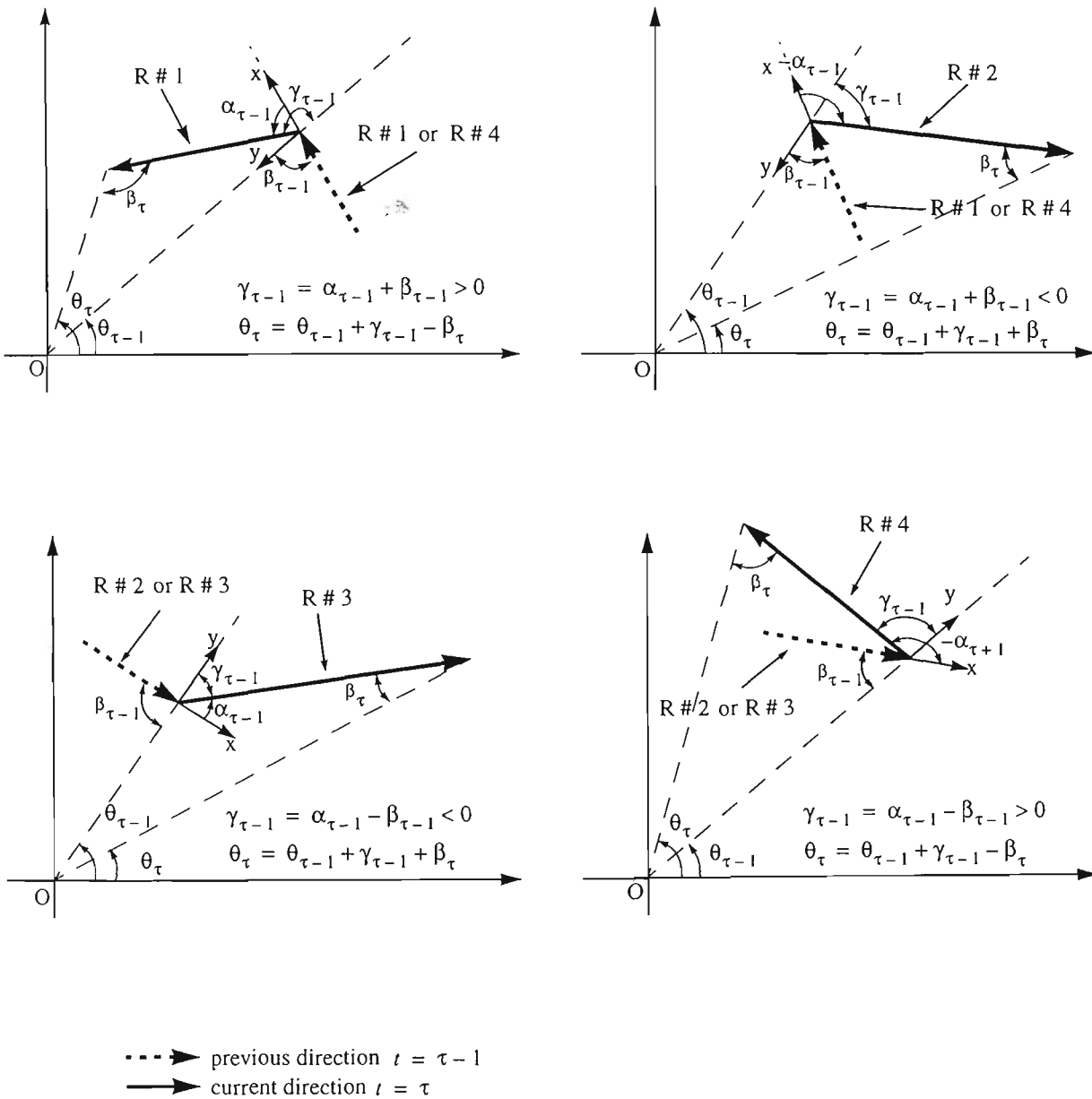
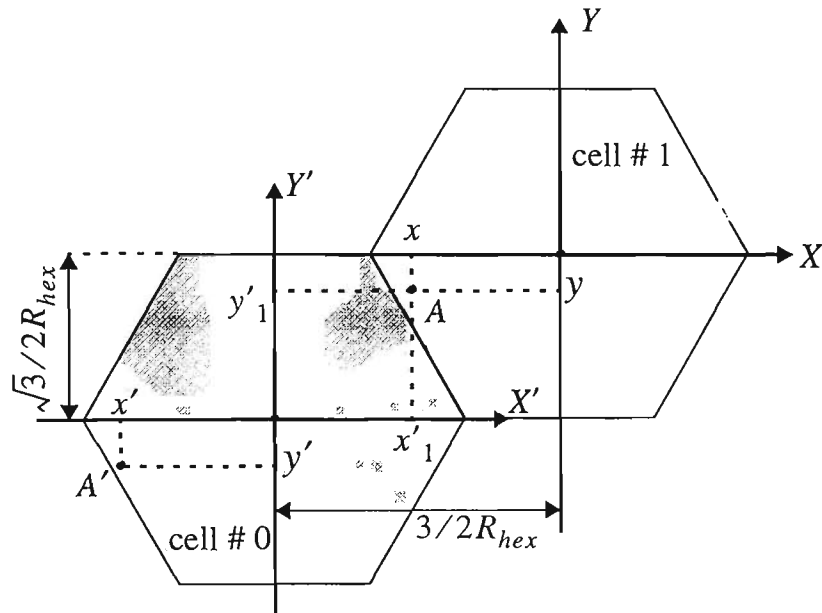


Fig. 3.7. Relations to trace a mobile between different regions.

### 3.2 Tracing of mobile outside the cell

In order to follow the trajectory of a mobile moving outside a cell, it is necessary to trace it as it moves to adjacent cells. However, the simulation of a large number of cells is cumbersome and requires extensive computer resources. To overcome this difficulty, a mobile moving into an adjacent cell is relocated at a corresponding position inside the original cell. This idea leads to a simpler formulation of the mobile trajectory and ultimately reduces the entire problem to the case of a single cell.

In [103], a mobile handed over to another cell is brought back to the original cell by applying the mirror reflection principle. The main drawback of this method is that the cell boundary crossing point has to be on the line joining the centres of the two cells. Therefore, the positions of the neighbouring cells are subject to change according to the location of the mobile leaving (or re-entering) the cell. This problem is surmounted by re-entering mobile in the initial cell as illustrated in Fig. 3.8 where a mobile enters from *cell#0* to *cell#1*. Let us define two coordinate systems with the origins locating at the base station sites i.e.  $(X, Y)$  for the *cell#1* and  $(X', Y')$  for the *cell#0*. The mobile location  $A$  in the new cell (*cell#1*) can be determined by  $(x, y)$  with respect to the coordinate system of  $(X, Y)$ , and can also be determined by  $(x'_1, y'_1)$  with respect to the coordinate system of  $(X', Y')$ . By re-entering the mobile back in the initial cell (*cell#0*), we locate the mobile at  $A'$  with the coordinate  $(x', y')$  such that it is equivalent to the position in its previous cell. This means that the coordinate  $(x', y')$  in the coordinate system  $(X', Y')$  is equivalent to the coordinate  $(x, y)$  in the coordinate system  $(X, Y)$ . Inspecting mobile location at



**Fig. 3.8.** Coordinates of a mobile position at point A with respect to two different coordinates systems.

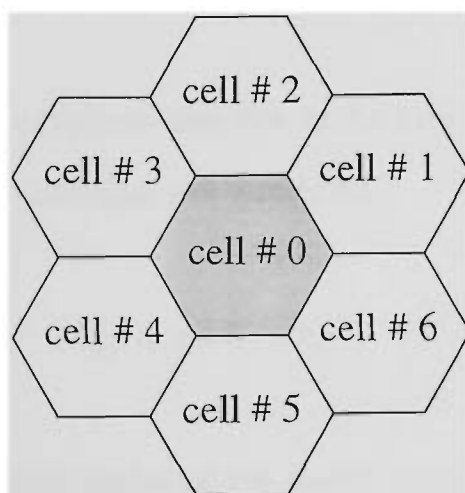


**Fig. 3.9.** Neighbour cells numbering.

points  $A$  and  $A'$  with respect to the coordinate system  $(X', Y')$ , it is possible to derive the following relations:

$$\begin{aligned}x' &= x'_1 - 3/2R_{hex} \\y' &= y'_1 - \sqrt{3}/2R_{hex}\end{aligned}\tag{3.10}$$

Depending on the neighbouring cell to which the mobile enters, the mobile's corresponding location inside the original cell coordinate system  $(x', y')$  can be obtained as follows:

$$\begin{array}{lll}cell\ No\ 1 & y' = y'_1 - \sqrt{3}/2R_{hex} & x' = x'_1 - 3/2R_{hex} \\cell\ No\ 2 & y' = y'_1 - \sqrt{3} R_{hex} & x' = x'_1 \\cell\ No\ 3 & y' = y'_1 - \sqrt{3}/2R_{hex} & x' = x'_1 + 3/2R_{hex} \\cell\ No\ 4 & y' = y'_1 + \sqrt{3}/2R_{hex} & x' = x'_1 + 3/2R_{hex} \\cell\ No\ 5 & y' = y'_1 + \sqrt{3} R_{hex} & x' = x'_1 \\cell\ No\ 6 & y' = y'_1 + \sqrt{3}/2R_{hex} & x' = x'_1 - 3/2R_{hex}\end{array}\tag{3.11}$$

In order to maintain the appropriate direction in the new location, the start angle  $\alpha_0$  of the new direction in the substitute cell should be,

$$\alpha_0 = \gamma + \theta_1 - \theta_2\tag{3.12}$$

where  $\theta_1, \theta_2$  are the location angles of the mobile with respect to the original and substitute cells respectively, as in Fig. 3.10. This process can be repeated as many times as needed to keep a mobile inside the original cell. The following equations

could be used to calculate the values of  $\theta_2$ :

$$\begin{aligned}
 x' \geq 0 \text{ and } y' \geq 0 & \quad \theta_2 = \arccos \frac{x'}{\rho} \\
 x' \geq 0 \text{ and } y' < 0 & \quad \theta_2 = -\arccos \frac{x'}{\rho} \\
 x' < 0 \text{ and } y' \geq 0 & \quad \theta_2 = \frac{\pi}{2} + \arccos \frac{y'}{\rho} \\
 x' < 0 \text{ and } y' < 0 & \quad \theta_2 = \frac{\pi}{2} - \arccos \frac{y'}{\rho}
 \end{aligned} \tag{3.13}$$

and the value of  $\rho$  is obtained by,

$$\rho = \sqrt{x'^2 + y'^2} \tag{3.14}$$

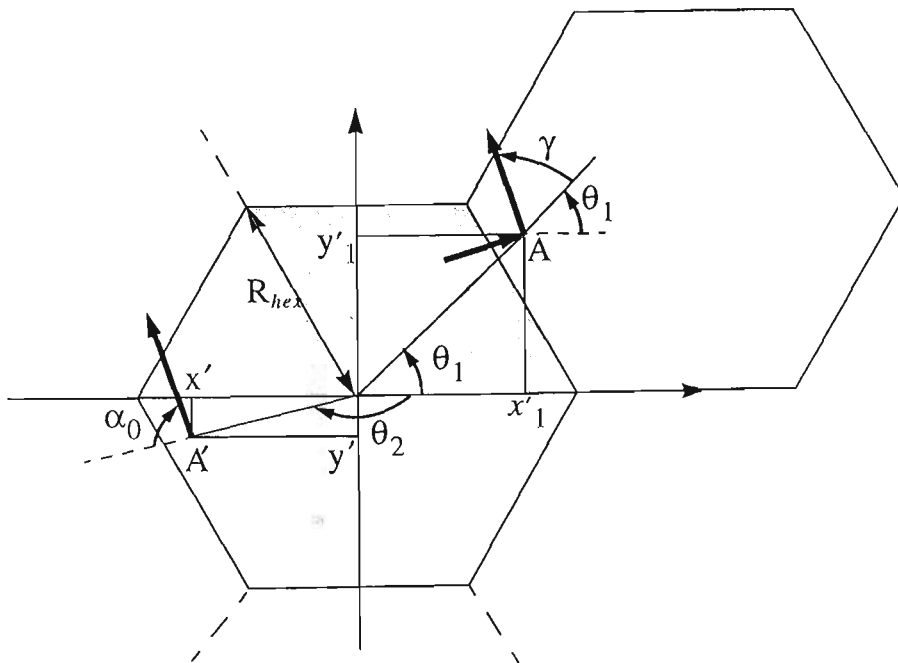


**Fig. 3.10.** Geometric relations between real location of a mobile  $A$ , and its image  $A'$  in the substitute cell.

### 3.3 Conclusions

In this Chapter, a mathematical formulation was developed for systematic tracking of the random movement of a mobile station in a cellular environment. It incorporates mobility parameters under generalized conditions, so that the model could be tailored to be applicable in most cellular systems. The proposed model traces mobiles systematically in a cellular environment where they are allowed to move in a quasi-random fashion with assigned degrees of freedom.

Two sets of equations have been derived to trace mobiles locations inside and outside the cell. These equations enable us to develop a computer simulation program to investigate the characteristics of different mobility related traffic parameters in a cellular system.



# ***Chapter 4***

## ***Cell Residence Time and Channel Holding Time Distributions***

There are two approaches commonly adopted in the incorporation of mobility in a cellular system simulation model. The first method, which is used in most simulations, considers mobility as a subsidiary function in the simulation program. Examples of this approach can be found in [4, 109, 113, 114, 115]. This method suffers from the disadvantage that every execution of the simulation requires mobility modelling. The second approach is to characterise different mobility related parameters. This method has the advantage that it can be used in analysis as well as in simulation. A review of the available literature on the characterisation of mobility related parameters reveals that only a few of the works have dealt with the related matter in detail, although the need for a comprehensive study is evident. Among

these works, we can refer to the following.

Guérin [103] has shown that the channel holding time follows a negative exponential distribution. Morales-Andres et al. [116], and Thomas et al. [107] have used fluid-flow model of mobility and analytically formulated the cell boundary crossing rate. Pollini et al. [117] have used these results to calculate the amount of signalling information needed to deliver calls to mobile stations. Seskar et al. [118] have shown via simulation that while the model given in [107] provides a good estimate of the boundary crossing rates for a Manhattan grid of streets, other conditions lead to crossing rates larger or smaller than those of the model. El-Hoiydi et al. [119] derive the probability of crossing the border of a circle and use it to extract the location update and paging rates. Nanda [49], and Hong et al. [101] have analysed the mean handover rate. In [108] the mean cell crossings per unit time has been proposed for a case of three dimensional space.

Among the different mobility-related traffic parameters, one that has not received sufficient attention so far is user's cell residence time. Therefore, an appropriate probability distribution that accurately describes the cell residence time remains an issue to be investigated. A literature survey shows that a relatively few in-depth papers have been published on this subject and most of these are restricted to simple mobility situations. Hong and Rappaport [101] have made an elaborate analysis to obtain the cell residence time probability density function (pdf) for a simplified case of mobility in which there is no change in speed or direction of the mobile. Further, in this work the initial speed of the mobile was assumed to follow a uniform distribution. Del Re, Fantacci and Giambene [102] have assumed that mobiles,

before crossing a cell, travel a distance uniformly distributed between 0 and  $2R_{hex}$ , where  $R_{hex}$  is the hexagonal cell side. They also assume a constant speed with uniform distribution and conclude that the pdf of cell residence time is different to that shown in [101]. Inoue, Morikawa and Mizumachi [120] have applied the procedure of [101] for a case of non-uniform speed distribution. However they end up with a set of unsolved integral equations. Yeung and Nanda [121, 122], Xie and Kuek [123], Xie and Goodman [124] have shown that contrary to the assumption made in [101], the speed and direction distributions of the in-cell mobiles are different from those of the cell-crossing mobiles. They have shown that a more precise distribution for the speed and direction can be obtained using the *Biased Sampling* formula.

While Sánchez Vargas [125], and Lue [126] have assumed cell residence time to be uniformly distributed over the call duration, Nanda [49], and Lin et. al [127, 128] have assumed a general distribution for the cell residence time. Malyan, Ng, Leung and Donaldson [129] have proposed a model where a mobile is positioned initially at the centre of a circular coverage area and its cell residence time is obtained by using a two dimensional random walk model. Generally, for the sake of simplicity, in the absence of any proved probability distribution, many authors dealing with the mobility problem have assumed either explicitly or implicitly, the cell residence time to be an exponentially distributed random variable [130, 131, 132, 133, 134, 135, 136, 137].

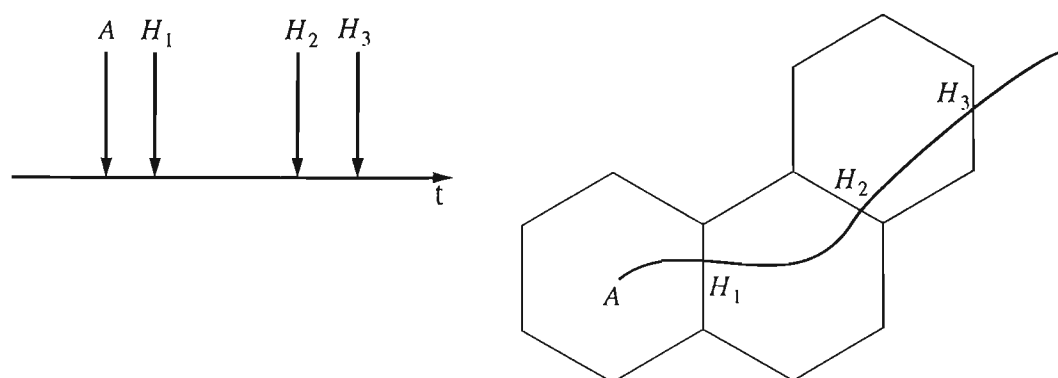
Another important parameter that appears in relation to cellular mobile systems is the channel holding (or occupancy) time. A knowledge of the channel holding time

probability distribution function is necessary to obtain an accurate analysis of many teletraffic issues that arise in planning and design of cellular mobile radio systems. Channel holding time of a cell is defined as the time during which a new or handover call occupies a channel in the given cell and is dependent on the mobility of the user. While this is similar to the call holding time in the fixed telephone network, it is often a fraction of the total call duration in a cellular mobile network and need not have the same statistical properties. Negative exponential distribution has been assumed to describe channel holding time in modelling large single cell systems [138, 139, 140]. Guérin [103] has extended this by attempting to describe the channel holding time in general by the negative exponential distribution.

The outline of this chapter is as follows. The distribution of the cell residence time for a simplified case (for comparison purposes) and the generalized case is studied in Section 4.1. Based on the formulation made in Chapter 3, a computer simulation is developed to obtain the behaviour of different mobility related parameters. Analysis of data obtained by simulation is used to show that the generalized gamma distribution function is a good approximation to describe the cell residence time distribution. Section 4.2 deals with the mean cell residence time. The effect of changes in direction and speed is analysed and empirical relationships that relate speed and direction changes to the cell size are obtained in Section 4.3. In Section 4.4, an expression to determine the average number of handovers in a cell is derived. In Section 4.5, it is shown that the channel holding time distribution of a cellular network is a negative exponential function.

## 4.1 Cell Residence Time Distribution

Depending on whether a call is originated in a cell or handed over from a neighbouring cell, two different cell residence times can be specified. They are the new call cell residence time and the handover call cell residence time, respectively. *New call cell residence time* is defined as the length of time a mobile station resides in the cell where the call originated before crossing the cell boundary. Similarly, the *handover call cell residence time* is defined as the time spent by a mobile in a given cell to which the call was handed over from a neighbouring cell before crossing to another cell, (Fig. 4.1). New call cell residence time  $\tau_n$  and the handover call cell residence time  $\tau_h$  are two random variables whose distributions have to be found. The term cell residence time is also labelled as the mobile sojourn time, dwell time or block holding time by some authors [122, 141, 142].



$AH_1$  - new call cell residence time

$H_1H_2$  and  $H_2H_3$  - handover call cell residence time

**Fig. 4.1.** Representation of cell residence time in time and space domains for a mobile moving across cells.

### 4.1.1 Simplified Case

In a cellular mobile system, the service area can be considered as a pattern of regular hexagonal cells of the same size with the cell radius  $R_{hex}$  [1]. The cell radius for a hexagonal shape is defined as the distance from the centre of the cell to a vertex of the hexagon. The coverage area is chosen to represent a purely random environment without any street grid, carrying homogenous traffic of equal density. In order to obtain simple but reliable criteria for examining cell boundary crossings, the hexagonal cells can be approximated by circles of the same area. If  $A_{cell}$  represents the cell area, the radius of the equivalent circle  $R$  can be approximated by (Fig. 4.2),

$$A_{cell} = \frac{3\sqrt{3}}{2}R_{hex}^2 \approx \pi R^2 \quad (4.1)$$

$$R \approx 0.91R_{hex}$$

Let us assume that users are independent and uniformly distributed over the entire region. The initial location of a mobile is represented by its distance  $\rho_0$  and direction  $\theta_0$  from the base station. Therefore, the probability density function of the mobile location in polar coordinates  $f(\rho_0, \theta_0)$  will be as follows (Appendix A):

$$f(\rho_0, \theta_0) = \begin{cases} \frac{\rho_0}{\pi R^2} & 0 \leq \rho_0 \leq R \quad \text{and} \quad 0 \leq \theta_0 \leq 2\pi \\ 0 & \text{otherwise} \end{cases} \quad (4.2)$$

Assuming that the direction of the mobile at the starting point  $\alpha_0$  is uniformly distributed and remains constant along its path, the pdf of the mobile initial direction

$f(\alpha_0)$  will be as follows:

$$f(\alpha_0) = \begin{cases} \frac{1}{2\pi} & 0 \leq \alpha_0 \leq 2\pi \\ 0 & \textit{otherwise} \end{cases} \quad (4.3)$$

Also assume that the initial speed of the mobile  $v_0$  is uniformly distributed in the range  $(0, V_m)$ , and remains constant along the mobile path. Therefore, the pdf of the mobile initial speed,  $f_{v_0}(v_0)$ , will be given by:

$$f_{v_0}(v_0) = \begin{cases} \frac{1}{V_m} & 0 \leq v_0 \leq V_m \\ 0 & \textit{otherwise} \end{cases} \quad (4.4)$$

Let  $f_{T_n}(t)$  and  $F_{T_n}(t)$  denote the probability density and the cumulative distribution functions of the new call cell residence time, respectively (random variable  $T_n$  has been shown in Fig. 4.2). These probability functions can be calculated from the following relations [101]:

$$f_{T_n}(t) = \begin{cases} \frac{8R}{3\pi V_m t^2} \left\{ 1 - \left[ 1 - \left( \frac{V_m t}{2R} \right)^2 \right]^{3/2} \right\} & 0 \leq t \leq \frac{2R}{V_m} \\ \frac{8R}{3\pi V_m t^2} & t \geq \frac{2R}{V_m} \end{cases} \quad (4.5)$$

$$F_{T_n}(t) = \begin{cases} \frac{2}{\pi} \operatorname{asin} \frac{V_m t}{2R} - \frac{4}{3\pi} \tan \left[ \frac{1}{2} \operatorname{asin} \frac{V_m t}{2R} \right] + \frac{1}{3\pi} \sin \left[ 2 \operatorname{asin} \frac{V_m t}{2R} \right] & 0 \leq t \leq \frac{2R}{V_m} \\ 1 - \frac{8R}{3\pi V_m t} & t \geq \frac{2R}{V_m} \end{cases} \quad (4.6)$$

A handover call starts from the boundary crossing of a cell by a mobile having a direction  $\alpha_0$  uniformly distributed over  $(-\pi/2, \pi/2)$ . Therefore, initial direction pdf  $f(\alpha_0)$  will be,

$$f(\alpha_0) = \begin{cases} \frac{1}{\pi} & -\frac{\pi}{2} \leq \alpha_0 \leq \frac{\pi}{2} \\ 0 & \text{otherwise} \end{cases} \quad (4.7)$$

where  $\alpha_0$  is the angle between the normal at the cell boundary crossing point, and the moving direction of the mobile. The pdf and the cdf of the handover call cell residence time,  $f_{T_h}(t)$  and  $F_{T_h}(t)$ , can be calculated in a similar manner to (4.5) and

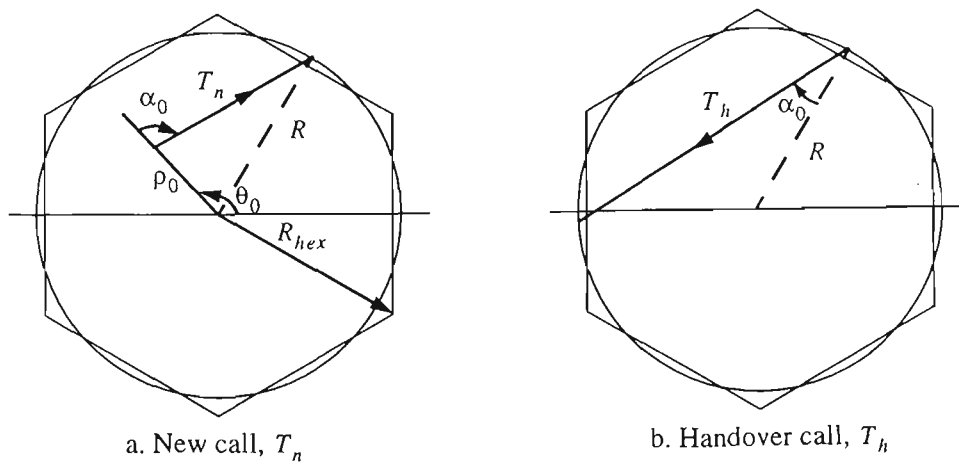


Fig. 4.2. Cell residence time illustration for two different cases.



(4.6) and is given by,

$$f_{T_h}(t) = \begin{cases} \frac{4R}{\pi V_m t^2} \left\{ 1 - \left[ 1 - \left( \frac{V_m t}{2R} \right)^2 \right]^{1/2} \right\} & 0 \leq t \leq \frac{2R}{V_m} \\ \frac{4R}{\pi V_m t^2} & t \geq \frac{2R}{V_m} \end{cases} \quad (4.8)$$

$$F_{T_h}(t) = \begin{cases} \frac{2}{\pi} \operatorname{asin} \frac{V_m t}{2R} - \frac{2}{\pi} \tan \left[ \frac{1}{2} \operatorname{asin} \frac{V_m t}{2R} \right] & 0 \leq t \leq \frac{2R}{V_m} \\ 1 - \frac{4R}{\pi V_m t} & t \geq \frac{2R}{V_m} \end{cases} \quad (4.9)$$

In [123, 124], it is shown that the speed and direction distributions of the in-cell mobiles are different from those of the cell-boundary crossing mobiles. Let  $f_{V_0}(v_0)$  denote the pdf of the speeds of the in-cell mobiles and  $f_{V_0}^*(v_0)$  denote the pdf of the speeds of cell-boundary crossing mobiles. Based on the Biased Sampling [143], it can be shown that,

$$f_{V_0}^*(v_0) = \frac{v_0 f_{V_0}(v_0)}{E[V_0]} = \begin{cases} \frac{v_0}{V_m E[V_0]} & 0 \leq v_0 \leq V_m \\ 0 & \text{otherwise} \end{cases} \quad (4.10)$$

where  $E[V_0] = \int_{-\infty}^{\infty} v_0 f_{V_0}(v_0) dv_0$  is the mean speed. Similarly, let  $f(\alpha_0)$  be the pdf of the directions of all mobile stations, which is uniform in the range  $(0, 2\pi)$ . Based on the Biased Sampling, the pdf of the directions of the cell-boundary crossing mobiles,  $f^*(\alpha_0)$ , can be obtained as:

$$f^*(\alpha_0) = \begin{cases} \frac{1}{2} \cos(\alpha_0) & -\frac{\pi}{2} \leq \alpha_0 \leq \frac{\pi}{2} \\ 0 & \textit{otherwise} \end{cases} \quad (4.11)$$

Equation (4.11) shows that the pdf of the direction of the cell-crossing mobile stations is not uniform, but has a direction biased towards the normal line on the border. Considering (4.10) and (4.11), the relations for  $f_{T_n}(t)$ ,  $F_{T_n}(t)$ ,  $f_{T_h}(t)$  and  $F_{T_h}(t)$  could be modified accordingly.

#### 4.1.2 Generalized Case

Eqs. (4.5)-(4.9) represent the new and handover call cell residence time distributions for the simplified case of mobility in which there is no change in speed and direction of the mobile and there is no biasing in speed or direction of the boundary crossing mobiles. In a general case, the mobility modelling should include changes in direction and speed of the mobile. Moreover, it is unrealistic to assume that the speed is uniformly distributed and remains constant. It is virtually impossible to extend the analysis of the simplified case to cover the general case of mobility. Instead a simulation approach appears to be the best way out. Based on the mobility model developed in Chapter 3, a computer simulation program can be developed to study the mobility under generalised assumptions for different mobility-related parameters.

##### 4.1.2.1 Simulation model

The simulation model is aimed at obtaining statistical estimates of the mobile cell

boundary crossings in a cellular environment in which the mobile is allowed to move freely with randomly varying velocities and directions within realistic bounds. In order that the simulation model be used in a variety of tasks, flexibility is provided in terms of its inputs and outputs. A simplified flow diagram of the simulation model is shown in Fig. 4.3. The objective of this simulation is to generate sufficient data to examine the boundary crossing phenomenon of a mobile as a function of cell size and mobility-related parameters. This would enable us to obtain the statistical distribution of the cell residence time and hence that of the channel holding time.

A uniform distribution is assumed for spatial location of the users. This assumption is valid, since throughout a cellular network, the relative orientation of streets and grids varies somewhat randomly, giving on the average, a nearly uniform distribution of possible directions. However, a suitable selection of input parameters allows modification of this to fit a particular pattern. Since the destination point of mobiles can be any point in the coverage area, mobiles are allowed to move away from the starting point in any direction with equal probability. Therefore, a uniform distribution in the range  $(-\pi, \pi)$  is suitable for the initial mobile direction. Depending on the structure of the cellular mobile coverage area, a mobile may move towards the destination point via different paths. However, in any case, the mobile direction is biased towards a destination to prevent it from circling around.

In order to make simulation processing time short, array processing is used. For this purpose, at any given time  $\tau$ , the locations of  $M$  mobiles in each of  $N$  concentric cells of radius  $nR$  ( $n= 1, 2, \dots, N$ ) can be represented by  $N \times M$  matrix pair,

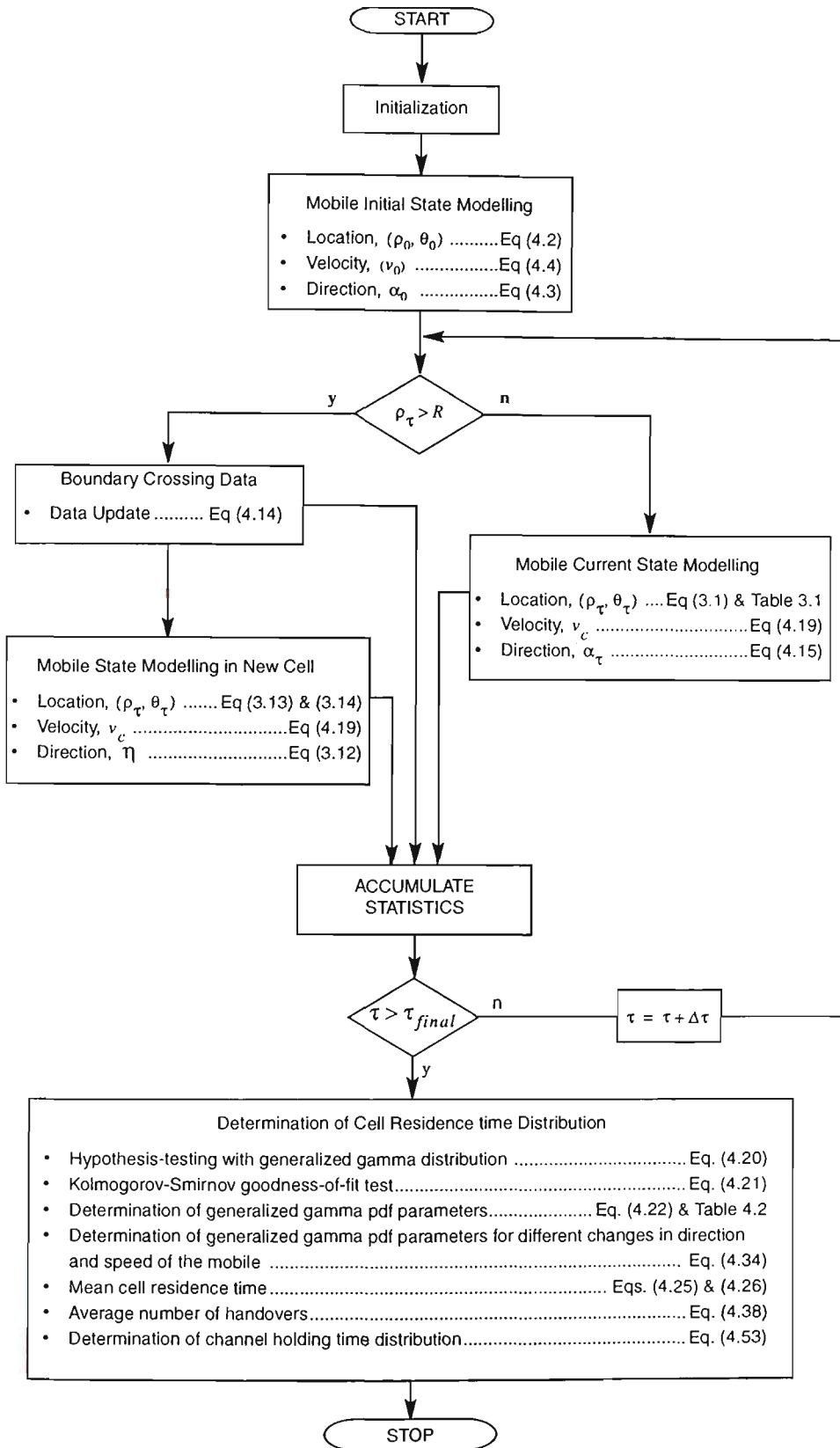


Fig. 4.3. Simplified flow diagram for analysing boundary crossing.

$$P_\tau = \begin{bmatrix} \rho_{11} & \rho_{12} & \dots & \rho_{1M} \\ \rho_{21} & \rho_{22} & \dots & \rho_{2M} \\ \dots & \dots & \dots & \dots \\ \rho_{N1} & \rho_{N2} & \dots & \rho_{NM} \end{bmatrix} \quad (4.12)$$

and,

$$\Theta_\tau = \begin{bmatrix} \theta_{11} & \theta_{12} & \dots & \theta_{1M} \\ \theta_{21} & \theta_{22} & \dots & \theta_{2M} \\ \dots & \dots & \dots & \dots \\ \theta_{N1} & \theta_{N2} & \dots & \theta_{NM} \end{bmatrix} \quad (4.13)$$

where any pair element of  $(P_\tau, \Theta_\tau)$  denotes location of a mobile in polar coordinates at time  $\tau$  after initiation of a call. Accordingly,  $(\rho_{nm}, \theta_{nm})$  shows position of  $m^{\text{th}}$  mobile in a cell of radius  $nR$  at time  $\tau$ . For the sake of simplicity, the position of an arbitrary mobile in a cell of radius  $nR$ , i.e.  $(\rho_{nm}, \theta_{nm})$ , at time  $\tau$  is denoted by  $(\rho_\tau, \theta_\tau)$ . The range of values of  $\rho_\tau$  is determined by the cell perimeter, i.e.  $0 < \rho_\tau \leq nR$ , and  $\theta_\tau$  can have any value in the range of  $-\pi \leq \theta_\tau \leq \pi$ . The time  $\tau = 0$  corresponds to the initial location of the mobile, and is synonymous with the instant of call establishment.

The simulation incorporates a sufficiently large mobile population, so that the influence of initial conditions and the variations due to the stochastic process behaviours can be ignored. In this simulation, a mobile population of  $M = 50,000$  is used to obtain the steady state statistics of the boundary crossing phenomena. With

this arrangement the system can be considered to be in statistical equilibrium, and the derived probabilities are not dependent on time.

Cell boundary crossing statistics for each mobile are determined by comparing the successive values of  $\rho_\tau$  with the related cell radius. The mobile remains inside a cell as long as  $\rho_\tau$  does not exceed the cell radius. As the time progresses, new locations of the mobiles are found using the mobility model and (4.12)-(4.13) are updated accordingly. Status of the boundary crossing is accumulated in  $N \times M$  tuples of integers where each element of it denotes the status of a mobile such that,

$$BC_{nm} = \begin{cases} 0 & \text{No boundary crossing} \\ 1 & \text{One boundary crossing} \end{cases} \quad (4.14)$$

where  $BC_{nm}$  denotes status of  $m^{\text{th}}$  mobile in a cell with the cell of radius  $nR$ . The probability of cell boundary crossing can be obtained by averaging results in each cell area over  $M$  users.

In the simulation model, the initial mobile direction is taken to be uniformly distributed in the cell area, and the directions at successive steps are allowed to change within a set bound referred herein as *drift*.

The probability distribution of the variation of the mobile direction  $\alpha_\tau$  along its path in successive steps is taken to be uniform in the range  $(-\varphi, +\varphi)$  degrees with respect to the current direction (Fig. 4.4).

$$f(\alpha_\tau) = \begin{cases} \frac{1}{2\varphi} & -\varphi \leq \alpha_\tau \leq \varphi \\ 0 & \text{otherwise} \end{cases} \quad (4.15)$$

The value of  $\varphi$  is chosen, depending on the street structure of the cell area, to be a low value for cells with more straight streets and a high value for cells with less straight streets. The effect of  $\varphi$  on the probability of boundary crossing can be examined by comparing different values of  $\varphi$  with respect to a reference. Taking a straight movement without any drift, i.e.  $\varphi = 0^\circ$  as the reference, the relative boundary crossing probability difference between reference cell and a cell with a drift  $\alpha$  in the range  $(-\varphi, +\varphi)$  degrees can be calculated by,

$$\delta P_\alpha(B) = P(B|\alpha=0) - P(B|\alpha=\varphi) \quad (4.16)$$

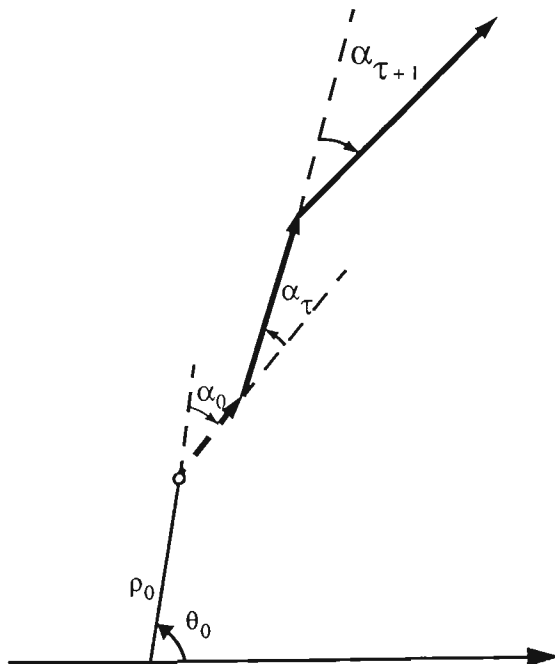


Fig. 4.4. Mobile movement in permissible directions.

where  $P(B|\alpha= 0)$  is the boundary crossing probability in the reference cell, and  $P(B|\alpha= \varphi)$  is the boundary crossing probability with a drift in the range  $(-\varphi, +\varphi)$  degrees.

The initial speed of a mobile station, at the instant the call is initiated, is taken as a random variable with truncated Gaussian probability density function,  $f_{v_0}(v_0)$ , with a mean  $\mu_v$  and a standard deviation  $\sigma_v$ . The choice of such a distribution seems reasonable, since the more extreme the speed value, the less likelihood of its occurrence. Also, it is unlikely that the speed exceeds a certain maximum value. Therefore if speed is limited in the range  $[V_{min} = 0, V_{max} = 100 \text{ Km/h}]$ , the initial speed of a mobile station pdf will be:

$$f_{v_0}(v_0) = \begin{cases} \frac{K}{\sigma_v \sqrt{2\pi}} e^{-\frac{(v_0 - \mu_v)^2}{2\sigma_v^2}} & V_{min} \leq v_0 \leq V_{max} \\ 0 & \text{otherwise} \end{cases} \quad (4.17)$$

where  $K$  is the normalization constant and is given by (Appendix B),

$$K = \left[ \operatorname{erf} \frac{V_{max} - \mu_v}{\sigma_v} - \operatorname{erf} \frac{V_{min} - \mu_v}{\sigma_v} \right]^{-1} \quad (4.18)$$

The mobile speed in the successive times is a random variable correlated with the previous speed,  $v_p$ . The current speed,  $v_c$ , of each mobile is taken to be a uniformly distributed random variable in the range  $\pm 10\%$  of the previous speed. Therefore the mobile current speed pdf  $f_{v_c}(v_c)$  will be,



$$f_{V_c}(v_c) = \begin{cases} \frac{1}{0.2v_p} & 0.9v_p \leq v_c \leq 1.1v_p \\ 0 & \textit{otherwise} \end{cases} \quad (4.19)$$

Any increase in the speed above 100  $Km/h$  is not allowed, and the minimum speed is taken to be  $0Km/h$ .

The speed of the mobile and its direction are updated at intervals which are exponentially distributed with an average value of one minute. The motivation for the choice of an exponential distribution for the length of time between two successive changes in direction and speed is based on the intuition that the time of the last change in direction or speed is virtually independent of the time of the next change in direction. In other words, the time distribution between two changes of direction or speed is assumed memoryless.

In order to check the validity of the proposed simulation model, a test run is made for the simplified case described in Sub-Section 4.1.1 with the same assumptions held. The probability distribution functions of the new and handover calls' cell residence time for this case is calculated using (4.6) and (4.9) and compared with the results obtained by the simulation. As shown in Fig. 4.5 the results obtained by simulation are in good agreement with the analytical results.

Since the moving direction and the speed of a mobile are non-deterministic processes, the path of a mobile will be a random trajectory. Fig. 4.6 shows 5 such trajectories when drift range is set to be  $\pm 20^\circ$ .

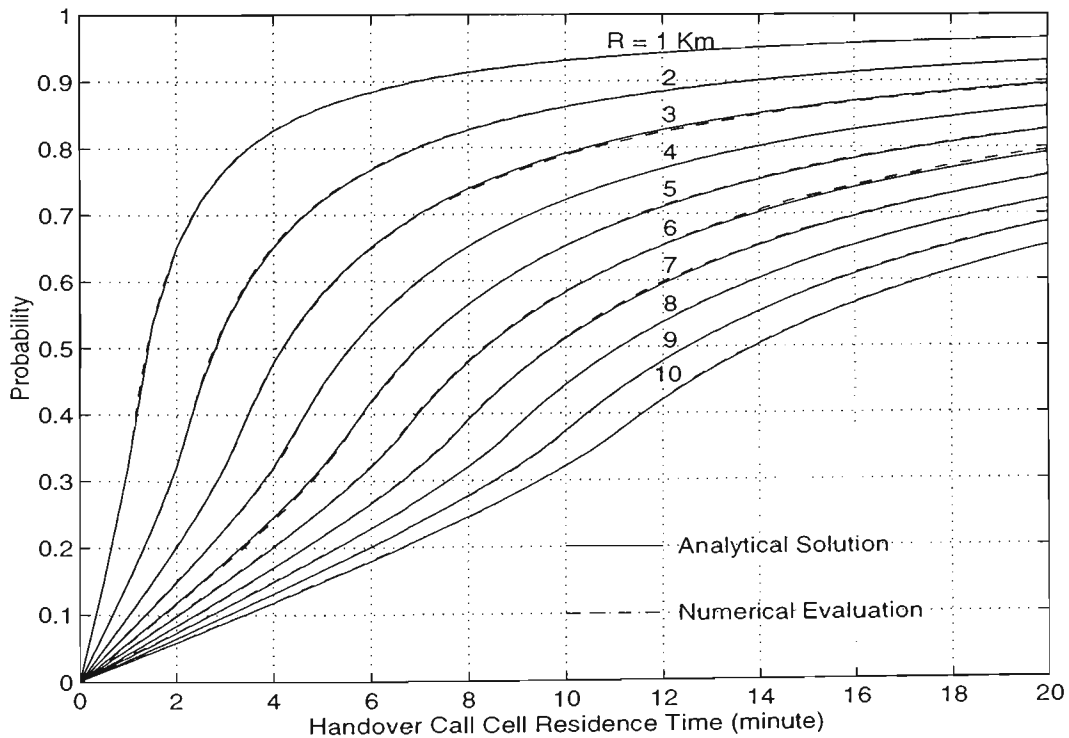
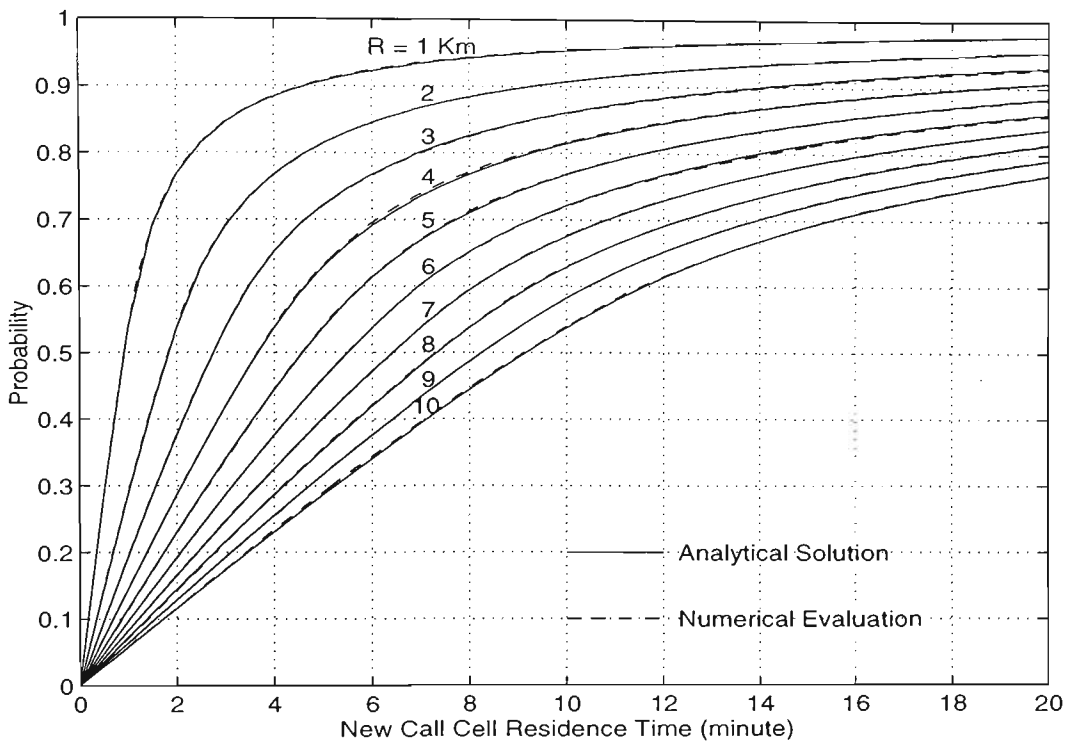


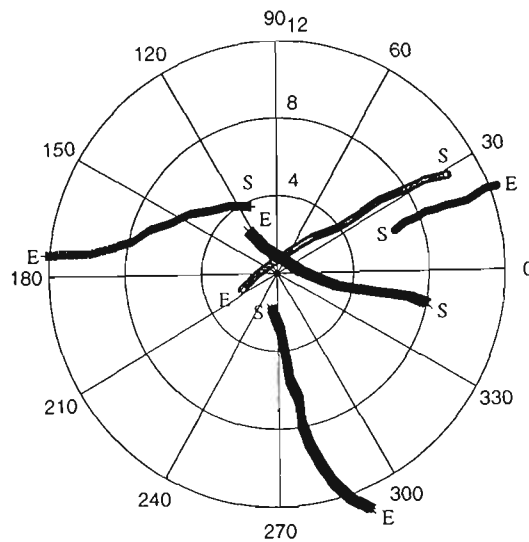
Fig. 4.5. New and handover calls' cell residence time distributions obtained analytically (Eqs. (4.6) and (4.9)) and by simulation with the same assumptions.

### 4.1.2.2 Data analysis

What is of importance here is not the actual mobile trajectories, but the distribution of the users' cell residence time. With this in mind, we wish to test the hypothesis that the new call and handover call residence time data follows a particular probability distribution. Following [144, 145], we proceed with the generalized gamma distribution which provides probability density functions of the form:

$$f_T(t; a, b, c) = \frac{c}{b^{ac} \Gamma(a)} t^{ac-1} e^{-\left(\frac{t}{b}\right)^c} \quad t, a, b, c > 0 \quad (4.20)$$

where  $\Gamma(a)$  is the gamma function, defined as  $\Gamma(a) = \int_0^{\infty} (x^{a-1}) e^{-x} dx$  for any real and positive number  $a$ . The parameters  $a, b, c$  can be classified on the basis of their



S, Start point of mobile movement  
 E, End point of mobile movement  
 $-20 < \alpha < +20$

Fig. 4.6. Paths of five sample mobile users.

physical or geometric interpretation, as one of the three types, namely location, scale and shape. A location parameter  $a$  specifies an abscissa ( $x$ -axis) location point of a distribution's range of values. As  $a$  changes, the associated distribution merely shifts left or right without any other change. A scale parameter  $b$  determines the scale of measurement of the values in the range of the distribution. A change in  $b$  compresses or expands the associated distribution without altering its basic form. A shape parameter  $c$ , distinct from location and scale, determines the basic form or shape of the distribution within the general family of distributions of interest. Substituting different values for  $a, b, c$  produces various distributions as shown in Table 4.1 and Fig. 4.7

The evaluation of the agreement between the distributions obtained by simulation and the best fitted generalized gamma distribution is done by using the Kolmogorov-Smirnov goodness-of-fit test [146]. Given the generalized gamma distribution as the hypothesized distribution, the values of the parameters  $a, b, c$  are found such that the maximum deviation  $\delta$  is a minimum. The maximum deviation shows the biggest divergence between the observed and the hypothesized distributions.

$$\begin{aligned} \delta &= \max |F_T(t) - F_{T_n}(t)| & \forall (t > 0) \\ \delta &= \max |F_T(t) - F_{T_h}(t)| & \forall (t > 0) \end{aligned} \quad (4.21)$$

where  $F_T(t), F_{T_n}(t), F_{T_h}(t)$  represent the probability distributions of the generalized gamma, new call and handover call cell residence times, respectively. Table 4.2 shows the values of  $a, b, c$  for the new call and the handover call cell residence times

**Table 4.1** Different distributions derived from generalized gamma distribution.

$f_T(t; 1, b, 1)$	<i>Exponential distribution</i>
$f_T(t; a, b, 1)$	<i>Gamma distribution</i>
$f_T(t; 1, b, c)$	<i>Weibull' distribution</i>
$f_T(t; n/2, 2, 1)$	<i>Chi-square distribution (n= degree of freedom)</i>
$f_T(t; 1, x\sqrt{2}, 2)$	<i>Rayleigh distribution (x &gt; 0)</i>
$f_T(t; K, 1/\mu, 1)$	<i>Erlang distribution (K= integer value)</i>

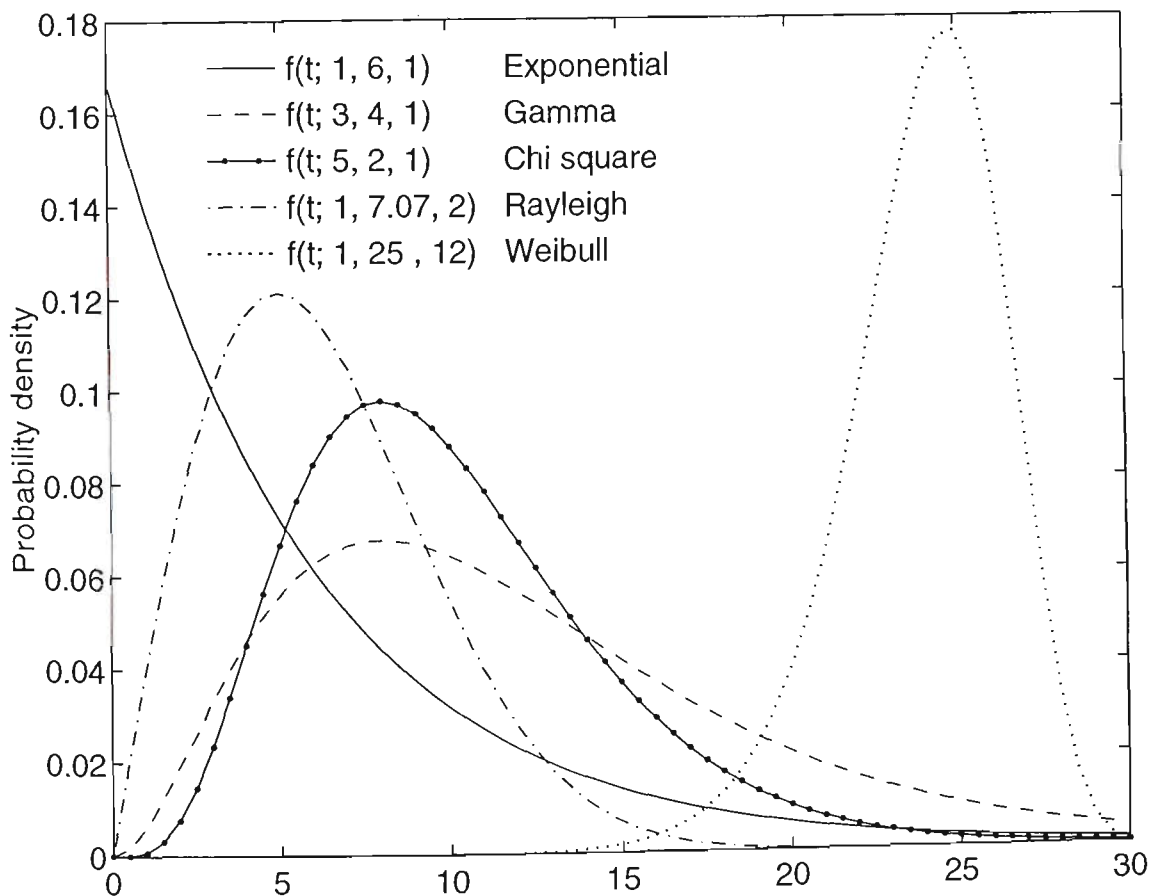


**Fig. 4.7.** Examples of generalized gamma density functions.

**Table 4.2 Best fitted gamma distribution parameters value for the new and handover call residence time.**

New Call			
$R(\text{Km})$	$a$	$b$	$c$
1	0.6201	1.8402	1.8803
2	0.6196	3.6799	1.8799
3	0.6202	5.5196	1.8798
4	0.6203	7.3603	1.8801
5	0.6196	9.2000	1.8798
6	0.6201	11.0397	1.8802
7	0.6197	12.8803	1.8799
8	0.6202	14.7200	1.8804
9	0.6200	16.5598	1.8799
10	0.6199	18.4002	1.8797
Handover Call			
$R(\text{Km})$	$a$	$b$	$c$
1	2.3101	1.2202	1.7203
2	2.3096	2.4405	1.7199
3	2.3102	3.6596	1.7198
4	2.3103	4.8797	1.7201
5	2.3096	6.0996	1.7198
6	2.3101	7.3197	1.7202
7	2.3097	8.5403	1.7199
8	2.3102	9.7604	1.7204
9	2.3100	10.9798	1.7199
10	2.3102	12.2002	1.7203

with a level of significance of 0.05<sup>1</sup>. The data represents the case of a reference cell where the cell radius is  $R$  and the mobiles move with an average speed of 50Km/h and zero drift. It can be observed that the values of  $a$  and  $c$  are constant and independent of cell size, while  $b$  varies with the cell size. The values of  $a, b, c$  for the new call and the handover call cell residence times can be summarised as the follow:

$$\begin{aligned}
 a &= \begin{cases} 0.62 & \text{new call} \\ 2.31 & \text{handover call} \end{cases} \\
 b &\approx \begin{cases} 1.84R & \text{new call} \\ 1.22R & \text{handover call} \end{cases} \\
 c &= \begin{cases} 1.88 & \text{new call} \\ 1.72 & \text{handover call} \end{cases}
 \end{aligned} \tag{4.22}$$

Fig. 4.8. illustrates the probability density function of the new call cell residence time, obtained by simulation and the equivalent generalized gamma function. Fig. 4.9 shows the distribution functions of new and handover cell residence times along with the respective generalized gamma distributions, respectively.

---

1. A 0.05 level of significance means that the probability of any disagreement between the observed distribution and the hypothesized distribution will not be more than 5 per cent of the time

## 4.2 Mean Cell Residence Time

The mean cell residence time for the new call and the handover call can be found by the following relations:

$$E[T_n] = \int_0^{\infty} t \cdot f_{T_n}(t) dt \quad (4.23)$$

$$E[T_h] = \int_0^{\infty} t \cdot f_{T_h}(t) dt \quad (4.24)$$

Yeung and Nanda [121, 122], have shown that for an arbitrary speed pdf and zero

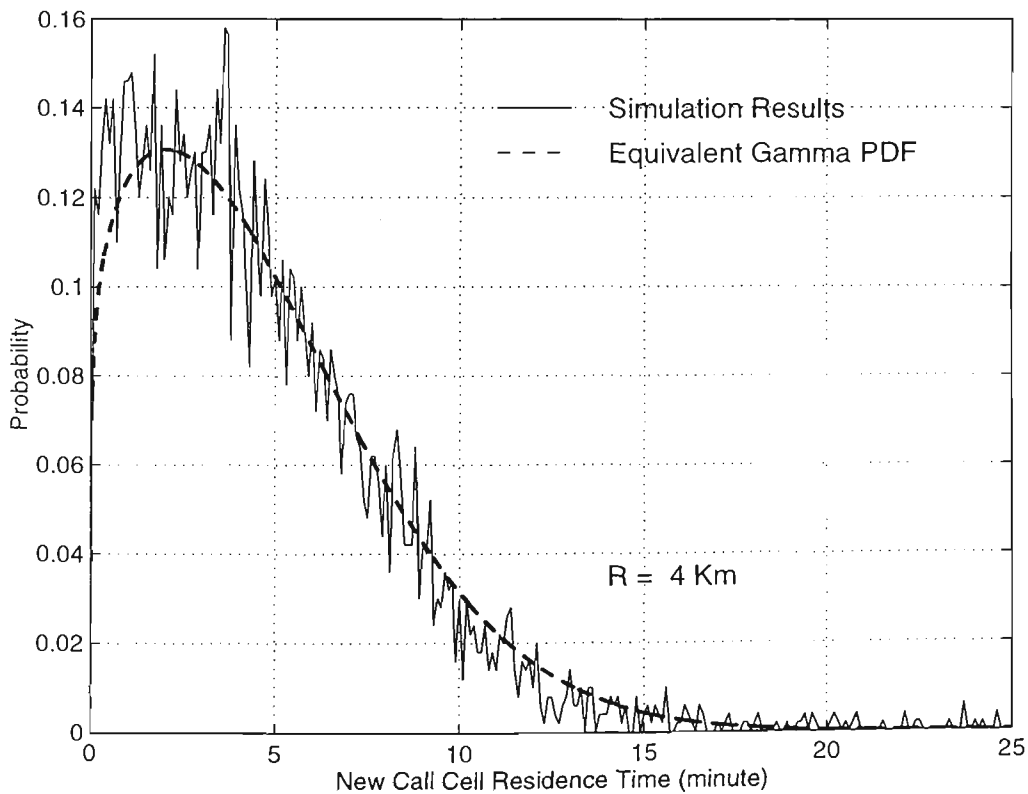


Fig. 4.8. New call cell residence time pdf.



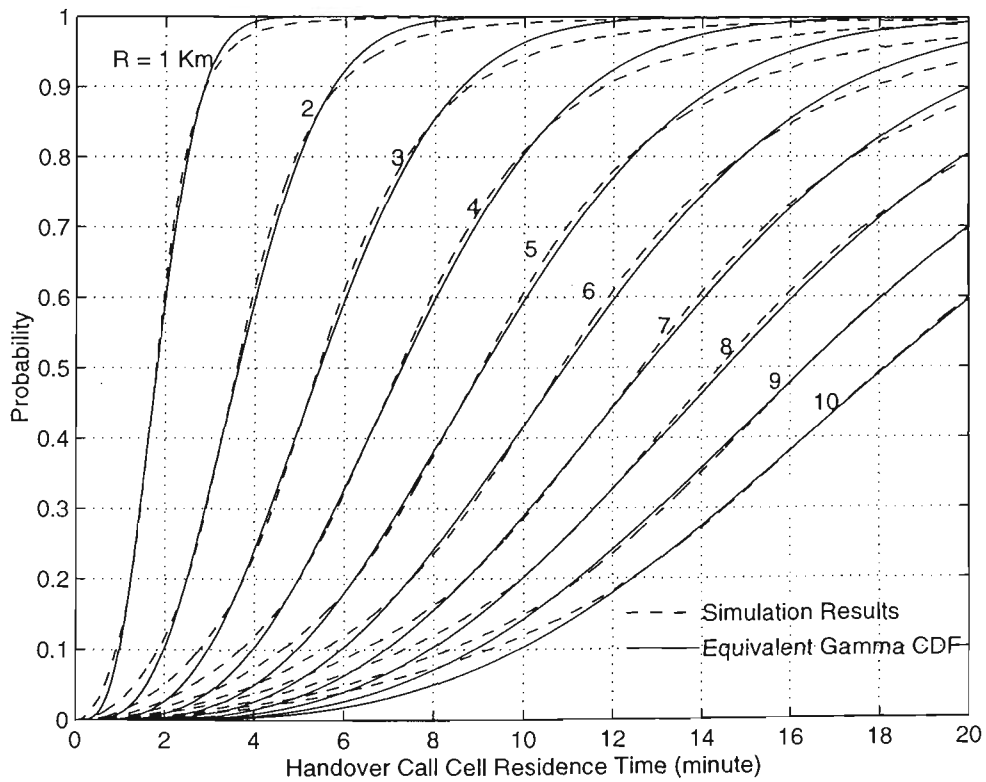
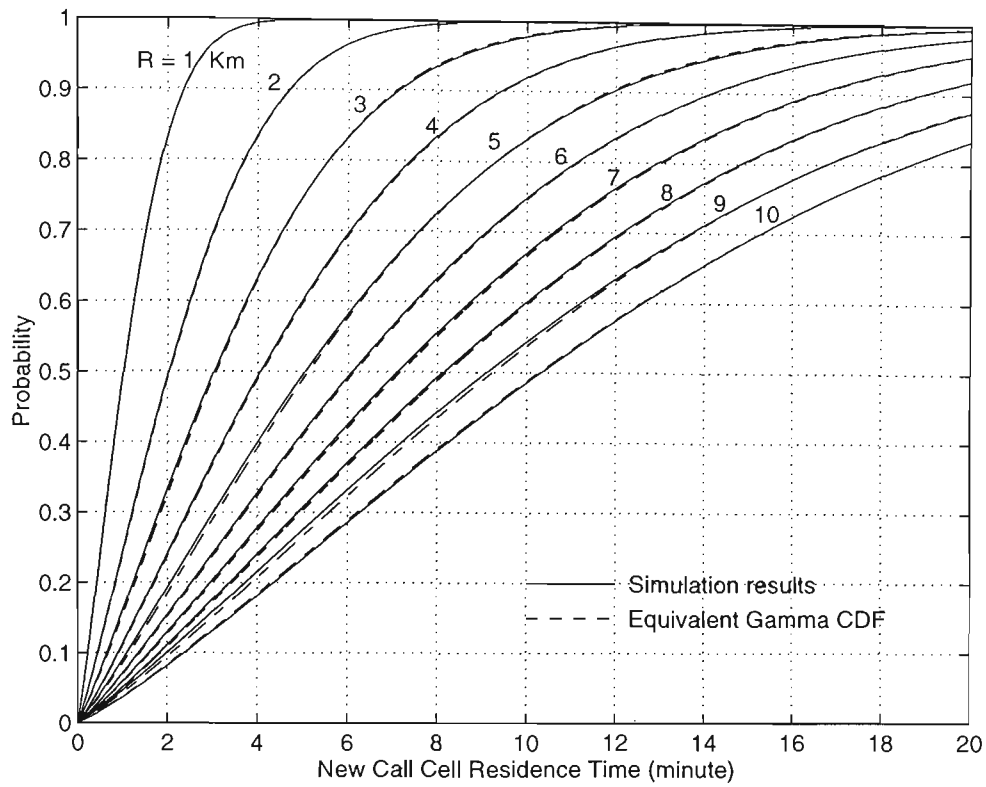


Fig. 4.9. New and handover call cell residence time cdf obtained by the simulation and by the assumption of the equivalent generalized gamma distributions.

drift the mean cell residence time can be obtained by the following equations:

$$E[T_n] = \frac{8R \cdot E[1/V]}{3\pi} \quad (4.25)$$

$$E[T_h] = \frac{\pi R}{2 \cdot E[V]} \quad (4.26)$$

where  $R$  is the cell radius and  $V$  is the speed of the mobile in the cell. A comparison of the results obtained from (4.25)-(4.26) with (4.23)-(4.24) assuming generalized gamma pdf for  $f_{T_n}(t)$  and  $f_{T_h}(t)$  shows that the difference (error) is less than 0.05% in the case of new calls and 0.015% in the case of handover calls (Table 4.3). This further justifies the adoption of generalized gamma distributions to describe the cell residence times.

### 4.3 Effect of Change in Direction and Speed

Depending on the street structure, a mobile can move in different paths and may possess different speeds. The extent of a mobile's change in direction (drift) and change in speed are the two parameters that govern its mobility pattern. The effect of mobile direction and/or speed variations on the boundary crossing for different cell sizes is illustrated in Fig. 4.10. The effect of change in direction or speed of mobiles can be considered as equivalent to a change in an average distance travelled or time spent by a mobile in the cell. Thus any increase in a mobile's drift can be treated as contributing to an effective increase in the cell radius. Similarly, any increase in speed of the mobile can be treated as contributing to a decrease in the cell residence

**Table 4.3** Comparison of results obtained from (4.25)-(4.26) with (4.23)-(4.24).

<i>R</i> (Km)	$E[T_n]$ (min.)			$E[T_h]$ (min.)		
	Eq (4.23)	Eq (4.25)	Error %	Eq (4.24)	Eq (4.26)	Error %
1	1.1876	1.1873	-0.0243	1.8852	1.8850	-0.0123
2	2.3734	2.3745	+0.0490	3.7705	3.7699	-0.0146
3	3.5622	3.5618	-0.0125	5.6550	5.6549	-0.0026
4	4.7509	4.7491	-0.0380	7.5399	7.5398	-0.0012
5	5.9335	5.9363	+0.0473	9.4239	9.4248	+0.0095
6	7.1243	7.1236	-0.0099	11.3091	11.3097	+0.0052
7	8.3081	8.3109	+0.0328	13.1947	13.1947	-0.0004
8	9.5006	9.4981	-0.0258	15.0796	15.0796	+0.0002
9	10.6851	10.6854	+0.0028	16.9651	16.9646	-0.0032
10	11.8710	11.8727	+0.0136	18.8496	18.8496	-0.0003

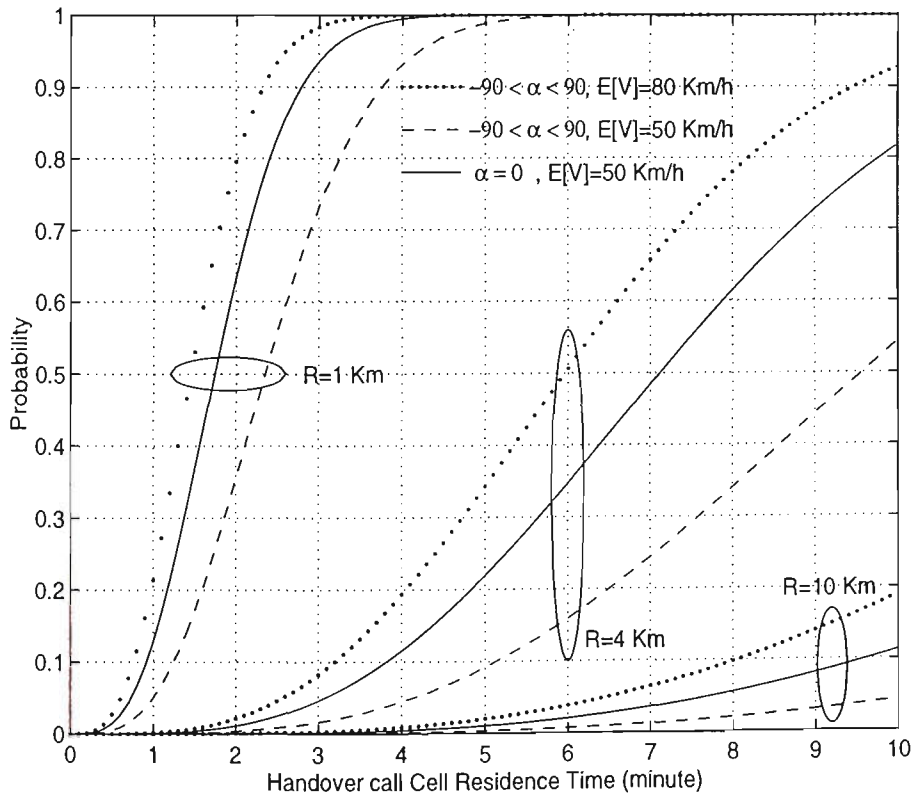
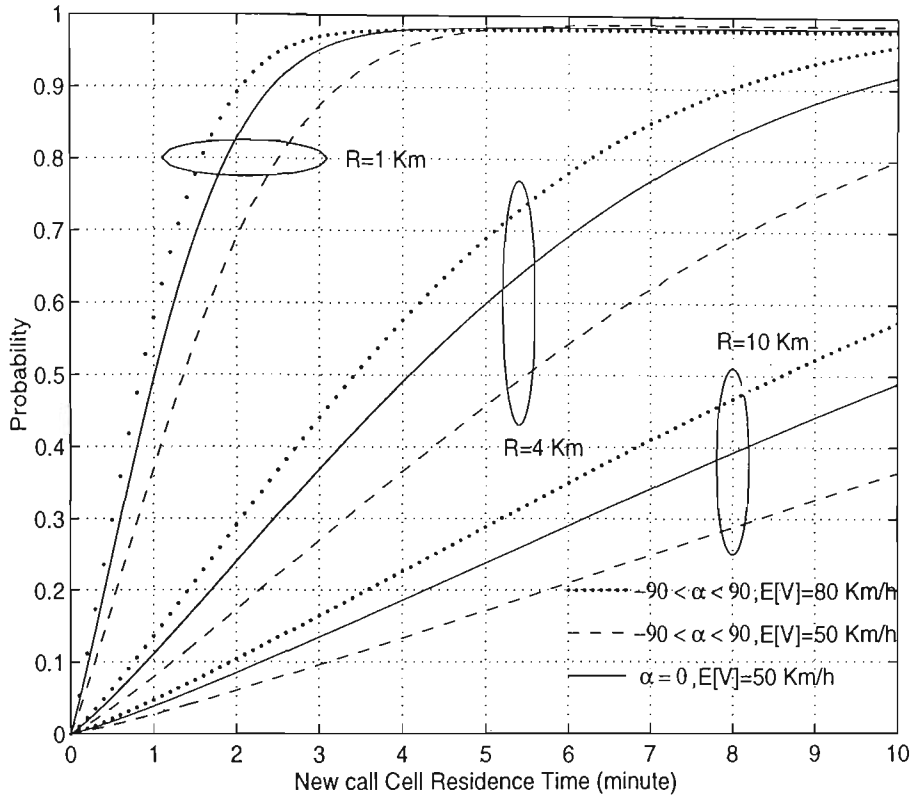


**Fig. 4.10.** Effect of change in mobile direction on the boundary crossing probability.

time which can be interpreted as an effective decrease in the cell size. Therefore, cells with a broad variety of mobility parameters can be replaced by an equivalent reference cell with an effective radius. The reference cell is defined as a cell with the following mobility parameters:

- mobile moves in a straight path, i.e.  $\alpha = 0^\circ$ .
- initial speed of a mobile follows a truncated Gaussian pdf with an average speed  $\mu_v = 50$  [Km/h] and standard deviation  $\sigma_v = 15$ [Km/h].

The main aim is to relate cells with given mobility parameters (i.e. drift  $\alpha$  and average speed  $\mu'_v$ ) to the reference cell. Two different cases are considered.

case i.) cells in which mobiles move with a drift pdf in the range  $-\varphi < \alpha < \varphi$  degrees and speed pdf similar to that of the reference cell. Radius of such cells is denoted by  $R_\alpha$ .

case ii.) cells in which mobiles move with zero drift (similar to the reference cell) and a truncated Gaussian speed pdf with an average value of  $\mu_v = \mu'_v$  [Km/h] and a standard deviation of  $\sigma_v = (\mu'_v - 5)/3$  [Km/h]. Radius of such cells is denoted by  $R_v$ .

Consider a cell with the radius of  $R_\alpha$  having mobility parameters according to case i. The radius of the equivalent cell  $\mathfrak{R}_\alpha$  (which has the same residence time but mobility parameters of the reference cell) is given by:

$$\mathfrak{R}_\alpha = R_\alpha + \Delta R_\alpha \quad (4.27)$$

where  $\Delta R_\alpha$  is the *excess cell radius*. Fig. 4.11 shows the excess cell radius for different drift limits. These curves allow handling of a variety of coverage areas with different streets orientations and traffic flows by representing those with mobility equivalent cells with zero drift. The data obtained by simulation satisfies the empirical relation of (4.28) in a least mean square sense.

$$\Delta R_\alpha = 0.0038\phi R_\alpha \quad (4.28)$$

Therefore the equivalent cell radius will be,

$$\mathfrak{R}_\alpha = K_\alpha R_\alpha \quad (4.29)$$

where  $K_\alpha$  is the proportionality factor and is equal to  $(0.0038\phi + 1)$ .

In the same manner, consider a cell with the radius of  $R_v$  and mobility parameters according to case ii. The radius of an equivalent reference cell  $\mathfrak{R}_v$ , which has the same cell residence time but mobility parameters of reference cell is given by:

$$\mathfrak{R}_v = R_v + \Delta R_v \quad (4.30)$$

where  $\Delta R_v$  is the excess cell radius. Fig. 4.12 shows the excess cell radius for different values of speed obtained by simulation. The data obtained by simulation satisfies the empirical equation of (4.31) in a least mean square sense.

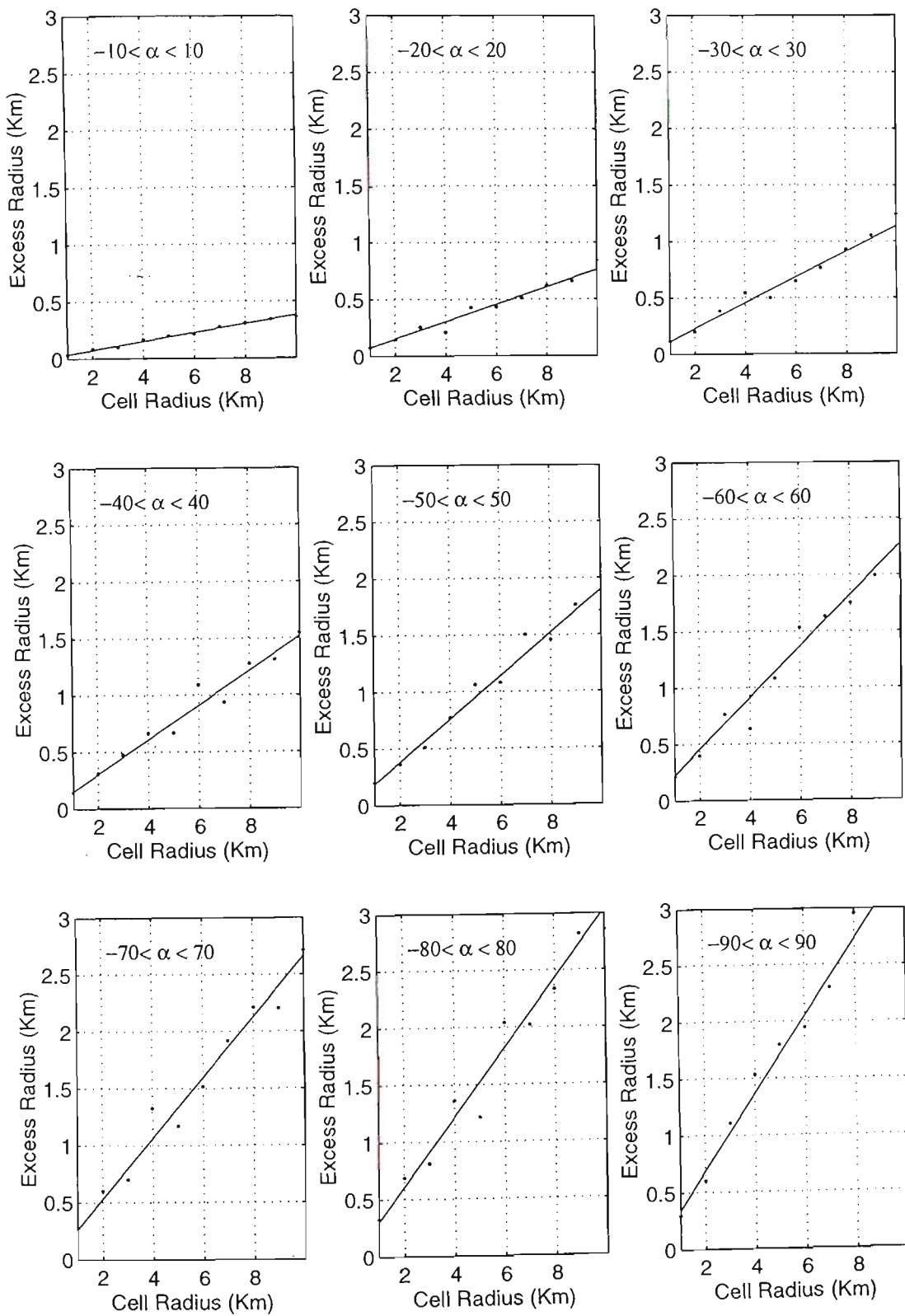


Fig. 4.11. Excess cell radius for different values of drift limits (in degrees).

$$\Delta R_v = \left( \frac{\mu_v}{\mu'_v} - 1 \right) R_v \quad (4.31)$$

Therefore the equivalent cell radius will be:

$$\mathfrak{R}_v = K_v R_v \quad (4.32)$$

where  $K_v$  is the proportionality factor and equals to  $(\mu_v/\mu'_v)$ .

In a case where both drift and speed are different from those of the reference cell, the equivalent cell radius  $\mathfrak{R}_{\alpha v}$  for a cell of radius  $R_{\alpha v}$  can be obtained by the following relation ( $R_{\alpha v}$  is the cell radius of a cell which supports mobility parameters of  $\alpha$  and

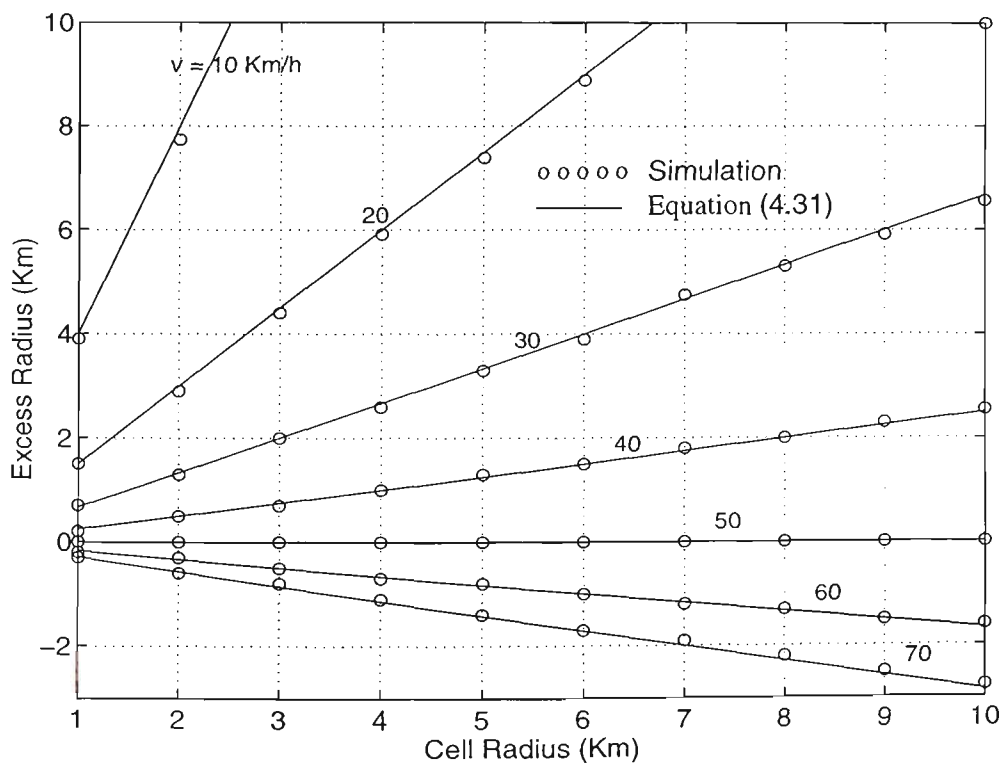


Fig. 4.12. Excess cell radius for different values of mean initial speed.



$\mu'_v$ ),

$$\mathfrak{R}_{\alpha v} = K_v K_\alpha R_{\alpha v} \quad (4.33)$$

Therefore, in a cell of radius  $R_{\alpha v}$ , the gamma distribution parameter  $b$  for a mobile with an average speed  $\mu'_v$  and a drift  $(-\varphi^\circ < \alpha < \varphi^\circ)$  can be described as per (4.22).

$$b = \begin{cases} 1.84 \mathfrak{R}_{\alpha v} & \text{new call} \\ 1.22 \mathfrak{R}_{\alpha v} & \text{handover call} \end{cases} \quad (4.34)$$

The values of  $a$  and  $c$  are constant and given by,

$$a = \begin{cases} 0.62 & \text{new call} \\ 2.31 & \text{handover call} \end{cases} \quad (4.35)$$

$$c = \begin{cases} 1.88 & \text{new call} \\ 1.72 & \text{handover call} \end{cases}$$

#### 4.4 Average Number of Handovers

A mobile can move through several cells while being involved in a call. The number of times a mobile crosses different boundaries during a call is a random variable dependent on the cell size, call holding time and mobility parameters. Each handover requires network resources to reroute the call through a new base station. It is preferred to have as few handovers as possible in order to alleviate the switching load and to decrease the processing burden required in the system. The number of

handovers has a lower bound<sup>1</sup> which is equal to the number of boundary crossings a mobile undergoes. As the number of handovers increases, the handover decision algorithms need to be enhanced so that the perceived QoS does not deteriorate and the cellular infrastructure cost does not skyrocket. In the following sub-sections, we present two different methods to determine the average number of handovers in a cellular system.

#### 4.4.1 Method I

The average number of times a non-blocked call is successfully handed over to the neighbour cell during the call can be obtained from:

$$E[H] = \sum_k k \cdot Prob\{H = k\} \quad (4.36)$$

where  $Prob\{H = k\}$  is the probability that a non-blocked call has  $k$  successful handovers to the successive cells during its life time, and  $H$  is an integer random variable. Let  $P_n$  be the probability that a non-blocked new call will require at least one handover before completion,  $P_h$  denote the probability that a non-failed handover call will require at least one more handover before completion, and  $P_{Fh}$  be the probability that a handover attempt fails. Then [101],

---

1. Uncertainty in the received signal power due to the fading will make many unnecessary handovers during each boundary crossing. This is explained in Chapter 7.

$$\begin{aligned}
\text{Prob}\{H=0\} &= (1 - P_n) + P_n P_{Fh} \\
\text{Prob}\{H=1\} &= P_n(1 - P_{Fh})(1 - P_h + P_h P_{Fh}) \\
\text{Prob}\{H=2\} &= P_n(1 - P_{Fh})P_h(1 - P_{Fh})(1 - P_h + P_h P_{Fh}) \\
&\dots \\
\text{Prob}\{H=k\} &= P_n(1 - P_{Fh})[P_h(1 - P_{Fh})]^{k-1}(1 - P_h + P_h P_{Fh})
\end{aligned} \tag{4.37}$$

Substituting (4.37) in (4.36) gives the average number of handovers per call  $E[H]$  as the following:

$$E[H] = \frac{P_n(1 - P_{Fh})}{1 - P_h(1 - P_{Fh})} \tag{4.38}$$

Let random variables  $T_n$ ,  $T_h$ ,  $T_c$  denote new call residence time, handover call residence time and the call holding time respectively. From classical teletraffic theories it is well known that the call holding time follows negative exponential distribution, i.e., probability that any randomly selected call holding time will end in time duration  $t$  is,

$$F_{T_c}(t) = 1 - e^{-\mu_c t} \tag{4.39}$$

where  $E[T_c] = 1/\mu_c$  is the average call holding time.

The value of  $P_n$  can be obtained as follows:

$$P_n = Prob\{T_c > T_n\} = \int_0^{\infty} Prob\{T_c > t | T_n = t\} \cdot Prob\{T_n = t\} dt \quad (4.40)$$

$T_n$  is mainly dependent on the mobility of the users, and has no influence on the call duration,  $T_c$ . Therefore,

$$\begin{aligned} P_n &= \int_0^{\infty} Prob\{T_c > t\} \cdot Prob\{T_n = t\} dt \\ &= \int_0^{\infty} [1 - F_{T_c}(t)] \cdot f_{T_n}(t) dt \\ &= \int_0^{\infty} e^{-\mu_c t} \cdot f_{T_n}(t) dt \end{aligned} \quad (4.41)$$

Similarly, assuming that call holding time  $T_c$  has an exponential distribution, the value of  $P_h$  can be obtained by the following equation,

$$P_h = Prob\{T_c > T_h\} = \int_0^{\infty} e^{-\mu_c t} \cdot f_{T_h}(t) dt \quad (4.42)$$

The values of  $P_n$  and  $P_h$  can be numerically evaluated by substituting generalized gamma pdf for  $f_{T_n}(t)$  and  $f_{T_h}(t)$  in (4.41)-(4.42) respectively.

#### 4.4.2 Method II

Consider a mobile traversing a path with consecutive cell residence times  $t_1, t_2, \dots$  as

in Fig. 4.13. Assume that a call starts at point  $S$  so that the remaining cell residence time in the cell is  $t'$ . In other words, the random variable  $T_h = \{t_1, t_2, \dots\}$  is handover call cell residence time and the random variable  $T_n = \{t'\}$  is new call cell residence time. The random variables  $T_h$  and  $T_n$  are assumed to be independent and identically distributed with general distributions of  $f_{T_h}(t)$  and  $f_{T_n}(t)$ . The Laplace transform of the handover call cell residence time  $f_h^*(\mu_c)$  can be defined as:

$$f_h^*(\mu_c) = \int_0^{\infty} f_{T_h}(t) e^{-\mu_c t} dt = E[e^{-\mu_c t}] \quad (4.43)$$

From excess life theorem [147] (or residual service time [148]), the Laplace transform of the new call cell residence time  $f_n^*(\mu_c)$  can be obtained as the following:

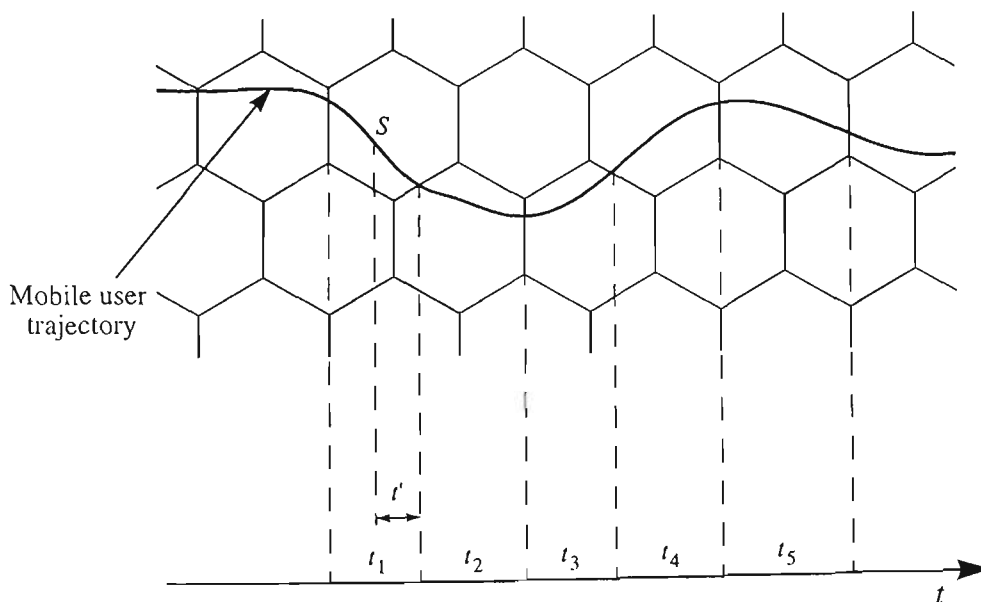


**Fig. 4.13.** Cell residence times for a mobile travelling across cells.

$$f_n^*(\mu_c) = \frac{1}{\mu_c E[T_h]} [1 - f_h^*(\mu_c)] \quad (4.44)$$

The number of handovers experienced by the call depends on the call holding time (which is exponentially distributed with mean  $1/\mu_c$ ), and can be obtained as follows [49]:

$$\begin{aligned} E[H|t', t_2, t_3, \dots] &= 1. \int_{t'}^{t'+t_2} \mu_c e^{-\mu_c x} dx + 2. \int_{t'+t_2}^{t'+t_2+t_3} \mu_c e^{-\mu_c x} dx + 3. \int_{t'+t_2+t_3}^{t'+t_2+t_3+t_4} \mu_c e^{-\mu_c x} dx + \dots \\ &= \int_{t'}^{\infty} \mu_c e^{-\mu_c x} dx + \int_{t'+t_2}^{\infty} \mu_c e^{-\mu_c x} dx + \int_{t'+t_2+t_3}^{\infty} \mu_c e^{-\mu_c x} dx + \dots \\ &= e^{-\mu_c t'} [1 + e^{-\mu_c t_2} [1 + e^{-\mu_c t_3} [1 + \dots \end{aligned} \quad (4.45)$$

Considering  $E[E[H|t', t_2, t_3, \dots]] = E[H|t']$  and using (4.43) we rewrite (4.45) as follows:

$$E[H|t'] = e^{-\mu_c t'} [1 + f_h^*(\mu_c) [1 + f_h^*(\mu_c) [1 + \dots] = \frac{e^{-\mu_c t'}}{1 - f_h^*(\mu_c)} \quad (4.46)$$

Taking the expectation of (4.46) and considering (4.43) and (4.44), we will have,

$$\begin{aligned} E[H] &= \frac{f_n^*(\mu_c)}{1 - f_h^*(\mu_c)} \\ &= \frac{1}{\mu_c E[T_h]} \end{aligned} \quad (4.47)$$

It should be noted that (4.47) is only valid for the case of  $P_{Fh} = 0$ . Fig. 4.14 shows

the average number of handovers per call for a reference cell described in Section 4.3. This figure compares the results obtained from (4.38) and (4.47). Agreement of the two results is another justification for the validity of the proposed cell residence time distributions.

#### 4.5 Channel Holding Time Distribution

The channel holding (or occupancy) time is a random variable defined as the length of time starting from the instant a channel in a cell is seized by the arrival of either a new or a handover call, until the time the channel is released either by completion of the call or by handing over to another cell. In other words, the time spent by a user on

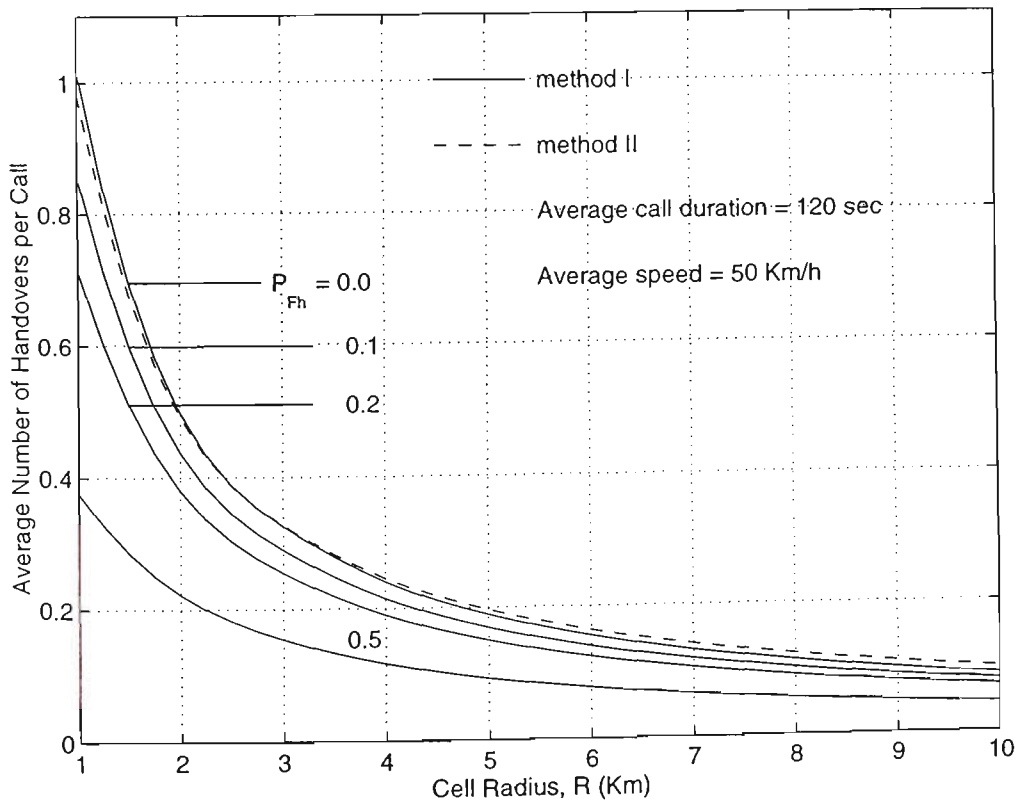


Fig. 4.14. Average number of handovers experienced by a call for different probabilities of handover failures  $P_{Fh}$ .

a particular channel in a given cell is the channel holding time. Channel holding time resembles the call duration in the fixed telephone network. However, in the case of cellular mobile networks, most often, it only corresponds to a portion of the total call duration in which the mobile is located in an associated cell.

Channel holding time is a function of the system parameters such as cell size, user location, user mobility, and call duration. In Fig. 4.15 the time intervals between points  $(A_1, H_{11})$ ,  $(A_2, C_2)$  and  $(A_3, H_{31})$  show channel holding time for three new calls originating at points  $A_1$ ,  $A_2$  and  $A_3$ . The time intervals between points  $(H_{11}, C_1)$ ,  $(H_{31}, H_{32})$  and  $(H_{32}, C_3)$  show the channel holding time for handover calls. When a new call is set up, a channel is occupied until the call is completed in the originating cell ( $SB$  in Fig. 4.16a.) or the mobile moves out of the cell ( $SE$  in Fig. 4.16a). Therefore, channel holding time of the new call  $T_N$ , is either  $T_n$  or  $T_c$  whichever is less.

$$T_N = \min(T_n, T_c) \quad (4.48)$$

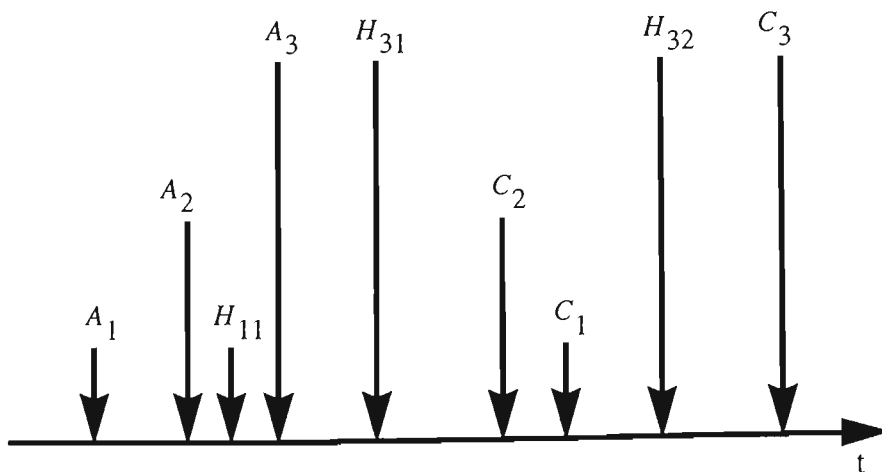


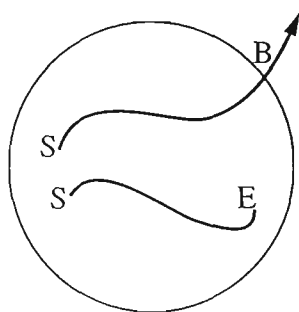
Fig. 4.15. Illustration of handover within various call duration.



A similar reasoning applies to a call which is handed over from a neighbouring cell. In this case, the channel is occupied until the call is completed ( $CE$  in Fig. 4.16b) or the mobile moves out to another cell ( $AB$  in Fig. 4.16b). Therefore, because of the memoryless property of the exponential distribution, the residual call time after a handover is independent of the time elapsed since the start of the call. As a result, the probability distribution of the residual call time given the time elapsed since the start of the call is the same as that of the original call duration  $T_c$ . Therefore, channel holding time of the handover call  $T_H$ , is either  $T_h$  or  $T_c$  whichever is less,

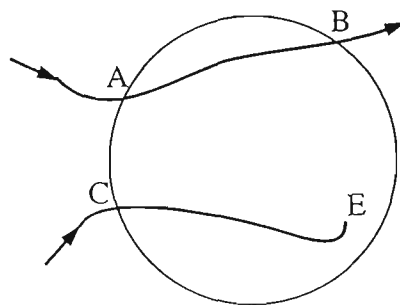
$$T_H = \min(T_h, T_c) \quad (4.49)$$

Since  $T_n$  and  $T_h$  are mainly dependent on the physical movement of the mobile, and have no influence on the total call duration  $T_c$ , it is reasonable to assume that the random variables  $T_n$  and  $T_h$  are independent of  $T_c$ . Therefore, distribution function



$SB \equiv T_n$  New call cell residence time  
 $SE \equiv T_c$  Call holding time

(a)



$AB \equiv T_h$  Handover call cell residence time  
 $CE \equiv T_c$  Residual call time

(b)

**Fig. 4.16.** Illustration of the new and handover call cell residence time.

of the  $T_N$  and  $T_H$  can be calculated by (Appendix C):

$$\begin{aligned} F_{T_N}(t) &= F_{T_c}(t) + F_{T_n}(t) - F_{T_c}(t)F_{T_n}(t) \\ F_{T_H}(t) &= F_{T_c}(t) + F_{T_h}(t) - F_{T_c}(t)F_{T_h}(t) \end{aligned} \quad (4.50)$$

The distribution of channel holding time in a given cell is a weighted function of  $F_{T_N}(t)$  and  $F_{T_H}(t)$ . If  $\zeta$  is the fraction of the average non-blocked new calls out of average total number of calls in a cell, the fraction of the average number of successful handed over calls will be  $1 - \zeta$ . Therefore, the distribution function of the channel holding time including both new and handover calls will be,

$$F_{T_{ch}}(t) = \zeta F_{T_N}(t) + (1 - \zeta)F_{T_H}(t) \quad (4.51)$$

$\zeta$  can be expressed in terms of the average number of handovers per call  $E[H]$  as:

$$\zeta = \frac{1}{1 + E[H]} \quad (4.52)$$

Eq. (4.51) can be rewritten in terms of the cell residence time and call holding time distributions as:

$$F_{T_{ch}}(t) = F_{T_c}(t) + \frac{1}{1 + E[H]}(1 - F_{T_c}(t))(F_{T_n}(t) + E[H]F_{T_h}(t)) \quad (4.53)$$

A numerical solution to (4.53), assuming generalized gamma distribution for  $T_n$  and  $T_h$  indicates that the distribution function of the channel holding time in a cell

follows exponential distribution. Fig. 4.17 shows distribution functions of the random variables  $T_n$ ,  $T_h$ ,  $T_c$  and  $T_{ch}$  for a cell of size 3 Km using generalized gamma distribution for  $T_n$ ,  $T_h$ , exponential distribution for  $T_c$  and (4.53) for  $T_{ch}$ . The same figure shows comparison of an exponential distribution with the same average value as of  $T_{ch}$ . It can be seen that the channel holding time distribution fits well with the exponential distribution. This agrees with the result obtained in [103] and assumed in [101]. The average channel holding time in a cell,  $E[T_{ch}] = 1/\mu_{ch}$ , can be obtained by (Appendix D):

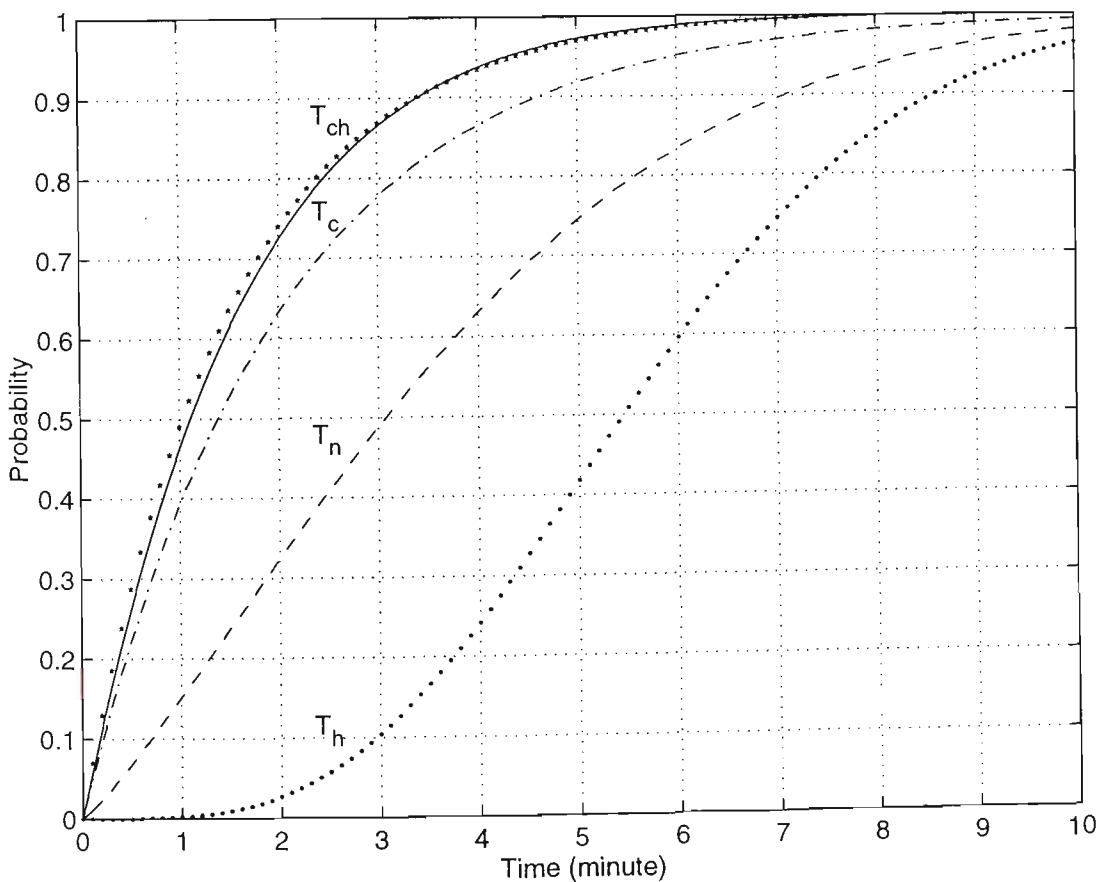


**Fig. 4.17.** Cdf of different random variables for a cell size of 3 Km. Cdf of  $T_{ch}$  is shown as per (4.53) with solid lines as well as a negative exponential distribution with stars.

$$E[T_{ch}] = t_0 - \int_0^{t_0} F_{T_{ch}}(t) dt \quad (4.54)$$

where  $t_0$  is the maximum channel holding time. The average channel holding time is a function of cell parameters such as mobility, and cell size as well as average call holding time. Fig. 4.18 illustrates the variation of the average channel holding time with cell size of the reference cell. It shows that as the cell size increases, the average channel holding time  $E[T_{ch}]$  approaches the average call holding time  $E[T_c]$  which could be expected.

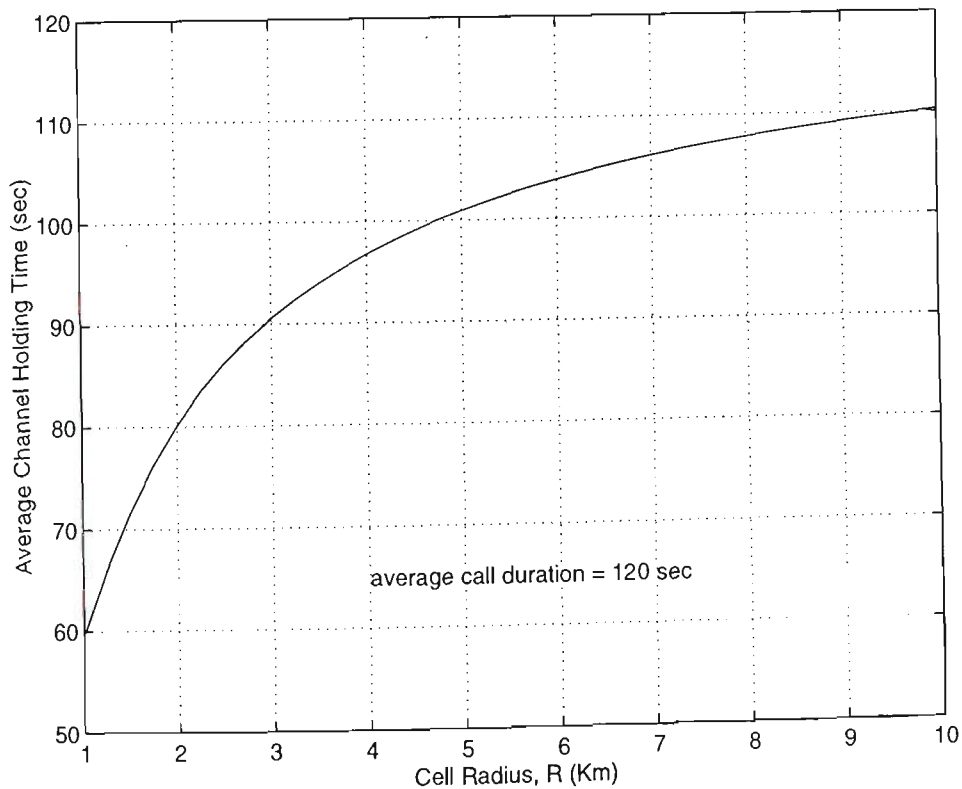


Fig. 4.18. Variation of the average channel holding time with cell size in the reference cell.

## 4.6 Conclusions

The mobility model developed in Chapter 3 has been used to characterise different mobility related traffic parameters in a cellular mobile communication system. These include the distribution of the cell residence time of both new and handover calls, channel holding time and the average number of handovers per call. Results show that the generalized gamma distribution is adequate to describe the cell residence time distribution of both new and handover calls. It is also shown that the negative exponential distribution is a good approximation for the channel holding time distribution in cellular mobile systems.

In order that the results could be made applicable to a wide range of cellular environments, it was shown that an increase in mobile drift in a cell can be treated as contributing to an effective increase in the cell radius. Similarly, it was shown that an increase in the speed of a mobile in a cell can be treated as contributing to a decrease in the cell size, and vice versa. Taking this excess cell radius into account for different values of drift and speed, a broad variety of cell coverage areas with different street orientations and traffic flows can be proportionate to an equivalent reference cell. Therefore, the distributions for the new call and handover call cell residence times as well as the channel holding time distribution can be determined for different cellular environments with various mobility parameters.

# *Chapter 5*

## *Effect of Handover on the Teletraffic Performance Criteria*

Unlike a fixed network, a cellular network must support mobile customers. In a cellular mobile communication network, the number of users associated with a base station at any given time instant is a random variable due to the mobile nature of the users. This inherent feature affects the behaviour of the cellular network in terms of its offered traffic and requires a new approach for teletraffic performance analysis. Consideration has to be given to issues such as handover attempt failure, call dropout and so on. In this Chapter, different radio resource allocation schemes are explained, a basis for teletraffic performance evaluation is explained, and an analytical model for teletraffic analysis is described. Also, some traffic policies that give a higher level of protection to handover calls are analysed, and their effect on the overall traffic

performance is assessed. Finally, a teletraffic simulation program which uses the next-event time-advance approach is described.

The random variables involved in modelling teletraffic in a cellular network are not totally amenable to analytical representation. Therefore a simulation procedure based on next-event time-advance approach could be utilized. This requires the generation of all attributes of the on-going and up-coming calls in the network, by simulation. In traditional fixed telephone networks, such attributes are confined to the call duration and interarrival time only. However, in a cellular mobile network, a channel could be occupied by the arrival of a new call or a handover call and it could be released either by the completion of the call or by handing it to the neighbour cell. Therefore, in cellular mobile communication networks, other attributes, namely the cell residence time of both new and handover calls, should also be taken into account. In Chapter 4, it has been shown that the cell residence time follows the generalized gamma distribution in the general case where the movement of users is governed by a set of random variables. Based on this result, a teletraffic model is developed to investigate the impact of handover on the cellular network performance. In particular it is aimed at studying how traffic performance is related to different system parameters such as user mobility and cell size.

## 5.1 Radio Resource Allocation

Efficient utilization of the radio resource (i.e., spectrum allocated for the cellular communications) is certainly one of the major challenges in cellular system design. All of the proposed schemes suggest the reuse of the same radio frequencies in

non-interfering cells and have given rise to several channel assignment strategies.

Channel<sup>1</sup> assignment strategies [149] can be classified as fixed (FCA) [4, 150] and dynamic (DCA) [4, 138, 139, 151, 152]. In between the extremes of fixed and dynamic channel assignments, there are many possible alternatives, such as hybrid schemes [153, 154], load sharing schemes (including directed retry [155] and directed handover [156]) and channel borrowing schemes [149, 157, 158]. These other schemes are described under flexible channel assignment in this Chapter.

### 5.1.1 Fixed Channel Assignment (FCA)

In the FCA scheme, each cell has its own distinct channel subset which is different from the channel subset allocated to its neighbouring cells. The channel subsets are reused in cells separated by a prescribed distance, called the reuse interval. So, when a call-in-progress crosses into a new cell, a new channel will have to be found for the call. If an idle channel is not found, the call-in-progress is terminated abruptly. This will happen even though there may be vacant channels in adjacent cells. Therefore, FCA could not attain a high efficiency of total channel usage over the whole service area if the traffic varies dynamically from cell to cell. However, FCA has the advantage that it requires a moderate amount of radio equipment in base station and a simple control algorithm. FCA is superior when traffic demand is high.

### 5.1.2 Dynamic Channel Assignment (DCA)

---

1. Channels can be time slots, frequencies, spreading codes or a combination of these



At the other extreme is the dynamic channel assignment scheme, where “dynamic” means that the channels are not preassigned to base stations but are allocated according to their needs. The dynamic channel assignment implies the lack of a fixed relationship between cells and channels. In this approach, all channels are kept in a central pool and allocated to cells as required by the real time traffic load. Since it is not permanently attached to any particular base station, a dynamic channel can float with the mobile as it moves from cell to cell. The only restriction is that the cochannel interference constraint should be satisfied. When a mobile moves into a new cell, the originally-assigned dynamic channel is checked at the new base station and all base stations within the reuse interval. If the channel passes this check (i.e. it is not already in use at those stations), it is allowed to continue serving the call. However, if the original channel is busy elsewhere within a reuse interval of the new base station, a whole new dynamic channel search is undertaken, identical to the one used for new calls. If a substitute channel is not available, then the call is terminated. Such assignment method can significantly increase the traffic capacity of the network, especially if serving calls can be assigned new channels according to the demand arising from new and handover calls.

A particular advantage of dynamic channel assignment is that the system can adapt to time varying traffic requirements. This allows real-time network traffic management in a cellular network. The disadvantage of dynamic channel assignment is that its practical implementation requires a great deal of processing power to determine optimal allocations, and a heavy signalling load on the system to implement all the channel changes. Among different DCA techniques, the Maximum Packing algorithm introduced by Everitt et al. [159] is of special theoretical interest as it

claims to achieve optimum performance. Since this algorithm requires system-wide information, the complexity of searching all possible re-allocations renders this strategy hard to implement. While DCA uses channels more efficiently than FCA at low traffic intensity, it does not show better performance and can even get worse at high traffic intensity. The reason for this can be explained as follows: Assume that  $D$  is the distance between two cells using the same channel and  $D_R$  is the minimum distance necessary to prevent co-channel interference. In the case of FCA, the channels are assigned to cells in advance so that  $D$  equals to  $D_R$ . In the case of DCA, since the channels are assigned dynamically on demand,  $D$  tends to be greater than  $D_R$ . This makes the number of the reusable channels in DCA less than that of FCA, especially when traffic intensity is high.

### 5.1.3 Flexible Channel Assignment

In between the extremes of fixed and dynamic channel assignments, there are many possible alternatives, such as hybrid channel assignment, channel borrowing and schemes such as directed retry and directed handover, which take advantage of the fact that some percentage of the mobiles may be able to obtain sufficient signal quality from two or more cells. With the hybrid scheme, one subset of channels is fixed and the rest is kept in a common pool. This scheme is meant to gain advantages of both fixed and dynamic channel assignments.

In most systems the mobiles are always connected to the base station to which they receive the strongest received signal. However, in some situations the utilization of the spectrum can be improved if mobiles are permitted to use base stations besides

the strongest. In fact, this happens mostly in the overlap area where received signal strength from different base stations could be enough to be connected. Based on this, Eklundh has proposed a variation of FCA called directed retry. In this approach, if the base station with the highest signal power can not accommodate another call, the mobile with the new call has the opportunity to establish a connection with the base station with the second highest power. Directed retry preserves the metrics of the FCA and at the same time, reduces the blocking probability of a cell by increasing its channel utilization. The improvement is accomplished at the expense of an increased number of handovers and an increased level of cochannel interference. A traffic analysis of directed retry can be found in [160]. In [156], the scheme was enhanced in a way that both on-going calls and new calls were allowed to be redirected to another base station. Hence, the traffic load is shared among the base stations and the blocking probability is decreased. This method is called directed handover. The disadvantage with these load sharing methods (i.e. directed retry and directed handover) is that if a mobile does not use the base station with the highest signal power it becomes more sensitive to interference.

During the operation of a cellular system, unexpected growth of traffic may develop in various cells and create traffic congestions. Therefore, a method which is adaptive to such a change will improve the capacity efficiency. Channel borrowing scheme is known to be a viable solution to alleviate congestions. In this method all channels are nominally pre-allocated to the base stations (same as FCA), but may be borrowed on demand by other base stations.

Lin, Noerpel and Harasty [161] recently have proposed a new channel assignment

scheme called sub-rating scheme (SRS) that creates a new channel on a blocked base station for a handover access attempt by sub-rating an existing call. Sub-rating means an occupied full-rate channel is temporarily divided into two channels at half the original rate: one to serve the existing call and the other to serve the handover request.

## 5.2 Teletraffic Performance Parameters

The teletraffic performance can be assessed in terms of the grade of service, the traffic carried by the network, the channel utilisation, and the spectrum efficiency. The grade of service is defined as any practical interpretation of a congestion function [162]. In a fixed network, this parameter refers to the probability that a call trying to access the system is denied because of channel unavailability. However, in the case of a cellular network, because of its unique features, this simple definition is insufficient, and the grade of service (GoS) is defined to include a combination of the following probabilities.

### 5.2.1 Setup channel blocking probability

In a cellular network, a control channel is often allocated exclusively for setting-up the calls. When a mobile attempts to make a call, it accesses the network first through the setup channel. The setup channel may handle the arriving traffic on a delay basis or on a loss basis. For the delay case, the call setup delay can be calculated using the Erlang *C* formula. For the loss case, the setup channel may be of ALOHA type with a collision probability, or of blocked-calls-cleared (BCC) type discipline with the

probability of loss  $P_{Bs}$  calculated according to the Erlang  $B$  formula.

### 5.2.2 New call blocking probability

If the setup channel is free, the mobile station transmits a seizure message requesting a voice radio channel. The new call blocking probability  $P_{Bn}$  represents the probability that a call attempt which succeeds in accessing the setup channel fails to access the network because of the unavailability of a free radio channel. This probability can be defined as:

$$\begin{aligned}
 P_{Bn} &= \text{Prob}\{\text{a new call arrives in a cell when all channels are occupied}\} \\
 &= \frac{\text{number of new calls fail to obtain a channel}}{\text{number of new call attempts}} \quad (5.1)
 \end{aligned}$$

### 5.2.3 Fixed network blocking probability

Most of the mobile calls pass through the fixed network. Therefore, any blocking due to unavailability of link through the fixed network affects the GOS of the mobile radio network. It is usually assumed that the blocking probability of the fixed network  $P_{Bl}$  is much smaller than that of the cellular network due to the limited availability of the mobile radio channels. For the mobile to mobile call, the fixed network may not be involved (if they are in the same cell), and hence its reliability does not affect the GOS. In this situation, the fixed network blocking probability is replaced by the probability of blocking of the radio channel in the other cell within which the called party is reached.

### 5.2.4 Handover attempt failure probability

A distinct feature of cellular networks is the handover where a mobile crossing its cell boundary during a call needs to be allocated a new channel in a new cell. The probability that this reallocation cannot be achieved is referred to as handover call blocking, or handover attempt failure probability,  $P_{Fh}$ . The handover failure probability represents the proportion of handover requests which are blocked during handover request. This parameter can be defined as:

$$\begin{aligned}
 P_{Fh} &= \text{Prob}\{\text{a handover call arrives when all channels are occupied}\} \\
 &= \frac{\text{number of handover calls fail to obtain a channel}}{\text{number of handover call attempts}} \quad (5.2)
 \end{aligned}$$

Handover failure probability is a good performance measure, because it reflects on the number of boundary crossings and hence the mobility of the mobile.

### 5.2.5 Dropout probability

The probability that a call will be dropped out during a call is another measure of traffic performance. This may arise either due to insufficient signal strength through fading of the radio signal, or through an unsuccessful handover attempt. Even if one neglects the dropout through signal fading, the probability of dropout is different from the handover blocking probability, because a mobile may cross several cell boundaries successfully before striking a boundary where it is blocked. The dropout probability  $P_D$  is defined as the probability that a non-blocked new call will be dropped out at some point during a call, while the handover blocking probability is

simply the same measure per cell boundary crossing. A forced termination (i.e. dropout) can be preceded by several successful handovers. Therefore,

$$\begin{aligned}
 P_D &= \text{Prob}\{\text{Forced termination of a call due to a handover failure}\} \\
 &= \frac{\text{number of calls forced to terminate}}{\text{number of the non blocked new call attempts}} \quad (5.3)
 \end{aligned}$$

A fraction of the new calls which are not blocked will eventually be forced into termination if it succeeds in each of the first  $(l-1)$  handover attempts, but fails on the  $l$ th handover attempt, i.e.,

$$P_D = \sum_{l=1}^{\infty} \text{Prob}\{(l-1)\text{successful handover}\} \cdot \text{Prob}\{l \text{ th handover fails}\} \quad (5.4)$$

where,

$$\begin{aligned}
 \text{Prob}\{(l-1)\text{successful handover}\} &= P_n(1-P_{Fh}) \cdot P_h(1-P_{Fh}) \cdot \dots \cdot P_h(1-P_{Fh}) \\
 &= P_n \cdot P_h^{l-2} \cdot (1-P_{Fh})^{l-1} \quad (5.5)
 \end{aligned}$$

and,

$$\text{Prob}\{l \text{ th handover fails}\} = P_h \cdot P_{Fh} \quad (5.6)$$

where  $P_n$  is the probability that a non-blocked new call will require at least one

handover before completion, and  $P_h$  denotes the probability that a non-failed handover call will require another handover before completion. Hence:

$$\begin{aligned}
 P_D &= P_{Fh} P_n \sum_{l=1}^{\infty} (1 - P_{Fh})^{l-1} P_h^{l-1} \\
 &= \frac{P_{Fh} P_n}{1 - (1 - P_{Fh}) P_h}
 \end{aligned} \tag{5.7}$$

### 5.2.6 Unsuccessful call probability

Assuming that setup channel and fixed network blocking probabilities are negligible, the probability of an unsuccessful call  $P_u$  is the probability that a call is not completely served due to either the initial blocking of the call attempt or the failure of a subsequent handover request. Therefore,  $P_u$  is the sum of the probabilities of blocking at the start of the call and dropping out afterwards and could be obtained by,

$$P_u = P_{Bn} + P_D(1 - P_{Bn}) \tag{5.8}$$

## 5.3 Teletraffic Analysis

Due to the occurrence of handover and forced call termination, the simple Erlang loss formulas or other product form solutions cannot be applied directly in cellular systems [132, 163]. To clarify this point, Fig. 5.1 shows the Markov chain reflecting traffic in two isolated adjacent cells with each cell supporting up to  $n$  simultaneous calls. A state of the system is shown by  $(n_1, n_2)$ , where  $n_1$  is the number of calls in



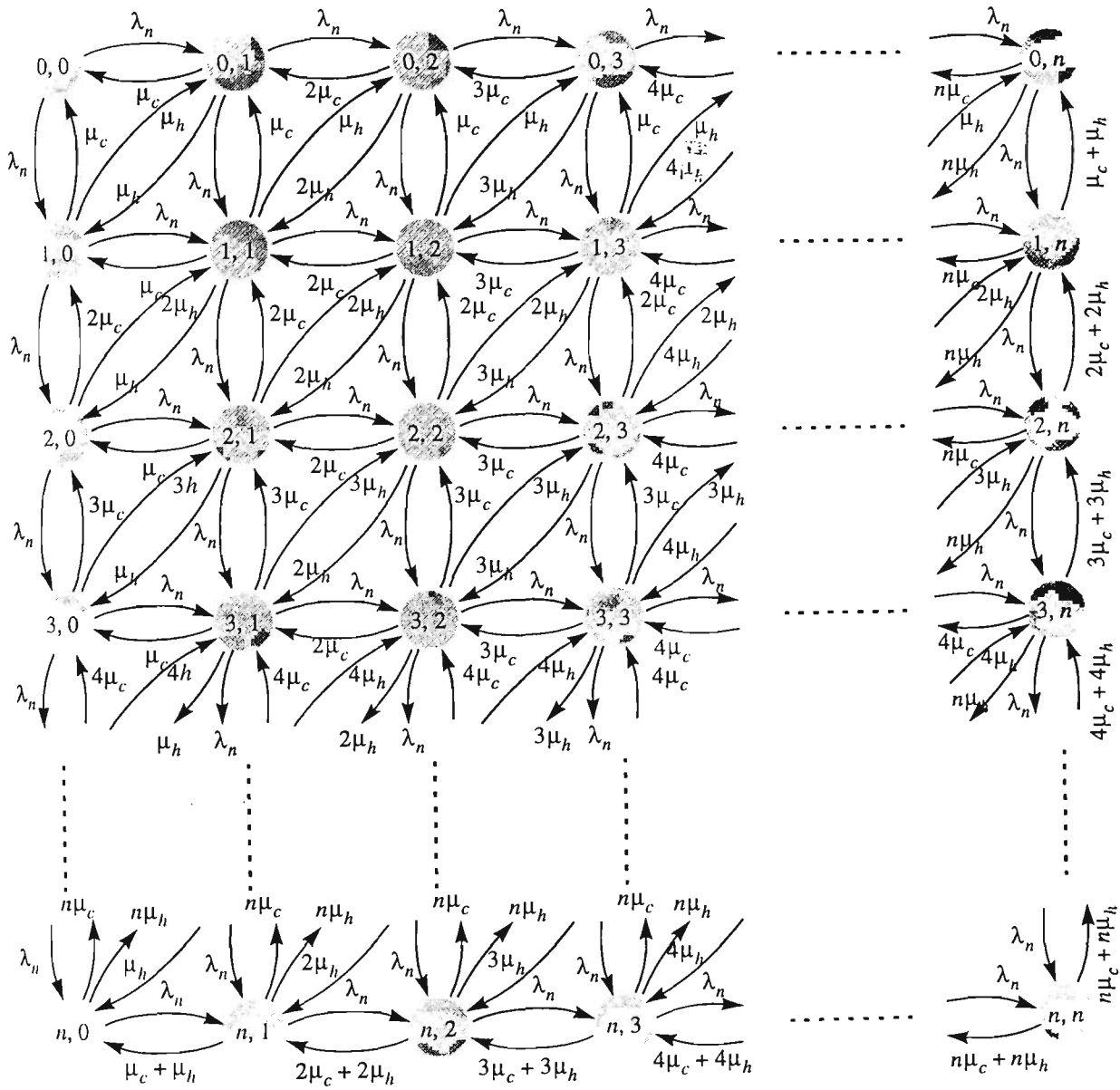


Fig. 5.1. Markov chain representation of two cells with  $n$  channels.

progress in cell 1 and  $n_2$  is the number of calls in progress in cell 2. Let  $\mu_c$  and  $\mu_h$  be the call completion rate and handover rate respectively per cell. The transition rates from state  $(n_1, n_2)$  to state  $(n_1 - 1, n_2)$  and from state  $(n_1, n_2)$  to state  $(n_1, n_2 - 1)$  are given by  $n_1\mu_c$  and  $n_2\mu_c$  respectively. However, the transition rates for the boundary states where  $n_1 = n$  or  $n_2 = n$  are given by  $n_1(\mu_c + \mu_h)$  and  $n_2(\mu_c + \mu_h)$  respectively. Only when  $\mu_h = 0$  (which corresponds to a system without handovers such as a fixed telephone network), the equilibrium state distribution has a product form solution given by:

$$p(n_1, n_2) = p_0 \binom{n_1}{n_1!} \binom{n_2}{n_2!} \quad (5.9)$$

where  $p(n_1, n_2)$  represents the steady state probability of having  $n_1$  calls in cell 1 and  $n_2$  calls in cell 2. Here,  $p_0$  is the normalization constant, and  $\rho_o$  is the offered traffic in the network given by  $\rho_o = \lambda_n / \mu_c$ , where  $\lambda_n$  is the average new call arrival rate per cell. However, if the number of handovers is not negligible, the exact steady state distribution does not have a product form solution. In this case, analytical modelling can be performed using the following approximation.

Let the arrival of calls to a cell consist of the newly initiated calls within the cell (new calls) and the calls handed over from the neighbouring cells (handover calls). Assuming that both new and handover call arrivals are Poisson processes with average call arrival rates  $\lambda_n$  and  $\lambda_h$ , respectively, the total call arrival rate  $\lambda_t$  per cell will be the superposition of the two Poissonian streams such that,

$$\lambda_t = \lambda_n + \lambda_h \quad (5.10)$$

Considering the fact that superposition of the two Poissonian streams is also a Poisson process, the total call arrival rate will be a Poisson process. A channel completion time (the length of time that a call remains in a cell) is determined by the time the channel becomes free after a call completion or a call handed over to another cell. Therefore, the total channel service rate  $\mu_{ch}$  will be the sum of the call completion rate  $\mu_c$  and the call handover rate  $\mu_h$ .

$$\mu_{ch} = \mu_c + \mu_h \quad (5.11)$$

Hence, the total effective traffic intensity in a cell due to new and handover calls will be:

$$\rho_e = \lambda_t / \mu_{ch} \quad (5.12)$$

Let  $P_B$  be the overall blocking probability in a cell. Then, the total departure rate of calls from the cell is  $\lambda_t(1 - P_B)$ . Therefore,

$$\lambda_h = \lambda_t(1 - P_B) \frac{\mu_h}{\mu_h + \mu_c} \quad (5.13)$$

where  $\mu_h / (\mu_h + \mu_c)$  is the probability that a call will hand over to neighbour cell, otherwise it will terminate inside the cell. Rearrangement of (5.13) will result in:

$$\lambda_i = \frac{\lambda_n(\mu_h + \mu_c)}{\mu_c + \mu_h P_B} \quad (5.14)$$

From (5.11)-(5.14), after some algebraic manipulation, the effective offered traffic  $\rho_e$  can be found as,

$$\rho_e = \lambda_n / (\mu_c + \mu_h P_B) \quad (5.15)$$

If the product of the average call holding time and the average velocity of a mobile is small compared to the cell size (i.e.,  $v/\mu_c \ll R$ ), the probability of the mobile crossing a cell boundary during a call is low. In this case, the probability of new call blocking is the major indication of system traffic performance and the offered traffic to a cell in the absence of any handover calls will simply be  $\lambda_n/\mu_c$ . Any decrease in cell size results in an increase in the handover rate resulting an increase in handover blocking probability. A premature call termination due to failure during handover forces the mean effective call duration to decrease (or call departure rate to increase). In order to make the system in Fig. 5.1 reversible and to take the overall call blocking probability  $P_B$  into account, it is assumed that the effective call duration of a new call is exponentially distributed with mean  $1/\mu_e$ , where  $\mu_e = \mu_c + \mu_h P_B$ .

In the case where there is no assigned priority to handover calls, a handover call entering a cell requires a channel in the new cell just as a call originating in the cell does. Hence, the same fraction of either category of calls will be unsuccessful. That is, the blocking probability of a new call  $P_{Bn}$ , the failure probability of a handover call  $P_{Fh}$ , and the overall call blocking probability  $P_B$  will be the same and can be

found using Erlang-B formula as per (5.16),

$$P_B = P_{Bn} = P_{Fh} = \frac{\rho_e^C / C!}{\sum_{i=0}^C \rho_e^i / i!} \quad (5.16)$$

where  $C$  is the number of channels allocated to a cell. Equation (5.16) should be solved iteratively, since  $\rho_e$  is related to the blocking probability.

## 5.4 Handover Prioritization Schemes

When all channels assigned to a cell are occupied, any handover attempt to that cell will be blocked, causing a forced termination of the call in progress. Such an interruption is perceived as more annoying to a user than a failure to set up a new call which only contributes to a delay in establishing a communication link. It is therefore necessary to establish traffic policies that minimize the probability of forced termination of calls in progress due to handover failures, while not penalizing the new calls too much. The probability of handover call failure can be decreased by giving some form of priority to handover requests over the new call attempts. Two generic handover prioritization schemes have been proposed and studied to reduce the dropout probability, namely:

- Reserved channel scheme [101, 164],
- Queueing prioritization schemes [101, 127, 165, 166].

Other prioritization schemes can be viewed as variations of the above. Handover prioritization schemes, in general, result in a decrease in handover failures and an increase in new call blocking which, in turn, reduces total carried traffic.

### 5.4.1 Reserved channel scheme

In the reserved channel scheme, a fixed or dynamically adjustable number of channels are exclusively reserved for handover requests. These channels are not available for setting up new calls and therefore the probability of a blocked new call will increase, but this may be the price we are willing to pay for a reliable handover. Let  $C_h$  be the number of reserved channels among the  $C$  available channels per cell reserved to protect handover calls, and the remaining  $C - C_h$  channels are shared by both new calls and handover calls. The aim is to determine an appropriate value for  $C_h$  in order to protect handover calls from excessive blocking without unduly increasing the blocking of new calls. The total call arrival rate in a cell  $\lambda_t$  is equal to  $\lambda_n + \lambda_h$  if the number of calls present in the system is less than  $C - C_h$ , and  $\lambda_h$  if there are  $C - C_h$  calls or more in the system. At statistical-equilibrium, the probability of finding  $i$  busy channels can be calculated using basic queueing theory [148, 167] as,

$$P(i) = \begin{cases} \frac{\rho_e^i}{i!} P(0) & i = 1, 2, \dots, C - C_h \\ \frac{\rho_e^{C - C_h} \rho_h^{i - (C - C_h)}}{i!} P(0) & i = C - C_h + 1, \dots, C \end{cases} \quad (5.17)$$

where,  $\rho_h = \lambda_h / \mu_{ch}$ ,  $\rho_e = (\lambda_n + \lambda_h) / (\mu_c + \mu_h)$  and  $P(0)$  is merely a normalizing

factor so that the state probabilities add up to 1, i.e.,

$$P(0) = \frac{1}{\sum_{k=0}^{C-C_h} \frac{\rho_e^k}{k!} + \rho_e^{C-C_h} \sum_{k=C-C_h+1}^C \frac{\rho_h^{k-(C-C_h)}}{k!}} \quad (5.18)$$

Therefore, the new call blocking and handover failure probabilities can be obtained by,

$$P_{Bn} = Prob(i \geq C - C_h) = \sum_{i=C-C_h}^C P(i) \quad (5.19)$$

$$P_{Fh} = Prob(i \geq C) = P(C)$$

i.e.,

$$P_{Bn} = \left[ \rho_e^{C-C_h} \sum_{i=C-C_h}^C \frac{\rho_h^{i-(C-C_h)}}{i!} \right] P(0) \quad (5.20)$$

$$P_{Fh} = \frac{\rho_e^{C-C_h} \rho_h^{C_h}}{C!} P(0)$$

It is clear that when  $C_h = 0$ ,  $P_{Bn} = P_{Fh}$ . Evaluation of the two blocking probabilities in (5.20) as illustrated in Fig. 5.2 reveals that the rates of change of two blocking probabilities are different. This implies that the decrease in blocking probability of handover calls with increasing number of reserved channels is greater than the corresponding increase in the blocking probability of new calls. This is what makes the reserved channel scheme useful.

Let's define the efficiency of the reserved channel method as:

$$\begin{aligned}
 \varepsilon_g &= 1 - \frac{P_{Fh}}{P_{Bn}} \\
 &= 1 - \frac{\rho_h^{C_h} / C!}{\sum_{i=C-C_h}^C \frac{\rho_h^{i-(C-C_h)}}{i!}} \\
 &= 1 - \frac{\rho_h^C / C!}{\sum_{i=C-C_h}^C \frac{\rho_h^i}{i!}}
 \end{aligned} \tag{5.21}$$

This definition is more appropriate compared to Guérin's [168] where it was defined

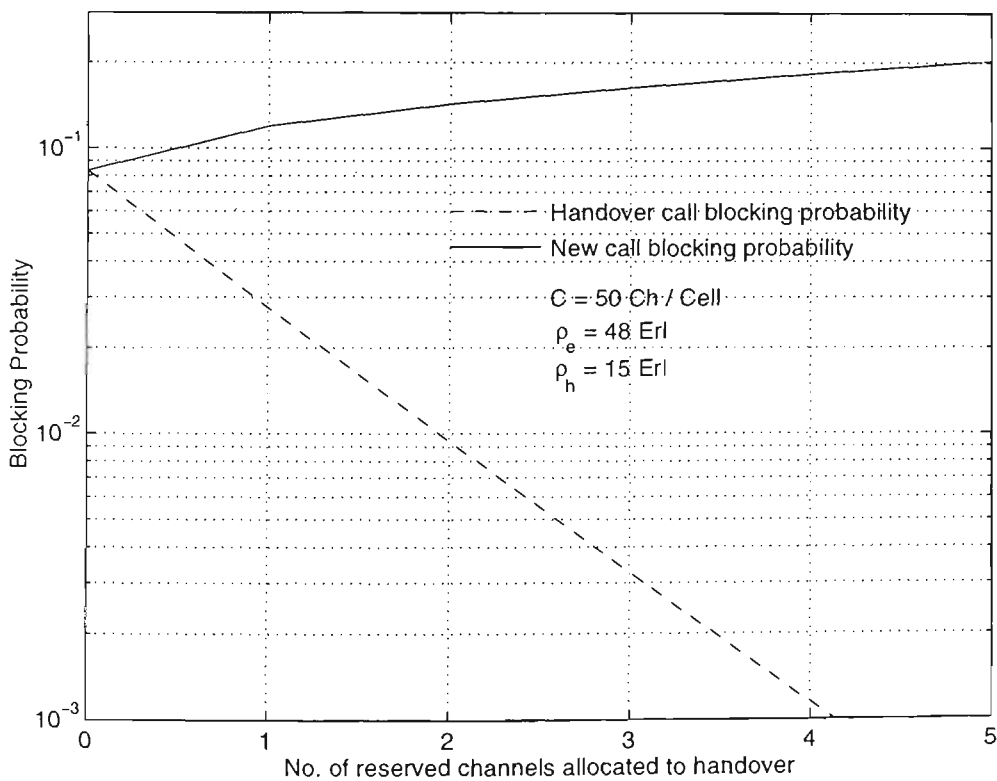


Fig. 5.2. Blocking probabilities for the networks with reserved channel scheme



as equal to  $P_{Fh}/P_{Bn}$ , the reason being that when the number of reserved channels is 0, the efficiency of the reserved channel scheme has to be 0. However, increasing the number of reserved channels makes the efficiency approaches 1. Note that with no reserved channels  $P_{Fh} = P_{Bn}$ .

Fig. 5.3 illustrates the efficiency of this scheme for handover calls. As it is shown, decreasing the traffic offered by handover calls increases the efficiency of the reserved channel scheme. Inspecting Fig. 5.3, we see that the increase in efficiency is greater than 16% when the number of reserved channels increases from 1 to 2 in heavy traffic (i.e. 15 Erlangs), whereas the same increase in the number of reserved channels in light traffic (i.e. 5 Erlangs) makes the efficiency increase only by 8%.

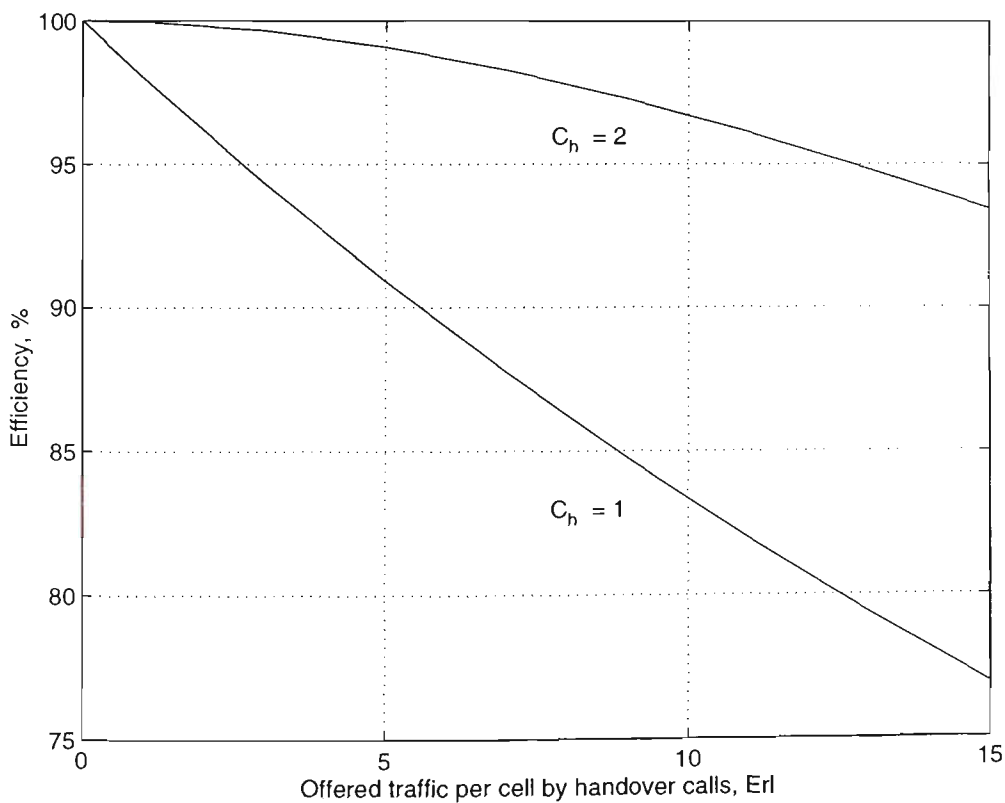


Fig. 5.3. Efficiency of the reserved channel scheme.

This reduction in efficiency at light traffic is not penalizing however, since at low traffic blocking of handover calls is less likely. This shows that the reserved channel scheme is most efficient when traffic is heavy and handover calls are most likely to be blocked.

### 5.4.2 Queueing prioritization schemes

Queueing prioritization schemes, with or without reserving channels for handover, is another method of reducing the probability of forced termination at the expense of increased new call blocking probability and a decrease in the ratio of carried-to-offered traffic. The reason is that no new call is granted a channel before the handover requests in the queue are served. Queueing prioritization schemes take advantage of the fact that adjacent cells in a cellular network overlay each other. Thus, there is an area where a call can be handled by either of the base stations. This area is called the *handover area*. When a mobile station with an ongoing call enters a handover area, it checks if there is a channel available on the new base station. If not, handover request is buffered in a waiting queue, and the channel on the current base station is used until a new channel is available. The fact that a successful handover can take place anywhere in the handover area marks a certain amount of tolerance in the delay in actual channel assignment after a handover request. The call eventually is forced terminated if no channel is found in the new base station by the time the mobile moves out of the handover area. Previous studies [101, 127, 165, 166] indicate that the queueing schemes effectively reduce the forced termination probability at the cost of slightly increasing the blocking probability of new call attempts. However, the total number of unsuccessful calls of these schemes are roughly the same as those of nonprioritized schemes. Note that the performance of

the queueing schemes depend on the time that a mobile station stays in the handover area. Two different methods are known for queueing prioritization schemes,

- First-In-First-Out scheme (FIFO)
- Measurement-Based Priority Scheme (MBPS)

In the FIFO scheme [101], when a channel is released, the base station first checks if the waiting queue is empty. If not the released channel is assigned to a handover call in the queue based on the FIFO queueing policy. MBPS [165] is also similar to the FIFO scheme, except for the queueing policy. MBPS uses a non-preemptive dynamic priority policy, for which priority calls are placed in the queue before all non-priority calls, but never interrupt a call in progress. The priorities are defined by the power level that the mobile station receives from the current base station. The network monitors the power level of the queued handover calls dynamically, and assigns a channel to the one with the weakest received signal.

In the general case, we consider queueing prioritization schemes in terms of reserving channels for handovers. For this purpose three distinct cases can be identified. a) The number of calls present in the system is less than  $C - C_h$ , where all calls are served without any distinction of type. b) The number of calls present in the system is equal or more than  $C - C_h$  and less than  $C$ , where new calls are blocked and handover calls are served. c) The number of calls present in the system is more than  $C$ , and the new calls are blocked while the handover calls are queued. Basic queueing theory shows that the probability of being in state  $i$  is ([148], Chapter 3 Section 1),

$$P(i) = \begin{cases} \frac{\rho_e^i}{i!} P(0) & 0 \leq i \leq C - C_h \\ \frac{\rho_e^{C-C_h} \rho_h^{i-(C-C_h)}}{i!} P(0) & C - C_h \leq i \leq C \\ \frac{\rho_e^{C-C_h} \rho_h^{i-(C-C_h)}}{C! C^{i-C}} P(0) & C \leq i \end{cases} \quad (5.22)$$

where,  $P(0)$  is the normalizing factor so that the state probabilities add up to 1, i.e.,

$$P(0) = \frac{1}{\sum_{i=0}^{C-C_h-1} \frac{\rho_e^i}{i!} + \rho_e^{C-C_h} \sum_{i=C-C_h}^{C-1} \frac{\rho_h^{i-(C-C_h)}}{i!} + \frac{\rho_e^{C-C_h} \rho_h^{C_h}}{(C-1)!(C-\rho_h)}} \quad (5.23)$$

Therefore, the blocking probability of the new calls  $P_{Bn}$  will be,

$$P_{Bn} = Prob(i \geq C - C_h) = \left[ \left( \frac{\rho_e}{\rho_h} \right)^{C-C_h} \sum_{i=C-C_h}^{C-1} \frac{\rho_h^i}{i!} + \frac{\rho_e^{C-C_h} \rho_h^{C_h}}{(C-1)!(C-\rho_h)} \right] P(0) \quad (5.24)$$

It can be seen that the blocking probability of new calls when handover calls are allowed to queue, is slightly greater than that of the case without queuing facility. The fact that we have assumed infinite queuing capacity for handover calls implies that no handover call will be blocked, even if it undergoes a long waiting time. Probability of a handover call being delayed  $P_{Hd}$ , can be obtained from the state probabilities given in (5.22),

$$P_{Hd} = Prob(i \geq C) = \frac{\rho_e^{C-C_h} \rho_h^{C_h}}{(C-1)!(C-\rho_h)} P(0) \quad (5.25)$$

## 5.5 Simulation model

The main aim of building a teletraffic simulation model is to obtain the appropriate blocking probabilities, and for this purpose the length of time the network remains in a certain state is not of any significance. Therefore, the proposed teletraffic simulation model is based on the next-event time-advance approach which uses all attributes of the current and next calls. These attributes include call duration, call interarrival time, new call cell residence time and handover call cell residence time. A very large population of mobile users is assumed in each cell, so that the mean call arrival rate will be independent of the number of calls in progress. Mobiles are assumed to be indistinguishable in the sense that the traffic originated per mobile is the same. Call attempts associated with each mobile are taken to be one type only and are assumed to arrive at the network according to a Poisson process. The call holding times are assumed to be independent and identically distributed (iid<sup>1</sup>) random variables, which follow the negative exponential distribution with a mean value of  $1/\mu_c$  sec. The blocked-calls-cleared (BCC) queuing discipline has been selected. New and handover call cell residence time distributions are taken to be generalized gamma according to the results of mobility modelling in Chapter 4. It is also assumed that a handover occurs from a cell to each of its six neighbouring cells with an equal probability of  $1/6$ . Further it is assumed that all base stations use omnidirectional

---

1. Identically distributed means that different calls from different mobiles have the same probability distribution for the call holding time.

antennas.

### 5.5.1 Cellular Mobile Coverage Area

A cellular mobile network usually covers a wide area, and is often difficult to examine in its entirety by analytical means. In general, simulations are the only way out of this situation. However, results from simulations are valid only if the cells under consideration are sufficiently far away from the border of the cell structure. An ideal cell structure would consist of an infinite number of cells and will have no border which can affect the results. However, simulation of such a system is impractical, since it needs virtually infinite memory and unacceptably long running times. An alternative approach would be to find a finite network which approximately represents the infinite network. One important issue arising from changing an infinite network into an approximate finite one is the introduction of edge effects in the finite network. Different types of approximate finite networks are discussed in [169]. One way of accomplishing an approximately infinite cell pattern is to wrap around the cellular layout with a limited number of cells [170]. By doing this the cells are arranged in such a manner that they effectively constitute a continuous toroidal surface. The problem with this kind of finite network is the introduction of artificial dependencies between cells. If the chosen number of cells is sufficiently large, this effect is reduced. Fig. 5.4 shows the system which we have used in the present simulation. The system comprises 49 cells with a reuse cluster size of 7 cells. Once the network is wrapped around, the cells with dashed lines will become neighbours of the cells with solid lines.

### 5.5.2 Analysis of computer simulation results

Fig. 5.5 illustrates how new and handover call blocking probabilities vary with the new call attempt rate per cell for various cell sizes. This figure shows that with increasing cell radius, blocking probability approaches the Erlang-B curve. The same data is shown in Fig. 5.6, as a function of offered traffic considering effective call holding time. As illustrated in Fig. 5.6, the variation of blocking probability with effective offered traffic per cell is independent of cell size as considered in (5.16). This means that for a given new call arrival rate, the effective call holding time in a cell is such that the consequent traffic intensity remains constant.

It should be noted that two networks with the same handover blocking probability could have different dropout probabilities. For example, a network with mobiles of low mobilities will experience a relatively lower number of boundary crossing

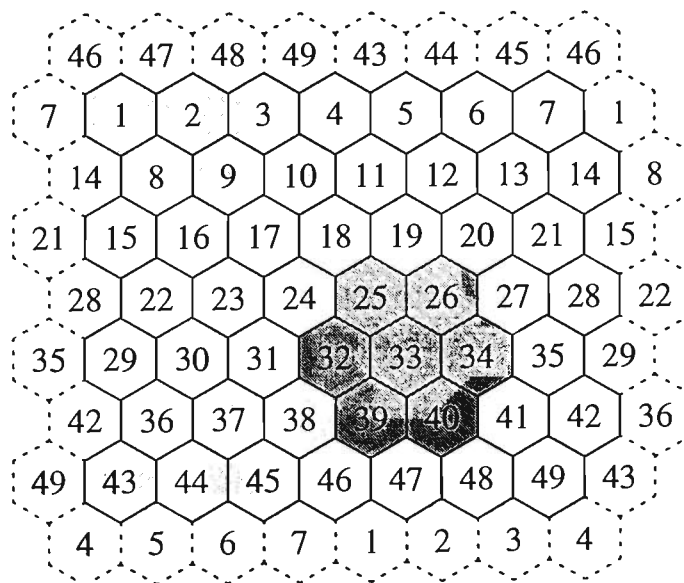


Fig. 5.4. Layout for a toroidal 49-cell system (reuse cluster for the cell number 33 highlighted).

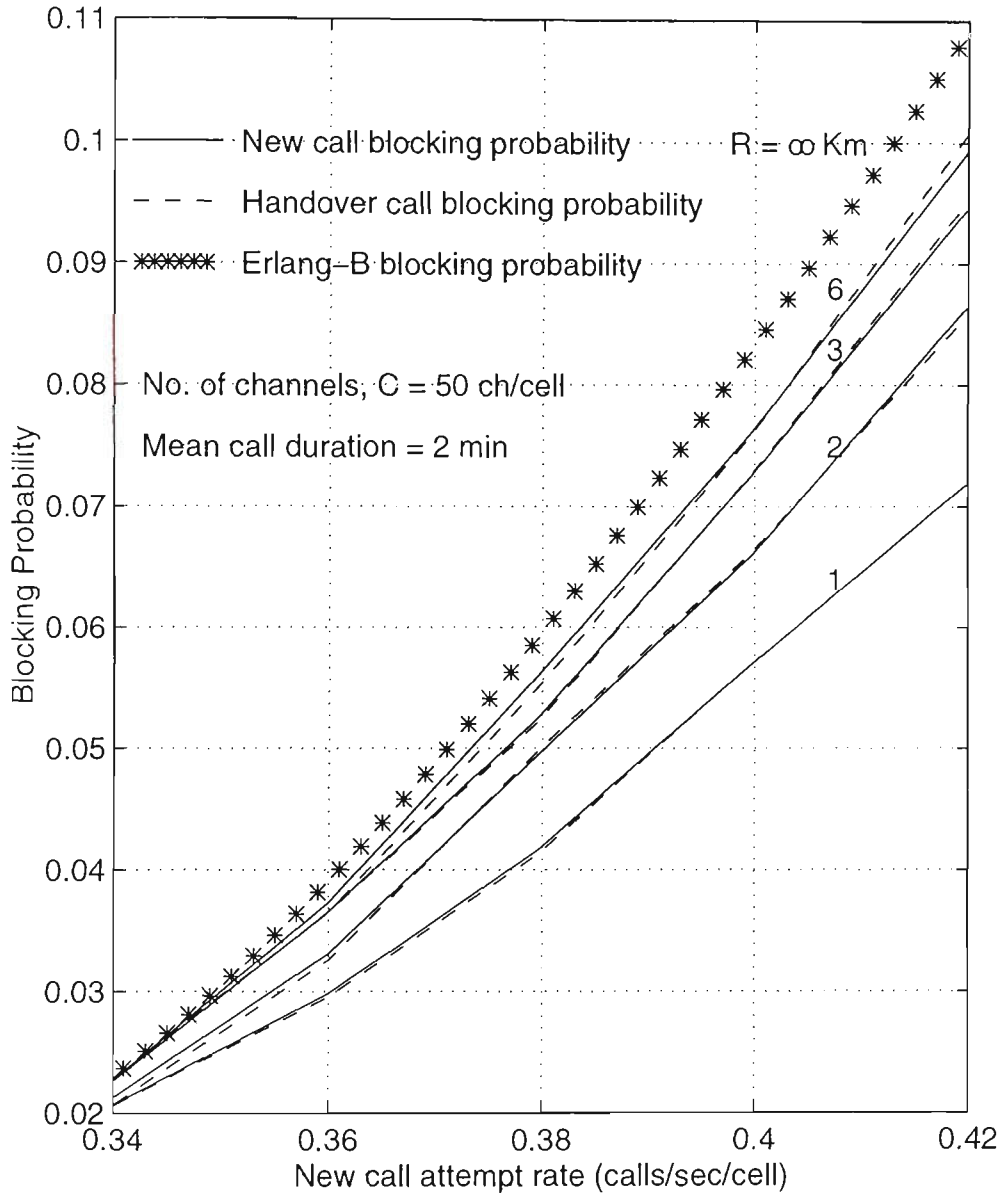


Fig. 5.5. New and handover call blocking probabilities for different cell sizes.



attempts than a network with mobiles of higher mobilities. The greater the number of boundary crossings occur, the greater will be the dropout probability for the same handover blocking probability. Fig. 5.7 shows dropout probability versus handover call blocking probability. It can be observed that the dropout probability depends on the cell size, and the mobility of users. Fig. 5.8 shows how the dropout probability decreases with increasing cell size for a given new call rate.

Having exclusive handover channels is seen to bear the risk of inefficient spectrum utilization. However, this policy has the advantage of simplicity and provides an efficient way of reducing the blocking probability of handover calls, while slightly increasing the blocking probability of new calls. The price paid for is a small decrease in the total carried traffic. Fig. 5.9 shows the effect of the number of

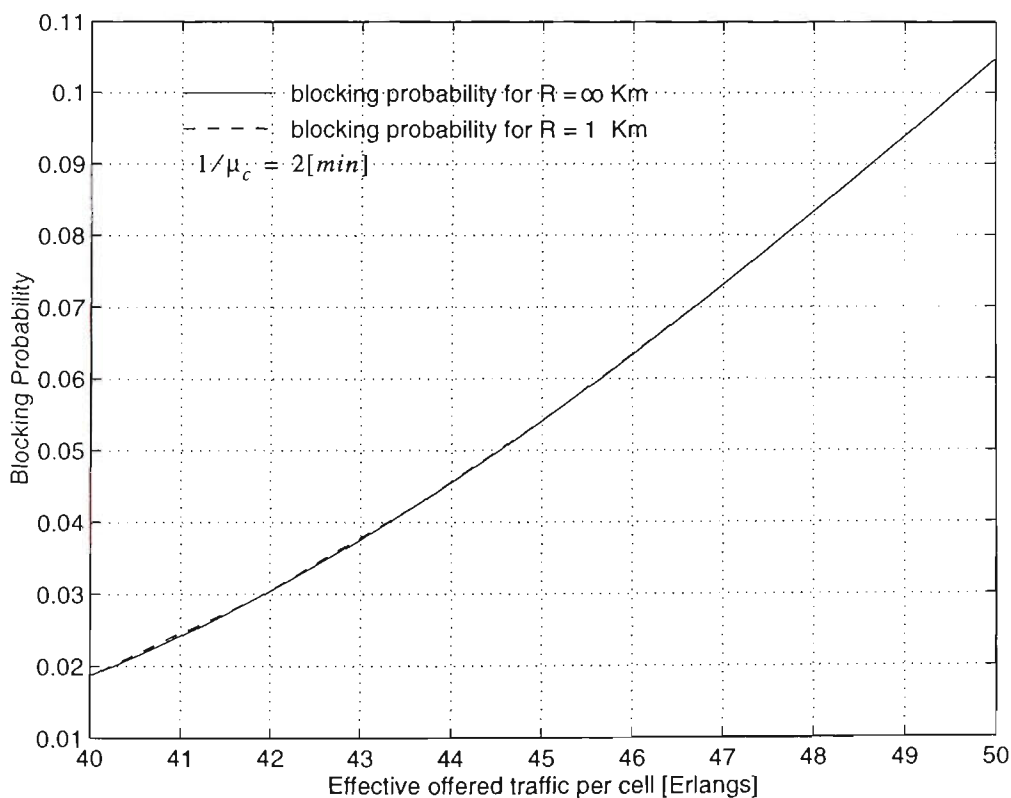
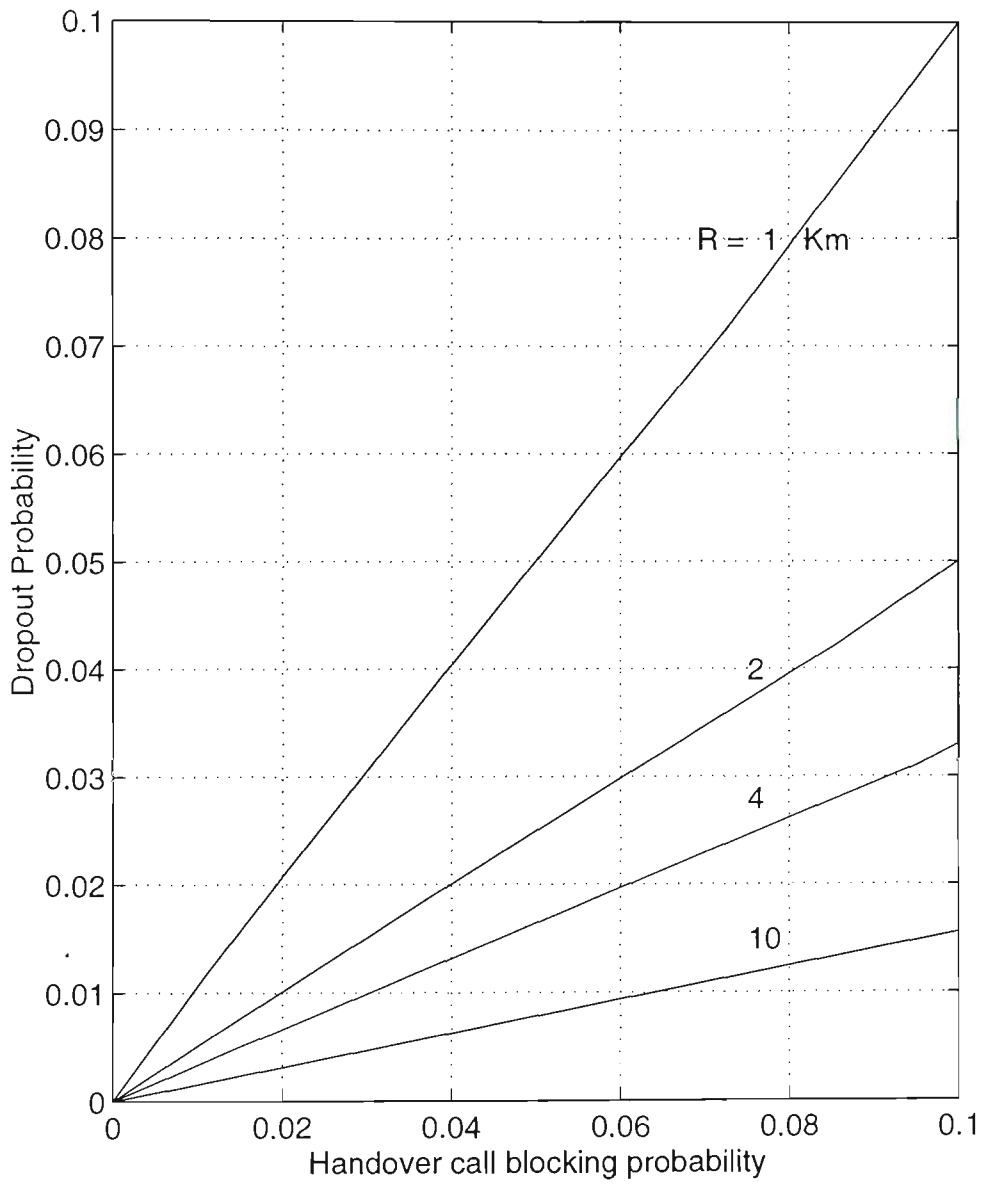
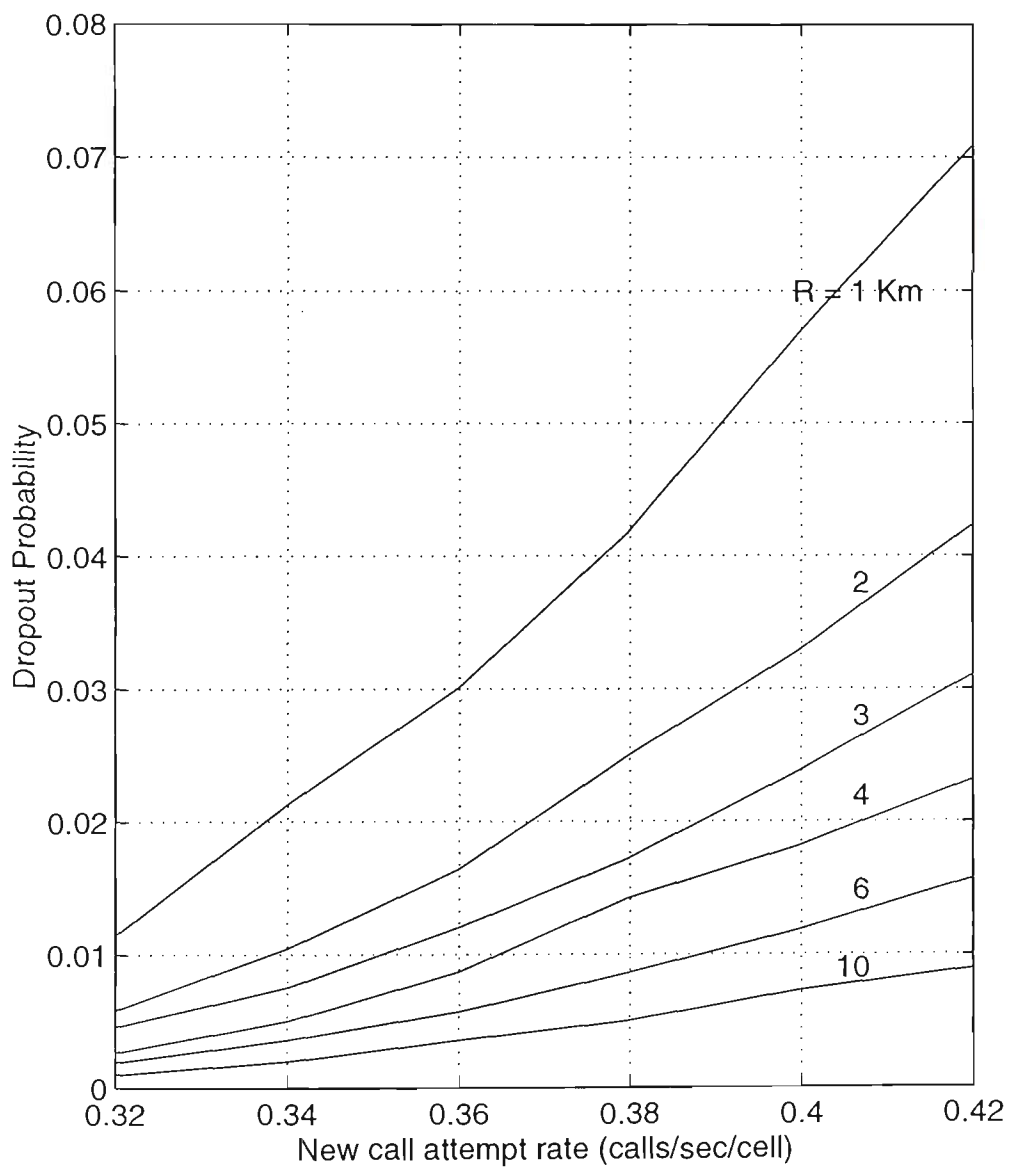


Fig. 5.6. Comparison of offered traffic for different cell sizes.



**Fig. 5.7.** Dropout probability versus handover call blocking probability.  
(No channel reservation).



**Fig. 5.8.** Dropout probability versus new call attempt rate.  
(No channel reservation)

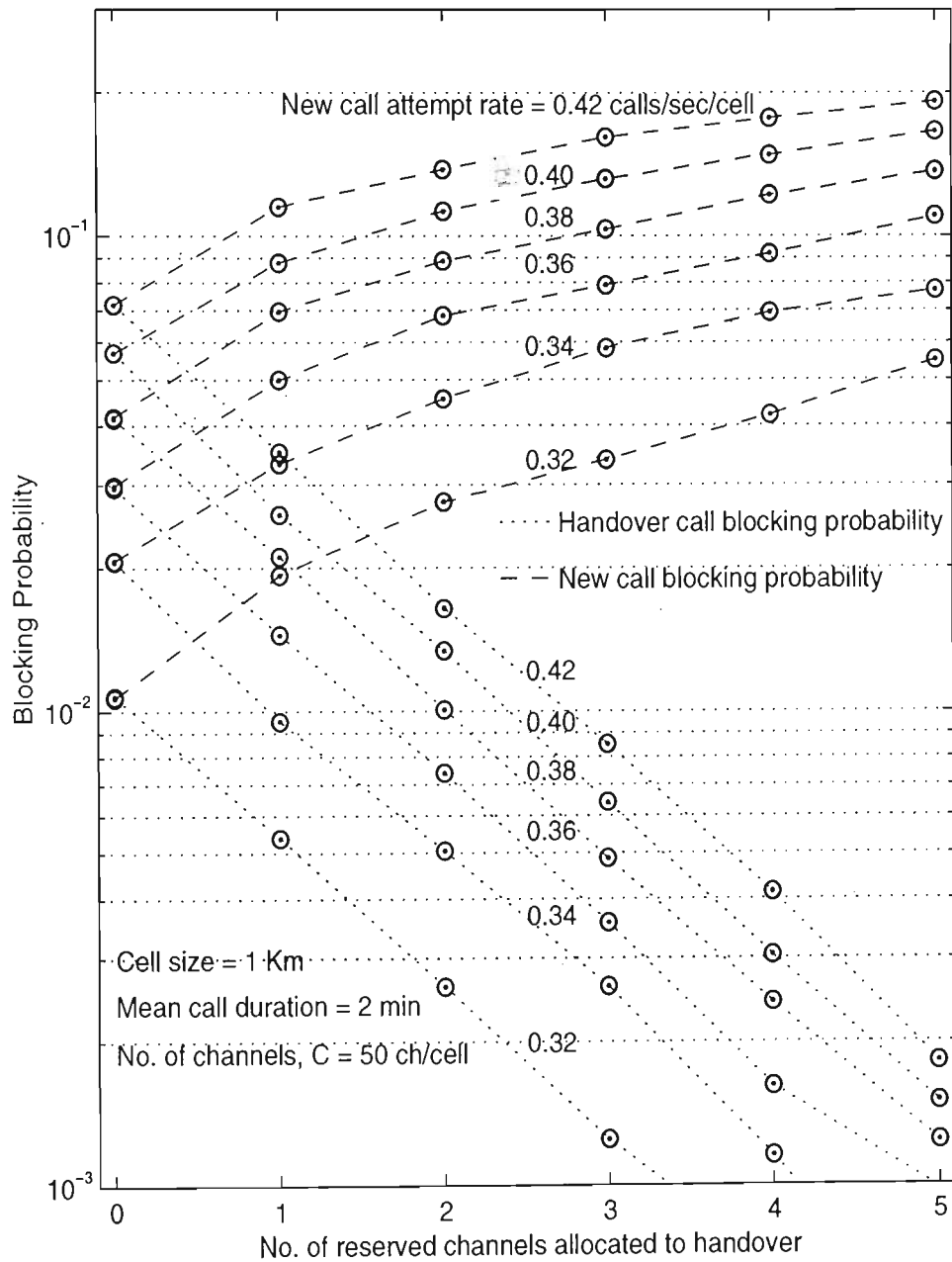


Fig. 5.9. New and handover call blocking probabilities with reserved channels for handover calls.

reserved channels allocated to handover on the probability of handover attempt failure and the new call blocking probability. As can be seen, the rate at which the blocking probability of handover calls decrease with increasing number of reserved channels is much bigger than the rate at which the new call blocking probability increases.

The use of reserved channels requires careful determination of the optimum number of reserved channels. This in turn requires the knowledge of the traffic pattern of the area, and an estimation of the channel occupancy time distributions. Reserving channels for handover means less channels are left for new calls so that the total carried traffic is reduced. This disadvantage can be minimised by carefully selecting the number of reserved channels. Also, it can be overcome to a certain extent by allowing queueing of new call attempts, which are considerably less sensitive to delays than handovers.

As it was mentioned earlier, using channel reservation priority scheme reduces dropout probability. Fig. 5.10 shows the effect of the number of reserved channels on the dropout probability for different offered traffic. It can be seen that the dropout probability decreases with the increasing number of reserved channels. This reduction is paid for by an increase in the new call blocking probability. The possible compromise between the new call blocking probability and the dropout probability can be established by allocating a threshold level on the dropout probability. Fig. 5.11 indicates the necessary number of channels exclusively dedicated to handover in order to obtain a certain limit on dropout probability.

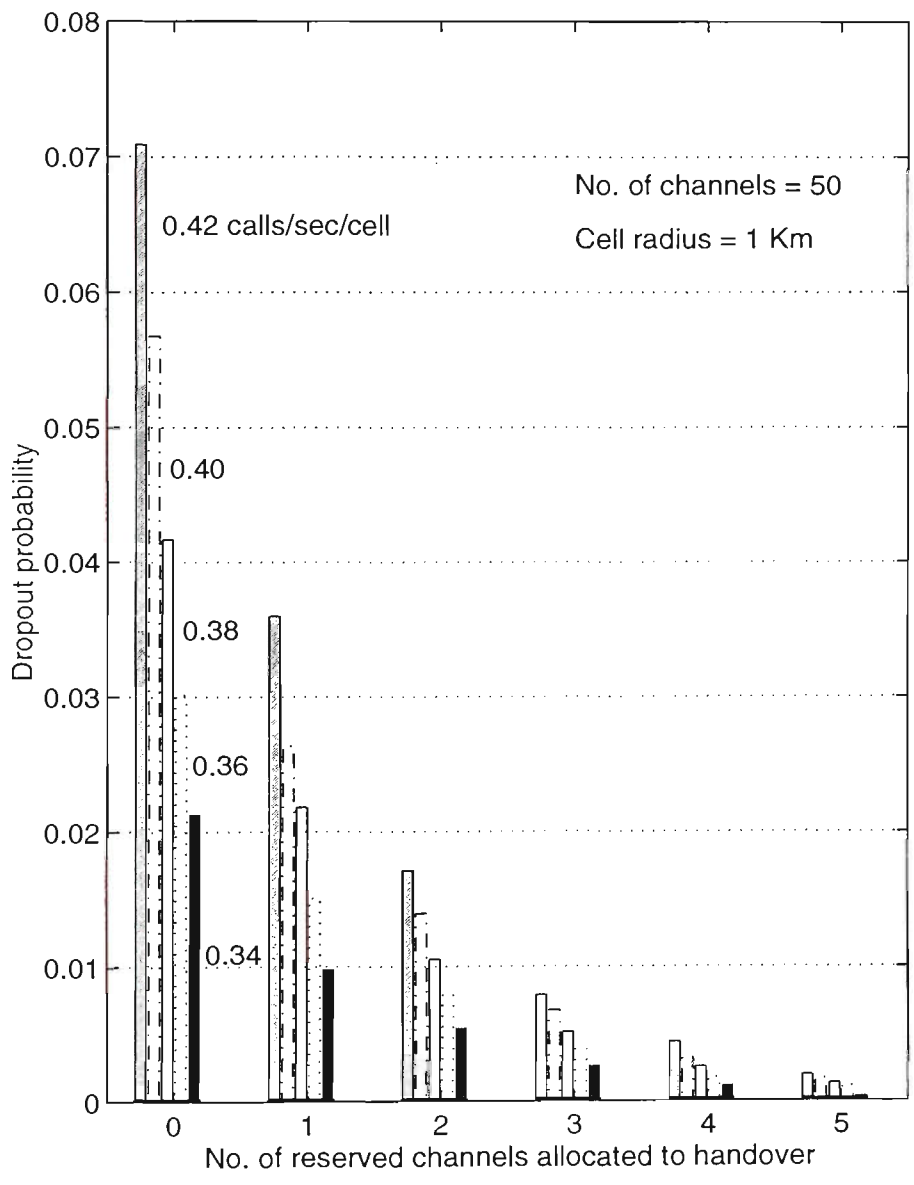


Fig. 5.10. Dropout probability variation with the number of reserved channels for handover.

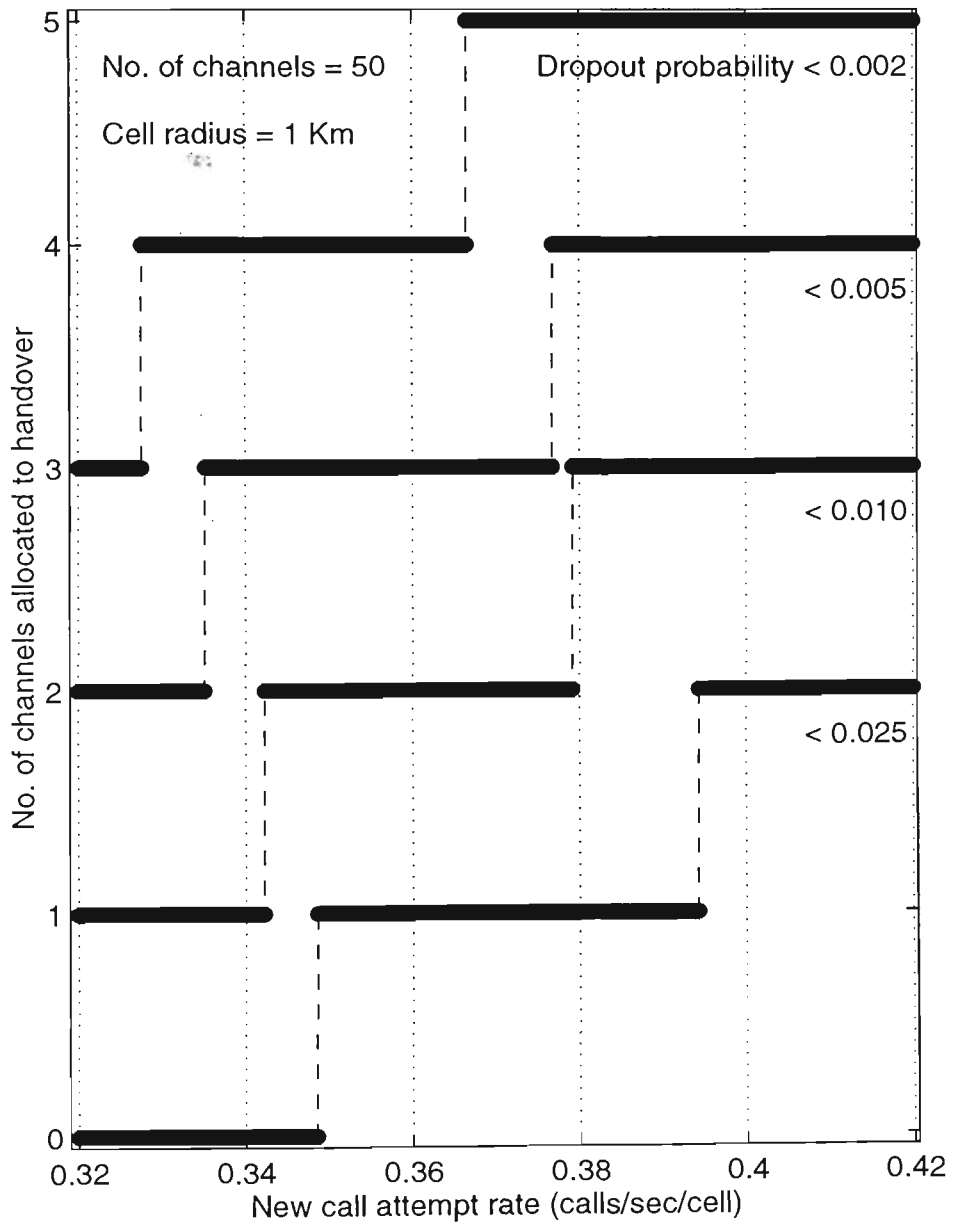


Fig. 5.11. Optimum number of reserved channels for different dropout levels

## 5.6 Conclusions

In this Chapter different radio resource allocation schemes were explained, teletraffic performance criteria were defined, and an analytical model for teletraffic analysis was presented. Also, some traffic policies that give a higher level of protection to handover calls were analysed, and their effects on the overall traffic performance were described. Based on the results obtained in Chapter 4, a teletraffic model that takes the user mobility into account was presented and was substantiated using a computer simulation based on the next-event time-advance approach. Furthermore, the influence of cell size on new and handover call blocking probabilities was examined. The effect of handover channel reservation policy on call dropout and handover failure probabilities was also examined to determine the optimum number of reserved channels required for handover.

It was found that blocking probabilities of the new and handover calls are the same when there are no reserved channels for handover calls. These probabilities become different with the allocation of some channels for handover calls. The variation of blocking probabilities of new and handover calls are such that any decrease in the blocking probability of the handover calls is much bigger than the corresponding increase in blocking probability of the new calls. This fact makes the reserved channel scheme attractive. An efficiency factor was defined to show the effectiveness of this scheme. It was shown that the reserved channel method is most efficient when the traffic is heavy and handover calls are most likely to be blocked.

It was also shown that with increasing cell radius, blocking probability approaches the Erlang-B curve. However, the blocking probability variation with respect to the effective



offered traffic per cell is independent of the cell size and follows Erlang-B formula. This means that for a given new call arrival rate, the effective call holding time in a cell is such that the consequent traffic intensity remains constant. It was also found that the dropout probability decreases with increasing number of reserved channels. This reduction is paid for by an increase in the new call blocking probability. The compromise between the new call blocking probability and the dropout probability is established by allocating a threshold level on the dropout probability.

# ***Chapter 6***

## ***Mobile Radio Channel Modelling for Handover Analysis***

In cellular systems, a knowledge of received signal behaviour is essential to analyse the handover, power control, and dynamic channel allocation. In fact, signal strength measurement represents the most important parameter for any reliable handover. Consequently, a thorough investigation and characterization of signal strength is required. The propagation of radio waves is always associated with the unpredictability of the medium which generally varies in space and time. In cellular mobile radio communication systems, the mobile nature of the users and small clearance of the mobile antenna from the ground impose additional constraints on the predictability of the received signal.

The mobile radio channel environment belongs to the class of *non stationary random fields*, where the received signal is affected by different factors such as base and mobile station characteristics as well as natural terrain and man-made structures.

In planning service areas for mobile radio communication systems, calculation of the path loss as well as precise estimation of the signal variability is absolutely necessary. The complex nature of the radio propagation in the real world makes exact analytical computation impossible. Whilst these data can be obtained from field surveys, the problem with this approach is that it is time consuming and expensive. Therefore, computer simulations are widely used. The models employed for these simulations are mainly a mixture of both theoretical and empirical relations as well as added stochastic processes. In generic system studies, a suitable model for variability of propagation phenomena can be derived by applying statistical communication theories, without considering any specific terrain data.

## 6.1 Radio Signal Components

A mobile radio channel is usually characterized by the superposition of three different, mutually independent, multiplicative, and approximately separable components with small-, medium-, and large-scale propagation effects. The small-scale quasi-stationary variations, mostly referred to as *multipath fading*, are fairly rapid in space. Medium-scale effect, mostly referred to as *shadowing*, is influenced by the spatial movements of the order of tens of wavelengths and creates random variations in the average power of the received signal which typically follows a lognormal distribution. In the large-scale effect, spatial movements of the

order of hundreds of meters make the median average power level vary in power-law fashion with path length. Large-scale variation is mostly referred to as *path loss*. Shadowing creates local variations (narrow area median), while path loss creates long range variations (wide area median).

The instantaneous radio signal received at the mobile can be expressed as  $r(t)e^{j\varphi(t)}$ , where  $\varphi(t)$  is a random variable, denoting phase angle of the received signal. In this work, we are interested in the received signal envelope  $r(t)$ , which can be described as the product of a slow varying signal  $s_o(t)$  (shadow fading component), and of a rapid variation factor  $r_o(t)$  (multipath fading component) [171]. Therefore,

$$r(t) = s_o(t) \cdot r_o(t) \quad (6.1)$$

The received signal envelope  $r(t)$  at time  $t$  is an average over the modulation (e.g., over the data symbols in digital cellular), so that it can be studied without regard to the particulars of the modulation. Equation (6.1) can also be expressed in the spatial domain, since the time fluctuations result from subscriber movement through the spatial fluctuations of signal power density. Therefore,

$$r(x) = s_o(x) \cdot r_o(x) \quad (6.2)$$

### 6.1.1 Multipath fading component

Local scatterers around the mobile produce several time-delayed and attenuated versions of the original transmitted signal. Consequently, the received signal

comprises a summation of several signals which can add together either constructively or destructively. The resultant field strength in such an environment follows a spatially-fluctuating standing-wave pattern with minimum and maximum values a quarter-wavelength apart. Movement of a mobile station through such a space-selective fading field makes the receiver sense a time-selective fading signal. The rate of fluctuation depends on the velocity of the mobile and the result is a received signal level which experiences very large and fast variations. The assumption that different scattered wave components are mutually uncorrelated with random phase leads to the conclusion that the local statistics of the received signal envelope follows a Rayleigh distribution. The signal envelope  $r$  has a Rayleigh distribution, if measured over distances of a few tenths of a wavelength, where the average signal is a quasi-stationary process (approximately constant) over small areas. Therefore, the probability density function of the received signal envelope  $r$  relative to the local mean  $s_o = \langle r \rangle$ , can be represented by [84, 172],

$$f(r|s_o) = \frac{\pi r}{2s_o^2} e^{-\frac{\pi r^2}{4s_o^2}} U(r) \quad (6.3)$$

where  $U(r)$  is the unit step function.

In a microcellular environment, radio propagation often includes a line-of sight (LOS) path which makes the short-term statistics of the received faded signal envelope to include a constant term. In this case, examination of statistical distribution of the received signal envelope relative to the local mean shows that it

most likely conforms to Rician distribution and suffers significantly less multipath fading, compared to the case of Rayleigh faded channel. Therefore, the probability density function of the received signal envelope relative to the local mean can be represented by:

$$f(r|s_o) = \frac{\pi r}{2s_o^2} e^{-\frac{\pi(r^2 + \xi^2)}{4s_o^2}} I_0\left(\frac{\xi\pi r}{2s_o^2}\right) U(r) \quad (6.4)$$

where  $\xi$  is the positive offset value from the Rayleigh distribution (amplitude of direct wave), and  $I_0(\cdot)$  is the modified Bessel function of the first kind zero order.

### 6.1.2 Shadow fading component

As the vehicle moves, changes in the obstacles along the propagation path lead to the gradual changes in local mean level  $s_o$ . Analysis of mobile radio propagation measurement results from different surveys has shown that the local mean of the signal envelope  $r$  is adequately described by a lognormal distribution. That is, the local mean  $s = 20 \log_{10} \frac{s_o}{s_o}$  in  $dB$  is a Gaussian random variable, with a probability density function given by:

$$f(s) = \frac{1}{\sqrt{2\pi}\sigma_s} e^{-\frac{(s-\mu)^2}{2\sigma_s^2}} \quad (6.5)$$

where  $\sigma_s$  is the standard deviation of the local mean in  $dB$  due to the shadowing of

the signal (*location variability*), and  $\mu = \langle s \rangle$  is the average of the received signal local mean level (*area average*) in  $dB$ . Area average reflects the median logarithmic attenuation and can be determined by the path loss. The value of  $\sigma_s$  has been experimentally found to lie between  $3 \sim 12dB$  [173, 174]. This broad range can be attributed to variations between experiments in the presence or absence of the LOS component (LOS component increases  $\sigma_s$ ), the height of the antennas used (lower antennas decrease  $\sigma_s$ ), the spatial averaging window length (longer windows decrease  $\sigma_s$ ), or the type of the terrain. Mogensen et al. [175] have shown that  $\sigma_s$  is relatively independent of frequency. Berg et al. [176] and Goldsmith et al. [173] have proposed a value of  $4dB$  in urban microcell areas, whereas for suburban areas containing macrocell areas the value is more likely to be  $8dB$  [177].

### 6.1.3 Path loss component

In the mobile radio environment, due to the fact that the mobile antenna height is close to the ground, the signal received from the base station is affected by three main sources of loss, namely, free space loss, ground wave loss and diffraction loss. The path attenuation depends on many variables, some of which can be controlled (e.g., frequency, antenna height); some can be measured (e.g., distance); and some can neither be controlled nor be measured deterministically (e.g., climate, topography of the environments, terrain). Considering all these factors, it is apparent that the path loss prediction of mobile radio signals is a formidable task. Although there is no easy analytical solution to the problem, it is possible to create a propagation prediction model to estimate the median path loss. These models vary in complexity, accuracy, and capability. Among different methods, Hata's empirical formula based on

Okumura's measurements is the most widely used relation that predicts the median propagation path loss in macrocells [178]. The median path loss,  $L_p$ , in decibels between two isotropic base and mobile antennas, with a separation distance denoted by  $d$  in kilometre is formulated as:

$$L_p = A + 10\gamma \log d \quad (6.6)$$

where  $\gamma$  is the slope factor and depends on the base station effective antenna height  $h_b$ , and is weakly affected by the carrier frequency. A good approximation yields  $\gamma = 4.49 - 0.655 \log h_b$ . The value of  $A$  for different frequency and environment settings such as urban area, suburban area, open area can be obtained through Hata and Okumura recommendations [178]. Therefore, in case a transmitter emits a signal with the power of  $P_{tx}[dB]$ , the received signal level  $P_{rx}[dB]$  due to the path loss will be:

$$P_{rx} = P_{tx} - L_p = K_1 - K_2 \log d \quad (6.7)$$

where,  $K_1 = P_{tx} - A$  and  $K_2 = 10\gamma$ . Hata's formula does not consider propagation from low base station antenna heights (less than  $30m$ ) or over the short distance (less than  $1Km$ ). Therefore, in a microcellular environment, where cell radius is usually below  $1Km$ , and base station antenna height is lowered down the surrounding buildings at the street-lamp elevation, Hata's formula is not valid.

One of the main distinctions between the propagation characteristics of the microcells and macrocells is the existence of a LOS wave. The presence of a LOS



path in the microcell environment implies that, in a region near the base station, the environmental features are unlikely to have a prominent influence on the propagation conditions, and the path loss exponent will be very close to that of free space propagation. When the link distance grows beyond a limit, namely a breakpoint distance, environmental factors dominate and path loss exponent increases, which leads to extra attenuation. The exact position of the breakpoint has been reported anywhere from 150 – 300m by a number of authors [54, 179]. Xia et al. [180] demonstrate that the breakpoint is the point where the Fresnel zone between the two antennas touches the ground assuming a flat earth. Therefore, the propagation path loss in microcells can be characterized by two straight lines with different slopes.

Another issue which commonly exist in microcells of Manhattan type is the street corner effect. Turning around a street corner causes a dramatic decrease in the received signal strength of the mobile station, due to the blockage of LOS component. In order to minimise the error occurring from this in the microcellular environment propagation model, the propagation phenomena are broken down to two categories as line-of-sight (LOS) and non-line-of-sight (NLOS) emissions.

The received signal strength  $p_{rx}$ , at a distance of  $x$  from a transmitter with the output power of  $p_t$ , and the wavelength of  $\lambda$  can be predicted by [176]:

$$p_{rx} = \frac{P_t}{L(x)} \cdot \left(\frac{\lambda}{4\pi}\right)^2 \cdot g_t \cdot g_r \quad (6.8)$$

where  $g_t$  and  $g_r$  are the transmitter and the receiver antenna gains relative to the

isotropic counterparts.  $L(x)$  is given by:

$$L(x) = \left(\frac{x}{x_0}\right)^2 \cdot q \sqrt{1 + \left(\frac{x}{x_L}\right)^{q \cdot (m-2)}} \quad (6.9)$$

where  $q$  is a form factor which determines the smoothness of the variation of the path loss at the transition region around the breakpoint  $x_L$ .  $x_0, m$  are two parameters whose values along with the values of the parameters  $q, x_L$  are chosen as suggested in [176]. Assuming that a fictitious transmitter is located at the street crossing, at a distance  $x_a$  from the base station, a similar loss relation in a side street for NLOS case can be found. In this case (6.9) can be stated as the following:

$$L(y) = \left(\frac{y}{y_0}\right)^2 \cdot q \sqrt{1 + \left(\frac{y}{y_L}\right)^{q \cdot (n-2)}} \quad (6.10)$$

Again the values of parameters  $y_0, y_L, q, n$  are chosen as suggested in [176]. Fig. 6.1 illustrates definition of  $x, x_a, y, y_0$ . The total loss along a NLOS street is determined by:

$$L(x_a, y) = L(x_a) \cdot L(y) \quad (6.11)$$

The received signal power could be obtained by substituting  $L(x_a, y)$  in place of  $L(x)$  in (6.8).

## 6.2 Mobile Radio Channel Characterization for Handover Analysis

A handover is executed only if the signal of the channel degrades for a reasonable interval of time. Considering that the Rayleigh fading pitch period is given by  $T = \lambda/(2v)$  [72], for a speed of the mobile  $v = 50\text{Km/hr}$  and wavelength of the signal  $\lambda = 35\text{cm}$  the pitch period will be  $T = 0.0126\text{s}$ . The fluctuations of such small duration cannot trigger handover decision, because the handover procedure with its associated signalling and switching requirements would take more time than the pitch period of the Rayleigh fading. However, compared to the multipath fading, shadow fading has a slower time-dependence rate which can cause long term variations in the received mean signal level and is very important in handover decision making.

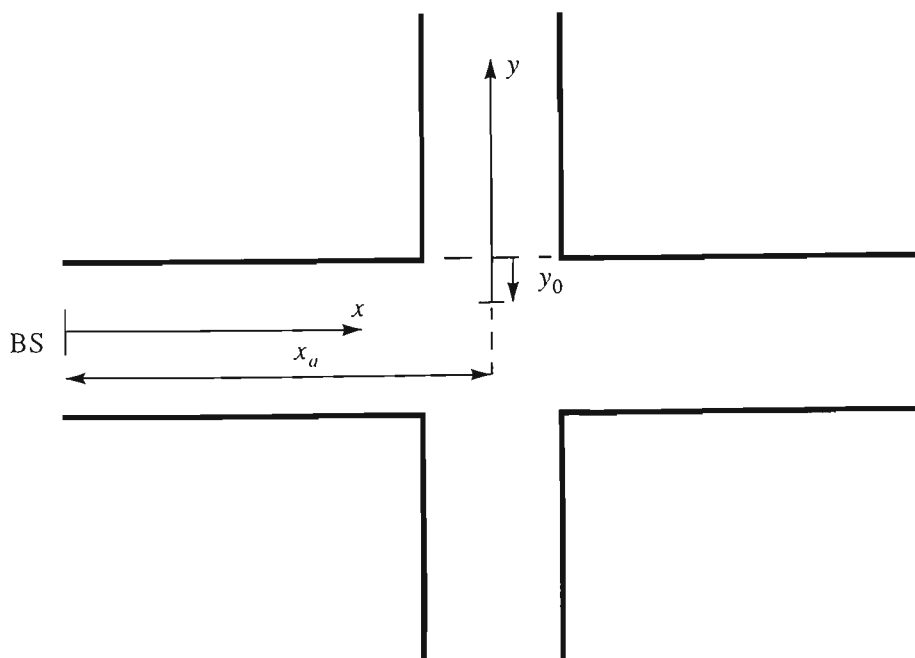


**Fig. 6.1.** Illustration of the parameters for determination of the LOS and NLOS path losses.

A proper selection of the size of spatial window is needed to effectively smooth out the Rayleigh fading variation. Lee [47] and Austin et. al [85], have investigated guidelines for the minimum distance averaging interval needed to eliminate fading in macrocells and microcells, respectively. Work carried out by Lee [47] suggests a length of  $40\lambda$  as a suitable distance in the case of macrocells. If the length is shorter than  $40\lambda$ , the average output would still retain a weaker portion of Rayleigh fading. If the length is greater than  $40\lambda$ , the excessive length of averaging also smooths out the local mean information. In practice, a spatial window in the range  $20\lambda$  to  $40\lambda$  is acceptable.

Examination of data taken from microcells shows that Rayleigh fading variation is less severe but the local mean could suffer quite large variations over short distances. In microcells, moreover, large window length may conceal the steep decrease of the signal strength when the mobile turns around a street-corner. Green [181] suggests a spatial window size of  $5\lambda$  as an appropriate averaging length for microcells. Velocity adaptive sampling is assumed to maintain spatial window lengths at a constant value. The received signal strength averaged over the window  $s(t)$  is a stochastic process where the first order statistics of that, at any instant of time or equivalently at any distance, can be modelled as a correlated lognormally distributed variable  $s$  with an average value of  $\mu$  and a standard deviation of  $\sigma_s$ . Since signal variation is a limited amount,  $s$  can be considered as a truncated normal distribution bounded within the range  $\pm 3\sigma_s$ . The mean received signal level can be predicted using a model which consists of a median path loss  $\mu$  and a log-normal variation of the local mean due to shadowing,  $S$ . Therefore,

$$s = \mu + S \quad (6.12)$$

where  $S$  models the shadow fading as a zero mean stationary Gaussian variable with the same standard deviation as that of  $s$ . From the model of  $s$ , it is also possible to obtain the model for  $s(t)$  at any instant of time or  $s(r)$  at any distance. The autocorrelation function of the shadow fading component has been experimentally found to be a decreasing function over distance. Gudmundson [177] has proposed a spatial correlation between two samples separated by a distance  $\Delta d$  to be,

$$Cor(\Delta d) = \sigma_s^2 \rho_{d_0}^{\Delta d/d_0} \quad (6.13)$$

where  $\rho_{d_0}$  is the spatial correlation at a distance  $d_0$ . The measurement data reveals that for macrocells in suburban areas  $\rho_{100[meters]} = 0.82$  when  $\sigma_s = 7.5$ , and for microcells in urban areas  $\rho_{10[meters]} = 0.3$  when  $\sigma_s = 4.3dB$  [177]. Work performed by Berg, Bownds and Lotse [176] shows that the average value of the spatial autocorrelation of shadow fading components also depends to some extent on the distance from base station. The average value of the standard deviation does not vary significantly either along LOS streets or along NLOS streets. Considering shadow fading as a random process with Gaussian probability density function and an autocorrelation factor  $\rho = \rho_{d_0}^{\Delta d/d_0}$ , the pdf of the slow fading signal samples at  $\Delta d$  meters apart can be represented as [182],

$$f(S(n)|S(n-1)) = \frac{1}{\sigma_s \sqrt{2\pi(1-\rho^2)}} e^{-\frac{(S(n)-\rho S(n-1))^2}{2\sigma_s^2(1-\rho^2)}} \quad (6.14)$$

where  $S(n)$  and  $S(n-1)$  are the adjacent samples of the slow fading signal with a standard deviation of  $\sigma_s$ . Eq. (6.14) suggests a simple AR-1 model which can be implemented by a digital filter as shown in Fig. 6.2 for simulating the shadow fading signal,

$$S(n)|S(n-1) = \rho S(n-1) + \sigma_s \sqrt{1-\rho^2} \mathfrak{N}(0,1) \quad (6.15)$$

where  $\mathfrak{N}(0,1)$  represents a normal random variable with a mean of 0 and standard deviation of 1. Fig. 6.3 shows a typical received signal level along a LOS and a NLOS street in a microcell with superimposed correlated shadow fading. The received signal level in the case of macrocells with superimposed correlated shadow fading is shown in Fig. 6.4.

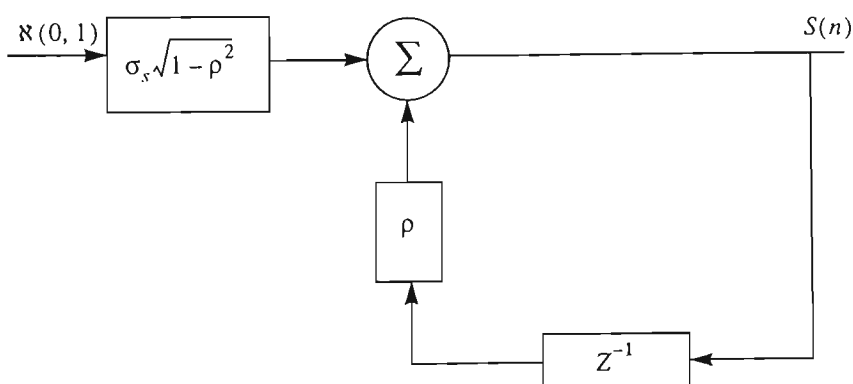


**Fig. 6.2.** Digital filter for producing slow fading signal component.

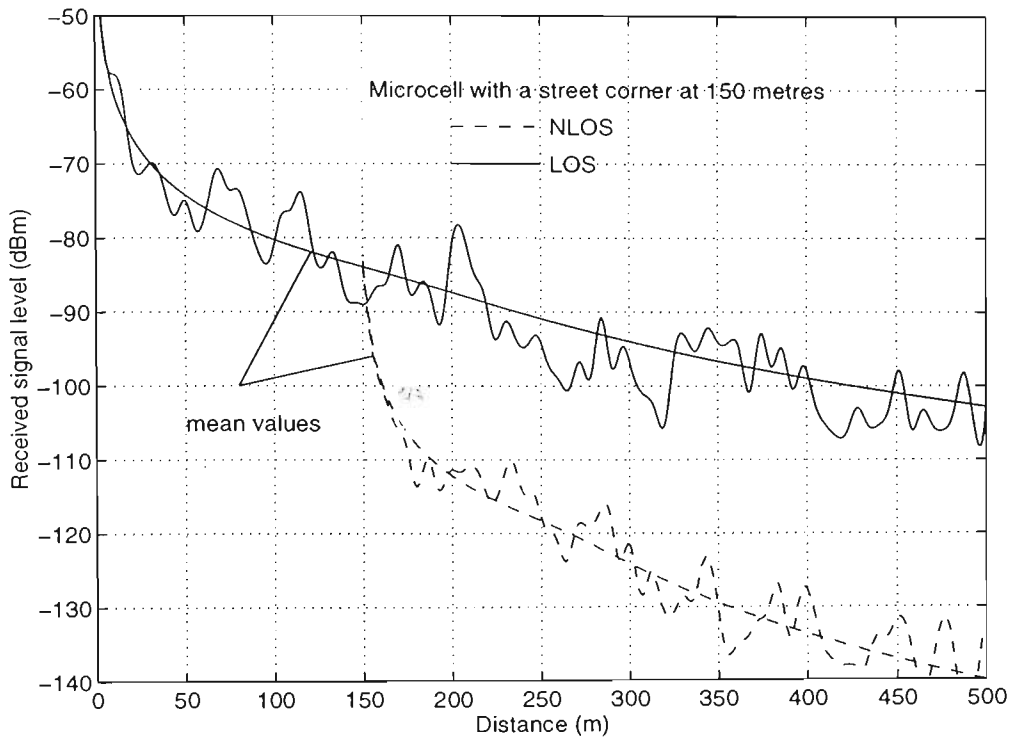


**Fig. 6.3.** Received signal level along a LOS and a NLOS streets in a microcell with superimposed correlated shadow fading.

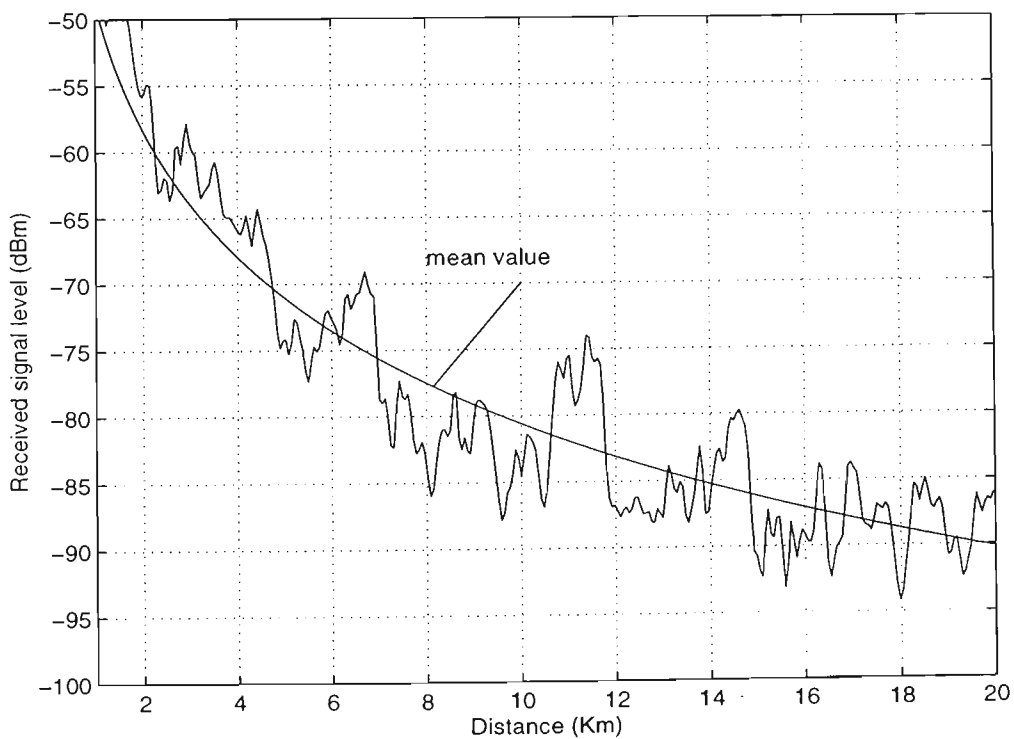


**Fig. 6.4.** Received signal level along a path in a macrocell with superimposed correlated shadow fading.

### 6.3 Conclusions

The contributions of three different components of a mobile radio signal are considered, and a propagation model suitable for micro- and macro-cells has been presented. Emphasis is made on the effect of shadow fading (the medium-scale propagation component), which is most important in handover decision making in cellular networks. It has been shown that a simple AR-1 model can be implemented by a digital filter for simulating the shadow fading signal taking correlation between adjacent samples into account.



# ***Chapter 7***

## ***Optimum Hysteresis Level, Signal Averaging Time and Handover Delay***

Performance of inter-cell handover algorithm is critical to the overall performance of a cellular mobile communication system. When a mobile station crosses a cell boundary between two base stations, handover is required to switch the radio link of the mobile station from the departing base station to the approaching base station in order to maintain the connection. The crucial part of handover is to decide exactly at which point a handover should take place. In analog systems this is solely determined by the received signal strength profile of the mobile station. In digital cellular systems other criteria have also been suggested. In GSM, quality of the received signal (as reflected by the bit error rate), and the distance between mobile and the

base station (as measured by the timing advance), have been recommended. However, careful examination of the handover algorithms chosen for implementation by several equipment manufacturers of GSM system indicates that these other criteria serve mainly in recognition of abnormal operating conditions (known as alarm conditions) rather than in providing a primary input to the handover decision making process. Thus, even in digital cellular systems, it is the mobile received signal strength that provides the vital information required for handover decision making.

As is discussed in Chapter 6, in the environments in which the cellular mobile systems operate, the received signal strength of a mobile station along its path is hardly a monotonic function even when the mobile moves in a straight line directly across cell boundaries separating the two base stations. The irregularities of terrain, the built up structures in urban areas and the like cause fluctuations in the received signal strength, making it difficult to determine the exact position at which the handover should occur.

The mobile received signal can be considered as consisting of three components, namely, the path loss component, the slow fading shadow component and the fast fading multipath component. The path loss component is determined primarily by the distance between the base station and the mobile station. In the absence of fading, this causes the signal strength to decrease gradually with distance. It is the path loss component that provides the best guide in the determination of the appropriate point of handover. However this is often obscured by the presence of the fading components of the signal causing confusion in making an appropriate handover

decision. As a result the radio link may be switched back and forth between neighbouring base stations jeopardizing the call quality and increasing the chance of a lost call. This phenomenon, i.e. repeated handovers between two base stations, is called the *ping-pong* effect. An improperly designed handover algorithm results in an unacceptably high level of ping-ponging which could give rise to high signalling costs in addition to increasing the probability of forced termination of calls.

An optimal handover algorithm should reflect the optimal tradeoff between the call quality (i.e., higher signal to noise ratio) and the signalling cost. If the handovers could be accomplished without any signalling cost, the best algorithm will be the one which connects the mobile station to a base station with the highest signal strength at each instant. However, in the presence of non-zero signalling costs, a better handover algorithm is one which also minimises the number of unnecessary handovers. The handover algorithm proposed in GSM provides, among other things, a handover margin (hysteresis) to be incorporated in the process as a means of preventing unnecessary handovers. However, a suitable value for this parameter has to be determined in conjunction with the other parameters involved in the processing of the mobile received signal.

For instance, a short signal averaging time may result in an increase in unnecessary handovers, while a long averaging time may result in a failure to detect a necessary handover. Introduction of a hysteresis level ensures that necessary handovers occur, while the unnecessary handovers are reduced if not eliminated totally. However, application of the hysteresis level leads to a delay in the handover decision and has to be kept as small as possible. Therefore, care should be taken in choosing the signal

averaging period and the hysteresis level to achieve the optimum trade-off between the number of unnecessary handovers and the delay in handover.

## 7.1 Handover Initiation Parameters

The two significant design factors influencing the performance of the handover initiation based on the received signal strength include: (a) control mechanisms to limit the numbers of unnecessary handovers, such as the hysteresis level, the signal threshold level, the length and shape of averaging window and, (b) parameters effecting the time of a handover decision such as the averaging period, sample interval size and the detection time.

Both experimental and analytical models for handover algorithms have been reported in the literature. Gudmundson [59] has proposed a class of linear handover algorithms, in which the decision is based on the linear characteristics of the signal. He suggests that an optimal handover decision is possible when the future value of the signal is known exactly. Chia and Warburton [58] have presented experimental results for handover using signal strength averaging. They examined the probability of handover and the effects of hysteresis. Vijayan and Holtzman [57, 183] have studied the dynamic behaviour of handover algorithms based on field strength measurements in a fading environment. The analysis is carried out in terms of level crossings of a stochastic process which is the difference between two processes, each representing the signal strength from a base station. At first, the level crossing process was assumed to be stationary; later work [62] included the nonstationary case. Zhang and Holtzman [69] have extended the case of relative strengths to the

case of combined absolute and relative strengths. The reported results indicate the possible tradeoff between delay and the expected number of unnecessary handovers when the averaging interval is fixed. They show that as either the hysteresis margin is raised or the signal threshold level lowered, the mean number of unnecessary handovers decreases and the expected delay increases. When the hysteresis level is small for the considered parameters, the threshold has a greater influence on the expected number of unnecessary handovers and crossover points. Murase, Symington and Green [61] also have looked into the effect of signal averaging time on the hysteresis level and handover performance. Ruggieri et. al [184] have extended the model in [57] to account for the effects of the mobile's movement direction, the effects of the cross-correlation of shadow fading and the presence of more than two base stations.

Corazza et al. [185] have evaluated the trade-off between delay and number of unnecessary handovers based on a simulation study. Their work have focused on the shape of the averaging window, and have considered both rectangular windows and exponential windows with various weights. Results show that long averaging periods reduce the number of unnecessary handovers but increase the delay. Kwon et al. [186] have investigated handover algorithms for various hysteresis levels and overlap conditions. Bernhardt [187] has studied the performance of handover in a frequency-reuse time-division multiplexed system via a computer simulation. He has shown that handover based on the comparison of time-averaged relative power of different channels, combined with hysteresis, can be the nucleus of an effective trigger mechanism.

Dassanayake [56] has investigated the effects of averaging the measurement samples of signal strength and the hysteresis setting of the handover algorithms on the elimination of unnecessary handover requests. A computer simulation based on a four cell model consisting of a serving cell, a target cell and two neighbouring cells has been used. Senadji et. al [188] have studied optimization of two conflicting criteria, the number of unnecessary handovers and the number of lost calls due to dropout. Their study was based on the Bayes criterion which is commonly used in detection and estimation techniques. However, this algorithm requires a real-time computation of a dynamic threshold. This computation leads to an increase in decision time which is an undesirable effect.

Senarath et. al [189] have shown that under realistic prediction schemes, depending on the mobile environment (mobile speed and direction, shadowing correlation and cell layout), an improvement in the call dropout performance can be obtained through hysteresis schemes in addition to the improvement obtainable in unnecessary handover performance. Kapoor et. al [71] have adopted an adaptive prediction based decision to improve the handover performance. The proposed algorithm makes use of the correlation properties of the shadow fading and attempts to make an optimal decision by predicting the future value of the signal strength:

A handover algorithm based on the fuzzy logic is discussed in literature [190, 191]. In [191], it is proposed that a fuzzy adaptive averaging interval for the received signal measurement. The algorithm consists of two fuzzy logic controllers. The first controller takes into account the signal variation and the change the averaging interval accordingly. The second controller dynamically adapts the hysteresis level

with signal differences between two stations.

## 7.2 Received Signal Statistics

At any time, mobile station scans all broadcast control channels as shown in Fig. 7.1. Averaging  $n$  successive samples will constitute the received signal level at a given location. The period between sampling times  $\Delta T$  is chosen long enough to mitigate the effect of Rayleigh fading. Let the sampled signal level at time  $i\Delta T$  be defined as  $r_i \triangleq r(i\Delta T)$ . Then the sample mean of the received signal  $\hat{r} = \frac{1}{n} \sum_{i=1}^n r_i$  can be used to determine the unbiased estimate of the received signal local mean level. According to the central limit theorem, the received signal estimated level  $\hat{r}$  is a Gaussian random variable with mean  $\mu$  and standard deviation  $\sigma$ . Therefore, pdf of the

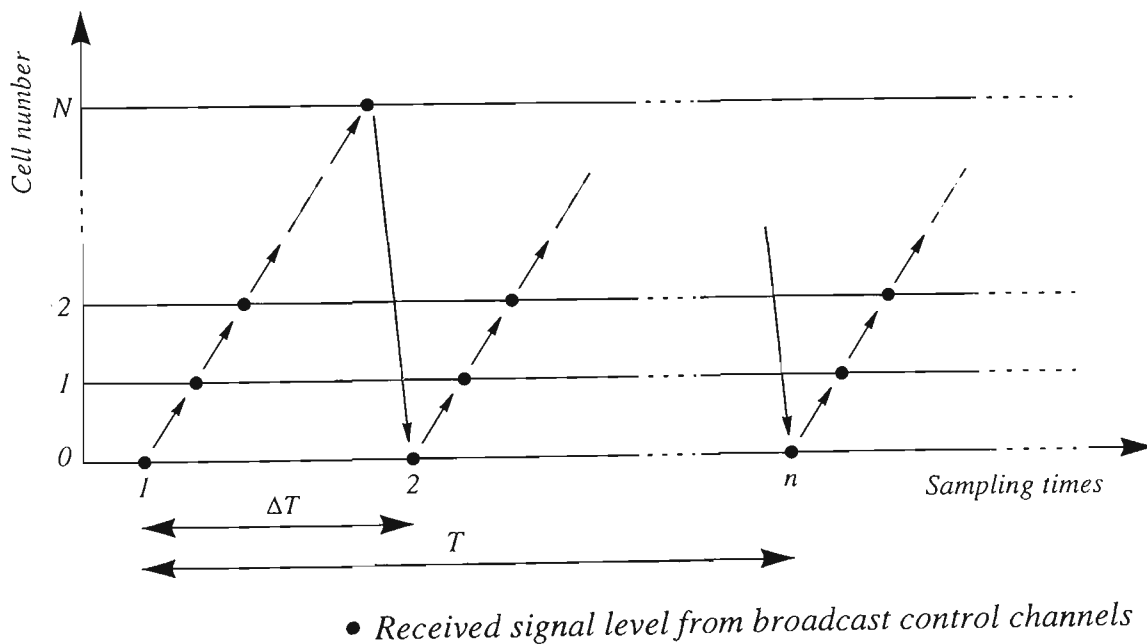


**Fig. 7.1.** Control channel measuring sequence. Cell number 0 stands for the current cell and other cell numbers stand for the neighbour cells [61].

estimated signal level will be,

$$f_{\hat{R}}(\hat{r}) = \frac{1}{\sqrt{2\pi}\sigma} e^{-\frac{(\hat{r}-\mu)^2}{2\sigma^2}} \quad (7.1)$$

### 7.2.1 Mean of the received signal level

Assuming all the sample signals have the same mean,  $\bar{r}_i = \mu$ , the mean value is given by,

$$E\{\hat{r}\} = \frac{\bar{r}_1 + \bar{r}_2 + \dots + \bar{r}_n}{n} = \mu \quad (7.2)$$

The mean of the signal levels received from the two base stations separated by  $D[Km]$  at a point  $d[Km]$  from communicating base station can be formulated as,

$$\mu_0(d) = K_1 - K_2 \log d \quad d \in (0, D) \quad (7.3)$$

$$\mu_1(d) = K_1 - K_2 \log(D - d) \quad d \in (0, D) \quad (7.4)$$

where  $K_1$  and  $K_2$  are the parameters representing the respective path losses.

### 7.2.2 Variance of the received signal level

Shadowing behaves as a Gaussian noise with an average value of zero and a standard



deviation of  $\sigma_s$ . Shadowing is a slow phenomenon, having correlation effects over several tens of meters. To model such a correlation, power spectrum of the shadow fading  $S_s(f)$  can be assumed to be flat as per [192],

$$S_s(f) = \begin{cases} \sigma_s^2/2f_m & |f| \leq f_m \\ 0 & |f| > f_m \end{cases} \quad (7.5)$$

where  $f_m$  is the maximum shadow fading rate. This rate is significantly lower than the fast fading rate (i.e. maximum Doppler rate) that would apply to the mobile terminal's carrier envelope [193]. The auto-correlation function  $R_s(\tau)$  of the shadow fading signal of  $s(t)$ , is derived from (7.5) and is given by:

$$\begin{aligned} R_s(\tau) &= \mathfrak{S}^{-1}[S_s(f)] = \int_{-f_m}^{f_m} \sigma_s^2/2f_m e^{j2\pi f\tau} df \\ &= \sigma_s^2 \text{sinc}(2f_m\tau) \end{aligned} \quad (7.6)$$

where  $\mathfrak{S}^{-1}[\ ]$  denotes the inverse Fourier transform, and  $\text{sinc}(X) = \sin(\pi X)/(\pi X)$ . Therefore, the auto-correlation function of the received signal  $R_r(\tau)$  and its auto-covariance  $Cov(\tau)$  will be:

$$\begin{aligned} R_r(\tau) &= R_s(\tau) + \mu^2 \\ &= \sigma_s^2 \text{sinc}(2f_m\tau) + \mu^2 \end{aligned} \quad (7.7)$$

$$Cov(\tau) = \sigma_s^2 \text{sinc}(2f_m\tau) \quad (7.8)$$

The variance of the mean received signal will be:

$$\begin{aligned}
 \text{Var}\{\hat{r}\} &= \text{Var}\left\{\sum_{i=1}^n r_i/n\right\} \\
 &= \frac{1}{n^2} E\left\{\left[\sum_{i=1}^n r_i - \sum_{i=1}^n \bar{r}_i\right]^2\right\} \\
 &= \frac{1}{n^2} E\left\{\left[\sum_{i=1}^n (r_i - \bar{r}_i)\right]^2\right\} \\
 &= \frac{1}{n^2} E\left\{\sum_{i=1}^n \sum_{j=1}^n (r_i - \bar{r}_i)(r_j - \bar{r}_j)\right\} \tag{7.9} \\
 &= \frac{1}{n^2} \sum_{i=1}^n \sum_{j=1}^n E\{(r_i - \bar{r}_i)(r_j - \bar{r}_j)\} \\
 &= \frac{1}{n^2} \left\{ \sum_{i=1}^n \text{Var}(r_i) + 2 \sum_{i=1}^n \sum_{j=i+1}^n \text{Cov}(r_i, r_j) \right\} \\
 &= \frac{1}{n} \left\{ \text{Cov}(0) + 2 \sum_{i=1}^n \left(1 - \frac{i}{n}\right) \text{Cov}(i \Delta T) \right\}
 \end{aligned}$$

Using (7.8), the variance of the mean received signal can be expressed as:

$$\text{Var}\{\hat{r}\} = \frac{\sigma_s^2}{n} \left[ 1 + 2 \sum_{i=1}^n \left(1 - \frac{i}{n}\right) \text{sinc}(2f_m i \Delta T) \right] \tag{7.10}$$

Thus the standard deviation of the received signal  $\sigma$  depends on the number of samples  $n$  and the time between two successive samples  $\Delta T$  and can be obtained as,

$$\sigma = \sigma_s \sqrt{\frac{1}{n} \left[ 1 + 2 \sum_{i=1}^n \left( 1 - \frac{i}{n} \right) \text{sinc}(2f_m i \Delta T) \right]} \quad (7.11)$$

The is the same result as that of [61, 192], though we have obtained it by a different approach. Depending on the type of the terrain, the shadow standard deviation  $\sigma_s$  lies in the range 3 to 12dB [173, 174]. The maximum shadow fading rate  $f_m$  is assumed to be 1/200<sup>th</sup> of the maximum Rayleigh fading rate [192] i.e.,

$$f_m = \frac{v}{100\lambda} \quad (7.12)$$

In the case of a mobile with speed  $v = 20\text{Km/h}$  and carrier signal wavelength  $\lambda = 30\text{cm}$ , we have  $f_m = 0.2\text{Hz}$ . For cases where an estimate of shadow standard deviation is important, Sampath et al. [194] provide a method to estimate the shadow standard deviation from the average difference of signal strengths. The method requires knowledge of the correlation decay model for the shadows, and is claimed to be relatively insensitive to model mismatches. Vijayan et al. [195] also report that the correlation decay factor between shadows has little effect on handover performance. A careful examination of (7.11), as illustrated in Fig. 7.2, reveals that the received signal standard deviation is quite sensitive to changes in shorter averaging periods than longer ones.

### 7.3 Handover Algorithm with Hysteresis

In cellular mobile networks, like GSM and DECT, the handover decision is mainly

based on relative difference between the signal levels of a communicating base station and neighbouring base stations. In the simplest case, the received signal level of the communicating base station decreases monotonically as the mobile station moves away from the base station. By contrast, the signal level of the neighbouring base station increases correspondingly. Assuming that both base stations have the same characteristics and transmit power, a mobile station will experience an approximately same signal level from both base stations at a location half-way between the two base stations (point A in Fig. 7.3). The point A is the ideal location to set the handover threshold, in which the handover request will be uniquely controlled by the two signal profiles. In practice due to the uncertainty arising from

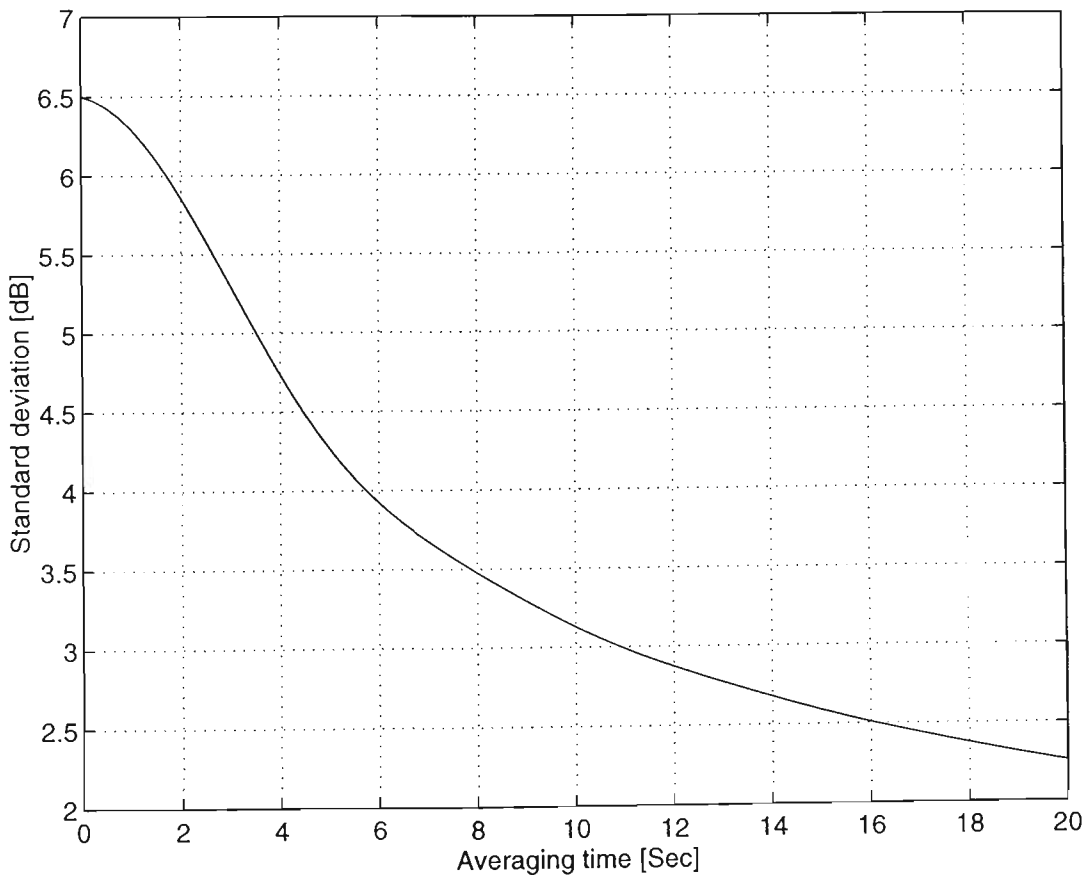


**Fig. 7.2.** Standard deviation as a function of averaging period.

the fluctuation of the received signals, setting such a point as the handover threshold will give rise to a numerous amount of unnecessary handovers (ping-pong effect) before capturing the target base station. To avoid ping-pong effect a hysteresis level is applied for handover decision. Adoption of hysteresis level can result in intelligent decisions as to determine whether and when handovers should take place. However, applying hysteresis level  $h$  [dB] shifts the handover decision (threshold) from point  $A$ , (where  $\mu_0(d_1) - \mu_1(D - d_1) = 0$ ) (Fig. 7.3), to point  $B$ , (where  $\mu_0(d_2) - \mu_1(D - d_2) = h$ ). It is obvious that in a uniform cellular network with similar base stations, we will have  $d_1 = D/2$ .

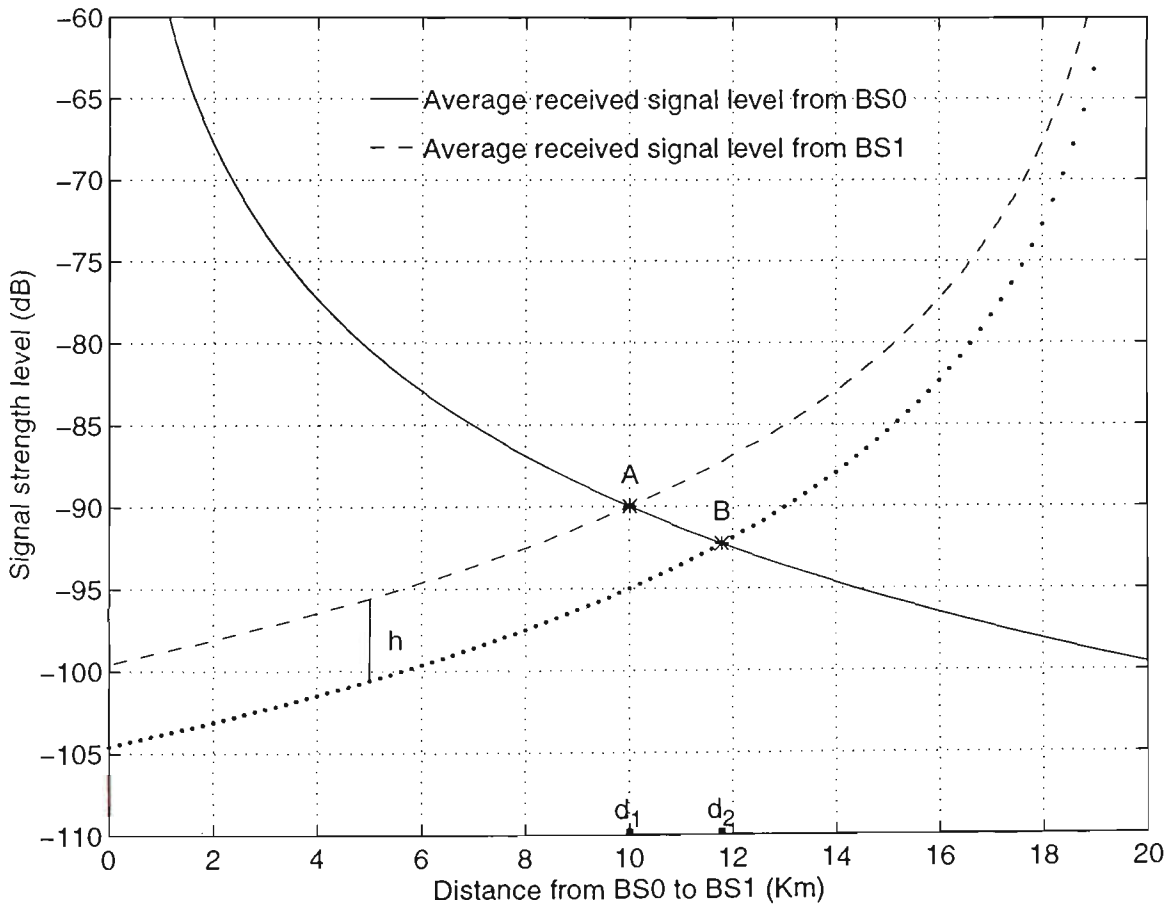


Fig. 7.3. Received signal level from two base stations without shadow fading.

## 7.4 Unnecessary Handovers

The probability of an unnecessary handover  $P_U$  is defined as the probability that a mobile station performs a handover from the existing base station  $BS0$  to the neighbouring base station  $BS1$  and then initiates another handover back to  $BS0$ . Let  $\hat{R}_{\#0}$  be the signal estimated level in  $dB$  received at the mobile station from the communicating base station, and  $\hat{R}_{\#1}$  be the signal estimated level received from the neighbouring base station which has the strongest level among all other neighbouring base stations. Then, the respective handover probabilities (connection from  $BS0$  to  $BS1$  and back from  $BS1$  to  $BS0$ ) can be defined by,

$$prob\{BS0 \rightarrow BS1\} = \int_{\hat{r}=-\infty}^{\hat{r}=\infty} prob\{\hat{R}_{\#1} = \hat{r}\} \cdot prob\{\hat{R}_{\#0} < (\hat{r} - h)\} \cdot d\hat{r} \quad (7.13)$$

$$prob\{BS1 \rightarrow BS0\} = \int_{\hat{r}=-\infty}^{\hat{r}=\infty} prob\{\hat{R}_{\#0} = \hat{r}\} \cdot prob\{\hat{R}_{\#1} < (\hat{r} - h)\} \cdot d\hat{r} \quad (7.14)$$

where,

$$prob\{\hat{R}_{\#1} = \hat{r}\} = F_{\hat{R}_{\#1}}(\hat{r} + d\hat{r}) - F_{\hat{R}_{\#1}}(\hat{r}) \quad (7.15)$$

and  $f_{\hat{R}_{\#1}}(\hat{r})$  has a normal pdf as in (7.1). Considering,

$$f(x) = \mathfrak{N}(0, 1) = \frac{1}{\sqrt{2\pi}} e^{-x^2/2} \quad (7.16)$$

as the normalised received signal pdf, the  $prob\{\hat{R}_{\#1} = \hat{r}\}$  will be equal to:

$$\begin{aligned} prob\{\hat{R}_{\#1} = \hat{r}\} &= F_X(x+dx) - F_X(x) \\ &= prob\{X = x\} \end{aligned} \quad (7.17)$$

where,  $x = \frac{\hat{r} - \mu_1}{\sigma}$ . The same argument will result in,

$$\begin{aligned} prob\{\hat{R}_{\#0} < (\hat{r} - h)\} &= F_{\hat{R}_{\#0}}(\hat{r} - h) \\ &= F_X\left(\frac{\hat{r} - h - \mu_0}{\sigma}\right) \\ &= F_X\left(\frac{\hat{r} - h - \mu_1 + \Delta L}{\sigma}\right) \\ &= F_X\left(x - \frac{h - \Delta L}{\sigma}\right) \\ &= prob\left\{\left(X - \frac{h - \Delta L}{\sigma}\right) < x\right\} \end{aligned} \quad (7.18)$$

where  $\Delta L = \mu_1 - \mu_0$  is the difference between the two received signal levels due to the path loss difference from the two base stations. Considering (7.17) and (7.18), we can replace (7.13) with the following relation (Fig. 7.4),

$$\begin{aligned} prob\{BS0 \rightarrow BS1\} &= \int_{x=-\infty}^{x=\infty} \left[ prob\{X = x\} \cdot prob\left\{\left(X - \frac{h - \Delta L}{\sigma}\right) < x\right\} \right] dx \\ &= \int_{-\infty}^{\infty} f(x) \left[ \int_{-\infty}^x f\left(x - \frac{h - \Delta L}{\sigma}\right) dx \right] dx \end{aligned} \quad (7.19)$$

The same procedure will result in,

$$\begin{aligned}
 \text{prob}\{BS1 \rightarrow BS0\} &= \int_{x=-\infty}^{x=\infty} \left[ \text{prob}\{X=x\} \cdot \text{prob}\left\{\left(X - \frac{h + \Delta L}{\sigma}\right) < x\right\} \right] dx \\
 &= \int_{-\infty}^{\infty} f(x) \left[ \int_{-\infty}^x f\left(x - \frac{h + \Delta L}{\sigma}\right) dx \right] dx
 \end{aligned} \tag{7.20}$$

Therefore,

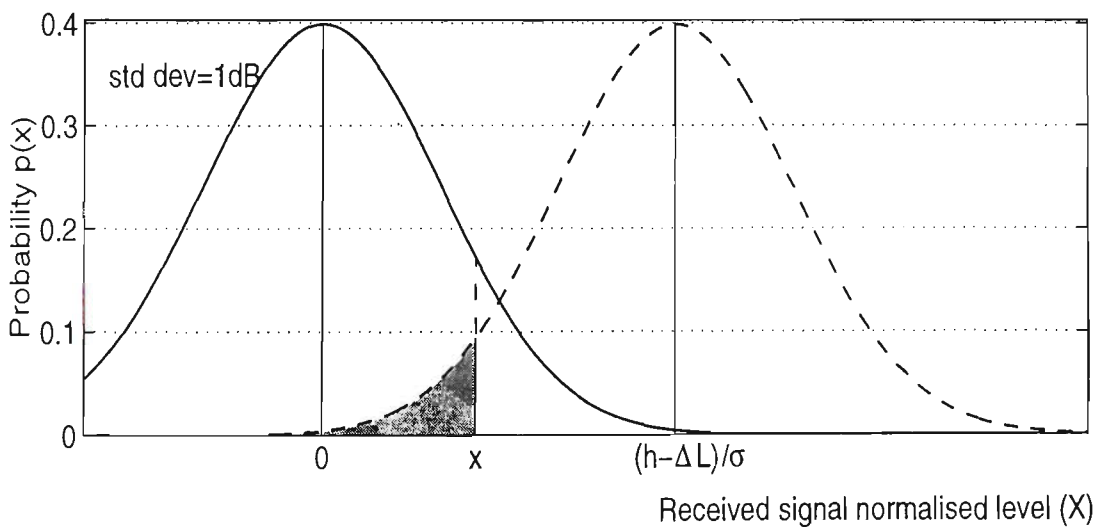
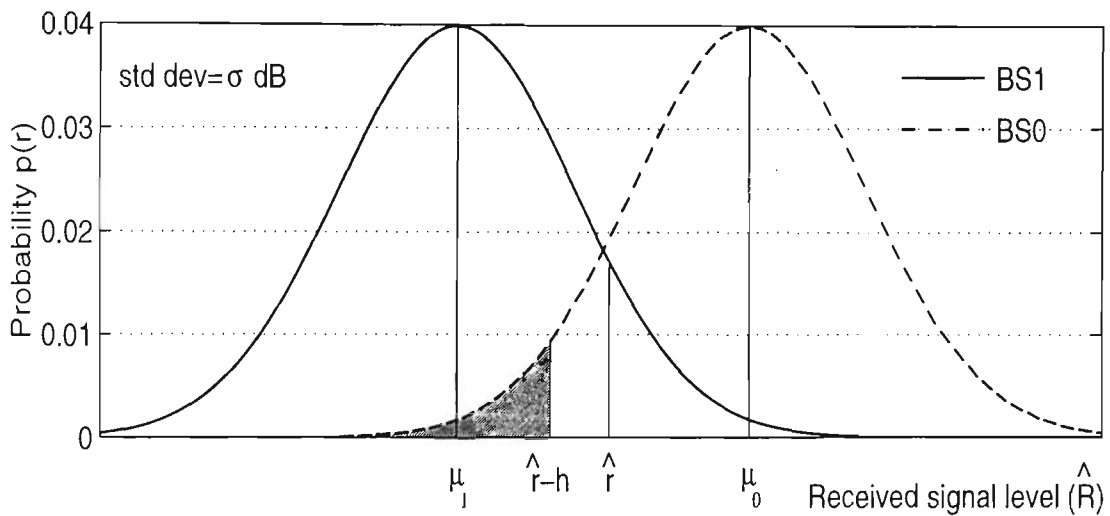


**Fig. 7.4.** Conversion of the normal distributions to the equivalent standardized normal distributions.



$$\begin{aligned}
P_U &= \int_{-\infty}^{\infty} f(x) \left[ \int_{-\infty}^x f\left(x - \frac{h - \Delta L}{\sigma}\right) dx \right] dx \times \int_{-\infty}^{\infty} f(x) \left[ \int_{-\infty}^x f\left(x - \frac{h + \Delta L}{\sigma}\right) dx \right] dx \\
&= \int_{-\infty}^{\infty} f(x) \left[ \frac{1}{2} + \operatorname{erf}\left(x - \frac{h - \Delta L}{\sigma}\right) \right] dx \times \int_{-\infty}^{\infty} f(x) \left[ \frac{1}{2} + \operatorname{erf}\left(x - \frac{h + \Delta L}{\sigma}\right) \right] dx
\end{aligned} \tag{7.21}$$

where,  $\operatorname{erf}(x) = \int_0^x f(x) dx$ . This result agrees with that of [61], where it was stated without proof. The closed-form solution of (7.21) is difficult and a numerical integration performed within the limits of  $\pm 3\sigma$  for different values of  $\Delta L$  and  $h$  gives the results illustrated in Fig. 7.5. It can be seen that the probability of unnecessary handovers is maximum when a mobile station is moving on the cell boundary, i.e.  $\Delta L = 0$ .

A numerical solution of (7.11), (7.21) could explain the dependencies between standard deviation of the sample averaged received signal  $\sigma$ , standard deviation of the shadow fading  $\sigma_s$ , received signal averaging time  $T$ , hysteresis level  $h$  and unnecessary handover probability  $P_U$ . Fig. 7.6 shows the variation of unnecessary handover probability with the averaging time, for two different hysteresis levels. It is clear from the figures that this probability decreases rapidly with increasing averaging time. The amount of averaging time required to reduce inappropriate handover requests is dependent on the variance of shadow fading to which the signal is subjected. Under light shadowing conditions (less variance) the handover algorithm performs better with low values of hysteresis levels. In this situation a high hysteresis level could extend the cell boundary beyond acceptable limits, causing both cochannel and adjacent channel interference in neighbouring cells. The same results have been extracted by Dassanayake [56] via simulation.

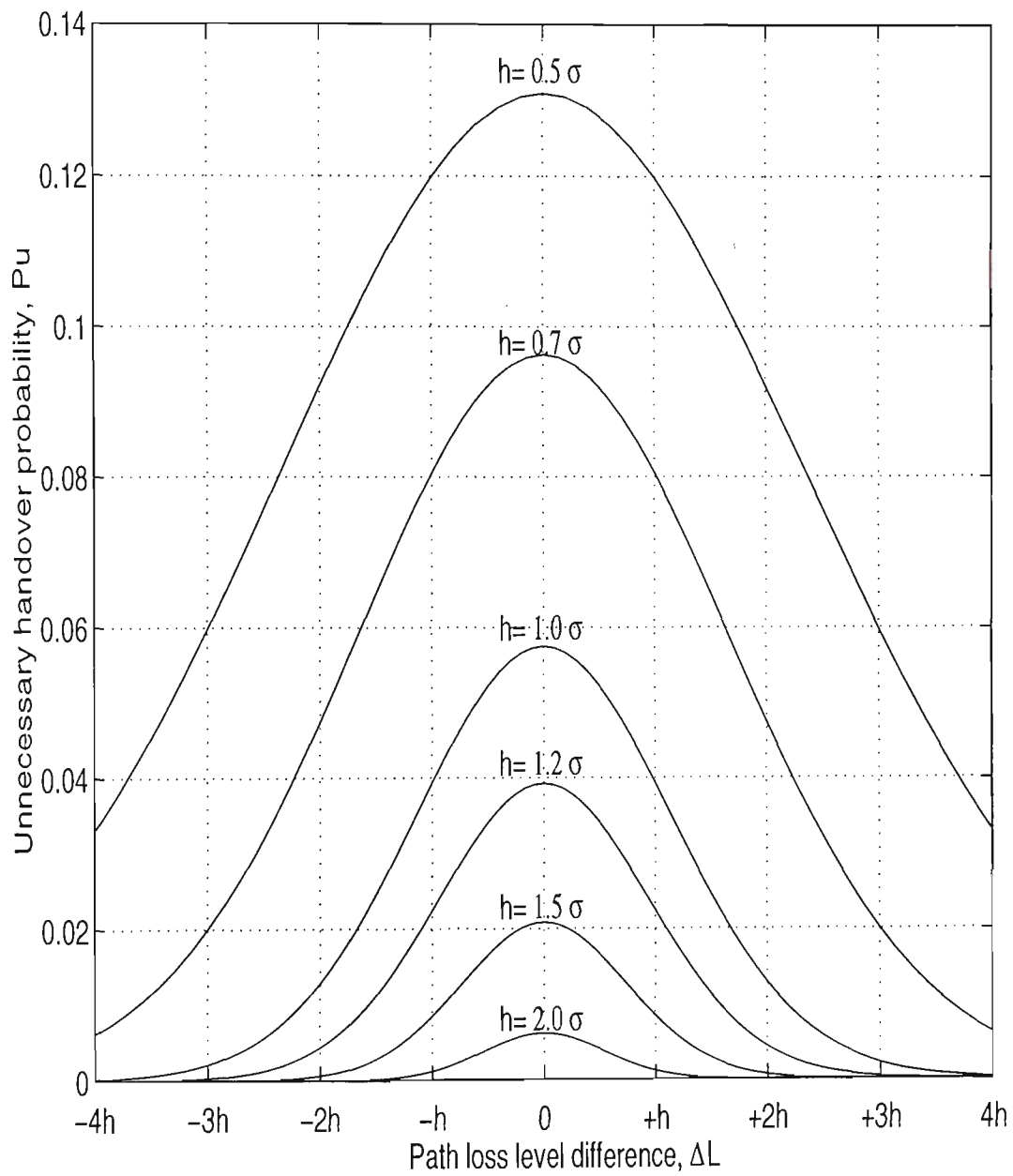


Fig. 7.5. Unnecessary handover probability versus path loss difference normalised to hysteresis level.

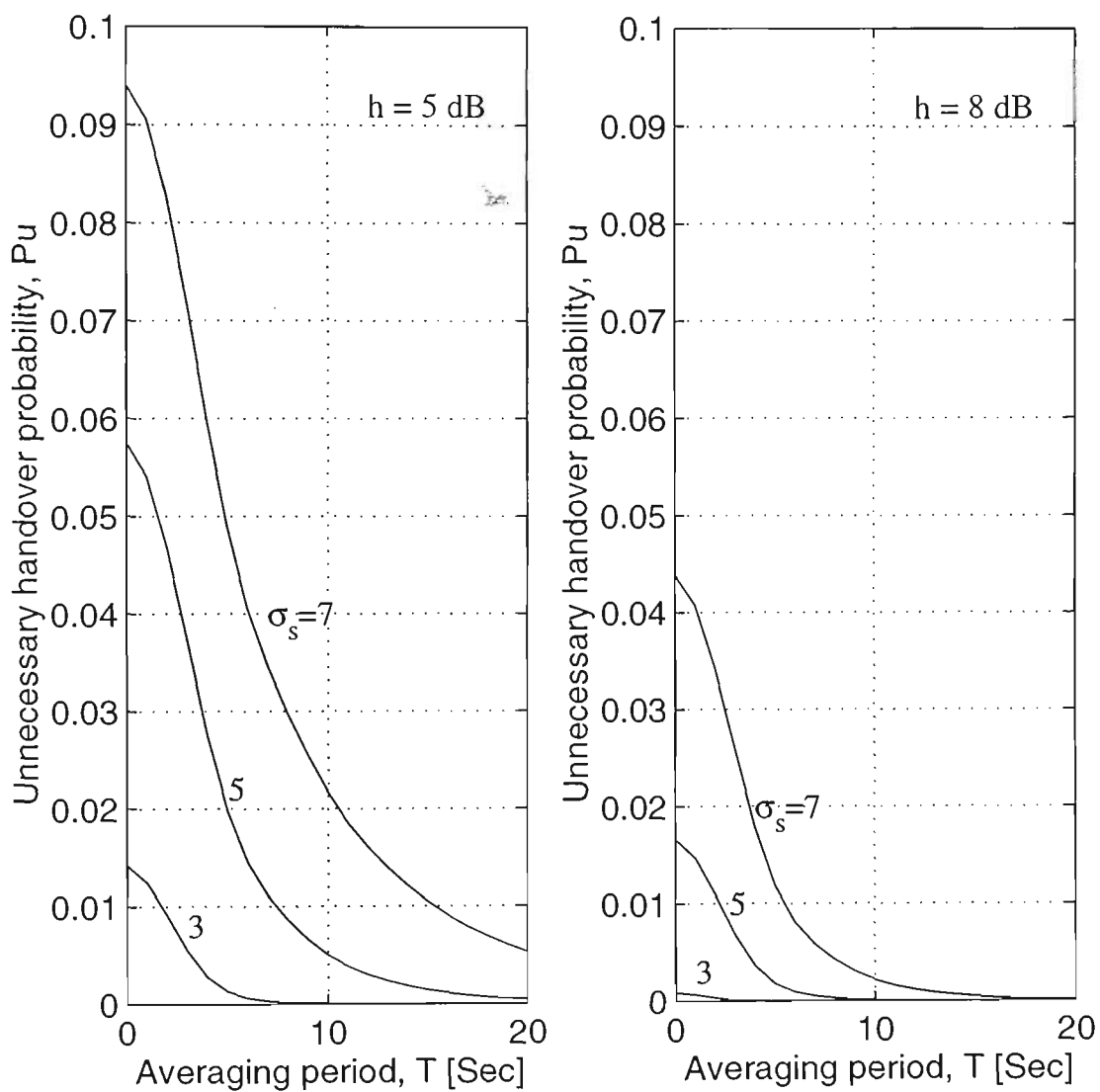


Fig. 7.6. Effect of shadow fading variance and hysteresis level on unnecessary handover probability.

Fig. 7.7 shows probability of unnecessary handovers for different hysteresis levels on the cell boundary. It can be seen that the probability of unnecessary handovers decreases as the hysteresis level increases. By using (7.11) and (7.21), the relationship between the signal averaging period and the hysteresis level for different probabilities of unnecessary handover can be obtained as shown in Fig. 7.8. For example, in order to have the probability of unnecessary handover less than 1%, the hysteresis level should not be less than 5.8[dB] when the received signal averaging period  $T$  is 10[sec].

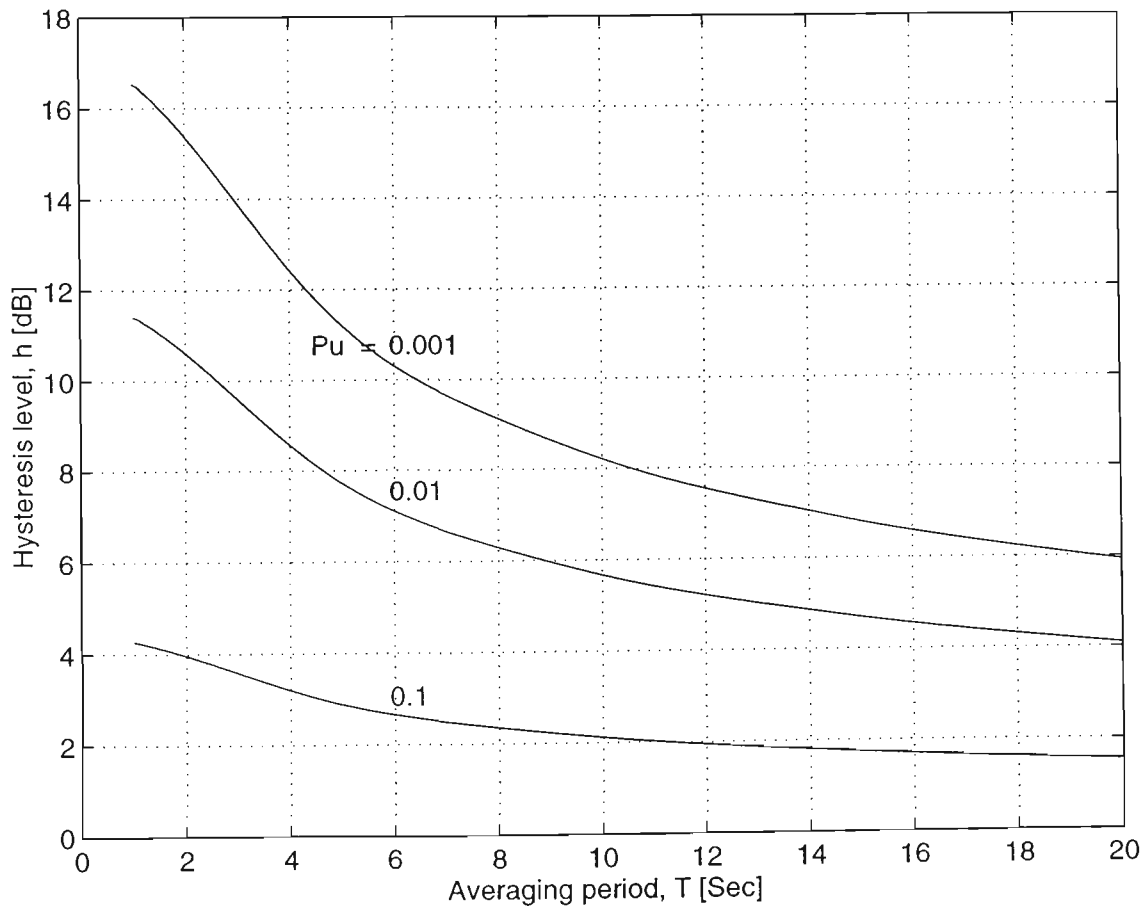


Fig. 7.8. Relation between three parameters of  $h$ ,  $T$ ,  $P_u$ .

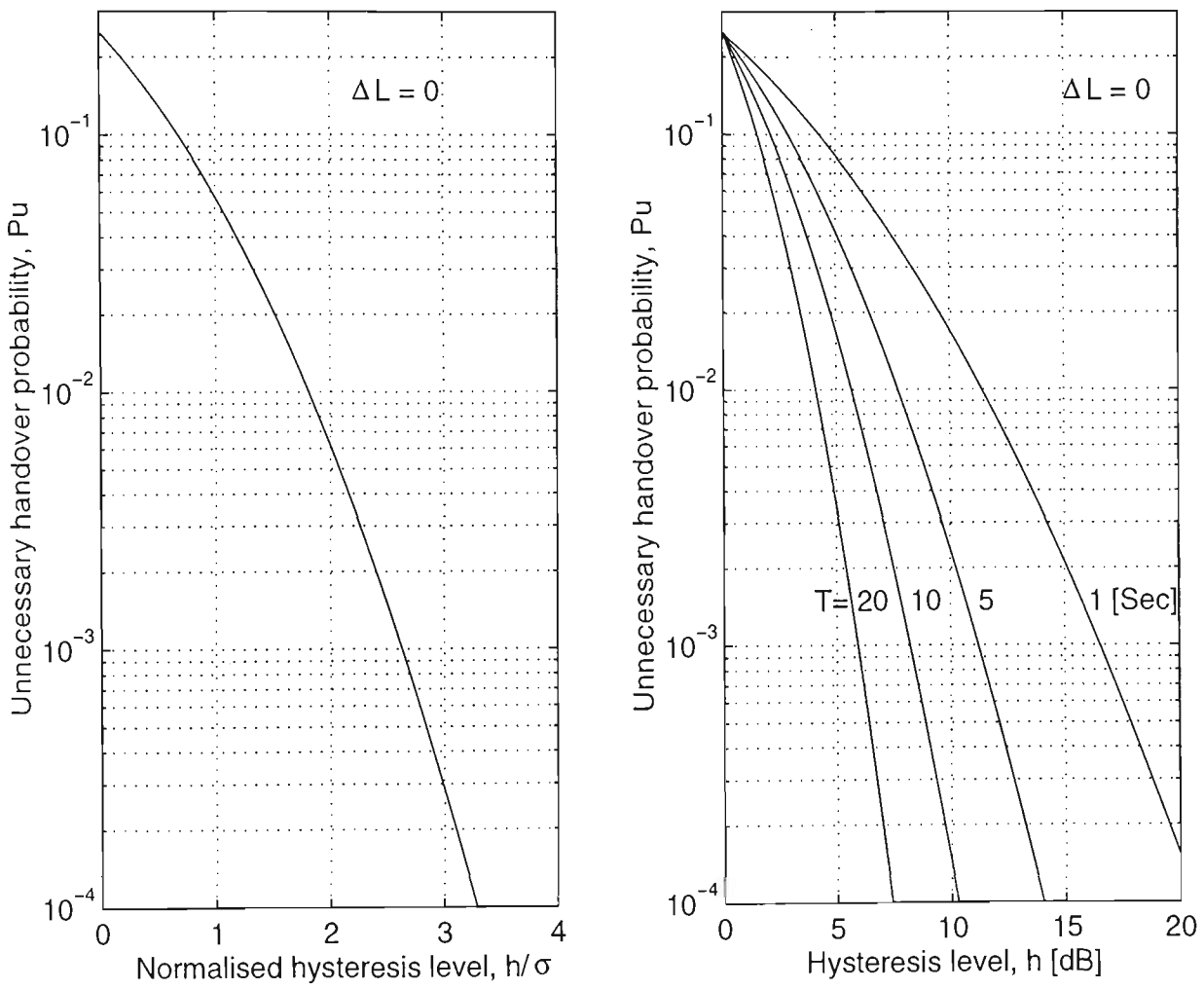


Fig. 7.7. Unnecessary handover probability versus hysteresis level for different signal averaging time.

## 7.5 Handover Delay

Handover delay is another issue of concern in the design of handover algorithms. If handover does not occur quickly, the quality of service (QoS) may deteriorate below an acceptable level. Minimizing delay also minimizes co-channel interference. If the signal quality changes fast the handover algorithm must react promptly in order to save the call. The time involved in the handover process is mainly due to the time taken for measuring and processing the signal strength, and making a decision for handover initiation, if actual switching time is ignored.

One other consideration that has to be taken into account when designing handover schemes is that fast handover algorithms can be unstable, while slower handover algorithms can result in poor signal quality. Unstable handover schemes consume a lot of computational resources just for handover management; resources that could be better used for other tasks. A slow algorithm can cause a mobile to remain connected to a base station even when it has moved well inside the cell of a closer base station.

The handover delay can be taken as the time delay occurring due to signal averaging and setting of a hysteresis margin. The averaging period  $T$  includes  $n$  samples with half of them extracted from the past samples. Therefore, the averaging would create a constant delay of  $T/2$ . Moreover, applying hysteresis level causes an additional delay. Hysteresis delay  $\delta_h$  is defined as the time associated between optimal point of handover and the actual point of handover with hysteresis. The optimal point (or crossover point) is the point where the probability of mobile being assigned to either

stations is equal. The sum of averaging delay and hysteresis delay constitutes the handover delay.

Since the probability of handover increases as the path loss difference decreases, most of the handovers are initiated before the path loss difference becomes equal to  $h$ . Let the standard deviation  $\sigma$  of the averaged received signal be the same for any of the base stations. Then we can assume that most handovers will be initiated when the path loss difference approaches  $(h - \sigma)$ .

Depending on the type of the cell (macro- or micro-), the amount of the handover delay involved can be calculated as shown in the following sub-sections.

### 7.5.1 Handover delay in macrocells

As is stated above, the handover occurs at a point where the difference between the two signals is  $h - \sigma$ , i.e. at point  $B$  in Fig. 7.9.

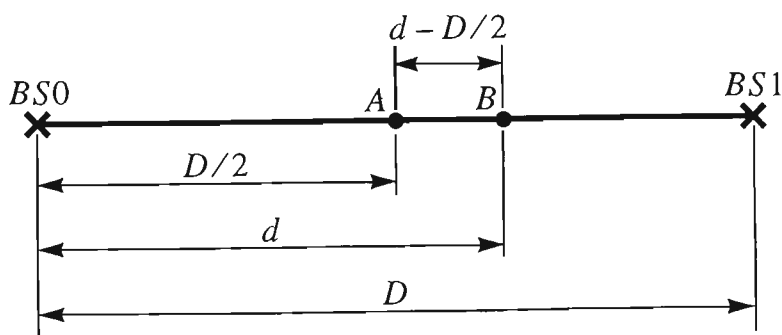


Fig. 7.9. Definition of parameters for delay calculation.

$$h - \sigma = \mu_1 - \mu_0 \quad (7.22)$$

Let  $d$  be the distance of handover point from the  $BS_1$ , and  $D$  be the distance between two base stations as shown in Fig. 7.9. Using (7.3) and (7.4), with (7.22) the hysteresis margin can be obtained as follows,

$$h - \sigma = K_2 \log \frac{d}{D - d} \quad (7.23)$$

Therefore,

$$\frac{d}{D - d} = 10^{\frac{h - \sigma}{K_2}} \quad (7.24)$$

After some algebraical manipulation the following relation can be obtained,

$$\frac{2d - D}{D} = \left( 10^{\frac{h - \sigma}{K_2}} - 1 \right) / \left( 10^{\frac{h - \sigma}{K_2}} + 1 \right) \quad (7.25)$$

A mobile moving at a speed  $v$  will be subjected to a delay in handover decision making which (from Fig. 7.9) can be calculated as the time interval associated between points  $A$  and  $B$ . Therefore, handover delay is,

$$\delta_h = \frac{d - D/2}{v} \quad (7.26)$$



Considering (7.25) and (7.26) we have,

$$\delta_h = \frac{D}{2v} \left\{ \left( 10^{\frac{h-\sigma}{K_2}} - 1 \right) / \left( 10^{\frac{h-\sigma}{K_2}} + 1 \right) \right\} \quad (7.27)$$

This result is similar to that of [61], where it was stated without proof. Let the cell size be normalized with respect to the speed of the mobile and be shown by  $K_{Rv} = D/2v$ . Then the total handover delay in a macrocell  $\delta_{hM}$  will be:

$$\delta_{hM} = \frac{T}{2} + K_{Rv} \left\{ \left( 10^{\frac{h-\sigma}{K_2}} - 1 \right) / \left( 10^{\frac{h-\sigma}{K_2}} + 1 \right) \right\} \quad (7.28)$$

Fig. 7.10 illustrates the handover delay as a function of hysteresis for different values of signal averaging period and normalized cell size,  $K_{Rv}$ . It can be seen that the handover delay and the hysteresis level are linearly related to each other. The proportionality factor (i.e. the increase in handover delay for an increase in hysteresis) increases with increasing normalized cell size. This is because the path loss slope near the cell boundaries decreases as the cell radius increases.

The delay in handover for a given probability of unnecessary handover increases as the hysteresis level increases and the averaging period decreases. Therefore, in case of macrocells where  $K_{Rv}$  is large, it is preferable to have a longer averaging period and smaller hysteresis level. This phenomenon is shown in Fig. 7.11. Since any change in the speed of the mobile will vary  $K_{Rv}$ , it is best to choose velocity adaptive signal averaging intervals. Different velocity estimators have been suggested in [4,

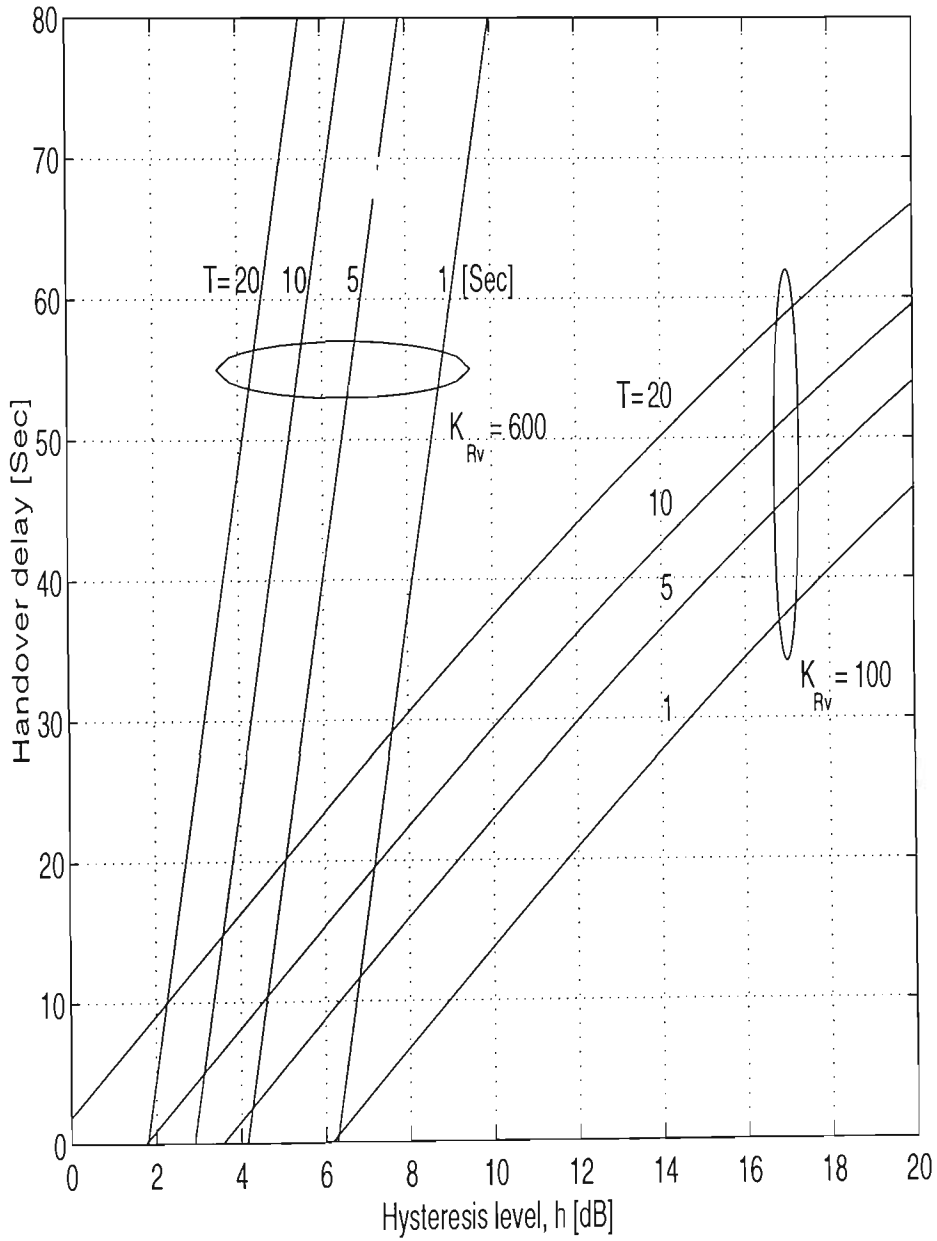


**Fig. 7.10.** Handover delay versus hysteresis levels for different signal averaging periods and cell sizes.

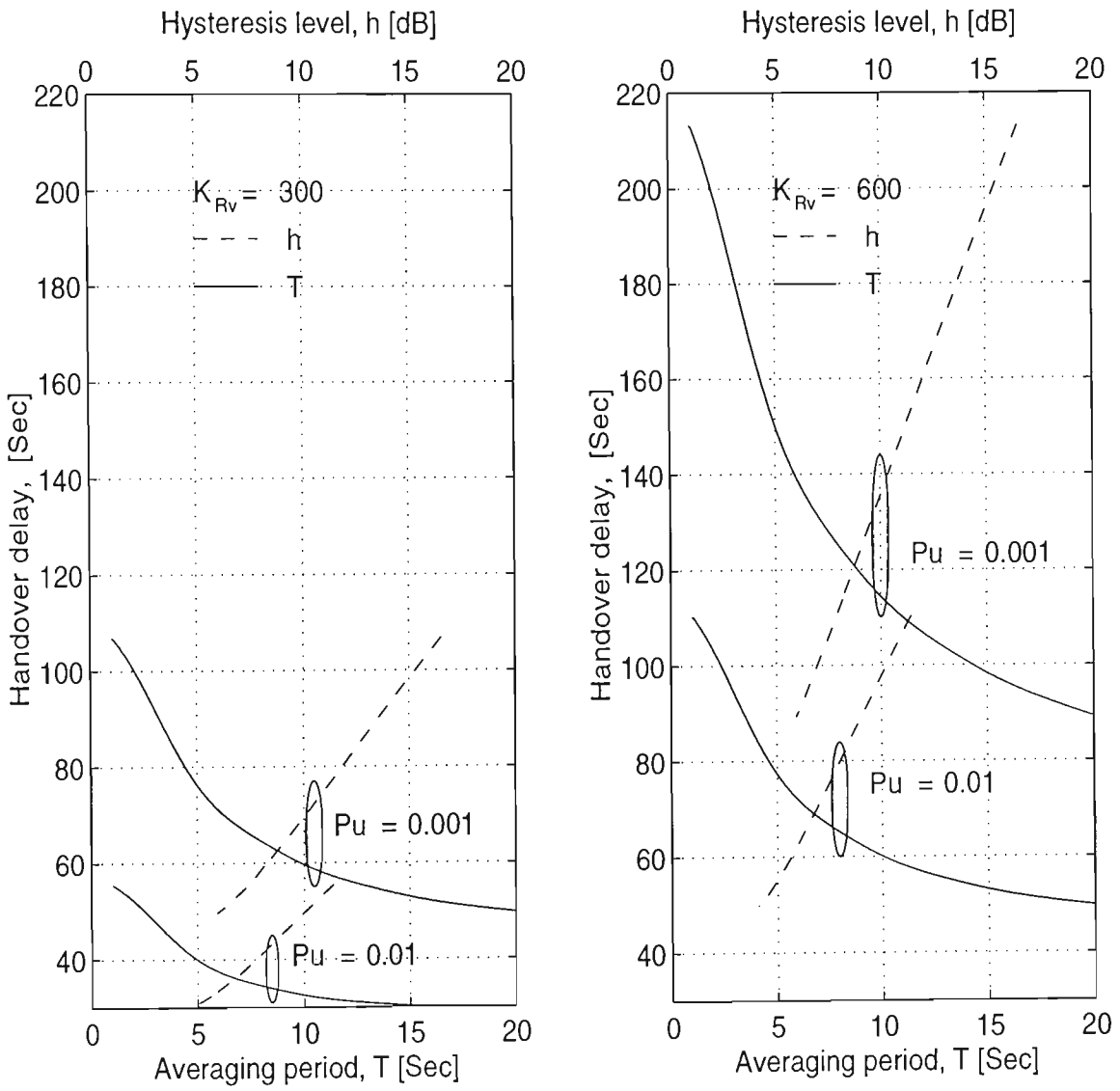


Fig. 7.11. Handover delay versus signal averaging period and hysteresis level as a function of unnecessary handovers for different cell sizes.

84, 85, 86, 196, 197]. Alternatively, this improvement can also be obtained with an adaptive hysteresis level. The idea of adjusting the hysteresis level according to the received signal strength, offers a means of fast handover in cases of the weak received signal levels. The simplest means of adjusting hysteresis level would be a linear adaptation where the hysteresis level is directly proportional to the received signal strength.

### 7.5.2 Handover delay in microcells

The received signal level from a microcell base station can suddenly fall when the mobile station makes a turn off from a main street in which the microcell base station is located. The drop in signal level is usually very sharp and could be greater than  $15dB$  within several meters from the turning point. In such cases, it is important that fast handover is carried out to prevent any connection interruption. The hysteresis delay in microcells  $\delta_h$  can be calculated by examining the geometrical relations exhibited by the signal strength profile in the vicinity of handover. With reference to Fig. 7.12, we have:

$$\frac{\delta_h}{h - \sigma} = \frac{T/2}{2L} \quad (7.29)$$

where,  $L$  is the drop in signal level (in  $dB$ ) at the street corner. Therefore,

$$\delta_h = \frac{T(h - \sigma)}{4L} \quad (7.30)$$

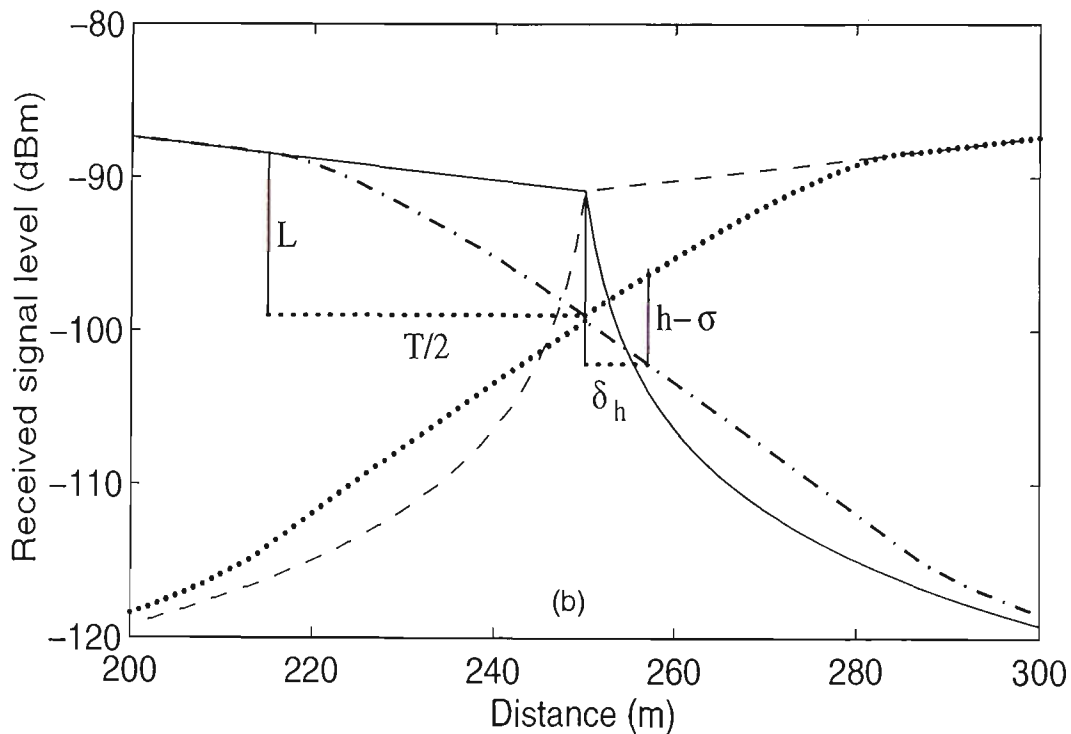
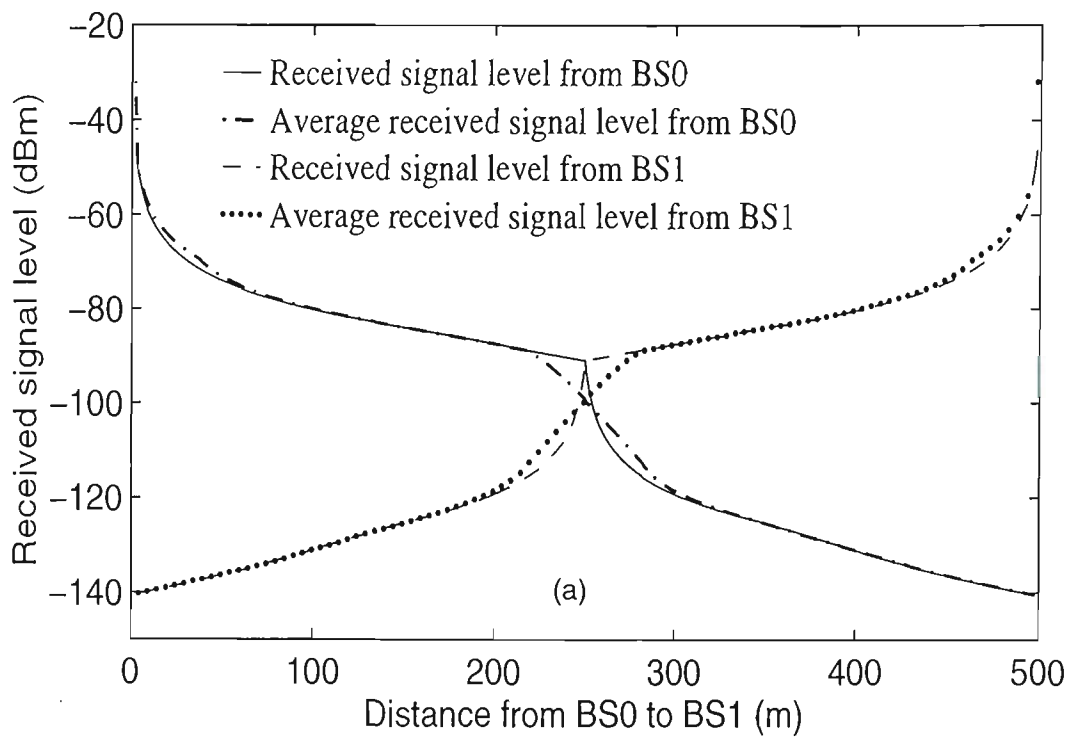


**Fig. 7.12.** Illustration of handover delay parameters in a micro-cell (figure (b) shows a zoomed region of figure (a) around the optimal point).

Taking the delay due to the averaging period also into account, the total handover delay in microcells  $\delta_{h\mu}$  can be obtained as:

$$\delta_{h\mu} = \frac{T}{2} + \frac{T(h - \sigma)}{4L} \quad (7.31)$$

## 7.6 Conclusions

In this Chapter the possibility of characterising the cell environment in terms of signal strength statistics (namely, variance) and its influence on the handover algorithm parameter settings (namely, signal averaging time and the hysteresis level) have been discussed. Improvement to handover performance has been investigated in terms of achieving less unnecessary handovers and less delay in handover decision making. An analytical approach has been developed to see how the different parameters involved in handover decision making could be optimized in both micro- and macro-cellular systems. The relationships between critical parameters including received signal averaging period, hysteresis margin and the handover delay have been discussed. It was found that the handover algorithms are quite sensitive to changes in the received signal standard deviation when averaging period is small. The possible compromise between handover parameters (i.e. the signal averaging period and the hysteresis level) under the influence of shadow fading was demonstrated. It was shown that for an accurate and stable handover, a small signal averaging period and a large hysteresis level would be appropriate for microcells, while the opposite is true for macrocells. These results are useful in setting the parameter values of the handover algorithm for its optimum performance (to achieve less

delay in handover decision making and less unnecessary handovers). The results also suggest that a hybrid handover algorithm with microcell and macrocell sensors could be used to achieve optimum performance. When the macrocell sensor is triggered a long averaging period and a short hysteresis level should be selected, while the reverse should occur when the microcell sensor is triggered.

In order to account for the velocity, it is best to choose velocity adaptive signal averaging intervals. This improvement can also be obtained with an adaptive hysteresis level. The idea of adjusting the hysteresis level according to the received signal strength offers a means of fast handover in cases of weak received signal levels.

# *Chapter 8*

## *Conclusions*

In this thesis, three important issues related to the handover process of cellular mobile systems have been investigated. They are the following,

- Effect of mobility on handover,
- Effect of handover on teletraffic performance criteria,
- Effect of propagation environment on handover decision making.

The results of this thesis are applicable to any analogue or digital cellular system in which the concept of channel is applicable.



## 8.1 Effect of mobility on handover

In Chapter 3 a mathematical formulation has been developed for systematic tracking of the random movement of a mobile station in a cellular environment. It incorporates mobility parameters under most generalized conditions so that the model could be tailored to be applicable in most cellular systems. The proposed model traces mobiles systematically in a cellular environment where they are allowed to move in a quasi-random fashion with assigned degrees of freedom. It enables the development of a computer simulation to investigate the characteristics of different mobility related traffic parameters in a cellular system. These parameters include the distribution of the cell residence time of both new and handover calls, channel holding time and the average number of handovers per call. Results show that the generalized gamma distribution is adequate to describe the cell residence time distribution of both new and handover calls. Results also show that the negative exponential distribution is a good approximation for the channel holding time distribution in cellular mobile systems. In order that these results could be made applicable to a wide range of cellular environments, it was shown that any velocity change in the mobile in a cell can be treated as contributing to an effective change in the cell radius. Taking this excess cell radius that corresponds to different values of velocity into account, a broad variety of cell coverage areas with different street orientations and traffic flows can be handled.

Further investigation is proposed to extend this method to cover the cases of microcells (CBD street structures with traffic light effects) and picocells (in-building 3D structures with slow motion).

## 8.2 Effect of handover on teletraffic performance criteria

In Chapter 5, different radio resource allocations were explained, teletraffic performance criteria were defined and an analytical model for teletraffic performance evaluation was presented. Also some traffic policies that give a higher level of protection to handover calls were described and their effect on the overall traffic performance were analysed. Based on the results obtained for cell residence time distribution, a teletraffic model that takes the user mobility into account has been presented and substantiated using a computer simulation using the next-event time-advance approach. Furthermore, the influence of cell size on new and handover call blocking probabilities has been examined. The effect of the handover channel reservation on call dropout probability has been investigated to determine the optimum number of reserved channels required for handover.

It was found that blocking probabilities of new and handover calls are the same when there are no reserved channels for the handover calls. However, these blocking probabilities become different when a portion of channels are reserved for handover calls. The rate of change of blocking probabilities of the new and handover calls with the number of reserved channels is such that the decrease in blocking probability of the handover calls due to an increase in the number of reserved channels is significantly bigger than the corresponding increase in the blocking probability of new calls. This is what makes the reserved channel scheme attractive. An efficiency factor was defined to estimate the effectiveness of this scheme. It was found that the scheme is most efficient when traffic is heavy and handover calls are most likely to be blocked.

It was also shown that with increasing cell radius, blocking probability approaches the Erlang-B results. Furthermore, the variation of the blocking probability with effective offered traffic per cell is independent of the cell size and is equal to Erlang-B results. This means that for a given new call arrival rate the consequent effective traffic intensity in a cell remains constant and is independent of cell size.

It was also shown that the dropout probability decreases with increasing number of reserved channels. This reduction is paid for by an increase in new call blocking probability. A compromise between the new call blocking probability and the dropout probability could be established by allocating a threshold level on the dropout probability.

### **8.3 Effect of propagation environment on handover decision making**

In Chapter 6, the contributions of the three different components of the mobile radio signal were considered, and propagation models suitable for micro- and macro-cells were presented. Emphasis was made on the effect of shadow fading which is by far the most important component in handover decision making in cellular networks. It was shown how a simple AR-1 model could be implemented using a digital filter to simulate the shadow fading component of the signal.

In Chapter 7, the possibility of characterising the cell environment in terms of signal strength statistics (namely, variance) and its influence on the handover algorithm parameter settings (namely, signal averaging time and the hysteresis level) have been discussed. Improvement to handover performance has been investigated in terms of

reductions in unnecessary handovers and handover delay time. An analytical approach has been developed to see how the different parameters involved in handover decision making could be optimized for both micro- and macro-cellular systems. The relationships between critical parameters including the received signal averaging period, the hysteresis level and the handover delay have been discussed.

It was found that the handover algorithms are quite sensitive to changes in the received signal standard deviation when averaging periods are small. The possible compromise between handover parameters (i.e. the signal averaging period and the hysteresis level) under the influence of shadow fading has been demonstrated. It was shown that for an accurate and stable handover, a small signal averaging period and a large hysteresis level would be appropriate in microcells, while the reverse would be true in macrocells. These results could be used in setting the parameters of the handover algorithm to achieve less delay in handover decision making and less unnecessary handovers. A hybrid handover algorithm with microcell and macrocell sensors could be used for optimum decision making such that when the macrocell sensor is triggered a long averaging period and a short hysteresis are chosen while the opposites are chosen when microcell sensor is triggered. In order to account for the velocity, it is best to choose velocity adaptive signal averaging intervals. This improvement can also be obtained with adaptive hysteresis levels. The idea of adjusting the hysteresis level according to the received signal strength offers a means of adopting fast handover in situations where received signal falls below the nominal levels.

## References

- [1] V. H. MacDonald, "Advanced mobile phone service: The cellular concept," *The Bell System Technical Journal*, vol. 58, no. 1, pp. 15-41, Jan. 1979.
- [2] Bell System, "Advanced mobile phone service," *The Bell System Technical Journal (special issue)*, vol. 58, no. 1, Jan. 1979.
- [3] F. H. Blecher, "Advanced mobile phone service," *IEEE Transactions on Vehicular Technology*, vol. 29, no. 2, pp. 238-244, May 1980.
- [4] W. C. Jakes, *Microwave Mobile Communications*. New York: John Wiley and Sons, 1974.
- [5] M. Mouly and M. B. Pautet, *The GSM system for mobile communications*. France: Mouly, Palaiseau, 1992.
- [6] D. J. Goodman, "Second generation wireless information networks," *IEEE Transactions on Vehicular Technology*, vol. 40, no. 2, pp. 366-374, May 1991.
- [7] K. Kinoshita, M. Kuramoto and Nakajima, "Development of a TDMA digital cellular system based on Japanese standard," *41st. IEEE Vehicular Technology Conference (VTC'91)*, St. Louis, pp. 642-645, May 1991.
- [8] TIA/EIA IS54, "Digital system dual-mode mobile station base station compatibility standard," Technical report 80-7814 Rev DCR 03567, Apr. 1992.
- [9] Qualcomm Inc., "An overview of the application of code division multiple access (CDMA) to digital cellular systems and personal cellular network," *Technical report EX60-10010*, May 1992.
- [10] A. Salmasi and K.S. Gilhousen, "On the system design aspects of code division multiple access (CDMA) and personal communications networks," *41st. IEEE*

- Vehicle Technology Conference (VTC'91)*, St. Louis, pp. 57-62, May 1991.
- [11] Steedman, "The common air interface MPT 1375," *Cordless Telecommunications in Europe*, W.H. W. Tuttlebee, ed., Springer Verlag, 1990.
- [12] ETSI, *Digital European Cordless Telecommunications-Common interface, Version 05.03*, May 1991.
- [13] K. Ogawa, K. Kohiyama and T. Kobayashi. "Towards the personal communication era- a proposal of the radio access concept from Japan," *International Journal Wireless information networks*, vol. 1, no 1, pp. 17-27, Jan. 1994.
- [14] Research and development centre for radio systems (RCR), "Personal handy phone systems," *RCR STD-28*, Dec. 1993.
- [15] Bellcore, "Generic criteria for version 0.1 wireless access communications systems (WACS) and supplement," Bellcore, Tech. Rep. TR-INS-001313, issue 1, 1994.
- [16] D. C. Cox, "Wireless network access for personal communications," *IEEE Communications Magazine*, vol. 30, no. 12, pp. 96-115, Dec. 1992.
- [17] ANSI J-STD, "Personal access communication system air interface standard," 1995
- [18] D. C. Cox, "Personal communications-A viewpoint," *IEEE Communications Magazine*, vol. 128, no. 11, pp. 8-20, Nov. 1990.
- [19] J. E. Padgett, C. G. Günther and T. Hattori, "Overview of wireless personal communications," *IEEE Communications Magazine*, vol. 33, no. 1, pp. 28-41, Jan. 1995.
- [20] F. Abrishamkar and E. Biglieri, "An Overview of wireless communications," *IEEE Military Communications Conference, (MILCOM'94)*, Fort Monmouth, NJ, pp. 900-905, Oct. 1994.
- [21] L. Grubb, "The travellers dream come true," *IEEE Communication Magazine*, vol. 29, no. 11, pp. 48-51, Nov. 1991.
- [22] J. C. B. Dende, R. Nevoux and J.C. Dang, "Networks, users and terminals in UMTS/FPLMTS," *IEEE Transactions on Vehicular Technology*, vol. 43, no. 3, pp. 681-685, Aug. 1994.
- [23] J. M. Nijhof, I. S. Dewantara and R. Prasad, "Base station system configurations

- for third generation mobile telecommunication systems," *43rd. IEEE Vehicular Technology Conference (VTC'93)*, New Jersey, pp. 621-624, May 1993.
- [24] B. Jabbari, G. Colombo, A. Nakajima and J. Kulkarni, "Network issues for wireless communications," *IEEE Communications Magazine*, vol. 33, no. 1, pp. 88-98, Jan. 1995
- [25] M. M. Zonoozi and P. Dassanayake, "Impact of mobility in mobile communication systems," A book chapter in *Mobile communications technology, tools, applications, authentication and security*, pp. 141-148, London: Chapman and Hall, 1996.
- [26] M. M. Zonoozi and P. Dassanayake, "A novel modelling technique for tracing mobile users in a cellular mobile communication system," *International Journal of Wireless Personal Communications (Kluwer Academic publishers)*, vol. 4, no. 2, pp. 185-205, Mar. 1997.
- [27] M. M. Zonoozi, P. Dassanayake and M. Faulkner, "Effect of cell structure and the user mobility on the probability of boundary crossing in the cellular mobile communication systems," *IEEE International Conference on Universal Wireless Access*, Melbourne, pp. 179-183, April 1994.
- [28] M. M. Zonoozi, P. Dassanayake and M. Faulkner, "Effect of mobility on the traffic analysis in cellular mobile networks," *IEEE International Conference on Networks & Information Engineering (IEEE SICON/ICIE)*, Singapore, pp. 407-410, July 1995.
- [29] M. M. Zonoozi, P. Dassanayake and M. Faulkner, "Mobility modelling and channel holding time distribution in cellular mobile communication systems," *IEEE Global Telecommunication Conference (Globecom'95)*, Singapore, pp. 12-16, Nov. 1995.
- [30] M. M. Zonoozi, P. Dassanayake and M. Faulkner, "Systematic tracking of mobile users in cellular systems," *5th. IEEE International Conference on Universal Personal Communications, (ICUPC'96)*, Cambridge, pp. 607-611, Sep. 1996.
- [31] M. M. Zonoozi, P. Dassanayake and M. Faulkner, "An efficient algorithm for mobility modelling in cellular mobile communication systems," *Australian Telecommunication Networks and Application Conference (ATNAC'94)*, Melbourne, pp. 757-762, Dec. 1994.
- [32] M. M. Zonoozi, P. Dassanayake and M. Faulkner, "Mobility analysis of cellular mobile networks based on a generalized approach," *2nd International Conference on Mobile and Personal Communication Systems*, Adelaide, pp. 142-148, April

- 1995.
- [33] M. M. Zonoozi, P. Dassanayake and M. Faulkner, "Mobility modelling in cellular mobile communication systems," *3rd Iranian Conference on Electrical Engineering*, Tehran, vol. I, pp. 9-16, May 1995.
- [34] M. M. Zonoozi, P. Dassanayake and M. Faulkner, "Generalised gamma distribution for cell residence time in cellular systems," *Australian Telecommunication Networks and Application Conference (ATNAC'95)*, Sydney, pp. 407-411, Dec. 1995.
- [35] M. M. Zonoozi, P. Dassanayake and R. Berangi, "Generation of non-uniform distributed random numbers by MATLAB," *1st. Australian MATLAB Conference*, Melbourne, paper no. 1 electrical engineering session, Jan. 1996.
- [36] M. M. Zonoozi and P. Dassanayake, "An efficient stochastic model for predicting cell residence time distribution," *2nd International Mobile Computing Conference*, Taiwan, pp. 152-159, Mar. 1996.
- [37] M. M. Zonoozi, P. Dassanayake, and M. Faulkner, "Teletraffic modelling of cellular mobile networks," *46th. IEEE Vehicular Technology Conference (VTC'96)*, Atlanta, pp. 1274-1277, Apr. 1996.
- [38] M. M. Zonoozi and P. Dassanayake, "Effect of handover on the teletraffic performance criteria," *IEEE Global Telecommunication Conference (Globecom'96)*, London, pp. 242-246, Nov. 1996.
- [39] M. M. Zonoozi and P. Dassanayake, "Traffic performance evaluation of cellular systems," *4th Iranian Conference on Electrical Engineering (ICEE'96)*, Tehran, pp. 271-278, May 1996.
- [40] M. M. Zonoozi, P. Dassanayake and M. Faulkner, "Mobile radio channel characterization," *IEEE International Conference on Networks & Information Engineering (IEEE SICONICIE)*, Singapore, pp. 403-406, July 1995.
- [41] M. M. Zonoozi and P. Dassanayake, "Shadow fading in mobile radio channel," *7th. IEEE International Symposium on Personal, Indoor and Mobile Radio Communications (PIMRC'96)*, Taiwan, pp. 291-295, Oct. 1996.
- [42] M. M. Zonoozi and P. Dassanayake, "Optimization of hysteresis level for avoiding unnecessary handovers," *IEEE Singapore International Conference on Communication systems (ICC'96)*, Singapore, pp. 561-565, Nov. 1996.
- [43] M. M. Zonoozi, P. Dassanayake and M. Faulkner, "Optimum hysteresis level, sig-



- nal averaging time and handover delay," *47th. IEEE Vehicular Technology Conference (VTC'97)*, Phoenix, pp. 310-313, May 1997.
- [44] R. Berangi, P. Leung and M. M. Zonoozi, "Simulation of a mobile communication system," *1st. Australian MATLAB Conference*, Melbourne, paper no. 4 of simulation session, Jan. 1996.
- [45] M. M. Zonoozi, P. Dassanayake and M. Faulkner, "Characterization of Radio Channel in Microcellular Mobile Systems," *4th UK/Australian International Symposium on DSP for Communication Systems (DSPCS'96)*, Perth, Australia, pp 10-16, Sep. 1996.
- [46] M. M. Zonoozi and P. Dassanayake, "Optimum hysteresis level and signal averaging time selection for minimizing unnecessary handovers," *Australian Telecommunication Networks and Application Conference (ATNAC'96)*, Melbourne, pp. 327-332, Dec. 1996.
- [47] W. C. Y. Lee, *Mobile communications design fundamentals*. Indianapolis: Howard W. Sams, 1986.
- [48] G. Labedz, K. Lev, and D. Schaeffer, "Handover control issues in very high capacity cellular systems using small cells," *International Conference on Digital Land mobile Radio Communications*, Venice, Jul. 1987.
- [49] S. Nanda, "Teletraffic models for urban and suburban microcells: cell sizes and handoff rates," *IEEE Transactions on Vehicular Technology*, vol. 42, no. 4, pp. 673-682, Nov. 1993.
- [50] O. Kelly and V. V. Veeravalli, "A locally optimal handoff algorithm," *6th. IEEE International Symposium on Personal, Indoor and Mobile Radio Communications (PIMRC'95)*, Toronto, pp. 809-813, Sep. 1995.
- [51] G. P. Pollini, "Trends in handover design," *IEEE Communications Magazine*, vol. 34, no. 3, pp. 82-90, Mar. 1996.
- [52] G. N. Senarath and D. Everitt, "Comparison of alternative handoff strategies for microcellular mobile communication systems," *44th. IEEE Vehicular Technology Conference (VTC'94)*, Stockholm, pp. 1465-1469, Jul. 1994.
- [53] G. N. Senarath and D. Everitt, "Performance of handover priority and queuing systems under different handover request strategies for microcellular mobile communication systems," *45th. IEEE Vehicular Technology Conference (VTC'95)*, Chicago, pp. 897-901, Jul. 1995.

- 
- [54] O. Grimlund and B. Gudmundson, "Handoff strategies in microcellular systems," *41st. IEEE Vehicular Technology Conference (VTC'91)*, St. Louis, pp. 505-510, May 1991.
- [55] P. Dassanayake, "Dynamic adjustment of propagation dependant parameters in handover algorithms," *44th. IEEE Vehicular Technology Conference (VTC'94)*, Stockholm, pp. 73-76, Jun. 1994.
- [56] P. Dassanayake, "Effects of measurement sample averaging on performance of GSM handover algorithm," *Electronics Letters*, vol. 29, no. 12, pp. 1127-1128, Jun. 1993.
- [57] R. Vijayan and J. M. Holtzman, "A model for analysing handoff algorithms," *IEEE Transactions on Vehicular Technology*, vol. 42, no. 3, pp. 351-356, Aug. 1993.
- [58] S. T. S. Chia and R. J. Warburton, "Handoff criteria for city microcellular systems," *40th. IEEE Vehicular Technology Conference (VTC'90)*, Orlando, pp. 276-281, 1990.
- [59] M. Gudmundson, "Analysis of handover algorithms," *41st. IEEE Vehicular Technology Conference (VTC'91)*, St. Louis, pp. 537-542, May 1991.
- [60] W. R. Mende, "Evaluation of a proposed handover algorithm for the GSM cellular system," *40th. IEEE Vehicular Technology Conference (VTC'90)*, Orlando, pp. 264-269, May 1990.
- [61] A. Murase, I. C. Symington and E. Green, "Handover criterion for macro and microcellular systems," *41st. IEEE Vehicular Technology Conference (VTC'91)*, St. Louis, pp. 524-530, May 1991.
- [62] R. Vijayan and J. M. Holtzman, "Analysis of handoff algorithms using nonstationary signal strength measurements," *IEEE Global Telecommunication Conference (Globecom'92)*, Orlando, pp. 1405-1409, Dec. 1992.
- [63] E. A. Frech and C. L. Mesquida, "Cellular models and handoff criteria," *39th. IEEE Vehicular Technology Conference (VTC'89)*, San Francisco, pp. 128-135, May 1989.
- [64] K. G. Cornett and S.B. Wicker, "Bit error rate estimation techniques for digital land mobile radios," *41st. IEEE Vehicular Technology Conference (VTC'91)*, St. Louis, pp. 543-548, May 1991.
- [65] R. Steele, D. Twelves and L. Hanzo, "Effect of cochannel interference on hando-

- ver in microcellular mobile radio," *Electronics Letters*, vol. 25, no. 20, pp. 1329-1330, Sep. 1989.
- [66] ETSI, *GSM recommendation Version 05.08*, Jan. 1991.
- [67] R. Rezaaifar, A. M. Makowski, S. Kumar, "Stochastic control of handoffs in cellular networks," *IEEE Journal on Selected Areas in Communications*, vol. 13 no. 7, pp. 1348-1362, Sep 1996.
- [68] K. Loew, "Boundaries between radio cell influence of buildings and vegetation," *IEE Proceedings Part F*, vol. 132, no. 5, pp. 321-326, Aug. 1985.
- [69] N. Zhang and J. M. Holtzman, "Analysis of handoff algorithms using both absolute and relative measurements," *IEEE Transactions on Vehicular Technology*, vol. 45, no. 1, pp. 174-179, Feb. 1996.
- [70] D. Muñoz-Rodríguez, J. A. Moreno-Cadenas, M. C. Ruiz-Sánchez and F. Gomez-Castañeda, "Neural supported handoff methodology in micro cellular systems," *42nd. IEEE Vehicular Technology Conference (VTC'92)*, Denver, pp. 431-434, May 1992.
- [71] V. Kapoor, G. Edwards and Sankar, "Handoff criteria for personal communication networks," *IEEE International Conference on Communications (ICC'94)*, New Orleans, pp.1297-1301, May 1994.
- [72] W. C. Y. Lee, *Mobile cellular telecommunications: analog and digital systems*. New York: McGraw-Hill, 1995.
- [73] S. Yoshida, A. Hirai, G. L. Tan, H. Zhou and T. Takeuchi, "In-service monitoring of multipath delay-spread and C/I for QPSK signal," *42nd. IEEE Vehicular Technology Conference (VTC'92)*, Denver, pp. 349-354, May 1992.
- [74] S. Kozono, "Co-channel interference measurement method for mobile communication," *IEEE Transactions on Vehicular Technology*, vol. 36, no. 1, pp. 7-13, Feb. 1987.
- [75] N. R. Sollenberger, "Architecture and implementation of an efficient and robust TDMA frame structure for digital portable communications," *IEEE Transactions on Vehicular Technology*, vol. 40, no. 1, pp. 250-260, Feb. 1991.
- [76] I. M. Kostic, "Pseudo error rate of a PSK system with hardware imperfections, noise and cochannel interference," *IEE Proceedings-I*, vol. 136, no. 5, pp. 333-338, Oct. 1989.

- 
- [77] T. Nagura, K. Kawazoe, S. Kubota and S. Kato, "A prediction eye-monitoring method for carrier hopping TDMA-TDD systems," *4th. IEEE International Symposium on Personal, Indoor and Mobile Radio Communications (PIMRC'93)*, Yokohama, Japan, pp. 667-670, Sep. 1993.
- [78] S. Sakagami, S. Aoyama, K. Kuboi and S. Shirota and A. Akeyama, "Vehicle position estimation by multi-beam antennas in multipath environments," *IEEE Transactions on Vehicular Technology*, vol. 41, no. 1, pp. 63-67, Feb. 1992.
- [79] S. C. Swales and M. A. Beach, "Direction finding in the cellular land mobile radio environment," *IEE 5th International Conference on Radio Receiver and Associated Systems*, pp. 192-196, 1990
- [80] M. Feuerstein and T. Pratt, "A local area position location system," *5th IEE International Conference on Mobile Radio and Personal Communication*, Coventry, UK, pp. 79-83, Dec. 1989
- [81] P. Goud, A. Sesay and M. Fattouche, "A spread spectrum radio location technique and its application to cellular radio," *IEEE Pacific Rim Conference on Communications, Computers and Signal Processing*, pp. 661-664, May 1991
- [82] M. Hata and T. Nagatsu, "Mobile location using signal strength measurements in cellular systems," *IEEE Transactions on Vehicular Technology*, vol. 29, no. 2, pp. 245-251, May 1980.
- [83] R. Simon, R. Beck, A. Gamst and E. G. Zinn, "Influence of handoff algorithm on the performance of cellular radio networks," *37th. IEEE Vehicular Technology Conference (VTC'87)*, Florida, pp. 855-858, Jun. 1987.
- [84] A. Mehrotra, *Cellular radio performance engineering*. Boston: Artech House, 1994.
- [85] M. D. Austin and G. L. Stüber, "Velocity adaptive handoff algorithms for micro-cellular systems," *IEEE Transactions on Vehicular Technology*, vol. 43, no. 3, pp. 549-561, Aug. 1994.
- [86] J. M. Holtzman and A. Sampath, "Adaptive averaging methodology for handoffs in cellular systems," *IEEE Transactions on Vehicular Technology*, vol. 44, no. 1, pp. 59-66, Feb. 1995.
- [87] A. Sampath and J. M. Holtzman, "Estimation of maximum Doppler frequency for handoff decisions," *43rd. IEEE Vehicular Technology Conference (VTC'93)*, New Jersey, pp. 859-862, May 1993.

- [88] M. K. Simon and D. Divsalar, "Doppler corrected differential detection of MPSK," *IEEE Transactions on Communication*, vol. 37, no. 2, pp. 99-109, Feb. 1989.
- [89] E. Biglieri, F. Abrishamkar and Y. C. Jou, "Doppler frequency shift estimation for differentially coherent CPM," *IEEE Transactions on Communications*, vol. 38, no. 3, pp. 1659-1663, Oct. 1990.
- [90] M. D. Austin and G. L. Stüber, "Eigen-based Doppler estimation for differentially coherent CPM," *IEEE Transactions on Vehicular Technology*, vol. 43, no. 3, pp. 781-785, Aug. 1994.
- [91] T. Kanai and Y. Furuya, "A handoff control process for microcellular systems," *38th. IEEE Vehicular Technology Conference (VTC'88)*, Philadelphia, pp. 170-175, May 1988.
- [92] S. T. S. Chia and W. Johnston, "Handover performance from microcell to indoor picocell," *Electronics Letters*, vol. 28, no. 3, pp. 315-316, Jan. 1992.
- [93] M. D. Austin and G. L. Stüber, "Direction biased handoff algorithms for urban microcells," *44th. IEEE Vehicular Technology Conference (VTC'94)*, Stockholm, pp. 101-105, Jun. 1994.
- [94] D. Muñoz-Rodríguez and K. W. Cattermole, "Multiple criteria for handoff in cellular mobile radio," *Electronics Letters*, vol. 27, no. 23, pp. 85-88, Nov. 1987.
- [95] D. Muñoz-Rodríguez and K. W. Cattermole, "Hand-off procedure for fuzzy defined radio cells," *37th. IEEE Vehicular Technology Conference (VTC'87)*, Florida, pp. 38-44, Jun. 1987.
- [96] P. S. Kumar and J. Holtzman, "Analysis of handoff algorithm using both bit error rate (BER) and relative signal strength," *3rd. IEEE International Conference on Universal Personal Communications (ICUPC'94)*, San Diego, pp 1-5, 1994.
- [97] R. C. Bernhardt, "Cost considerations of macroscopic diversity architectures for universal digital portable communications," *IEEE Global Telecommunication Conference (Globecom'85)*, New Orleans, Dec. 1985.
- [98] R. C. Bernhardt, "RF performance of macroscopic diversity in universal portable radio communications: frequency reuse considerations," *IEEE International Conference on Communications (ICC'86)*, Toronto, pp. 65-71, Jun. 1986.
- [99] R. C. Bernhardt, "RF performance of macroscopic diversity in universal portable radio communications: signal strength considerations," *IEEE Global Telecommu-*

- nication Conference (Globecom'85)*, New Orleans, Dec. 1985.
- [100] S. W. Wang and I. Wang, "Effect of soft handoff, frequency reuse and non-ideal antenna sectorization on CDMA system capacity," *43rd. IEEE Vehicular Technology Conference (VTC'93)*, New Jersey, pp. 850-854, May 1993.
- [101] D. Hong and S. S. Rappaport, "Traffic model and performance analysis for cellular mobile radio telephone systems with prioritized and nonprioritized handoff procedures," *IEEE Transactions on Vehicular Technology*, vol. 35, no. 3, pp. 77-92, Aug. 1986.
- [102] E. Del Re, R. Fantacci and G. Giambene, "Handover and dynamic channel allocation techniques in mobile cellular networks," *IEEE Transactions on Vehicular Technology*, vol. 44, no. 2, pp. 229-237, May 1995.
- [103] R. A. Guérin, "Channel occupancy time distribution in a cellular radio system," *IEEE Transactions on Vehicular Technology*, vol. 35, no. 3, pp. 89-99, Aug. 1987.
- [104] S. Tekinay, *Modelling and analysis of cellular networks with highly mobile heterogeneous traffic sources*. Ph.D. thesis, George Mason University, Fairfax, Virginia, 1994.
- [105] K. Kim, M. Cho, S. Kwon, K. Cho and K. Cho, "An optimal location area decision method considering mobile power status," *5th. IEEE International Conference on Universal Personal Communications, (ICUPC'96)*, Cambridge, pp. 612-616, Sep. 1996.
- [106] B. H. Cheung and V. C. M. Leung, "Network configurations for seamless support of CDMA soft handoffs between cell-clusters," *5th. IEEE International Conference on Universal Personal Communications, (ICUPC'96)*, Cambridge, pp. 295-299, Sep. 1996.
- [107] R. Thomas, H. Gilbert, and G. Mazziotto, "Influence of the movement of the mobile station on the performance of a radio cellular network," *3rd Nordic Seminar*, Copenhagen, Paper 9.4, Sep. 1988.
- [108] T. S. Kim and D. K. Sung, "The effects of handoffs on the microcell-based PCN networks," *IEEE Global Telecommunication Conference (Globecom'94)*, pp. 1316-1320, 1994.
- [109] X. Luo and D. Everitt, "Handoff effects in microcellular systems," *42nd. IEEE Vehicular Technology Conference (VTC'92)*, Denver, pp. 654-657, May 1992.
- [110] S. A. El-Dolil, W. C. Wong and R. Steele, "Teletraffic performance of a highway

- microcell with overlay macrocell," *IEEE Journal on Selected Areas in Communications*, vol. 7, no 1, pp. 71-78, Jan. 1989.
- [111] M. Frodigh, "Performance bounds for power control supported DCA-algorithms in highway micro cellular radio systems," *IEEE Transactions on Vehicular Technology*, vol. 44, no. 2, pp. 238-243, May. 1995.
- [112] T. S. Kim, M. Y. Chung, D. K. Sung and M. Sengoku, "A mobility analysis in 3-dimensional PCS environments," *46th. IEEE Vehicular Technology Conference (VTC'96)*, Atlanta, pp. 237-243, Apr. 1996.
- [113] E. Bitar, M. McDonnell and N. D. Georganas, "Channel hand-off strategies in cellular mobile communication systems," *Canadian Electrical Engineering Journal*, vol. 12, no. 3, pp. 99-104, 1987.
- [114] P. Dassanayake and L. X. Jun, "Modelling of signal level profile for a random mobile trajectory in a cellular mobile system," *2nd. International Conference on Modelling and Simulation*, Melbourne, pp 135-142, Jul. 1993.
- [115] C. M. Simmonds, M. A. Beach, "Network planning aspects of DS-CDMA with particular emphasis on soft handoff," *43rd. IEEE Vehicular Technology Conference (VTC'93)*, New Jersey, pp. 855-858, May 1993.
- [116] G. Morales-Andres and M. Villen-Altamirano, "An approach to modelling subscriber mobility in cellular radio networks," *5th World Telecommunication Forum*, Geneva, pp. 185-189, Nov. 1987.
- [117] G. P. Pollini and D. J. Goodman, "Signalling system performance evaluation for personal communications" *IEEE Transactions on Vehicular Technology*, vol. 45, no. 1, pp. 131-138, Feb. 1996.
- [118] I. Seskar, S. Maric, J. Holtzman and J. Wasserman, "Rate of location area updates in cellular systems," *42nd. IEEE Vehicular Technology Conference (VTC'92)*, Denver, pp. 694-697, May 1992.
- [119] A. El-Hoitdi and R. J. Finean, "Location management for the satellite-universal mobile telecommunication system," *5th. IEEE International Conference on Universal Personal Communications, (ICUPC'96)*, Cambridge, pp. 739-744, Sep. 1996.
- [120] M. Inoue, H. Morikawa and M. Mizumachi, "Performance analysis of microcellular mobile communication systems," *44th. IEEE Vehicular Technology Conference (VTC'94)*, Stockholm, pp. 135-139, Jun. 1994.

- [121] K. L. Yeung and S. Nanda, "Optimal mobile-determined micro-macro cell selection," *6th. IEEE International Symposium on Personal, Indoor and Mobile Radio Communications (PIMRC'95)*, Toronto, pp. 294-299, Sep. 1995.
- [122] K. L. Yeung and S. Nanda, "Channel management in microcell/macrocell cellular radio systems," *IEEE Transactions on Vehicular Technology*, vol. 45, no. 4, pp. 601-612, Nov. 1996.
- [123] H. Xie, S. Kuek, "Priority handoff analysis," *43rd. IEEE Vehicular Technology Conference (VTC'93)*, New Jersey, pp. 855-858, May 1993.
- [124] H. Xie, D. J. Goodman, "Mobility models and biased sampling problem," *2nd. IEEE International Conference on Universal Personal Communications (ICUPC'93)*, Ottawa, pp 804-807, Oct. 1993.
- [125] J. H. Sánchez Vargas, "Teletraffic performance of cellular mobile radio systems," Ph.D thesis, University of Essex, England, 1988.
- [126] X. Luo, "Investigation of traffic performance in mobile cellular communication systems," Master of Engineering thesis, University of Melbourne, Australia, 1991.
- [127] Y. B. Lin, S. Mohan and A. Noerpel, "Queuing priority channel assignment strategies for PCS handoff and initial access," *IEEE Transactions on Vehicular Technology*, vol. 43, no. 3, pp. 704-712, Aug. 1994.
- [128] Y. B. Lin, L. F. Chang and A. Noerpel, "Modelling hierarchical microcell/macrocell PCS architecture," *IEEE International Conference on Communications (ICC'95)*, Seattle, pp.405-409, Jun 1995.
- [129] A. D. Malyan, L. J. Ng, V. C. M. Leung, R. W. Donaldson, "Network architecture and signalling for wireless personal communications," *IEEE Journal on Selected Areas in Communications*, vol. 11, no 6, pp. 830-841, Aug. 1993.
- [130] H. Jiang and S. Rappaport, "Handoff analysis for CBWL schemes in cellular communications," *3rd. IEEE International Conference on Universal Personal Communications (ICUPC'94)*, San Diego, pp 496-500, 1994.
- [131] W. M. Jolley and R. E. Warfield, "Modelling and analysis of layered cellular mobile networks," *13th International Teletraffic Congress (ITC-13)*, Copenhagen, pp. 161-166, Jun. 1991.
- [132] M. Naghshineh and A. S. Acampora, "Design and control of micro-cellular networks with QOS provisioning for real time traffic," *3rd IEEE International Con-*



- ference on Universal Personal Communications (ICUPC'94)*, San Diego, pp 376-381, Sep. 1994.
- [133] F. N. Pavlidou, "Two-dimensional traffic models for cellular mobile systems," *IEEE Transactions on Communication*, vol. 42, no. 2/3/4, pp. 1505-1511, Feb./Mar./Apr. 1994.
- [134] C. Purzynski and S. S. Rappaport, "Multiple call hand-off problem with queued hand-offs and mixed platform types," *IEE Proceedings on Communications*, vol. 142 no 1, pp. 31-39, Feb. 1995.
- [135] S. S. Rappaport, "The multiple-call handoff problem in high capacity cellular communications systems," *IEEE Transactions on Vehicular Technology*, vol. 40, no. 3, pp. 546-557, Aug. 1993.
- [136] S. Rappaport and L. R. Hu, "Microcellular communication systems with hierarchical macrocell overlays: traffic performance models and analysis," *Proceedings of IEEE*, vol. 82, no. 9, pp. 1383-1397, Sep. 1994.
- [137] S. S. Rappaport and C. Purzynski, "Prioritized resource assignment for mobile cellular communication systems with mixed services and platform types," *IEEE Transactions on Vehicular Technology*, vol. 45, no. 3, pp. 443-458, Aug. 1996.
- [138] D. C. Cox and D. O. Reudink, "Dynamic channel assignment in high-capacity mobile communications systems," *The Bell System Technical Journal*, vol. 50, no. 6, pp. 1833-1857, Jul. 1971.
- [139] D. C. Cox and D. O. Reudink, "Increasing channel occupancy in large scale mobile radio systems: dynamic channel reassignment," *IEEE Transactions on Communications*, vol. 21, no. 11, pp. 1302-1306, Nov. 1973.
- [140] L. Schiff, "Traffic capacity of three types of common-user mobile radio communication systems," *IEEE Transactions on Communication technology*, vol. 18, no. 1, pp. 12-21, Feb. 1970.
- [141] S. S. Rappaport, "Blocking, handoff and traffic performance for cellular communication systems with mixed platforms," *IEE Proceedings-I*, vol. 140, no. 5, pp. 389-401, Oct. 1993.
- [142] W. C. Wong, "Packet reservation multiple access in a metropolitan microcellular radio environment," *IEEE Journal on Selected Areas in Communications*, vol. 11, no 6, pp. 918-925, Aug. 1993.
- [143] D. R. Cox and P. A. W. Lewis, *The statistical analysis of series of events*. London:

Chapman and Hall, 1978.

- [144] A. M. Law and W. D. Kelton, *Simulation modelling and analysis*. New York: McGraw-Hill, 1991.
- [145] G. A. Mihram, *Simulation: statistical foundations and methodology*. New York: Academic press, 1972.
- [146] R. J. Serfling, *Approximation theorems of mathematical statistics*. New York: John Wiley and Sons, 1980.
- [147] S. M. Ross, *Stochastic process*. New York: John Wiley and Sons, 1983.
- [148] L. Kleinrock, *Queueing systems. Volume 1: Theory*. New York: John Wiley and Sons, 1975.
- [149] I. Katzela and M. Naghshineh, "Channel assignment schemes for cellular mobile telecommunication systems: A comprehensive survey," *IEEE Personal Communications Magazine*, vol. 3, no. 3, pp. 10-31, Jun. 1996.
- [150] D. C. Cox and D. O. Reudink, "A comparison of some channel assignment strategies in large scale mobile communication systems," *IEEE Transactions on Communications*, vol. 20, no. 11, pp. 190-195, Apr. 1972.
- [151] G. Falciasecca, M. Frullone, G. Riva, M. Sentinelli and M. Serra, "Investigation on a dynamic channel allocation for high capacity mobile radio systems," *39th. IEEE Vehicular Technology Conference (VTC'89)*, san Francisco, pp. 176-181, May 1989.
- [152] K. Okada and F. Kubota, "On dynamic channel assignment in cellular mobile radio systems," *IEEE International Symposium on Circuits and systems*, Singapore, pp. 938-941, Jun. 1991.
- [153] W. Yue, "Analytical methods to calculate the performance of a cellular mobile radio communication system with hybrid channel assignment," *IEEE Transactions on Vehicular Technology*, vol. 40, no. 2, pp. 453-460, May 1991.
- [154] T. J. Kahwa and N. D. Georganas, "A hybrid channel assignment scheme in large scale, cellular-structured mobile communication systems," *IEEE Transactions on Communication*, vol. 26, no. 4, pp. 432-438, Apr. 1978.
- [155] B. Eklundh, "Channel utilization and blocking probability in a cellular mobile telephone system with directed retry," *IEEE Transactions on Communication*, vol. 34, no. 4, pp. 329-337, Apr. 1986.

- [156] J. Karlsson and B. Eklundh, "A cellular mobile telephone system with load sharing-An enhancement of directed retry," *IEEE Transactions on Communication*, vol. 37, no. 5, pp. 530-535, May. 1989.
- [157] S. M. Elnoubi, R. Singh and S. C. Gupta, "A new frequency channel assignment algorithm in high capacity mobile communications systems," *IEEE Transactions on Vehicular Technology*, vol. 31, no. 3, pp. 125-131, Aug. 1982.
- [158] H. Jiang and S. Rappaport, "Channel borrowing without locking for sectorized cellular communications," *IEEE Transactions on Vehicular Technology*, vol. 43, no. 4, pp. 1067-1077, Nov. 1994.
- [159] D. Everitt and N. W. Macfadyen, "Analysis of multi-cellular mobile radiotelephone systems with loss", *British Telecom Technology journal*, Vol. 1, No. 2, pp 37-45, Oct. 1983.
- [160] T. S. P. Yum and K. L. Yeung, "Blocking and handoff performance analysis of directed retry in cellular mobile systems," *IEEE Transactions on Vehicular Technology*, vol. 44, no. 3, pp. 645-650, Aug. 1995.
- [161] Y. B. Lin, A. R. Noerpel and D J. Harasty, "The sub-rating channel assignment strategy for PCS hand-offs," *IEEE Transactions on Vehicular Technology*, vol. 45, no. 1, pp. 122-130, Feb. 1996.
- [162] J. H. Weber, "Dictionary of English language traffic terms," *IEEE Transactions on Communication*, vol. 16, no. 3, pp. 365-369, Jul. 1968.
- [163] M. Naghshineh and A. S. Acampora, "Design and control of micro-cellular networks with QOS provisioning, Part A: real time traffic," IBM Research Report1994.
- [164] C. H. Yoon and K. Un, "Performance of personal portable radio telephone systems with and without guard channels," *IEEE Journal on Selected Areas in Communications*, vol. 11, no 6, pp. 911-917, Aug. 1993.
- [165] S. Tekinay and B. Jabbari, "A measurement-based prioritization scheme for handovers in mobile cellular networks," *IEEE Journal on Selected Areas in Communications*, vol. 10, no 8, pp. 1343-1350, Oct. 1992.
- [166] S. Tekinay, B. Jabbari, "Handover and channel assignment in mobile cellular networks," *IEEE Communication Magazine*, vol. 29, no. 11, pp. 42-46, Nov. 1991.
- [167] R. B. Cooper, *Introduction to queueing theory, 2nd edition*, New York: Elsevier-North Holland, 1981.

- [168] R. Guerin, *Queuing and traffic in cellular radio*. Ph.D. thesis, California Institute of Technology, Pasadena, California, 1986.
- [169] D. L. Pallant and P. G. Taylor, "Performance analysis of homogeneous cellular mobile systems with dynamic channel allocation," *7th Australian teletraffic research seminar, Mannum, South Australia*, pp. 403-414, Nov. 1992.
- [170] K. Sallberg, B. Stavenow and B. Eklundh, "Hybrid channel assignment and reuse partitioning in a cellular mobile telephone system," *37th. IEEE Vehicular Technology Conference (VTC'87)*, Florida, pp. 405-411, Jun. 1987.
- [171] W. C. Y. Lee, *Mobile communications engineering*. New York: McGraw-Hill, 1982.
- [172] R. C. French, "The effect of fading and shadowing on for channel reuse in mobile radio," *IEEE Transactions on Vehicular Technology*, vol. 28, no. 3, pp. 171-181, Aug. 1979.
- [173] A. J. Goldsmith, L. J. Greenstein and G. J. Foschini, "Error statistics of real-time power measurement in cellular channels with multipath and shadowing," *43rd. IEEE Vehicular Technology Conference (VTC'93)*, New Jersey, pp. 108-111, May 1993.
- [174] J. D. Parsons, *The mobile radio propagation channel*. London: Pentech press, 1992.
- [175] P. E. Mogensen, P. Eggers, C. Jensen and J.B. Andersen, "Urban area radio propagation measurements at 955 and 1845 Mhz for small and micro cells," *IEEE Global Telecommunication Conference (Globecom'91)*, Phoenix, pp. 1297-1301, 1991.
- [176] J. Berg, R. Bownds and F. Lotse, "Path loss and fading models for microcells at 900 MHz," *42nd. IEEE Vehicular Technology Conference (VTC'92)*, Denver, pp. 666-671, May 1992.
- [177] M. Gudmundson, "Correlation model for shadow fading in mobile radio systems," *Electronics Letters*, vol. 27, no. 23, pp. 2145-2146, Nov. 1991.
- [178] M. Hata, "Empirical formula for propagation loss in land mobile radio services," *IEEE Transactions on Vehicular Technology*, vol. 29, no. 3, pp. 317-325, Aug. 1980.
- [179] P. Harley, "Short distance attenuation measurements at 900 MHz and 1.8 GHz using low antenna heights for microcells," *IEEE Journal on Selected Areas in*

*Communications*, vol. 7, no 1, pp. 5-11, Jan. 1989.

- [180] H. H. Xia, H. L. Bertoni, L. R. Maciel, A. Lindsay-Stewart, R. Rowe and L. Grindstaff, "Radio propagation measurement and modelling for line-of-sight microcellular systems," *42nd. IEEE Vehicular Technology Conference (VTC'92)*, Denver, pp. 349-354, May 1992.
- [181] E. Green, 'Radio link design for microcellular systems', *British Telecom Technology journal*, Vol. 8, No. 1, pp 85-96, Jan. 1990
- [182] A. Papoulis, *Probability, Random Variables, and Stochastic Processes*. New York: McGraw-Hill, 1965.
- [183] R. Vijayan and J. M. Holtzman, "The dynamic behaviour of handoff algorithms," *1st. IEEE International Conference on Universal Personal Communications (ICUPC'92)*, Dallas, pp 39-43, Sep. 1992.
- [184] M. Ruggieri, F. Graziosi, M. Pratesi and F. Santucci, "Modelling of handover initiation in a multicell system scenario," *46th. IEEE Vehicular Technology Conference (VTC'96)*, Atlanta, pp. 1505-1509, Apr. 1996
- [185] G. E. Corazza, D. Giancrisofaro and F. Santucci, "Characterization of handover initialization in cellular mobile radio networks," *44th. IEEE Vehicular Technology Conference (VTC'94)*, Stockholm, pp. 1869-1872, Jun. 1994.
- [186] D. Kwon and K. W. Sarkies, "Handover algorithm analysis combined with overlap conditions," *46th. IEEE Vehicular Technology Conference (VTC'96)*, Atlanta, pp. 1331-1335, Apr. 1996.
- [187] R. C. Bernhardt, "The effect of multipath fading on automatic link transfer for a random walk trajectory," *IEEE Transactions on Vehicular Technology*, vol. 42, no. 4, pp. 456-465, Nov. 1993.
- [188] B. Senadji, S. Tabbane and B. Boashash, "A handover decision procedure based on the minimization of Bayes criterion," *44th. IEEE Vehicular Technology Conference (VTC'94)*, Stockholm, pp. 77-81, Jul. 1994.
- [189] G. N. Senarath and D. Everitt, "Controlling handoff performance using signal strength prediction schemes & hysteresis algorithms for different shadowing environments," *46th. IEEE Vehicular Technology Conference (VTC'96)*, Atlanta, pp. 1510-1514, Apr. 1996.
- [190] G. Edwards and R. Sankar, "Handoff using fuzzy logic," *IEEE Global Telecommunication Conference (Globecom'95)*, Singapore, pp. 524-528, Nov. 1995.

- 
- [191] S. S. Lau, K. Cheung and J. C. Chuang, "Fuzzy logic adaptive handoff algorithm," *IEEE Global Telecommunication Conference (Globecom'95)*, Singapore, pp. 509-513, Nov. 1995.
- [192] C. Miller and R. Wyrwas, "Probabilistic analysis of handover algorithms," *IEEE International Conference on Universal Wireless Access, Melbourne*, pp. 77-81, April 1994.
- [193] P. P. S. Carter and A. M. D. Turkmani, "Performance evaluation of Rayleigh and log-normal GMSK signals in the presence of cochannel interference," *IEE Proceedings-I*, vol. 139, no. 2, pp. 156-164, Apr. 1992.
- [194] A. Sampath and J. M. Holtzman, "Adaptive handoffs through the estimation of fading parameters," *IEEE International Conference on Communications (ICC'94)*, New Orleans, pp. 1131-1135, May 1994.
- [195] R. Vijayan and J. M. Holtzman, "Sensitivity of handoff algorithms to variations in the propagation environment," *2nd. IEEE International Conference on Universal Personal Communications (ICUPC'93)*, Ottawa, pp 158-162, Oct. 1993.
- [196] K. Kawabata, T. Nakamura and E. Fukuda, "Estimating velocity using diversity reception," *44th. IEEE Vehicular Technology Conference (VTC'94)*, Stockholm, pp. 371-374, Jul. 1994.
- [197] Y. Kim, K. Lee and Y. Chin, "Analysis of multi-level threshold handoff algorithm," *IEEE Global Telecommunication Conference (Globecom'96)*, London, pp. 1141-1145, Nov. 1996.

## APPENDIX A

### *User Distribution*

Initial location of the mobiles can be represented by their distance  $\rho_0$  and direction  $\theta_0$  from the base station. The base station is located at the centre of the cell. The model assumes that the users are independent and uniformly distributed over the entire region. In order to meet conditions for uniform distribution of mobiles throughout the coverage area, the probability of locating mobiles in a strip of width  $d\rho_0$  with a distance of  $\rho_0$  from the centre should be (Fig. A.1),

$$P(\rho_0) = K \cdot 2\pi\rho_0 d\rho_0 \quad (\text{A.1})$$

where K is the normalization constant such that:

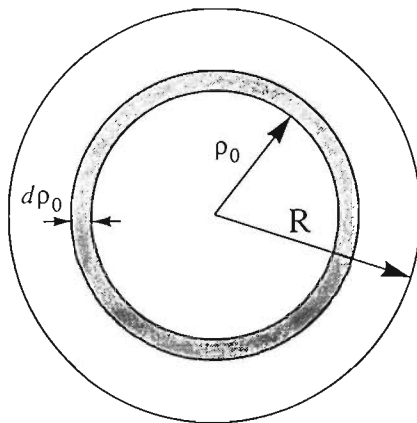


**Fig. A.1.** User distribution in a strip.

$$\int_0^R K \cdot 2\pi\rho_0 \, d\rho_0 = K \cdot \pi R^2 = 1 \quad (\text{A.2})$$

$$K = \frac{1}{\pi R^2}$$

Therefore the probability density function of the mobile locations in cylindrical coordinates  $(\rho_0, \theta_0)$  will be of the form,

$$f_{R_0}(\rho_0) = \begin{cases} \frac{2\rho_0}{R^2} & 0 \leq \rho_0 \leq R \\ 0 & \text{otherwise} \end{cases} \quad (\text{A.3})$$

$$f_{\Theta_0}(\theta_0) = \begin{cases} \frac{1}{2\pi} & 0 \leq \theta_0 \leq 2\pi \\ 0 & \text{otherwise} \end{cases}$$

Since  $\rho_0$  and  $\theta_0$  are independent, therefore,

$$f(\rho_0, \theta_0) = \begin{cases} \frac{\rho_0}{\pi R^2} & 0 \leq \rho_0 \leq R \quad \text{and} \quad 0 \leq \theta_0 \leq 2\pi \\ 0 & \text{otherwise} \end{cases} \quad (\text{A.4})$$

The cumulative distribution function (cdf) for the random variable  $\rho_0$  will be,



$$\begin{aligned} F_{R_0}(\rho_0) &= \int_{-\infty}^{\rho_0} f_{R_0}(\rho_0) d\rho_0 \\ &= \frac{\rho_0^2}{R^2} \end{aligned} \tag{A.5}$$

Using the probability integral transformation theorem, random numbers  $R_0$  with the cdf of  $F_{R_0}(\rho_0)$  can be generated by a sequence of uniformly distributed numbers,  $U$ , in the range of  $[0, 1]$  by,

$$R_0 = R\sqrt{U} \tag{A.6}$$

## APPENDIX B

### ***User's Speed Distribution***

The speed of a mobile unit is considered to be a random variable with truncated Gaussian probability density function.

$$f_V(v) = \begin{cases} \frac{K}{\sigma_v \sqrt{2\pi}} e^{-\frac{(v-\mu_v)^2}{2\sigma_v^2}} & V_{min} \leq v \leq V_{max} \\ 0 & \text{otherwise} \end{cases} \quad (\text{B.1})$$

where K is the normalization constant such that:

$$\int_{V_{min}}^{V_{max}} f_V(v) dv = 1 \quad (\text{B.2})$$

Considering definition of the error function (erf), i.e.  $\text{erf } x = \frac{1}{\sqrt{2\pi}} \int_0^x e^{-\frac{y^2}{2}} dy$ , it is easily concluded that:

$$\frac{1}{\sigma_v \sqrt{2\pi}} \int_{V_{min}}^{V_{max}} e^{-\frac{(v-\mu_v)^2}{2\sigma_v^2}} dv = \text{erf} \frac{V_{max} - \mu_v}{\sigma_v} - \text{erf} \frac{V_{min} - \mu_v}{\sigma_v} \quad (\text{B.3})$$

Hence,

$$K = \frac{1}{\left[ \operatorname{erf} \frac{V_{max} - \mu_v}{\sigma_v} - \operatorname{erf} \frac{V_{min} - \mu_v}{\sigma_v} \right]} \quad (\text{B.4})$$

## APPENDIX C

### *Minimum Value of Two Random Variables*

If

$$Z = \min(X, Y), \quad (\text{C.1})$$

then,

$$F_Z(z) = F_X(z) + F_Y(z) - F_X(z)F_Y(z) \quad (\text{C.2})$$

Proof:

The random variable  $Z$  is so defined that its value  $Z(\zeta)$  for a given  $\zeta$  equals the minimum of the two numbers  $X(\zeta), Y(\zeta)$ . For a given  $z$ , the region  $D_z$  of the  $xy$  plane such that,

$$\min(x, y) \leq z \text{ that is } x \leq z \text{ or } y \leq z \quad (\text{C.3})$$

is shown in Fig. C.1. Hence, to find  $F_Z(z)$ , it suffices to determine the mass in  $D_z$ . This mass equals the mass  $F_X(z)$  in the half plane  $x \leq z$  plus the mass  $F_Y(z)$  in the half plane  $y \leq z$  minus the mass  $F_{XY}(z, z)$  in the region  $x \leq z$  and  $y \leq z$ .

$$F_Z(z) = F_X(z) + F_Y(z) - F_{XY}(z, z) \quad (\text{C.4})$$

If the random variable  $X$  and  $Y$  are independent, then the above yields,

$$F_Z(z) = F_X(z) + F_Y(z) - F_X(z)F_Y(z) \quad (\text{C.5})$$

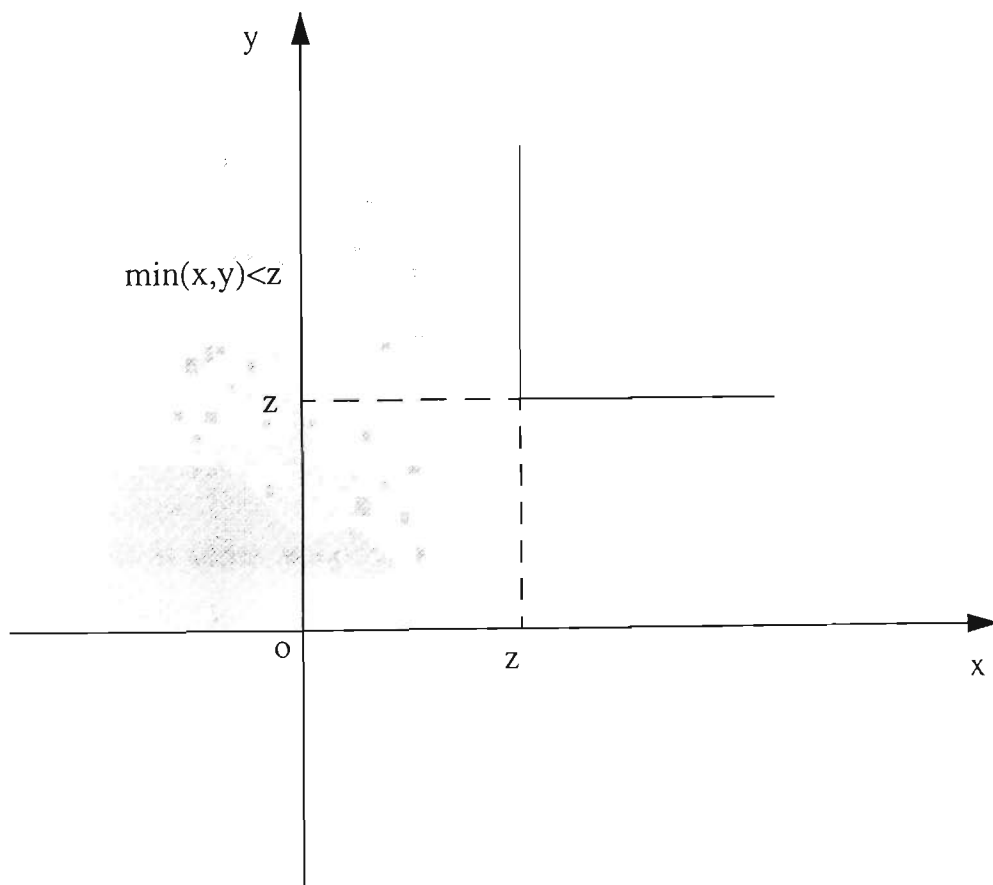


**Fig. C.1.** Region for a random variable  $Z$  which is the minimum of the two other random variables.

## APPENDIX D

### *Expected Value of a Distribution*

The average value of a random variable  $T_{ch}$  can be expressed directly in terms of its distribution  $F_{T_{ch}}(t)$ . Since the channel holding time is limited in the range  $0 < T_{ch} < t_0$  then,

$$\begin{aligned} F_{T_{ch}}(0) &= 0 \\ F_{T_{ch}}(t_0) &= 1 \end{aligned} \tag{D.1}$$

The average value of  $T_{ch}$  can be expressed in term of its density by,

$$E[T_{ch}] = \int_0^{t_0} t f_{T_{ch}}(t) dt \tag{D.2}$$

Integrating (D.2) by parts, we obtain,

$$\begin{aligned} \int_0^{t_0} t f_{T_{ch}}(t) dt &= t F_{T_{ch}}(t) \Big|_0^{t_0} - \int_0^{t_0} F_{T_{ch}}(t) dt \\ &= t_0 - \int_0^{t_0} F_{T_{ch}}(t) dt \end{aligned} \tag{D.3}$$

Hence, from (D.2) and (D.3), we obtain,

$$E[T_{ch}] = t_0 - \int_0^{t_0} F_{T_{ch}}(t) dt \quad (\text{D.4})$$

## APPENDIX E

### *Source Codes*

The software developed in this research is mostly written in MATLAB code. In this Appendix, some of the major programs has been shown.

*% This program with the name MainMobil.m uses different m-files InputMobil, InitialMobil, prob\_handover, NewLocation, NewAlpha, NewStateAndGama, DataSaveMobil and functions angleStar, Cdf2Rand, NormalEq and normalStar. It traces mobiles with different conditions including direction, speed. Data are collected and saved which later will be used to obtain behaviour of random motions in cellular environment.*

```
clear
InputMobil;
Tmean=[]; Dmean=[]; Tstd=[]; Dstd=[];
for drif=10:10:90
    drif_rad = drif * pi/180;Vstd=(Vave-5)/3;
    for R=inc:inc:rmax
        InitialMobil;
        for t=0:win:ht
            ProbHand
            NewLocation
            NewAlpha
            NewStateAndGama
        end;
        DataSaveMobil
    end;
end;
```

*% This program with the name InputMobil.m is used for entering required parameters.*

```
handover=input('1 for first handover any other numbers for second handover');
while 1
    rmax=input('enter max cell radius "default value is rmax = 10 Km"');
    disp('-----');
    if isempty(rmax),rmax=10; end;
    inc=input('enter space window size "default value is 1000 meters "');
    disp('-----');
    if isempty(inc),inc=1; else, inc=inc/1000; end;
    n=rmax/inc;
    if rem(n,1)~=0,disp('!!!invalid data!!!!try again!!!'),else break,end;
end;
while 2
    ht=input('enter max holding time "default value is ht=10 minutes"');
```



```

disp('----- ');
if isempty(ht),ht=10; end;
win=input('enter time window size "default value is 0.01 minutes ');
disp('----- ');
if isempty(win), win=.01; end;
m=ht/win;
if rem(m,1)~=0,disp('!!!invalid data!!!!try again!!!'),else break,end;
end;
user=input('enter number of users "default value is user=100000");
disp('----- ');
if isempty(user), user=100000; end;
Vave=input('enter average velocity"default value is Vave=50 km/hour");
disp('----- ');
if isempty(Vave),Vave=50; end;
Vstd=(Vave-5)/3;
vmax=input('enter max mobile velocity " default value is vmax =100 km/hour");
disp('----- ');
if isempty(vmax),vmax=100; end;
chn=input(' enter change of velocity per minute " default is chn= 10 % ');
disp('----- ');
if isempty(chn),chn=10; end;
DIS=input('Type of time interval distribution, 1 for uniform 2 for exponential');

```

*% This program with the name InitialMobil.m is used for initialization of mobiles position, speed and direction according to the appropriate distributions.*

```

n=1;
s=ones(user,n)*(1:n) .* R;
ZERO=zeros(user,n);
ZERO1=zeros(1,n);
userr=user;
sampleTime=[];
sampledistance=[];
Aved=[];
PresHoNo=[];
d1=ZERO;
T=1;
R,drif, % Let's know the stage of program.
if DIS==2, % Time interval distribution assumed to be exponential
    TimeChg=Exp(1,user,n); % Generates user-by-n matrix random variables with exponential
                           % distribution functions for the duration of time between two consequent
                           % changes in direction.
    temp=find(TimeChg<=win); if temp~=[],
    TimeChg(temp)=win.*ones(size(temp)); end;
    SpeedChg=Exp(1,user,n); % Generates user-by-n matrix random variables with exponential
                            % distribution functions for the duration of time between two consequent
                            % changes in speed.
else
    TimeChg=rand(user,n); % Time interval distribution between two consequent changes in speed
                          % assumed to be uniform
    SpeedChg=rand(user,n); % Time interval distribution between two consequent changes in speed

```

```

                                assumed to be uniform
end;
if handover==1
    roh=sqrt(rand(user,n)) .* s;      % Random choice of initial position ( magnitude)
    alpha = 2*pi .* rand(user,n) - pi; % Random choice of initial position (angle)
else
    roh=s;
    % The following part is to account for BIAS formula
    x=-pi./2:.004:pi./2;
    [Pdf,Cdf]=angleStar(x); % Creates pdf and cdf for direction as in Eq (4.11)
    [alpha]=Cdf2Rand(Cdf,x',user); % Generates random variables for direction.
    temp1=find(alpha<0);
    temp2=find(alpha>=0);
    alpha(temp1)=pi+alpha(temp1);
    alpha(temp2)=alpha(temp2)-pi;
end;
alphaO=alpha;
teta= 2*pi .* rand(user,n)-pi;
gama=alpha;
state=(alpha>=0).*1+(alpha<0).*3;
if handover==1
    x=0:.1:2.*vmax;
    [Pdf,Cdf,t]=NormalEq(Vave,Vstd,x,vmax); % Creates pdf and cdf for initial speed
    [v]=Cdf2Rand(Cdf,t',user); % Random choice of initial speed
else
    % This part is to account for BIAS formula
    x=0:.1:1.*vmax;
    [PdfStar,CdfStar,t]=normalStar(Vave,Vstd,x);% Creates pdf and cdf for the speed as in Eq (4.10)
    [v]=Cdf2Rand(CdfStar,t',user); % Generates random variables for initial speed for handover calls.
end;
tmean=[]; tstd=[]; dmean=[]; dstd=[];

% This program with the name ProbHand.m is used for collecting parameters of 1st or 2nd handover.
z=find((roh-s)>0);
if z==[]
    PresHoNo=[PresHoNo;ZERO1];
else
    temp=length(z);
    PresHoNo=[PresHoNo; temp];
    temp=d1(z);
    sampledistance=[sampledistance;temp];
    roh(z)=[]; s(z)=[]; gama(z)=[]; state(z)=[]; teta(z)=[]; alpha(z)=[]; alphaO(z)=[];
    d1(z)=[]; TimeChg(z)=[]; SpeedChg(z)=[]; v(z)=[]; ZERO(z)=[];
    userr=userr-length(z);
end;

% This program with the name NewLocation.m is used for creating new position of mobiles.
d=v * (1/60)*win;
d1=d1+d;

```

```

rohN=sqrt ( roh.^2 + d.^2 + 2 * ((roh .* d).*cos(gama)));
beta= abs(real(acos((rohN.^2+d.^2-roh.^2)/(2*(rohN.*d)))));
roh=rohN;
BetaSign=((state==2)+(state==3))-((state==1)+(state==4));
teta=teta+gama+beta.*BetaSign;
temp=find(teta> pi);
if temp~=[], teta(temp)=teta(temp)-2*pi; end;
temp=find(teta<-pi);
if temp~=[], teta(temp)=teta(temp)+2*pi;end;

```

*% This program with the name NewAlpha.m is used for creating new position, velocity and direction for active mobiles.*

```

alpha=ZERO;
temp=find(TimeChg<t+win & TimeChg>=t);
if temp~=[]
    if DIS==2
        TimeChg(temp)=Exp(1,length(temp),1)+t+win;
    else
        TimeChg(temp)=TimeChg(temp)+ones(size(temp));
    end;
alpha(temp)=2.*drif_rad .* rand(size(temp))-drif_rad;
alphaOO=alphaO(temp)+alpha(temp);
temp2=find(alphaOO>pi);
if temp2~=[], alphaOO(temp2)=alphaOO(temp2)-2*pi; end;
temp2=find(alphaOO<-pi);
if temp2~=[], alphaOO(temp2)=alphaOO(temp2)+2*pi; end;
alphatemp=alpha(temp);
ph=pi./2;
A= alphaO(temp)>0 & alphaO(temp)<ph & alpha(temp)>0 & alphaOO> ph;
B= alphaO(temp)>ph & alphaO(temp)<pi & alpha(temp)<0 & alphaOO< ph;
C= alphaO(temp)>-ph & alphaO(temp)<0 & alpha(temp)<0 & alphaOO<-ph;
D= alphaO(temp)>-pi & alphaO(temp)<-ph & alpha(temp)>0 & alphaOO>-ph;
E=A+B+C+D;
if find(E>1)~=[],disp('error') ;end;
temp1=find(E==1);
alphatemp(temp1)=zeros(size(temp1));
alpha(temp)=alphatemp;
alphaO(temp)=alphaO(temp)+alpha(temp);
TimeChgtemp=TimeChg(temp);
TimeChgtemp(temp1)=(t+win).*ones(size(temp1));
TimeChg(temp)=TimeChgtemp;
end;
temp=find(SpeedChg<t+win & SpeedChg>=t);
Speed_CHG=(2.*chn/100).* rand(user,n) - chn/100;
if temp~=[]
    v(temp)=Speed_CHG(temp).*v(temp)+v(temp);
    if DIS==2
        SpeedChg(temp)=Exp(1,length(temp),1)+t+win;
    else
        SpeedChg(temp)=SpeedChg(temp)+ones(size(temp));
    end;
end;

```

```

    end;
end;
v1=find(v>vmax); if v1~=[], v(v1)=vmax.*ones(size(v1)); end;
v2=find(v<=0); if v2~=[], v(v2)=0.0001.*ones(size(v2)); end;

```

*% This program with the name NewStateAndGama.m is used for creating new state and angle gamma of mobiles.*

```

stateOld=state;
region2=alpha< (-beta) | alpha> (pi-beta);
region1=alpha>=(-beta) & alpha<=(pi-beta);
region4=alpha> (beta) | alpha< (beta-pi);
region3=alpha<=(beta) & alpha>=(beta-pi);
if region1==[], region1=ZERO; end;
if region2==[], region2=ZERO; end;
if region3==[], region3=ZERO; end;
if region4==[], region4=ZERO; end
state= ((stateOld==1)+(stateOld==4)).*(region1+region2.*2)+...
        ((stateOld==2)+(stateOld==3)).*(region3.*3+region4.*4);
betaSign=(state==1)+(state==2)-(state==3)-(state==4);
gama=alpha+beta.*betaSign;

```

*% This program with the name DataSaveMobil.m is used for saving data.*

```

Dmean=mean(sampledistance);
Dstd=std(sampledistance);
RR=R.*1000;
p1=num2str(handover);
p2=num2str(Vave);
p3=num2str(drif);
p4=num2str(R);
filename=['~/MATLAB/mobility/data/H' p1 'V' p2 'drif' p3 'R' p4];
eval(['save' filename ' PresHoNo drif R ht win user Vave handover Dmean Dstd;']);

```

*% This function generates I-by-J matrix random variables with exponential distribution functions.*

```

function [B]=Exp(A,I,J)
B= - A.*log(rand(I,J));

```

*% This function generates pdf and cdf for direction as in Eq (4.11)*

```

function [Pdf,Cdf]=angleStar(x);
Pdf=0.5.*cos(x);
Cdf=.5+.5.*sin(x);

```

*% This function generates random variables for different distribution functions.*

```

function [RandNum]=Cdf2Rand(Cdf,t,No);
CdfSh=Cdf(1:(length(Cdf)-1));
temp=Cdf(2:length(Cdf))-CdfSh;
temp1=find(temp==0);

```

```

if temp1 ~= [], Cdf(temp1) = []; t(temp1) = []; end;
UU = min(Cdf) + (max(Cdf) - min(Cdf)) * rand(1, No);
RandNum = interp1(Cdf, t, UU);

```

*% This function creates truncated normal distributions.*

```

function [Pdf, Cdf, t] = NormalEq(Mu, Sigma, x, vmax);
A = (2 * pi).^0.5;
vmin = 0;
B = (vmax - Mu) / Sigma;
BB = 0.5 * erf(B / 2.^0.5);
C = (vmin - Mu) / Sigma;
CC = 0.5 * erf(C / 2.^0.5);
K = 1 / (BB - CC);
t = vmin : .01 : vmax;
Pdf = (K / (Sigma * A)) * exp(-(t - Mu).^2 / (2 * Sigma.^2));
X = (t - Mu) / Sigma;
Cdf = 0.5 + 0.5 * erf(X / (2.^0.5));

```

*% This function creates pdf and cdf for Eq (4.10).*

```

function [PdfStar, CdfStar, t] = normalStar(Mu, Sigma, x);
vmax = 100;
[Pdf, Cdf, t] = NormalEq(Mu, Sigma, x, vmax);
PdfStar = (t * Pdf) / Mu;
[CdfStar] = Pdf2Cdf(PdfStar, t);

```

*% This function calculates pdf and cdf as shown in Eqs (4.5), (4.6), (4.8) and (4.9).*

```

function [pdfHo1, pdfHo2, cdfHo1, cdfHo2, t] = RapHo(win, ht, vmax, rmax)
t = win : win : ht;
vmax1 = vmax / 60;
R = rmax * 0.91;
Limit = (2 * R) / vmax1;
temp1 = find(t >= Limit);
temp2 = find(t < Limit);
a = (2 / pi) * asin((vmax1 * t(temp2)) / (2 * R));
b = (4 / (3 * pi)) * tan((1 / 2) * asin((vmax1 * t(temp2)) / (2 * R)));
c = (1 / (3 * pi)) * sin(2 * asin((vmax1 * t(temp2)) / (2 * R)));
e = (8 * R) / (3 * pi * vmax1 * t(temp1));
f = 1 - e;
g = 1 - 1.5 * e;
cdfHo1 = a - b + c;
cdfHo1 = [cdfHo1, f];
cdfHo2 = a - b * 3 / 2;
cdfHo2 = [cdfHo2, g];
aa = (8 * R) / (3 * pi * vmax1 * t(temp2) * t(temp2));
bb = ((vmax1 * t(temp2)) / (2 * R)).^2;
cc = 1 - (1 - bb).^1.5;
dd = (8 * R) / (3 * pi * vmax1 * t(temp1) * t(temp1));
ce = 1 - (1 - bb).^0.5;

```

```

ddd=1.5.*dd;
pdfHo1=aa.*cc;
pdfHo1=[pdfHo1,dd];
pdfHo2=(aa.*1.5).*ee;
pdfHo2=[pdfHo2,ddd];
pdfHo1=[0,pdfHo1];
pdfHo2=[0,pdfHo2];
cdfHo1=[0,cdfHo1];
cdfHo2=[0,cdfHo2];
t=0:win:ht;

```

*% This program with the name RapNewCall.m plots new call residence time probability distributin for two different case of simulation and Eq (4.6) with the same mobility parameters. It is shown in Fig. 4.5.*

```

clear;
load ~/MATLAB/mobility/data/RAP/H1V100R1_10.mat % data file from simulation
t=0:win:ht;
PDF1=PresHoNo./(user.*win);
CDF1=cumsum(PresHoNo./user); % cdf as obtained from simulation
for r=inc:inc:rmax
    [pdfHo1,pdfHo2,cdfHo1,cdfHo2, tt]=RapHo(win.*10, ht, vmax, r);
    CDF_HO1=[CDF_HO1,cdfHo1']; % cdf as obtained from equation (4.8)
end
clg; figure(1)
plot(t,CDF1,'--'); % Plots simulation results
hold on; grid on
plot(tt,CDF_HO1); % Plots analytical results
xlabel('New Call Cell Residence Time (minute)')
ylabel('Probability')
hold off

```

*% This program with the name RapHoCall.m plots hanover call residence time probability distribution using two different cases of simulation and Eq (4.9) with the same mobility parameters. The figure is shown in Fig. 4.5.*

```

clear
load ~/MATLAB/mobility/data/RAP/H2V100R1_10.mat; % data file from simulation
t=0:win:ht;
PDF1=PresHoNo./(user.*win);
CDF1=cumsum(PresHoNo./user);
for r=inc:inc:rmax
    [pdfHo1,pdfHo2,cdfHo1,cdfHo2, tt]=RapHo(win.*10, ht, vmax, r);
    CDF_HO2=[CDF_HO2,cdfHo2']; % cdf as obtained from equation 4.9
end
clg; figure(1)
plot(t,CDF1,'--'); % Plots simulation results
hold on; grid on;
plot(tt,CDF_HO2); % Plots analytical results
xlabel('Handover Call Cell Residence Time (minute)')
ylabel('Probability')
hold off

```

*% This program with the name FitCdfGamma.m fits the obtained data for handover probability to a generalised gamma distribution*

```
clear
A1=[]; ERRORm=inf;Vave=50;drif=0; alpha=[];beta=[];
handover=input('enter 1 for new calls and 2 for handover calls');
alphaL=input('enter lower limit of alpha parameter')
alphaU=input('enter upper limit of alpha parameter')
alphaI=input('enter increment for the alpha parameter')
betaL=input('enter lower limit of beta parameter')
betaU=input('enter upper limit of beta parameter')
betaI=input('enter increment for the beta parameter')
pL=input('enter lower limit of p parameter')
pU=input('enter upper limit of p parameter')
pI=input('enter increment for the p parameter')
for R=10:10:100
    RR=R./10;
    p1=num2str(handover);
    p2=num2str(Vave);
    p3=num2str(drif);
    p4=num2str(R);
    filename=['~/MATLAB/mobility/data/H' p1 'V' p2 'drif' p3 'R' p4];
    eval(['load' filename]);
    t=(0:win:ht)';
    [Pdf]=Data2Pdf(PresHoNo,t);
    [Cdf]=Pdf2Cdf(Pdf,t);
    ERRORm=inf;
    for p=pL:pI:pU
        for alpha=alphaL:alphaI:alphaU
            for beta=betaL:betaI:betaU
                [PDF,CDF]=GammaEq(alpha,beta,p,t);
                Error=max(abs(CDF-Cdf));
                if ERRORm>Error
                    alphaO=alpha; betaO=beta; pO=p;
                    ERRORm=Error;
                end;
            end;
        end;
    end;
    betaR=betaO./R;
    A= [R alphaO, betaR, pO, ERRORm];
    A1=[A1;A]
end;
```

*% This function generates pdf for any input data. In our case input data is 'PresHoNo' which describes statistics for number of handovers.*

```
function [Pdf]=Data2Pdf(Data,t);
Pdf=Data./sum(Data);      % rough estimation of Pdf
PdfArea=trapz(t,Pdf);
Pdf=(Pdf./PdfArea);     % final result of Pdf
```

*% This function converts pdf to cdf*

```
function [Cdf]=Pdf2Cdf(Pdf,t);
if length(Pdf)~=length(t), error('error in Pdf2Cdf'), end;
if length(Pdf) > 200
    win=t(2)-t(1);
    Cdf=cumsum(Pdf(1:length(Pdf))).*win;
else
    Cdf=0;
    Bins_Area=0;
    for i=1:length(Pdf)-1
        BinArea=trapz([t(i), t(i+1)], [Pdf(i), Pdf(i+1)]);
        Bins_Area=BinArea+Bins_Area;
        Cdf=[Cdf; Bins_Area];
    end;
end;
```

*% This function generates pdf and cdf for the generalized gamma distribution.*

```
function [Pdf,Cdf]=GammaEq(alpha,beta,p,t);
a=exp(-(t./beta).^p);
b=t.^(p.*alpha-1);
c=beta.^(p.*alpha);
d=gamma(alpha);
Pdf=(p.*b.*a)./(c.*d);
[Cdf]=Pdf2Cdf(Pdf,t);
```

*% This program with the name BestRDrift.m chooses cells with different drifts with the best fit with a reference cell.*

```
clear
Vave=50; drif1=0;
handover=input('enter 1 for new calls and 2 for handover calls');
for drifdrif=10:10:90
    for RR=10:10:100
        p1=num2str(handover);
        p2=num2str(Vave);
        p3=num2str(drifdrif);
        p4=num2str(RR);
        filename=['~/MATLAB/mobility/data/H' p1 'V' p2 'drif' p3 'R' p4];
        eval(['load' filename]);
        RX=R;
        t=(0:win:ht);
        [Pdf]=Data2Pdf(PresHoNo,t);
        [Cdf]=Pdf2Cdf(Pdf,t);
        ERRORm=inf;
        for R1=RR:1:2.*RR
            p3=num2str(drif1);
            p4=num2str(R1);
            filename=['~/MATLAB/mobility/data/H' p1 'V' p2 'drif' p3 'R' p4];
            eval(['load' filename]);
```



```

        [PDF]=Data2Pdf(PresHoNo,t);
        [CDF]=Pdf2Cdf(PDF,t);
        Error=max(abs(CDF-Cdf))
        clear PresHoNo;
        if ERRORm>Error, ERRORm=Error; Rm=R1.*100; end;
    end
    p3=num2str(drifdrif);
    p4=num2str(RX);
    filename=['~/MATLAB/mobility/data/Drift/H' p1 'V' p2 'drif' p3 'R' p4];
    eval(['save' filename ' Rm ERRORm;']);
end;
end;

```

*% This program with the name BestRVel.m chooses cells with different speeds with the best fit with a reference cell.*

```

clear
Vave1=50; drif=0;
handover=input('enter 1 for new calls and 2 for handover calls');
for VaveVave=10:10:80
    for RR=10:10:100
        p1=num2str(handover);
        p2=num2str(VaveVave);
        p3=num2str(drif);
        p4=num2str(RR);
        filename=['~/MATLAB/mobility/data/H' p1 'V' p2 'drif' p3 'R' p4];
        eval(['load' filename]);
        RX=R;
        t=(0:win:ht);
        [Pdf]=Data2Pdf(PresHoNo,t);
        [Cdf]=Pdf2Cdf(Pdf,t);
        ERRORm=inf;
        for R1=1:1:1.*RR
            p2=num2str(Vave1);
            p4=num2str(R1);
            filename=['~/MATLAB/mobility/data/H' p1 'V' p2 'drif' p3 'R' p4];
            eval(['load' filename]);
            [PDF]=Data2Pdf(PresHoNo,t);
            [CDF]=Pdf2Cdf(PDF,t);
            Error=max(abs(CDF-Cdf));
            clear PresHoNo;
            if ERRORm>Error, ERRORm=Error; Rm=R1.*100; end;
        end;
        p2=num2str(VaveVave);
        p4=num2str(RX);
        filename=['~/MATLAB/mobility/data/Velocity/H' p1 'V' p2 'drif' p3 'R' p4];
        eval(['save' filename ' Rm ERRORm;']);
    end;
end;
end;

```

*% This program with the name diff\_gamma.m plots Fig. 4.7 which shows examples of different generalized gamma density functions.*

```
clear;
win=.5; ht=30;
t=0:win:ht;
figure(1)
alpha=1; beta=6; p=1;
[pdf,cdf]=GammaEq(alpha,beta,p,t); % Exponential distribution
plot(t,pdf,'m-')
hold on
alpha=3; beta=4; p=1;
[pdf,cdf]=GammaEq(alpha,beta,p,t); % Gamma distribution
plot(t,pdf,'--')
alpha=1; beta=25; p=12;
[pdf,cdf]=GammaEq(alpha,beta,p,t); % Weibull distribution
plot(t,pdf,'r:', 'LineWidth', 1)
alpha=1; beta=5.*2.^(1/2); p=2;
[pdf,cdf]=GammaEq(alpha,beta,p,t); % Rayleigh distribution
plot(t,pdf,'g-')
n=10; alpha=n./2; beta=2; p=1;
[pdf,cdf]=GammaEq(alpha,beta,p,t); % chi square distribution
plot(t,pdf,'w-')
ylabel('Probability density')
hold off
```

*% This program with the name Pdf\_GamaData\_HOI.m plots new or handover call residence time pdf using two different cases of simulation and generalized gamma distribution. The figure is shown in Fig. 4.8.*

```
clear;
handover=input('enter 1 for new calls and 2 for handover calls');
Vave=input('enter intial average velocity');
drif=input('enter the amount of drift');
R=input('enter the amount of cell size in Km');
R=R.*10;
eval(['load ~/MATLAB/mobility/data/H' num2str(handover) 'V' num2str(Vave) 'drif' num2str(drif) 'R'
num2str(R)])
t=(0:win:ht);
[Pdf]=Data2Pdf(PresHoNo,t); % Pdf according to simulation data
[Cdf]=Pdf2Cdf(Pdf,t); % Pdf according to simulation data
if handover=1, alpha=.62; beta=1.84.*R; p=1.88; end;
if handover=2, alpha=2.31; beta=1.22.*R; p=1.72; end;
[Pdf1,Cdf1]=GammaEq(alpha, beta, p, t); % Pdf according to equivalent gamma distribution.
figure
plot(t(1:10:length(t)),Pdf(1:10:length(Pdf)), 'g');
temp=max(Pdf);
axis([0,25,0,.16])
hold on
plot(t,Pdf1,'--', 'LineWidth', 2);
grid on;
```

*% This program with the name Cdf\_GamaData\_HO1.m plots new or handover call residence time pdf using two different cases of simulation and generalized gamma distribution. The figure is shown in Fig. 4.9.*

```
clear;
handover=input('enter 1 for new calls and 2 for handover calls');
Vave=input('enter initial average velocity');
drif=input('enter the amount of drift');
for R=10:10:100
    p1=num2str(handover);
    p2=num2str(Vave);
    p3=num2str(drif);
    p4=num2str(R);
    filename=['~/MATLAB/mobility/data/H' p1 'V' p2 'drif' p3 'R' p4];
    eval(['load' filename]);
    t=(0:win:ht);
    [Pdf]=Data2Pdf(PresHoNo,t);
    [Cdf]=Pdf2Cdf(Pdf,t);
    if handover=1, alpha=.62; beta=1.84.*R; p=1.88; end;
    if handover=2, alpha=2.31; beta=1.22.*R; p=1.72; end;
    [Pdf1,Cdf1]=GammaEq(alpha,beta,p,t);
    plot(t,Cdf);
    hold on;
    plot(t,Cdf1,'r--');
end;
axis([0,20,0,1]);
t=0:win:ht;
grid on;
if handover=1, xlabel('New Call Cell Residence Time (minute)'); end;
if handover=2, xlabel('Handover Call Cell Residence Time (minute)'); end;
ylabel('Probability');
hold off;
```

*% This program with the name MEAN.m compares the mean cell residence time for the new and the handover calls with different calculation methods as shown in Table 4.3*

```
V=50; drif=0;
handover=input('enter 1 for new calls and 2 for handover calls');
for R=1:1:10
    if handover=1, alpha=.62; beta=1.84.*R; p=1.88; end;
    if handover=2, alpha=2.31; beta=1.22.*R; p=1.72; end;
    p1=num2str(handover);
    p2=num2str(Vave);
    p3=num2str(drif);
    p4=num2str(R);
    filename=['~/MATLAB/mobility/data/H' p1 'V' p2 'drif' p3 'R' p4];
    eval(['load' filename]);
    t=(0:win:ht);
    [Pdf]=Data2Pdf(PresHoNo,t);
    [mu]=Pdf2mean(Pdf,t); % mean value according to the Eqs (4.23) and (4.24)
```

*% This program with the name EqRdrift.m compares simulation results with the empirical formula as shown in Fig. 4.11.*

```
Vave=50; r=1:1:10; j=0;
handover=input('enter 1 for new calls and 2 for handover calls');
for drif=10:10:90
    Extra=[]; Excess=[];
    for R=1:1:10
        p1=num2str(handover);
        p2=num2str(Vave);
        p3=num2str(drif);
        p4=num2str(R.*10);
        filename=['~/MATLAB/mobility/data/Drift/H' p1 'V' p2 'drif' p3 'R' p4];
        eval(['load' filename]);
        excess=Rm-R; % Excess cell radius for different values of drift by simulation
        extra=0.0038.*drif.*R; % Excess cell radius by empirical equation (4.28).
        Excess=[Excess, excess];
        Extra=[Extra, extra];
    end;
    j=j+1;
    subplot(3,3,j),
    plot(r, Extra, 'w.', r, Excess, 'g')
    axis([1,10,0,3])
    grid on; hold on;
    ylabel('Excess Radius (Km)');
    xlabel('Cell Radius (Km)');
end;
hold off
```

*% This program with the name EqRvelocityHO1.m compares simulation results with the empirical formula as shown in Fig. 4.12.*

```
clear
drif=0; r=1:1:10;
handover=input('enter 1 for new calls and 2 for handover calls');
for Vave=10:10:70
    Extra=[]; Excess=[];
    for R=1:1:10
        p1=num2str(handover);
        p2=num2str(Vave);
        p3=num2str(drif);
        p4=num2str(R.*10);
        filename=['~/MATLAB/mobility/data/Drift/H' p1 'V' p2 'drif' p3 'R' p4];
        eval(['load' filename]);
        excess=Rm-R; % Excess cell radius for different speeds by simulation
        extra=((50./Vave)-1).*R; % Excess cell radius by empirical equation (4.31).
        Excess=[Excess, excess];
        Extra=[Extra, extra];
    end;
    plot(r, Extra, 'w.', r, Excess, 'g')
    grid on; hold on;
```

```

    ylabel('Excess Radius (Km)');
    xlabel('Cell Radius (Km)');
    axis([1,10,-3,10])
    ylabel('Excess Radius (Km)')
    xlabel('Cell Radius (Km)')
    end;
hold off

% This function calculates the mean value for a given pdf
function [mu]=Pdf2mean(Pdf,t)
temp=t.*Pdf;
mu=trapz(t,temp);

% This program with the name ave_ho_Pfh.m calculates and plots (as in Fig. 4.14) average number of
handovers experienced by a random call for different probabilities of handover failures.

clear
Vave=50; drif=0; AveCallHoldTime=2; win=.01; ht=100;
t=0:win:ht;R=1:1:10; Ri=1:1./4:10;
for Pfh=[0,.1,.2,.5]
    AveH_G=[]; HH2=[]; HHg=[]; HH2g=[]; mu_InvTh=[];
    for RR=1:1:10
        handover=1; alpha=.62; beta=1.84.*RR; p=1.88;
        [Pdfn,Cdfn]=GammaEq(alpha,beta,p,t);
        handover=2; alpha=2.31; beta=1.22.*RR; p=1.72;
        [Pdfh,Cdfh]=GammaEq(alpha,beta,p,t);
        [Pn]=Pn_OR_Ph(Pdfn,AveCallHoldTime,t);
        [Ph]=Pn_OR_Ph(Pdfh,AveCallHoldTime,t);
        [H]=AveHoNo(Pn,Ph,Pfh);
        AveH_G=[AveH_G;H]; % First method
        if Pfh==0
            [mu_Th1]=Pdf2mean(Pdfh,t);
            HH=(AveCallHoldTime)./mu_Th1;
            AveH_T=[AveH_T; HH]; % Second method using equation (4.47)
        end
    end;
end;
AveH_Gi=interp1(R,AveH_G,Ri,'spline');
AveH_Ti=interp1(R,AveH_T,Ri,'spline');
plot(Ri, AveH_Gi)
hold on
plot(Ri, AveH_Ti,'r--');
ylabel('Average Number of Handovers per Call')
xlabel('Cell Radius, R (Km)')
hold off

% This function calculates probability that a handover call or a new call will require at least another
handover as in Eqs (4.41) and (4.42).

function [P]=Pn_OR_Ph(Pdf,AveCallHoldTime,t)
mu_c=1./AveCallHoldTime;

```

```
FUNCTION=Pdf.*exp(-mu_c.*t);
P=trapz(t,FUNCTION);
```

*% This function calculates average number of handovers per call as in (4.38)*

```
function [H]=AveHoNo(Pn,Ph,Pfh)
temp=1-Pfh;
H=(Pn.*temp)/(1-Ph.*temp);
```

*% This program with the name Th\_Tn\_Tc\_Tch.m calculates and plots (as in Fig. 4.17) different functions for a cell size of 3 Km.*

```
path(path,'/pgr/mahmood/_framemaker/figures/mobility');
path(path,'/pgr/mahmood/MATLAB/mobility/dataprocce/Functions');
path(path,'/pgr/mahmood/MATLAB/Distribution/Data2Dist');
path(path,'/pgr/mahmood/MATLAB/Distribution/Eq2Dist');
win=.1;ht=100;inc=1;rmax=10;
handover=1; Vave=50; drif=0; R=30;
eval(['load /pgr/mahmood/MATLAB/mobility/data/H' num2str(handover) 'V' num2str(Vave) 'drif'
num2str(drif) 'R' num2str(R)])
t=(0:win:ht);
[Pdfn]=Data2Pdf(PresHoNo,t);
[Cdfn]=Pdf2Cdf(Pdfn,t);
handover=2; R=30;
eval(['load /pgr/mahmood/MATLAB/mobility/data/H' num2str(handover) 'V' num2str(Vave) 'drif'
num2str(drif) 'R' num2str(R)])
[Pdfh]=Data2Pdf(PresHoNo,t);
{Cdfh}=Pdf2Cdf(Pdfh,t);
AveTime=2;
[PdfCall,CDFCall]=ExpEq(AveTime,t);
[CDFch]=CdfCh(Pdfn,Cdfn,Pdfh,Cdfh,AveTime,t);
[muCh]=Cdf2mean(CDFch,t);
[Pdfchannel,CDFchannel]=ExpEq(muCh,t);
[Pn]=Pn_OR_Ph(Pdfn,AveTime,t);
[Ph]=Pn_OR_Ph(Pdfh,AveTime,t);
Pfh=0;
[H]=AveHoNo(Pn,Ph,Pfh);% Ave Ho No First method
F_Tch=CDFCall+(1./(1+H)).*(1-CDFCall).*(Cdfn+H.*Cdfh);
z=1:10:length(t);
plot(t(z),Cdfn(z),'b-');hold on
axis([0, 10,0, 1])
plot(t(z),Cdfh(z),'r.','LineWidth',2)
plot(t(z),CDFCall(z),'g-')
plot(t(z),CDFchannel(z),'c')
text(t(z),F_Tch(z),'*','clipping','on','HorizontalAlignment','right','VerticalAlignment','top','FontSize',7)
axis([0, 10,0, 1]);
ylabel('Probability')
xlabel('Time (minute)')
hold off;
```

*% This function calculates pdf and cdf of the exponential distribution by using the related relation*

```
function [Pdf,Cdf]=ExpEq(AveTime,t);
Pdf=(1./AveTime).*exp(-t./AveTime);
Cdf=1-exp(-t./AveTime);
```

*% This function calculates call holding time distributions as in (4.53)*

```
function [CDFch]=CdfCh(Pdfn,Cdfn,Pdfh,Cdfh,AveCallHoldTime,t)
[Pn]=Pn_OR_Ph(Pdfn,AveCallHoldTime,t);
[Ph]=Pn_OR_Ph(Pdfh,AveCallHoldTime,t);
[PdfCall,CdfCall]=ExpEq(AveCallHoldTime,t);
ratio=Pn./(1-Ph);
ratio=ones(length(Cdfh),1)*ratio;
ratioI=1./(1+ratio);
CDFch=CdfCall+ratioI.*(1-CdfCall).*(Cdfn+ratio.*Cdfh);
```

*% This function calculates mean value from cdf*

```
function [mu]=Cdf2mean(Cdf,t)
CdfArea=trapz(t,Cdf);
mu=t(length(Cdf))-CdfArea;
```

*% This program with the name mu.m calculates and plots (as in Fig. 4.18) variation of the average channel holding time with different cell sizes*

```
clear;
Vave=50; drif=0; AveCallHoldTime=2;
win=.01; ht=100; t=0:win:ht; Pfh=0;
AveH_G=[]; HH2=[]; HHg=[]; HH2g=[]; mu=[];
for R=1:1:10
    handover=1; alpha=.62; beta=1.84.*R; p=1.88;
    [Pdfn,Cdfn]=GammaEq(alpha,beta,p,t);
    handover=2; lpha=2.31; beta=1.22.*R; p=1.72;
    [Pdfh,Cdfh]=GammaEq(alpha,beta,p,t);
    [CDFch]=CdfCh(Pdfn',Cdfn',Pdfh',Cdfh',AveCallHoldTime,t');
    [muCh]=Cdf2mean(CDFch,t);
    [mu]=[mu; muCh];
end;
mu=60.*mu;
R=1:1:10; Ri=1:1./4:10;
mui=interp1(R,mu,Ri,'spline');
plot(Ri,muCh3i)
```

*% This program creates data required for the traffic analysis*

```
clear
cellsize=1;ch=50;ch_ho=0; ch_new=ch - ch_ho;attempt=.33;
InitialTraffic;
for ch_ho=0:1:5
    ch=50; ch_new=ch - ch_ho;
```

```

for cellsize=1:10
    for attempt=.04:.002:.05 % minute per call
        landa=1./(attempt.*60)% call per second
        LANDA=round(landa.*100),% for deleting point in data saving
        InitialTraffic;
        LOOPSteady=30000;
        for i=1:LOOPSteady
            SteadyState
        end;
        savedataTraffic; % steady state data
        for i=1:LOOP
            BodyTraffic
        end;
        savedataTraffic
    end;
end;
end;

```

*% This program with the name InitialTraffic.m is used for initialization of parameters required for traffic analysis*

```

cells=49;
ARR=2; % mean call holding time [min];
LOOP=10000;
CDF_1_2
NewCall=zeros(1,cells); NewCallBlock=zeros(1,cells);
HoCall=zeros(1,cells); HoCallBlock=zeros(1,cells);
ChannelStatus=zeros(1,cells);
NoCallSuccess=zeros(1,cells);
st=inf.*ones(1,cells);
sp=inf.*ones(ch,cells);
ho=inf.*ones(ch,cells);
old_ho=inf.*ones(ch,cells);
dropout=zeros(1,cells);
sourceCell=inf.*ones(ch,cells); % attributes of calls in process
st(1,:)=Exp(attempt,1,cells); % attempt = duration between two successive call [min]
clock=min(min(st));
i=0; ii=0;

```

*% This program with the name SteadyState.m is used for approaching to the steady state condition.*

```

[a]=find(st==clock);
if a~=[],
    if length(a)>1, a=min(a); end;
    if ChannelStatus(a)<ch_new
        ChannelStatus(a)=ChannelStatus(a)+1;
        B=min(find(sp(:,a)==inf));
        sp(B,a)=Exp(ARR,1,1)+clock; % CallTime=Exp(ARR,1,1);
        ho(B,a)=Cdf2Rand(CDF1,X,1)+clock;
        sourceCell(B,a)=a;
    end;
end;

```



```

        st(a)=Exp(attempt,1,1)+clock;           % start time of the future call
end;
[A,a]=find(sp==clock);
if A~=[],
    if length(A)>1, A=min(A); a=min(a); end;
    sp(A,a)=inf; ho(A,a)=inf;
    ChannelStatus(a)=ChannelStatus(a)-1;
    sourceCell(A,a)=inf;
end;
[A,a]=find(ho==clock);
if A~=[]
    if length(A)>1, A=min(A); a=min(a); end;
    ho(A,a)=inf;
    ChannelStatus(a)=ChannelStatus(a)-1;
    CellN=CellNo(old_ho(A,a),a);
    old_ho(A,a)=inf;
    if ChannelStatus(CellN)<ch
        ChannelStatus(CellN)=ChannelStatus(CellN)+1;
        B=min(find(sp(:,CellN)==inf)); % to find place of empty channel
        sp(B,CellN)=sp(A,a);
        ho(B,CellN)=Cdf2Rand(CDF2,X,1)+clock;
        old_ho(B,CellN)=a; % gives the number of previous cell
        sourceCell(B,CellN)=sourceCell(A,a);
    end;
    sp(A,a)=inf;
    sourceCell(A,a)=inf;
end;
clock1=min(min(st)); % start time of the future call
clock2=min(min(sp)); % stop time of the current call
clock3=min(min(ho)); % ho time of the current call
clock=min([clock1, clock2, clock3]);

```

*% This program with the name savedataTraffic.m is used for saving data*

```

iii=ii+1;
ch_ho_ii_R_Att=[ch_ho ,ii, cellsize, LANDA ]
seed=rand('seed'); % seed for generating next variable
p1=num2str(cellsize);
p2=num2str(LANDA);
p3=num2str(ch);
p4=num2str(ch_ho);
filename=['~/MATLAB/traffic/data/R' p1 'E' p2 'C' p3 'H' p4];
clear X PDF1 CDF1 PDF2 CDF2
eval(['save ' filename]);
CDF_1_2

```

*% This program with the name BodyTraffic.m generates: attributes of the current call*

```

[a]=find(st==clock);
if a~=[],
    if length(a)>1, a=min(a); end;

```

```

NewCall(a)=NewCall(a)+1;
if ChannelStatus(a)<ch_new
    ChannelStatus(a)=ChannelStatus(a)+1;
    B=min(find(sp(:,a)==inf));
    sp(B,a)=Exp(Arr,1,1)+clock;% CallTime=Exp(Arr,1,1);
    ho(B,a)=Cdf2Rand(CDF1,X,1)+clock;
    sourceCell(B,a)=a;

else
    NewCallBlock(a)= NewCallBlock(a)+1;
end;
st(a)=Exp(attempt,1,1)+clock; % start time of the future call
end;
[A,a]=find(sp==clock);
if A~=[],
    if length(A)>1, A=min(A); a=min(a); end;
    sp(A,a)=inf; ho(A,a)=inf;
    ChannelStatus(a)=ChannelStatus(a)-1;
    sourceCell(A,a)=inf;
    NoCallSuccess(a)=NoCallSuccess(a)+1
end;
[A,a]=find(ho==clock);
if A~=[]
    if length(A)>1, A=min(A); a=min(a); end;
    ho(A,a)=inf;
    ChannelStatus(a)=ChannelStatus(a)-1;
    CellN=CellNo(old_ho(A,a),a);
    HoCall(CellN)=HoCall(CellN)+1;
    old_ho(A,a)=inf;
    if ChannelStatus(CellN)<ch
        ChannelStatus(CellN)=ChannelStatus(CellN)+1;
        B=min(find(sp(:,CellN)==inf)); % to find place of empty channel
        sp(B,CellN)=sp(A,a);
        ho(B,CellN)=Cdf2Rand(CDF2,X,1)+clock;
        old_ho(B,CellN)=a; % gives the number of previous cell
        sourceCell(B,CellN)=sourceCell(A,a);
    else
        HoCallBlock(CellN)= HoCallBlock(CellN)+1;
        dropout(sourceCell(A,a))=dropout(sourceCell(A,a))+1;
    end;
    sp(A,a)=inf;
    sourceCell(A,a)=inf;
end;
clock1=min(min(st)); % start time of the future call
clock2=min(min(sp)); % stop time of the current call
clock3=min(min(ho)); % ho time of the current call
clock=min([clock1, clock2, clock3]);

% This program with the name CDF_1_2.m creates pdf and cdf of the generalised Gamma distributions
X=(0:.01:100)';

```

```
alpha=0.62; beta=1.84.*cellsize; p=1.88; %handover=1;
[PDF1,CDF1]=GammaEq(alpha,beta,p,X);
alpha=2.31; beta=1.22.*cellsize; p=1.72; %handover=2;
[PDF2,CDF2]=GammaEq(alpha,beta,p,X);
```

*% This function creates the cell number to which a handover call is arrived.*

```
function [CellN]=CellNo(old,a)
U=fix(1+(7-1).*rand);
while U==7, U=fix(1+(7-1).*rand); end;
replace=['CellN=XX(U); while CellN==old, U=fix(1+(7-1).*rand); while U==7, U=fix(1+(7-1).*rand);
end; CellN=XX(U); end;'];
if a== 1, XX=[ 2  8 14  7 46 47]; eval(replace)
elseif a== 2, XX=[ 3  9  8  1 47 48]; eval(replace)
elseif a== 3, XX=[ 4 10  9  2 48 49]; eval(replace)
elseif a== 4, XX=[ 5 11 10  3 49 43]; eval(replace)
elseif a== 5, XX=[ 6 12 11  4 43 44]; eval(replace)
elseif a== 6, XX=[ 7 13 12  5 44 45]; eval(replace)
elseif a== 7, XX=[ 1 14 13  6 45 46]; eval(replace)
elseif a== 8, XX=[ 9 16 15 14  1 2]; eval(replace)
elseif a== 9, XX=[10 17 16  8  2 3]; eval(replace)
elseif a==10, XX=[11 18 17  9  3 4]; eval(replace)
elseif a==11, XX=[12 19 18 10  4 5]; eval(replace)
elseif a==12, XX=[13 20 19 11  5 6]; eval(replace)
elseif a==13, XX=[14 21 20 12  6 7]; eval(replace)
elseif a==14, XX=[ 8 15 21 13  7 1]; eval(replace)
elseif a==15, XX=[16 22 28 21 14  8]; eval(replace)
elseif a==16, XX=[17 23 22 15  8 9]; eval(replace)
elseif a==17, XX=[18 24 23 16  9 10]; eval(replace)
elseif a==18, XX=[19 25 24 17 10 11]; eval(replace)
elseif a==19, XX=[20 26 25 18 11 12]; eval(replace)
elseif a==20, XX=[21 27 26 19 12 13]; eval(replace)
elseif a==21, XX=[15 28 27 20 13 14]; eval(replace)
elseif a==22, XX=[23 30 29 28 15 16]; eval(replace)
elseif a==23, XX=[24 31 30 22 16 17]; eval(replace)
elseif a==24, XX=[25 32 31 23 17 18]; eval(replace)
elseif a==25, XX=[26 33 32 24 18 19]; eval(replace)
elseif a==26, XX=[27 34 33 25 19 20]; eval(replace)
elseif a==27, XX=[28 35 34 26 20 21]; eval(replace)
elseif a==28, XX=[22 29 35 27 21 15]; eval(replace)
elseif a==29, XX=[30 36 42 35 28 22]; eval(replace)
elseif a==30, XX=[31 37 36 29 22 23]; eval(replace)
elseif a==31, XX=[32 38 37 36 23 24]; eval(replace)
elseif a==32, XX=[33 39 38 31 24 25]; eval(replace)
elseif a==33, XX=[34 40 39 32 25 26]; eval(replace)
elseif a==34, XX=[35 41 40 33 26 27]; eval(replace)
elseif a==35, XX=[29 42 41 34 27 28]; eval(replace)
elseif a==36, XX=[37 44 43 42 29 30]; eval(replace)
elseif a==37, XX=[38 45 44 36 36 31]; eval(replace)
elseif a==38, XX=[39 46 45 37 31 32]; eval(replace)
elseif a==39, XX=[40 47 46 38 32 33]; eval(replace)
```

```

elseif a==40, XX=[41 48 47 39 33 34]; eval(replace)
elseif a==41, XX=[42 49 48 40 34 35]; eval(replace)
elseif a==42, XX=[36 43 49 41 35 29]; eval(replace)
elseif a==43, XX=[44 5 4 49 42 36]; eval(replace)
elseif a==44, XX=[45 6 5 43 36 37]; eval(replace)
elseif a==45, XX=[46 7 6 44 37 38]; eval(replace)
elseif a==46, XX=[47 1 7 45 38 39]; eval(replace)
elseif a==47, XX=[48 2 1 46 39 40]; eval(replace)
elseif a==48, XX=[49 3 2 47 40 41]; eval(replace)
elseif a==49, XX=[43 4 3 48 41 42]; eval(replace)
end;

```

*% This program with the name HoCall\_attributes.m generates: attributes of the handover call*

```

% a = current;
% CellN = future;
% old = previous;
ho(A,a)=inf;
ChannelStatus(a)=ChannelStatus(a)-1;
CellN=CellNo(old_ho(A,a),a);
HoCall(CellN)=HoCall(CellN)+1;
old_ho(A,a)=inf;
if ChannelStatus(CellN)<ch
    ChannelStatus(CellN)=ChannelStatus(CellN)+1;
    B=min(find(sp(:,CellN)==inf)); % to find place of empty channel
    sp(B,CellN)=sp(A,a);
    ho(B,CellN)=Cdf2Rand(CDF2,X,1)+clock;
    old_ho(B,CellN)=a;% gives the number of previous cell
    sourceCell(B,CellN)=sourceCell(A,a);
else
    HoCallBlock(CellN)= HoCallBlock(CellN)+1;
    dropout(sourceCell(A,a))=dropout(sourceCell(A,a))+1;
end;
sp(A,a)=inf;
sourceCell(A,a)=inf;

```

*% This function calculates blocking probability*

```

function [NCBP,HCBP,DP]=BlockProb(cellsize,LANDA,ch,ch_ho)
p1=num2str(cellsize);
p2=num2str(LANDA);
p3=num2str(ch);
p4=num2str(ch_ho);
eval(['load ~/MATLAB/traffic/data/R' p1 'E' p2 'C' p3 'H' p4])
NCBP=mean(NewCallBlock./NewCall);
HCBP=mean(HoCallBlock./HoCall);
DP=mean(dropout./(NewCall-NewCallBlock));
BP=mean((NewCallBlock+HoCallBlock)./(NewCall+HoCall));

```

*% This program calculates handover call attempt rate using the formula*

```

%    $\lambda_h = (\lambda_n \cdot (1 - PB_n) \cdot P_n) / (1 - (1 - P_{fh}) \cdot Ph)$ 
function [lambda_h,Pfh]=Landa_h(cellsize, AveCallHoldTime, lambda_n);
ch=50; ch_ho=0; ch_new=ch-ch_ho;
PBn1=[]; PBn=[]; Pfh1=[]; Pfh=[];
win=.001; ht=80; t=(0:win:ht);
handover=1; alpha=.5; beta=1.8.*cellsize; p=2.1;
[Pdfn,Cdfn]=GammaEq(alpha,beta,p,t);
handover=2; alpha=.5; beta=2.5.*cellsize; p=2.7;
[Pdfh,Cdfh]=GammaEq(alpha,beta,p,t);
[Pn]=Pn_OR_Ph(Pdfn,AveCallHoldTime,t);
[Ph]=Pn_OR_Ph(Pdfh,AveCallHoldTime,t);
for Erlang=40:2:50
    [PBn2,Pfh2,DP2]=BlockProb(cellsize,Erlang,ch,ch_ho);
    PBn=[PBn; PBn2];
    Pfh=[Pfh; Pfh2];
end;
lambda_h=(lambda_n.*(1-PBn).*Pn)./(1-(1-Pfh).*Ph)

```

*% This function calculates new call duration.*

```

function [mu_c]=Mu_c(cellsize, lambda_n)
ch=50; ch_ho=0; ch_new=ch-ch_ho;
DP=[]; NCBP=[];
AveCallHdTime_new1=[];
erl=30:.01:50;
NCBP_erl=ErlangB(ch_new,erl);
for Erlang=40:2:50
    [NCBP1,HCBP1,DP1]=BlockProb(cellsize,Erlang,ch,ch_ho);
    NCBP=[NCBP; NCBP1];
    DP=[DP; DP1];
end;
for i=1:6
    temp=find(NCBP_erl<=NCBP(i));
    MAX=max(temp);
    temp=erl(MAX)./lambda_n(i);
    AveCallHdTime_new1=[AveCallHdTime_new1; temp];
end;
mu_c=1./AveCallHdTime_new1;

```

*% This function calculates the probability of blocking using Erlang-B formula*

```

function [B]=ErlangB(C, rho)
XX=1;
X=1;
for i=1:C
    XX=(XX.*rho)./i;
    X=XX+X;
end;
B=XX./X;

```

*% This function calculates new call duration considering the dropout effect*

```
function [DP]=Mu_c1(cellsize, landa_n)
ch=50; ch_ho=0; ch_new=ch-ch_ho;
DP=[]; NCBP=[];
AveCallHdTime_new1=[];
erl=30:.01:50;
NCBP_erl=ErlangB(ch_new,erl);
for Erlang=40:2:50
    [NCBP1,HCBP1,DP1]=BlockProb(cellsize,Erlang,ch,ch_ho);
    NCBP=[NCBP; NCBP1];
    DP=[DP; DP1];
end;
T_c=(1-4.*DP./4).*2;
mu_cDP=1./T_c;
```

*% This program determines Blocking Probability including new and handover calls versus Offered traffic per cell [ATTEMPTS].*

```
ch=50; ch_ho=0;
ch_new=ch-ch_ho;
NCBP1=[]; NCBP=[]; HCBP1=[]; HCBP=[];
for cellsize=[1 2 3 6]
    for LANDA=32:2:40
        [NCBP2,HCBP2,DP2]=BlockProb(cellsize,LANDA,ch,ch_ho);
        NCBP1=[NCBP1; NCBP2];
        HCBP1=[HCBP1; HCBP2];
        DP1=[DP1; DP2];
    end;
    NCBP=[NCBP,NCBP1]; NCBP1=[];
    HCBP=[HCBP,HCBP1]; HCBP1=[];
    DP=[DP,DP1]; DP1=[];
end;
```

*% This program with the name ProbCalR2.m determines Blocking Probability including new and handover calls versus Offered traffic per cell [Erlangs].*

```
ch=50; ch_ho=0;
ch_new=ch-ch_ho;
NCBP1=[]; NCBP=[];HCBP1=[]; HCBP=[];DP=[];
AveCallHoldTime_new=[]; AveCallHdTime_new1=[];
Erlang=40:2:50;
landa_n=Erlang./(2.*60); % New call attempt rate (calls/sec/cell)
erl=30:.1:50;
NCBP_erl=ErlangB(ch_new,erl);
for cellsize=1:10
    NCBP1=[]; NCBP=[];
    HCBP1=[]; HCBP=[];DP1=[];
    AveCallHdTime_new1=[];
    for Erlang=40:2:50
        [NCBP2,HCBP2,DP2]=BlockProb(cellsize,Erlang,ch,ch_ho);
```

```

        NCBP=[NCBP; NCBP2];
        DP1=[DP1; DP2];
    end;
    DP=[DP,DP1];
    for i=1:6
        temp=find(NCBP_erl<=NCBP(i));
        MAX=max(temp);
        temp=erl(MAX)/landa_n(i);
        AveCallHdTime_new1=[AveCallHdTime_new1; temp];
    end;
    AveCallHoldTime_new=[AveCallHoldTime_new, AveCallHdTime_new1];
end
temp=ErlangB(ch_new,Erlang);
plot(Erlang,temp,'g*');
hold on, grid on
Erlang_new=landa_n'.*AveCallHoldTime_new(:,10);
temp=ErlangB(ch_new,Erlang_new);
plot(Erlang_new,temp,'r-');
Erlang=40:2:50;
A=(1-1.*DP./2).*120
plot(Erlang',AveCallHoldTime_new(:,1:2:10))
hold on; grid on
plot(Erlang',A(:,1:2:10),':')
temp=ErlangB(ch_new,Erlang);
plot(Erlang,temp,'g*');
hold on, grid on
Erlang_new=landa_n'.*A(:,10);
temp=ErlangB(ch_new,Erlang_new);
plot(Erlang_new,temp,'r-');

% This program with the name thomas.m compares our results with Thomas formula
Vave=50;drif=0; win=.01; ht=100; t=(0:win:ht)';
mu1=[];AveCellResTime=[]; AveCellResTimeH2=[];
handover=1
for cellsize=1:10
    if handover==2, alpha=2.5; beta=1.12.*cellsize; p=1.6;end;
    if handover==1, alpha=.5; beta=1.8.*(cellsize); p=2.1 ;end;
    [Pdf,Cdf]=GammaEq(alpha,beta,p,t);
    [AveCellResTime1]=Pdf2mean(Pdf,t);
    AveCellResTime=[AveCellResTime;AveCellResTime1];
end;
if handover==1
    Mu=50;Sigma=15;x=0.01:.01:100;vmax=100;
    [Pdf,Cdf]=NormalEq(Mu,Sigma,x,vmax);
    [mu]=PdfInv2mean(Pdf,x);
    Thomas=((8.*cellsize.*mu.*60)/(3.*pi))';
end;
if handover==2,
    Thomas=((pi.*cellsize.*60)/(2.*50))';
end;
end;

```

```
Error=100.*(Thomas-AveCellResTime)./Thomas;
[cellsize', Thomas, AveCellResTime Error]
```

*% This program with the name fig1.m plots (as in Fig. 5.5) Blocking Probability including new and handover calls versus Offered traffic per cell [Erlangs].*

```
clear
ProbCal;
landa=0.34:0.02:0.42 % call per sec
NCBP(1,:)=[];HCBP(1,:)=[];
figure(1)
plot(landa(2:length(landa)),NCBP)
hold on,grid on
plot(landa(2:length(landa)),HCBP,'--')
xlabel('New call attempt rate (calls/sec/cell)')
ylabel('Blocking Probability')
AttemptRate=.34:.002:.42;
Erlang=AttemptRate.*120;
temp=ErlangB(ch_new,Erlang); % Erlang-B formula calculation
plot(AttemptRate,temp,'g*');
hold off
```

*% This program with the name naghsh.m determines and plots (as in Fig. 5.6) Blocking Probability including new and handover calls versus Offered traffic per cell [Erlangs].*

```
clear
ch=50;ch_ho=0;ch_new=ch-ch_ho;
Mu=1./(2.*60); Ev=50./3600;
NCBP1=[]; NCBP=[];HCBP1=[]; HCBP=[];
cellsize=1
for LANDA=32:2:42
    [NCBP2,HCBP2,DP2]=BlockProb(cellsize,LANDA,ch,ch_ho);
    NCBP1=[NCBP1; NCBP2];
    HCBP1=[HCBP1; HCBP2];
end;
h=(2.*Ev)/(pi.*cellsize);
Mu_e=Mu+h.*NCBP1;
Erlang=landa./Mu_e;
temp=ErlangB(ch_new,Erlang);
plot(Erlang,temp,'r-'); hold on; grid on,
AttemptRate=.32:.002:.42;
Erlang=AttemptRate.*120;
temp=ErlangB(ch_new,Erlang);
plot(Erlang,temp,'g');
xlabel('Effective offered traffic per cell [Erlangs]')
ylabel('Blocking Probability')
```

*% This program with the name DP\_HCPB.m determines and plots (as in Fig. 5.7) dropout Probability versus handover call Blocking Probability.*

```
clear
```



```

ProbCal;
figure(1)
plot(HCBP, DP)
hold on,grid
xlabel('Handover call blocking probability')
ylabel('Dropout Probability')

```

*% This program with the name fig2.m determines and plots (as in Fig. 5.8) dropout Probability versus new call attempt rate.*

```

clear
ch=50; ch_ho=0;ch_new=ch-ch_ho;
DP1=[]; DP=[];
for cellsize=[1 2 3 4 6 10]
    for LANDA=32:2:42
        [NCBP2,HCBP2,DP2]=BlockProb(cellsize,LANDA,ch,ch_ho);
        DP1=[DP1; DP2];
    end;
    DP=[DP,DP1]; DP1=[];
end;
figure(1)
landa=0.32:0.02:0.42
plot(landa,DP)
xlabel('New call attempt rate (calls/sec/cell)')
ylabel('Dropout Probability')
grid on

```

*% This program with the name fig3L.m determines and plots (as in Fig. 5.9) Blocking Probability including new and handover calls versus Offered traffic per cell [Erlangs].*

```

ch=50; cellsize=1;
ch_ho=[0 1 2 3 4 5];
for LANDA=32:2:42
    for ch_ho=[0 1 2 3 4 5 ]
        [NCBP2,HCBP2,DP2]=BlockProb(cellsize,LANDA,ch,ch_ho);
        NCBP1=[NCBP1; NCBP2];
        HCBP1=[HCBP1; HCBP2];
    end;
    NCBP=[NCBP,NCBP1]; NCBP1=[];
    HCBP=[HCBP,HCBP1]; HCBP1=[];
end;
ch_ho=[0 1 2 3 4 5];
ch_hoi=0:.5:10;
NCBPi=interp1(ch_ho,NCBP,ch_hoi,'spline');
HCBPi=interp1(ch_ho,HCBP,ch_hoi,'spline');
figure(1)
semilogy(ch_ho,NCBP,'--'); hold on;
semilogy(ch_ho,HCBP,':');
xlabel('No. of reserved channels allocated to handover');
ylabel('Blocking Probability');
axis([-0.1, 5.1, .001,.3]);

```

*% This program with the name fig4.m determines and plots (as in Fig. 5.10) dropout probability for the systems with different priorities given to handover calls*

```

ch=50; cellsize=1;
DP1=[];DP=[];
for LANDA=34:2:42
    for ch_ho=[0 1 2 3 4 5 ]
        [NCBP2,HCBP2,DP2]=BlockProb(cellsize,LANDA,ch,ch_ho);
        DP1=[DP1; DP2];
    end;
    DP=[DP,DP1]; DP1=[];
end;
delta = .1;
ch_ho=[0 1 2 3 4 5 ]-3.5.*delta;
LINETYPE=['r--', 'c: ', 'y- ', 'm-.', 'r--'];
delta = .1;
figure(1)
set(gcf, 'defaultaxesXgrid','on');
set(gcf, 'defaultaxesBox','on');
grid;hold on;
for i=5:-1:1
    ch_ho=ch_ho +delta;
    bar1(ch_ho,DP(:,i),LINETYPE(i*3-2:i*3))
end
ch_ho1=[0 1 2 3 4 5 ]-3.*delta;
X=.01;
for i=6:-1:1
    temp=ch_ho1(i);
    patch([temp+X,temp+X,temp+delta-X,temp+delta-X],[0,DP(i,5),DP(i,5),0], 'y', 'EdgeColor', 'w')
end
for i=6:-1:1
    temp=ch_ho1(i)+4.*delta;
    patch([temp,temp,temp+delta,temp+delta],[0,DP(i,1),DP(i,1),0], 'r')
end
temp=3.*delta;
for i=0:1:5
    UNDER=[i-temp,i+temp-.1];
    plot(UNDER,[0,0], '-','LineWidth',3)
end;
axis([-5 5.5 0 0.08])
xlabel('No. of reserved channels allocated to handover')
ylabel('Dropout probability')

```

*%This program with the name fig5.m plots optimum number of reserved channels for different dropout threshold levels*

```

clear, clg;
NCBP1=[]; NCBP=[];HCBP1=[]; HCBP=[];
cellsize=1;ch=50;
Landa=0.32:.02:0.42;
LANDA=100.*Landa;

```

```

ch_ho=[0 1 2 3 4 5];
for LANDAI=LANDA
    for ch_ho1=ch_ho
        [NCBP2,HCBP2,DP2]=BlockProb(cellsize,LANDAI,ch,ch_ho1);
        NCBP1=[NCBP1; NCBP2];
        HCBP1=[HCBP1; HCBP2];
        DP1=[DP1; DP2];
    end;
    NCBP=[NCBP,NCBP1]; NCBP1=[];
    HCBP=[HCBP,HCBP1]; HCBP1=[];
    DP=[DP,DP1]; DP1=[];
end;
Landai=0.32:0.0001:0.42;
DPi=interp1(Landa,DP,Landai,'spline');
N=length(Landai);
DPlimit=[0.002 0.005 0.01 0.025];
for limit=DPlimit
    for i=1:N
        exact_chHo1=min((find(DPi(:,i)<=limit))-1);
        exact_chHo2=[exact_chHo2,exact_chHo1];
    end;
    exact_chHo=[exact_chHo;exact_chHo2]; exact_chHo2=[];
end;
figure(1)
set(gcf, 'defaultaxesYgrid','on');
set(gcf, 'defaultaxesBox','on');
grid;hold on;
for i=1:length(DPlimit)
    plot(Landai, exact_chHo(i,:), 'o', Landai, exact_chHo(i,:), '--');
    hold on
end;
hold off
xlabel('New call attempt rate (calls/sec/cell)')
ylabel('No. of channels allocated to handover')
text(.375,4.8,sprintf('Dropout probability < %5.3f,DPlimit(1)'))
text(.407,3.8,sprintf('< %5.3f,DPlimit(2)'))
text(.407,2.8,sprintf('< %5.3f,DPlimit(3)'))
text(.407,1.8,sprintf('< %5.3f,DPlimit(4)'))
text(.323,4.8,sprintf('No. of channels = 50'))
text(.323,4.5,sprintf('Cell radius = 1 Km'))

% This program with the name Pow_d_mic.m plots received signal level along a LOS and a NLOS streets
in a microcell with superimposed correlated shadow fading.

clear;clf
INC=6; Tx=-15; x_a=150; x_end=500; conditionX=1; conditionY=9; f=870; landa=300/f;
[Power, L_Los, x, PowerN, L_nLos, y, PowerT, xy]=BergFun(INC, Tx, x_a, x_end);
[Power1, L_Los, x1, PowerN1, L_nLos, y1, PowerT1, xy]=BergFun(INC, Tx, 500, x_end);
x1i=x1(1):INC./6:x1(length(x1));
y1i=y1(1):INC./6:y1(length(y1));
Power1i=interp1(x1,Power1,x1i,'spline');

```

```

PowerNi=interp1(y,PowerN,yi,'spline');
plot(x1i,Power1i); hold on;grid on;
plot(y,PowerN,'--'); hold on;grid on;
[S,Sn]=shadowFun(x1);
Si=interp1(x1,S,x1i,'spline');
SS=Si+Power1i;
plot(x1i,SS)
[S,Sn]=shadowFun(y);
Si=interp1(y,S,yi,'spline');
SS=Si+PowerNi;
plot(yi,SS,'--')
xlabel('Distance (m)')
ylabel('Received signal level')
axis([0 500 -140 -40])
text(150, -60, 'Microcell with the street corner at 150 metres')
plot([200,250],[-70,-70])
plot([200,250],[-65,-65],'--')
text(255,-70,sprintf('LOS'))
text(255,-65,sprintf('NLOS'))
axis([0 500 -140 -50])

```

*% This program with the name Pow\_d\_mac.m plots received signal level along a path in a microcell with superimposed correlated shadow fading.*

```

clear;clf
INC=6; Tx=-15; x_a=200; x_end=500; conditionX=1; conditionY=9; f=870; landa=300/f;
ht=100;type=2; hr=1.5;d=1:1:20; Tx=70;
[Loss, loss, Power, power, K1, K2]=hatafun(Tx, ht, type, d, hr, f);
di=d(1):INC./100:d(length(d));
Poweri=interp1(d,Power,di,'spline');
plot(di,Poweri);hold on;grid on;
Sigma_mac=4;
[S,Sn]=shadowFun(d,Sigma_mac);
Sni=interp1(d,Sn,di,'spline');
SS=Sni+Poweri;
plot(di,SS)
xlabel('Distance (Km)')
ylabel('Received signal level')
axis([1 20 -100 -50])

```

*% This function simulates shadow fading by using Eq. (6.14)*

```

function [S_mic, S_mac]=shadowFun(xy,Sigma_mac,Sigma_mic);
if nargin<3, Sigma_mic=4.3; end;
if nargin<2, Sigma_mac=7.5; end;
rho10=0.3;
rho100=0.82;
delta_d=xy(2)-xy(1);
d0_mac=.1;% in Km
d0_mic=10;% in m
rho_mac=rho100.^(delta_d./d0_mac);

```

```

rho_mic=rho10.^(delta_d./d0_mic);
S_mic=[];S_mac=[];
S1=0;
for x=xy
    N=randn.*Sigma_mic;
    while (N>3.*Sigma_mic | N<-3.*Sigma_mic), N=randn.*Sigma_mic; end;
    S1=rho_mic.*S1+((1-rho_mic.^2).^(1/2)).*N;
    S_mic=[S_mic,S1];
end;
S1=0;
for x=xy
    N=randn.*Sigma_mac;
    while (N>3.*Sigma_mac | N<-3.*Sigma_mac), N=randn.*Sigma_mac; end;
    S1=rho_mac.*S1+((1-rho_mac.^2).^(1/2)).*N;
    S_mac=[S_mac,S1];
end;

```

*% This function calculates mean path loss and received power by hata formulas (6.6) and (6.7).*

```

% Tx transmit power [dbm];
% ht height of base station antenna,30~200 (m)
% hr height of mobile station antenna,1~10 (m)
% f frequency, 150~1500 (Mhz)
% typ type of environment:1= medium-small city
%                2= large city
%                3= suburban area
%                4= open area
% d distance 1~20 (Km)
function [Loss, loss, Power, power, K1, K2]=hatafun(Tx, ht, typ, d, hr, f)
if nargin<6, f=900; end;% limit=150~1500 (Mhz)
if nargin<5, hr=1.5; end;% limit=1~10 (m)
if nargin<4, d=1:.5:20; end;% limit=1~20 (Km)
if nargin<3, typ=2; end;
if nargin<2, ht=100; end;% limit=30~200 (m)
% Tx=70;
K2=(44.9-6.55*log10(ht));
Lp = 69.55+26.16*log10(f)-13.82*log10(ht)
if typ == 1, Lp=Lp - ((1.1*log10(f)-.7)*hr-(1.56*log10(f)-.8)); end;
if typ == 2, Lp=Lp - (3.2*(log10(11.75*hr))^2-4.97); end;
if typ == 3, Lp=Lp - 2*(log10(f/28))^2-5.4; end;
if typ == 4, Lp=Lp - 4.78*(log10(f))^2+18.33*log10(f)-40.94; end;
Loss = Lp + K2.*log10(d);
loss=10.^Loss;
K1=Tx-Lp;
Power=K1-K2.*log10(d);
power=10.^Power;

```

*% This function calculates mean path loss and received power by Berg formula (6.11)*

```

% Tx transmit power [dbm];
% hb height of base station antenna, (m)

```

```

% hm height of mobile station antenna, (m)
% f frequency, 150~1500 (Mhz)
function [Power, L_Los, x, PowerN, L_nLos, y, PowerT, xy]=BergFun(INC, Tx, x_a, x_end, conditionX,
conditionY, f)
global y0 x0
if nargin<7, f=870; end;
if nargin<6, conditionY=9; end;
if nargin<5, conditionX=1; end;
if nargin<4, x_end=500; end;
if nargin<3, x_a=x_end./2; end;% length of LOS street to the junction
if nargin<2, Tx=-15; end;
q=4;hb=5;hm=2;landa=300/f;
if conditionX==1 , x0=2 ; xl=185 ; m=4 ;
elseif conditionX==2 , x0=1 ; xl=370 ; m=4 ;
elseif conditionX==3 , x0=1.4; xl=408 ; m=8.3;
elseif conditionX==4 , x0=1.7; xl=332 ; m=6.8;
elseif conditionX==5 , x0=.4 ; xl=126 ; m=4.4;
elseif conditionX==6 , x0=.5 ; xl=95 ; m=4 ;
elseif conditionX==7 , x0=1.2; xl=148 ; m=5.2;
elseif conditionX==8 , x0=1 ; xl=143 ; m=3.2;
elseif conditionX==9 , x0=1 ; xl=189 ; m=4.6;
elseif conditionX==10, x0=1 ; xl=209 ; m=6.2;
end;
if conditionY==1 , y0=3 ; yl=110 ; n=3.5 ;
elseif conditionY==2 , y0=7.9; yl=440 ; n=10.5;
elseif conditionY==3 , y0=3 ; yl=400 ; n=8;
elseif conditionY==4 , y0=4 ; yl=100 ; n=3;
elseif conditionY==5 , y0=3.2; yl=140 ; n=4.7 ;
elseif conditionY==6 , y0=3.5; yl=230 ; n=4.4 ;
elseif conditionY==7 , y0=1.5; yl=180 ; n=5.1 ;
elseif conditionY==8 , y0=4 ; yl=450 ; n=10 ;
elseif conditionY==9 , y0=2 ; yl=120 ; n=4.4 ; end;
x=x0:INC:x_a;
L_Los=((x./x0).^2).*((1+(x./xl).^((m-2).*q)).^(1/q));
L_Los=(1./L_Los).*((landa/(4.*pi)).^2);
L_Los= 10.*log10(L_Los);
L_Los_xa=((x_a./x0).^2).*((1+(x_a./xl).^((m-2)*q)).^(1/q));
y=y0:INC:x_end-x_a;
L_nLos=((y./y0).^2).*((1+(y./yl).^((n-2)*q)).^(1/q));
L_nLos=(1./(L_Los_xa.*L_nLos)).*((landa/(4.*pi)).^2);
L_nLos= 10.*log10(L_nLos);
y=y+x_a-y0;
A= 20.*log10(landa./(4.*pi));
Power=Tx+L_Los;
PowerN=Tx+L_nLos;
PowerT=[Power PowerN];
xy=[x y];

% This program with the name Sigma_T.m plots standard deviation as a function of averaging time
clear; clf

```

```

deltaT=0.25;
SIGMA=[];
for T=0:deltaT:20
    [SIGMA]=[SIGMA, SigmaFun(T,deltaT)];
end;
T=0:deltaT:20;
plot(T,SIGMA)
hold on; grid on;
axis([0 20 2 7])
xlabel('Averaging time [Sec]')
ylabel('Standard deviation [dB]')

```

*% This program with the name Power\_d\_2.m plots received signal level from two base stations without shadow fading*

```

Tx=61; ht=100; type=2; hr=1.5; f=900; increment=.2; d=1:increment:20; h=5;
[Loss, loss, PowerA, power,K1, K2]=hatafun(Tx, ht, type, d, hr, f);
PowerB=PowerA;
dB=19:-1.*increment:0;
PowerC=PowerB-h;
figure(1)
plot(d,PowerA,dB,PowerB,'r--',dB,PowerC,'g.')
xlabel('Distance from BS0 to BS1 (Km)')
ylabel('Received signal level (dB)')
grid;
hold on
axis([0 20 -110 -60])
d1=max(d)/2
[Loss, loss, Power1, power,K1, K2]=hatafun(Tx, ht, type, d1, hr, f);
plot(d1,Power1, '*')
temp=10.^(h./K2);
d2=(temp-1).*d1./(temp+1) + d1;
[Loss, loss, Power2, power,K1, K2]=hatafun(Tx, ht, type, d2, hr, f);
plot(d2,Power2, '*')
d3=15;
[Loss, loss, Power3, power,K1, K2]=hatafun(Tx, ht, type, d3, hr, f);
plot([5 5], [Power3 Power3-h])
plot([5,5.9], [-65, -65])
plot([5,5.9], [-68, -68], 'r--')
mean=pl_s;
% conversion of log normal mean & standard deviation to normal mean & standard deviation
std_n=sqrt(log(std^2./mean.^2+1));
mean_n=log(mean)-(0.5*(std_n.^2));
X=randn(1,39);
XX=std_n.*X+mean_n;
PL=exp(XX);
figure(2)
plot(d,PL,d,mean)
xlabel('distance (Km)')
ylabel('path loss (dB)')
title ('Path loss in suburban area')

```

```

grid
mean=pl_o;
% Conversion of log normal mean & standard deviation to normal mean & standard deviation
std_n=sqrt(log(std^2./mean.^2+1));
mean_n=log(mean)-(0.5*(std_n.^2));
X=randn(1,39);
XX=std_n.*X+mean_n;
PL=exp(XX);
figure(3)
plot(d,PL,d,mean)
xlabel('distance (Km)')
ylabel('path loss (dB)')
title ('Path loss in open area')
grid;
mean=pl_ul;
% conversion of log normal mean & standard deviation to normal mean & standard deviation
std_n=sqrt(log(std^2./mean.^2+1));
mean_n=log(mean)-(0.5*(std_n.^2));
X=randn(1,39);
XX=std_n.*X+mean_n;
PL=exp(XX);
figure(4)
plot(d,PL,d,mean)
xlabel('distance (Km)')
ylabel('path loss (dB)')
grid;

```

*% This program with the name Normal.m shows conversion of the normal distributions to the equivalent standardized normal distributions*

```

clf; clear
Mu2=10; Mu1=35; Sigma=10;
WP= -.004;% position of y for writing down to x axis
s=Mu1-1.2*Sigma;% point s
h=5; % hysteresis level
sh=s-h;
Muu2=0; Muu1=((Mu1-Mu2)+h)/Sigma; Sigmaa=1;
t1= -6.*Sigma-Mu1: 0.01 :6.*Sigma+Mu1;
t2= -6.*Sigma-Mu2: 0.01 :6.*Sigma+Mu2;
[Pdf1]=NormalPdf(Mu1,Sigma,t1);
[Pdf2]=NormalPdf(Mu2,Sigma,t2);
minx= Mu2-3.*Sigma; maxx= Mu1+3.*Sigma; miny= 0; maxy= max(Pdf1); maxy= 0.04;
figure(1)
sp1=subplot(211);
set(gca,'Box', 'on');
hold on; grid on
set(gca, 'XTick', []);
tp= -6.*Sigma-Mu1: 0.01 :sh;
[Pdfp]=NormalPdf(Mu1,Sigma,tp);
patch('XData',[tp(1) tp tp(length(tp))], 'YData', [0 Pdfp 0], 'FaceColor',[0.7 0.7 0.4]);
plot(t2,Pdf2, 'LineWidth', 1,'clipping','on');

```



```

plot(t1,Pdf1,'r--', 'LineWidth', 1,'clipping','on')
axis([minx,maxx,miny,maxy])
[Pdf11]=NormalPdf(Mu1,Sigma,sh);
plot([sh,sh],[0, Pdf11])
text(sh, WP,'r-h','HorizontalAlignment','center')
text(sh-1.5, WP+0.0015,'^','HorizontalAlignment','center')
[Pdf22]=NormalPdf(Mu2,Sigma,s);
plot([s,s],[0, Pdf22])
ylabel('Probability p(s)')
subplot(212)
text(-1.5,-0.0, '(b)')
t1= -6.*Sigmaa-Muu1: 0.01 :6.*Sigmaa+Muu1;
t2= -6.*Sigmaa-Muu2: 0.01 :6.*Sigmaa+Muu2;
[Pdf1]=NormalPdf(Muu1,Sigmaa,t1);
[Pdf2]=NormalPdf(Muu2,Sigmaa,t2);
x=(s-Mu2)./Sigma;
hold on; grid on
set(gca, 'XTick',[])
tp= -6.*Sigmaa-Muu1: 0.01 :x;
[Pdfp]=NormalPdf(Muu1,Sigmaa,tp);
patch('XData',[tp(1) tp tp(length(tp))], 'YData', [0 Pdfp 0], 'FaceColor',[.7 .7 .4]);
plot(t1,Pdf1,'r--', 'LineWidth', 1,'clipping','on')
plot([-2 6.5], [0 0])

```

*% This program with the name Pu\_DL\_h.m calculates and plots unnecessary handover probability versus path loss difference normalised to hysteresis.*

```

clear; clf
SIGMA=1;
for h=[ 0.5, 0.7, 1, 1.2, 1.5, 2].*SIGMA
    A=fix(10.*h./SIGMA);
    eval(['load /pgr/mahmood/MATLAB/handover/UnHo/data/H_' num2str(A)])
    deltaL=-4:.1./h:4;
    plot(deltaL,PU)
    hold on
end;
grid on;
axis([-4 4 0 .14])
ylabel('Unnecessary handover probability, Pu')

```

*% This program with the name Pu\_H.m calculates and plots unnecessary handover probability versus hysteresis level for different signal averaging time*

```

clear; clf
SIGMA=1;
delta_L=0;
deltaT=.25;
load /pgr/mahmood/MATLAB/handover/UnHo/data/DL_0; % PU(h/sigma)
for T=[1 5 10 20]
    [SIGMA]=SigmaFun(T,deltaT);
    H=h.*SIGMA;

```

```

        subplot(122)
        semilogy(H,Pu),
        hold on
end;
axis([0 20 0.0001 .3])
grid on;
xlabel('Hysteresis level, h [dB]')
ylabel('Unnecessary handover probability, Pu')
Sigma=1;
delta_L=0;
load /pgr/mahmood/MATLAB/handover/UnHo/data/DL_0; % PU(h/sigma)
subplot(121)
semilogy(h,Pu)
end;
axis([0 3 0.0001 1])
xlabel('Normalised hysteresis level, h/')
ylabel('Unnecessary handover probability, Pu')

% This program with the name H_T_PU.m calculates and plots relation between three parameters of h, T,
Pu

load /pgr/mahmood/MATLAB/handover/UnHo/data/H_T_PU;% H_T_Pu T Pu;
plot(T, H_T_Pu)
grid on;
A=50; B=0.4; C=1.5
text( T(A), H_T_Pu(1,A)+B, num2str(Pu(1)))
text( T(A), H_T_Pu(2,A)+B, num2str(Pu(2)))
text( T(A), H_T_Pu(3,A)+B, num2str(Pu(3)))
text( T(A)-C, H_T_Pu(3,A)+B, 'Pu = ')
xlabel('Averaging period, T [Sec]')
ylabel('Hysteresis level, h [dB]')

```

*% This program with the name Delay\_H\_T\_R.m calculates and plots handover delay versus hysteresis levels for different signal averaging time and cell radius.*

```

clear; clf
deltaT=0.25;
ht=100;
K2=(44.9-6.55*log10(ht));
for R_v=[100 600]
    Delay=[];
    h=0:1:30;
    T=[01 05 10 20];
    for t=T
        [SIGMA]=SigmaFun(t,deltaT);
        hh=(h-SIGMA);
        temp=10.^(hh./K2);
        temp=(temp-1)./(temp+1);
        temp=(R_v).*temp;
        delay=t./2 + temp;
        Delay=[Delay;delay];
    end
end

```

```

end;
plot(h, Delay)
hold on
if R_v==100
    A=15; B=3; C=.7;
    Rx=.3; Ry=14; x0=17;y0=48;samples=10;
    circle(Rx,Ry,x0,y0,samples);
    text(17.3, 33, 'K = 100')
    set(gcf,'defaulttextfontsize',8);
    text(17.6, 31, 'Rv ')
    set(gcf,'defaulttextfontsize',12);
    text( h(A), Delay(1,A)+B, num2str(T(1)))
    text( h(A), Delay(2,A)+B, num2str(T(2)))
    text( h(A), Delay(3,A)+B, num2str(T(3)),'HorizontalAlignment','center')
    text( h(A), Delay(4,A)+B, num2str(T(4)),'HorizontalAlignment','center')
    text( h(A)-C, Delay(4,A)+B, 'T=','HorizontalAlignment','center')
end;
if R_v==600
    delayi=60; C=.7; del=delayi+1.5;
    Rx=3; Ry=2; x0=6.5;y0=55;samples=10;
    circle(Rx,Ry,x0,y0,samples);
    text(9, 51, 'K = 600')
    set(gcf,'defaulttextfontsize',8);
    text(9.4, 49, 'Rv ')
    set(gcf,'defaulttextfontsize',12);
    text( interp1(Delay(1,:),h,delayi), del, num2str(T(1)),'HorizontalAlignment','right')
    text( interp1(Delay(1,:),h,delayi), del, ' [Sec]')
    text( interp1(Delay(2,:),h,delayi), del, num2str(T(2)),'HorizontalAlignment','right')
    text( interp1(Delay(3,:),h,delayi), del, num2str(T(3)),'HorizontalAlignment','right')
    text( interp1(Delay(4,:),h,delayi), del, num2str(T(4)),'HorizontalAlignment','right')
    text( interp1(Delay(4,:),h,delayi)-C,del, 'T=','HorizontalAlignment','right')
end;
end
axis([0 20 0 80])
grid on;
xlabel('Hysteresis level, h [dB]')
ylabel('Handover delay [Sec]')

```

*% This program with the name Delay\_T\_Pu\_H\_R.m calculates and plots handover delay versus signal averaging time and hysteresis level as a function of unnecessary handovers for different cell sizes*

```

clear; clf
R_v=[300 600];
A=120; B=10; C=3.5;
k=1;
load /pgr/mahmood/MATLAB/handover/UnHo/data/H_T_PU;% H_T_Pu T Pu;
delay=1:length(H_T_Pu);
for r_v=R_v
    SUBPLOT=120+k;
    subplot(SUBPLOT)
    for j=2:3

```

```

        for i=1:length(H_T_Pu)
            delay(i)=DelayFun(T(i), r_v, H_T_Pu(j,i));
        end;
        plot(T, delay)
        grid on; hold on
        plot(H_T_Pu(j,:), delay,'r--')
        text( T(A), delay(A)+B, num2str(Pu(j)))
        text( T(A)-C, delay(A)+B, 'Pu = ')
        A=A+20;B=B+5;
    end;
    A=120; B=20; C=3.5;
    k=k+1;
    xlabel('Averaging period, T [Sec]')
    ylabel('Handover delay, [Sec]')
    axis([0 20 30 220])
    text(5, 200, 'K = ')
    set(gcf,'defaulttextfontsize',8);
    text(6, 197, 'Rv ')
    set(gcf,'defaulttextfontsize',12);
    text(9, 200, num2str(r_v))
    plot([5 8], [190 190], '--')
    plot([5 8], [180 180], '-')
    text(9, 190, 'h')
    text(9, 180, 'T')
    text(0, 225, '0','HorizontalAlignment','center');
    text(5, 225, '5','HorizontalAlignment','center');
    text(10, 225, '10','HorizontalAlignment','center');
    text(15, 225, '15','HorizontalAlignment','center');
    text(20, 225, '20','HorizontalAlignment','center');
    text(10, 235, 'Hysteresis level, h [dB]','HorizontalAlignment','center');
end;
subplot(121)
Rx=.3; Ry=7; x0=8.5;y0=38;samples=10;
circle(Rx,Ry,x0,y0,samples);
Rx=.4; Ry=11; x0=10.5;y0=66;samples=10;
circle(Rx,Ry,x0,y0,samples);
subplot(122)
Rx=.4; Ry=12; x0=8;y0=72;samples=10;
circle(Rx,Ry,x0,y0,samples);
Rx=.4; Ry=17; x0=10;y0=127;samples=10;
circle(Rx,Ry,x0,y0,samples);
hold off

% this program with the name Power_d_2_micro.m calculates and plots handover delay in a micro-cell
clear;clf
global y0 FIX
INC=1;
[Power, L_Los, x, PowerN, L_nLos, y, PowerT, xy]=BergFun(INC);
ConvNum=71; POS=2;
[Mean]=MeanData(PowerT, ConvNum, POS);

```

```

XY=xy(length(xy):-1:1);
Inc=5;
PowerT1=PowerT(1:Inc:length(PowerT));
Mean1=Mean(1:Inc:length(Mean));
xy1=xy(1:Inc:length(xy));
XY1=XY(1:Inc:length(XY));
subplot(211)
plot(xy, PowerT,'r-');grid off, hold on
plot(xy , Mean , 'g-', 'LineWidth', 1.1);
plot(XY, PowerT, 'y--')
plot(XY1 , Mean1 , 'r.', 'LineWidth', 1)
axis([0 500 -150 -20])
ylabel('Received signal level (dB)')
xlabel('Distance from BS0 to BS1 (m)')
plot([50,70], [-30, -30], '-')
plot([50,70], [-50, -50], '--')
plot([50,70], [-40, -40], '-.', 'LineWidth', 1.1)
plot([50,55,60,65,70], [-60,-60,-60,-60,-60], '.', 'LineWidth', 1)
subplot(212)
plot(xy, PowerT,'r-'); grid off, hold on
plot(xy , Mean , 'g-', 'LineWidth', 1.1);
plot(XY, PowerT, 'y--')
plot(XY , Mean , 'r.', 'LineWidth', 1)
axis([200 300 -120 -80])
ylabel('Received signal level (dB)')
xlabel('Distance (m)')
AA=length(x)-FIX;
A=x(AA);
B=PowerT(AA);
C=Mean(length(x));
XData=[A A];
YData=[B C];
line(XData, YData, 'LineStyle', '-', 'LineWidth', .5)
DD=length(x);
D=x(DD);
E=Mean(DD);
XData=[A D];
YData=[E E];
line(XData, YData, 'LineStyle', ':', 'LineWidth', 1.5)
GG=length(x)+8;
G=xy(GG);
H=Mean(GG);
II=length(x)-8;
I=Mean(II);
XData=[G G];
YData=[H I];
line(XData, YData, 'LineStyle', '-', 'LineWidth', .5)
F=PowerT(length(x));
XData=[D D];
YData=[F H];
line(XData, YData, 'LineStyle', '-', 'LineWidth', .5)

```

```

I=Mean(II);
XData=[G D];
YData=[H H];
line(XData, YData,'LineStyle',':', 'LineWidth', 1.5)
Tx=(A+D)/2; Ty=C;
text(Tx,Ty-2,'T/2','HorizontalAlignment','center')
hx=G; hy=(I+H)/2;
text(hx,hy,' h-','HorizontalAlignment','left')
set(gcf,'defaulttextfontName','symbol')
text(hx,hy,' s','HorizontalAlignment','left')
set(gcf,'defaulttextfontName','times')
dx=(D+G)/2; dy=H;
set(gcf,'defaulttextfontName','symbol')
text(dx-1, dy-2,' d','HorizontalAlignment','right')
set(gcf,'defaulttextfontsize',8);
text(dx, dy-3,' m','HorizontalAlignment','center')
set(gcf,'defaulttextfontName','times')
text(dx, dy-3,' hys','HorizontalAlignment','center')
set(gcf,'defaulttextfontsize',12);
d_corx=A; d_cory=(B+C)/2;
text(d_corx,d_cory,' d','HorizontalAlignment','left')
set(gcf,'defaulttextfontsize',8);
text(d_corx,(d_cory-1),' cor','HorizontalAlignment','left')
set(gcf,'defaulttextfontsize',12);

```

*% This function determines mean value of data by smoothing data by convolution*

```

function [Mean]=MeanData(Data, ConvNum)
if nargin<1, ConvNum=21; end;
FIX=fix(ConvNum./2);
SIZE=length(Data);
Mean=conv(Data,ones(1,ConvNum));
Mean(1:ConvNum-FIX-1)=Mean(1:2:ConvNum-2)./(1:2:ConvNum-2);
Mean(ConvNum-FIX:SIZE-FIX)=Mean(ConvNum:SIZE)./ConvNum;
Mean(SIZE-FIX+1:SIZE)=Mean(SIZE+1:2:SIZE+ConvNum-1)./(ConvNum-1:-2:1);
Mean(1)=(Data(1)+Data(2))./3;
Mean(SIZE+1:length(Mean))=[];
end;

```

*% This function determines hysteresis delay*

```

function [delay]=DelayFun(T, R_v, H);
[SIGMA]=SigmaFun(T);
ht=100;
K2=(44.9-6.55*log10(ht));
hh=(H-SIGMA);
temp=10.^(hh./K2);
temp=(temp-1)./(temp+1);
temp=(R_v).*temp;
delay=T./2 + temp;

```

*% This function calculates unnecessary handover probability*

```
function [PU]=PuFun(x,h,deltaL,SIGMA);
x1=x-h./SIGMA + deltaL./SIGMA;
x2=x-h./SIGMA - deltaL./SIGMA;
Px=exp((-x.^2)./2)./(2.*pi).^5);% P(x)
Px1=exp((-x1.^2)./2)./(2.*pi).^5);% P(x1)
Px2=exp((-x2.^2)./2)./(2.*pi).^5);% P(x2)
Int_Px1=.5+.5.*erf(x1./2).^5);% integral of P(x1) between [-inf x]
A1=Px.*Int_Px1;          % P(x). * integral of P(x1)
B1=trapz(A1,x);          % integral of the above (A1)
Int_Px2=.5+.5.*erf(x2./2).^5);% integral of P(x2) between [-inf x]
A2=Px.*Int_Px2;          % P(x). * integral of P(x2)
B2=trapz(A2,x);          % integral of the above (A2)
PU=B1.*B2;
```

*% This function calculates received signal variance*

```
function [SIGMA]=SigmaFun(T,deltaT,SigmaS,SigmaR,Fm);
if nargin<5, Fm=0.2; end;
if nargin<4, SigmaR=5.57;end;
if nargin<3, SigmaS=6.5; end;
if nargin<2, deltaT=0.25;end;
n=T ./ deltaT+1;
A=0;
for i=1:n
    x=2.*Fm.*i.*deltaT;
    SINC=sinc(x);
    A=A+(1-i./n).*SINC;
end;
B=(1./n).*(1+2.*A);
SIGMA=SigmaS.*sqrt(B);
```

*% This program with the name dataCreateForH\_T\_Pu.m creates data for calculation of unnecessary handovers*

```
Pu=[.1 .01 0.001];
T=1:.1:20;
H_T_Pu=[];
for pui=Pu
    H_T=[];
    load ~/MATLAB/handover/UnHo/data/DL_0; % PU(h/sigma)
    len=length(PU);
    temp=find(PU(2:len)-PU(1:(len-1))==0);
    if (temp~=[]), PU(temp)=[]; h(temp)=[]; end;
    hi=interp1(PU, h, pui);
    for t=T
        [SIGMA]=SigmaFun(t);
        Hi=hi.*SIGMA;
        H_T=[H_T,Hi];
    end;
end;
```

```

    H_T_Pu=[H_T_Pu; H_T];
end;
save ~/MATLAB/handover/UnHo/data/H_T_PU H_T_Pu T Pu;

```

*% This program with the name dataCreateForH\_T\_de.m generates data necessary for delay calculation*

```

R_v=600
Delay=[20 40 60];
T=1:0.1:20;
H=(0:1:100);
for r_v=R_v
    H_T_Delay=[];
    for delayi=Delay
        H_T=[];
        for t=T
            [delay]=DelayFun(t, r_v, H);
            len=length(delay);
            temp=find(delay(2:len)-delay(1:(len-1))==0);
            if (temp~=[]), delay(temp)=[]; H(temp)=[]; end;
            Hi=interp1(delay, H, delayi);
            H_T=[H_T,Hi];
        end;
        H_T_Delay=[H_T_Delay; H_T];
    end;
    eval(['save ~/MATLAB/handover/data/H_T_Delay_R_v' num2str(r_v) ' H_T_Delay T Delay'])
end;

```

*% This program with the name dataCreateForPu.m generates data necessary for unnecessary handover probability*

```

SIGMA=1;
for h=[0.5, 0.7, 1, 1.2, 1.5, 2].*SIGMA
    PU=[];
    for deltaL=-4.*h:.1:4.*h
        x=-6.*SIGMA:0.001:6.*SIGMA;
        [Pu]=PuFun(x,h,deltaL,SIGMA);
        PU=[PU,Pu];
    end;
    A=fix(10.*h./SIGMA);
    eval(['save ~/MATLAB/handover/data/H_' num2str(A) ' SIGMA PU '])
end;

```